

G. De Vogeleeer

Reduced measuring strategies to assess ventilation rates in naturally ventilated animal houses



Promotors

Prof. dr. ir. Jan G. Pieters

Dr. ir. Peter Demeyer

Ghent University

Institute for Agricultural and Fisheries
Research (ILVO)

Faculty of Bioscience Engineering

Technology and Food Science Unit –

Department of Biosystems Engineering

Agricultural Engineering

Jan.Pieters@UGent.be

Peter.Demeyer@ilvo.vlaanderen.be

Examination committee

Dr. ir. Ann Dumoulin

Chairman

Ghent University, Belgium

Prof. dr. ir. Jan Pieters

Promotor

Ghent University, Belgium

Dr. ir. Peter Demeyer

Promotor

ILVO, Belgium

Prof. dr. ir. Herman Van
Langenhove

Ghent University, Belgium

Dr. ir. Bart Sonck

ILVO and Ghent University, Belgium

Dr. Ir. Nico Ogink

Wageningen University,
the Netherlands

Dr. Tomas Norton

University of Leuven, Belgium
Harper Adams University, United
Kingdom

Dean: Prof. dr. ir. Marc Van Meirvenne

Rector: Prof. dr. Anne De Paepe

G. De Vogeleeer

Reduced measuring strategies to assess ventilation rates in naturally ventilated animal houses

Thesis submitted in fulfilment of the requirements
for the degree of Doctor (PhD) in Applied Biological Sciences

Dutch translation of the title:

Ontwikkeling van gereduceerde meettechnieken voor ventilatiedebieten in een natuurlijk geventileerde stal

Please refer to this work as follows:

De Vogeleer G. (2017). Reduced measuring strategies to assess ventilation rates in naturally ventilated animal houses. PhD thesis, Faculty of Bioscience Engineering, Ghent University, Ghent, Belgium, pp. 229

Gerlinde De Vogeleer is supported by Institute for Agricultural and Fisheries Research, University of Ghent, Agency for Innovation by Science and Technology (IWT) and through a Ph.D. fellowship.

Cover:.

Copyright: 2017 Gerlinde De Vogeleer

ISBN: 978-90-5989-983-4

All rights reserved. No part of this thesis may be reproduced, stored in a retrieval system of any nature, or transmitted in any means, without permission of the author, or when appropriate, of the publishers of the publications.

Acknowledgements

Doctoreren, het is een speciale ervaring. Het doctoraatschrift kwam er absoluut niet vanzelf. Het is echt hard en zonder veel pauzes doorwerken geweest. Daar tegenover stond wel de flexibiliteit van het doctoreren die de mogelijkheid gaf om het gezinsleven te combineren met het harde werken. Ik kan terug kijken op een periode waarbij ik een doctoraat afgeleverd heb waarop ik toch trots ben. Ik heb er het beste uitgeperst met mijn vermogen en binnen de tijd die ik ter beschikking had. Uiteraard met hulp van veel mensen rondom mij.

Eerst en vooral wil ik Philippe bedanken. Aangezien we samen aan het NATVENT-project werkten, hebben we veel dicht contact gehad. Gelukkig klikte dat, stel u voor. Niet alleen konden we goed samen werken (en samen sukkelen), we konden ook nog eens dezelfde, soms ietwat foute, humor delen. We hebben ons geluk en miserie samen kunnen uitlachen en dat deed bij tijd echt veel deugd. En belangrijk Philippe, we zijn allebei over de horde geraakt :-). Ik hoop dat we af en toe nog eens een tertje door de ILVO-velden gaan kunnen zetten.

Jan en Peter, het is duidelijk dat ik niet de student ben die het meest zal uitblonken hebben in teksten schrijven. Maar kijk, we zijn er alle drie rustig bij gebleven en we hebben er het beste van gemaakt! Peter kon mijn teksten opwaarderen door mij te wijzen op de structuur en mijn aandacht proberen bij te houden bij de exacte bewoording. Jan had een heel andere stijl van werken. Als ik teksten van hem terug kreeg had ik gemengde gevoelens van enerzijds diepe schaamte over de kwaliteit en anders moest ik lachen met de manier waarop alles aangeduid werd. Hij schuwde geen uitroepingstekens, drukletters en uitdrukkingen als 'TE WOLLIG!'. Maar vooral belangrijk, ik kreeg altijd snel feedback op mijn teksten. Dit heb ik altijd zeer erg geapprecieerd aangezien het voor mij de mogelijkheid gaf goed te kunnen doorwerken zodat ik tijdig kon doctoreren!

Ook aan de collega's van onze milieutechniekgroep, het gaf echt een goed gevoel dat we elkaar konden helpen en dat het niet ieder voor zich was. Technische hulp en mentale steun top bij milieutechniek. En ja, misschien ga ik de stalgeurtjes van Caroline missen :-)

Anyone: "Raphael, how are you today?"

Raphael: "not too bad"

Yes, Raphael, maybe you didn't notice it, but you do have an impact on us by being

the one and only Raphael. We had a nice atmosphere in our ventilation office. Also with Luciano: knowledge, friendliness and the ability to bake amazing cakes in one package, very good combination for a close colleague :-). And of course I don't forget Sewoon, one day I will come to South Korea to check whether your country is indeed so beautiful as you say.

Stephanie, ik heb veel "ze duren maar 5 minuutjes"-vragen gehad voor jou. Altijd kreeg ik een antwoord met een glimlach en wat extra humor erbij. Ik was blij die noodzakelijke statistiek met jou te kunnen overleggen. Dat maakte het stukken minder mottig.

En ook aan de techniekers van TV115. Iedereen heeft zowat meegeholpen aan het NATVENT-project, maar ik denk dat Olav en Eric veruit het meest afgezien hebben door onze testconstructie in orde te zetten bij vriestemperaturen. Ik ben het nog altijd niet vergeten, jullie waarschijnlijk ook niet :-). En ja, zeker ook bedankt aan Bart Lannau, het was altijd leuk om samen in de stal te werken.

Vrollega's van ILVO... hoe zeer hebben we ons geamuseerd. Echt, ik heb heel graag in onze collegagroep gezeten. Ik durf niet teveel namen te noemen uit angst mensen te vergeten. Er is ook zoveel passage geweest, wat eigen is aan een onderzoeksinstelling met veel doctoraatsstudenten uiteraard. Tijdens de middag- en koffiepauzes, in de gang, in de bureaus, hoe neig hebben we ons niet geamuseerd. Ik vond het heerlijk dat echt aaaaalle soorten gesprekken aan bod kwamen (Ingrid hield het bij). Het middagmaal was toch veruit het favoriete moment van de werkdag! En ik was ook altijd blij om faalverhalen te horen van andere moeders, het was toch een soort van moedertherapie :-).

Aan de innova's: neen geen bedankt. Jullie blokkeerden altijd mijn airway system - niet ok-!!

Dear UGhent-colleagues, we also shared great times together (not with you Luis, not with you :-). The first two years I came to the university because I followed evening classes in Ghent. Afterwards, I just came because I needed my dose of contact with UGhent-colleagues. I even came for the beer events. And that's quite an achievement I must say, few people have seen me drink more than 1 beer. Ook heel erg bedankt aan Dieter, Lut en Thomas voor hun last-minute hulp. Hulp bij stress zijn dubbele punten en jullie hebben big-time gescoord! En ook merci aan Eddy, mijn contact met de buitenwereld :-).

Eveline Volcke, bedankt om aan mij te denken toen mijn doctoraatsfunctie nog openstond. En Lieve Herman zeker ook om me het vertrouwen te geven en me aan te werven.

Familie, heel erg bedankt voor al jullie geduld als ik al eens wat slechter gezind was

(echt niet he). Moeke en Martine, vooral ook bedankt om de kindjes op cruciale momenten op te vangen. En Karel, de tweeling is weer in balans! Gij ingenieur, ik ook. Gij doctor, ik ook! Voor dat vliegdiploma ga ik passen. Gij wint.

Opa, ik ben echt heel blij dat je me kan zien doctoreren. Niet over het feit dat je nog leeft om het te kunnen zien. Uiteraard niet, want ik moet je binnen 56 jaar ook nog kunnen zeggen hoe het voelt ouder dan 87 te zijn. Maar vooral omdat ik met hard werken en doorzetten er gekomen ben. En nu ga ik weer meer op bezoek komen, ik heb onze lange gesprekken teveel gemist de laatste weken!

Wolf en Hazel, ik had het soms moeilijk om toe te geven aan mijn collega's dat ik niet ging mee drinken omdat ik weer eens super moe was (letterlijk 3 jaar van mijn doctoraat dus) van het bukken, koken, lopen, springen, willetjes in toom houden, 's nachts opstaan en vooral rushen voor jullie. Maar ik moet maar 1 seconde jullie gezichtjes zien en ik weet waarom ik alles doe. Ik meen het dat ik zeg dat jullie mij veel geholpen hebben in het laatste jaar van mijn doctoraat. Elke dag had ik een werkstress-loze periode tussen 16 en 19u en kon ik genieten van jullie eigenzinnige persootjes. Jullie geven me meer energie dan dat ik er moet geven (en dat is behoorlijk wat: jullie zijn zeer actieve, maar heel lieve kindjes).

Hans. Gij staat het dichtst bij mij, dus ge stond op de eerste rij om de bagger op te vangen. Ge hebt mijn mentale afwezigheid (fysiek was ik er) best goed verdragen, al was het op het einde wel genoeg. Ik was altijd zo trots om te zeggen dat Wolf en Hazel niets van mijn doctoraat gemerkt hebben. Maar gij daarentegen hebt dubbel afgezien. Maar kijk, ik heb een doctoraat gedaan en gij zijt zelfstandig begonnen terwijl Hazel nog een baby was -Ik denk dat we nu wel quitte staan!- :-). Op een of andere manier functioneren we heel goed als koppel en als gezin met alle uitdagingen van werk, kinderen, verbouwingen, vrienden, familie,..... erbij, we doen het gewoon op ons tempo. Ik heb gelijk wel al in de mot dat er nooit echt zoiets zal zijn als 'veel tijd voor elkaar', ook niet na het doctoraat. Maar aangezien ik blijf werken voor de Vlaamse Overheid, moet ik nu wel rekening houden met hun campagne -www.tijdvoorjerelatie.be-. Dus vanaf nu donderdag date-dag?

Gent, April 2017 - Gerlinde

Table of Contents

ACKNOWLEDGEMENTS	V
TABLE OF CONTENTS	IX
LIST OF ABBREVIATIONS	XIII
LIST OF SYMBOLS	XV
SUMMARY	XVII
SAMENVATTING	XXIII
1 INTRODUCTION	1
1.1 Importance of the indoor climate	2
1.1.1 Ventilating livestock buildings	2
1.1.2 Efficient ventilation towards emission control	3
1.1.3 Natural vs. mechanical ventilation	4
1.2 Assessing the airflow rate in naturally ventilated buildings	5
1.2.1 Measuring techniques	6
1.2.2 Modelling techniques	11
1.3 Problem statement	17
1.4 Overall objective and thesis outline	18
2 EXPERIMENTS IN AN ANIMAL MOCK-UP BUILDING: ASSESSING AIRFLOW RATES*	21
2.1 Introduction	22
2.2 Materials and Methods	25
2.2.1 Animal mock-up building and instrumentation	25
2.2.2 Data Collection and Model Development Methods	28
2.2.3 Experimental data	33
2.3 Results	36
2.3.1 Assessing the airflow rate for uni-directional flows in the side vents	36
2.3.2 Assessing the airflow rate for bi-directional flows in the side vents	39
2.4 Discussion	42
2.5 Conclusions	44

3	EXPERIMENTS IN AN ANIMAL MOCK-UP BUILDING: ASSESSING AIRFLOW DISTRIBUTION IN VENTS	47
3.1	Introduction	48
3.2	Materials and Methods	50
3.2.1	Animal mock-up building, instrumentation and experimental setup	50
3.2.2	Reference airflow rate measurements and calculations	50
3.2.3	Data collection and model development	54
3.2.4	Experimental data	56
3.3	Results & discussion	57
3.3.1	Characterisation of the airflow rates through the vents	57
3.3.2	Distribution models for the ridge vent	58
3.3.3	Distribution models for the side vent	60
3.4	General discussion	65
3.5	Conclusions	66
4	EXPERIMENTS IN AN ANIMAL MOCK-UP BUILDING: EFFECT OF SAMPLING DENSITY ON THE ACCURACY OF AIRFLOW RATE MEASUREMENTS	69
4.1	Introduction	70
4.2	Materials and Methods	72
4.2.1	Animal mock-up building and experimental setup	72
4.2.2	Airflow rate methods	73
4.2.3	Sampling density reduction schemes	77
4.2.4	Analysis of the reliability of airflow rate measurements	78
4.3	Results and discussion	82
4.3.1	Direct airflow rate measurements	82
4.3.2	Indirect airflow rate measurements	87
4.4	General discussion	90
4.5	Conclusions	92
5	EXPERIMENTS IN A DAIRY BARN: EFFECT OF SAMPLING DENSITY ON THE ACCURACY OF AIRFLOW RATE MEASUREMENTS AND CORRELATIONS BETWEEN THE SAMPLING POINTS IN THE VENT AND AT THE METEOMAST	95
5.1	Introduction	96
5.2	Materials and Methods	97
5.2.1	Site and building description	98
5.2.2	Experimental set-up	100
5.2.3	Data processing	112
5.3	Results and discussion	115
5.3.1	Velocities of reduced sampling locations as predictors for the velocity profile	115
5.3.2	Predictability of the velocity pattern in the vents	132
5.3.3	Characterisation of airflow rates through side and ridge vent	142

5.4	General discussion	147
5.5	Conclusions	149
GENERAL DISCUSSION & PERSPECTIVES		153
5.6	Research questions	154
5.7	Feasibility of reduced sampling strategies	156
5.7.1	Reduced sampling strategies in the animal mock-up building	156
5.7.2	Reduced measurement strategies in a commercial animal house	157
5.7.3	Suggestions for an improved airflow sampling technique in the vents	159
5.8	Future perspectives	162
5.8.1	Linking with mechanistic models describing ammonia release at source level	162
5.8.2	Representativeness of measurement conditions	164
REFERENCES		167
CURRICULUM VITAE		179
Personal particulars		180
Basic education		180
Employment		180
Publications		182
Papers in international journals with reading committee		182
Oral presentations at conferences		183
Other conference contributions		184
MSc theses		184
BSc thesis		184

List of abbreviations

abbreviation	description
2D	2-dimensional
3D	3-dimensional
ACNV	Automatic Controlled Natural Ventilation
AER	Air exchange rates (1/h)
ANN	Artificial neural networks
AVG	Average
CC	Curtain Configuration
CFD	Computational Fluid Dynamics
Diff	Difference
E	East
EMR	Emission rate (g/h)
EFF	Opening effectiveness of the ventilation opening
hSL	Horizontally aligned sampling location
IA	Incidence angle
Max	Maximum
Min	Minimum
MM	Meteomast
MR	Model results
MV	Modelled Velocity
N	North
NE	North East
NW	North West

List of abbreviations

PAN	Programmatic Approach Nitrogen
RH	Ridge vent horizontal sampling line
RSL	Reduced sampling locations
RR	Reference results
RSM	Response Surface Method
RV	Reference Velocity
S	South
SC	Side vent chess pattern sampling locations
SE	South East
SH	Side vent horizontal sampling locations
SV	Side vent vertical sampling locations
SW	South West
SD	Standard Deviation
SG	Sensor Group
SL	Sensor Location
SR	Sensor ridge vent
VERA	Verification of Environmental Technologies for Agricultural Production)
W	West

List of symbols

abbreviation	characterization	unit
β_0	Slope Bland Altman	-
β_1	Intercept Bland Altman	m/s
ρ	Air density	kg/m ³
A	Surface area	m ²
a	Coefficient	-
b	Coefficient	-
c	Constant	-
C	Component	-
i	Index	-
j	Constant	m ²
H	Height	m
M	Molar weight	kg/mol
MMass	Molar mass	g/mol
n	Number of	-
p	Probability	-
Pr	Pressure	hPa
Q	Airflow rate	m ³ /h
T	Temperature	°C
\vec{U}	Velocity vector	m/s
v	Velocity	m/s
$ \vec{U} $	Total air velocity	m/s
x	Distance	m

List of symbols

$ \bar{X} $	Tangential (to the vents) air velocity component	m/s
$ \bar{Y} $	Perpendicular (to the vents) air velocity component	m/s

Subscript

characterization

b	Background
bi	Bi-directional
d	Discharge
m	Measured
ms	Measurements surface
MM	Meteomast
part	Partition
ref	Reference
tot	Total
uni	Unidirectional

Summary

This PhD research studied the feasibility of reduced measuring strategies using direct velocity measurements to assess ventilation rates in naturally ventilated animal houses. There exists a need for accurate and simple measurement techniques in order to determine emissions from animals cost-efficient and to improve ventilation control. The possibility of using simple (regression) models using wind velocity measurements at the meteor mast and local values in the vents, was investigated to predict the airflow rate through the building and the velocity distribution in the vents. Insight was gained on the influence of reduced sampling locations and varying wind conditions on the accuracy and precision of airflow rate measurements.

A well-designed ventilation system is essential to ensure optimal animal production in agricultural buildings. This, because animal welfare is strongly related to the quality of the air in animal houses. Beside controlling the quality of the indoor air by removing hazardous components as e.g. NH_3 and CH_4 , airflow (rate) assessment is also important to estimate the emissions of these hazardous gases from the buildings. Measuring emissions has gained in importance since the awareness to the effect of NH_3 on the environment increased. However, measuring the airflow rate in naturally ventilated buildings is a challenge because of highly varying wind conditions. Airflow rate measurements are difficult to conduct due to temporal and spatial variations of the velocity distribution in the vents and in the building. Notwithstanding a strong need for a reference measuring technique, still no undisputed reference is available. **Chapter 1** provides some background of the importance of developing an accurate reduced measuring strategy. This, in the context of animal health and for measuring emissions of the NEC-directive and the currently hot topic PAN (Programmatic Approach to Nitrogen). PAN has been imposed by the Flemish government with regard to the EU NATURA2000 program In order to reduce ammonia deposition in nature. To understand the complexity of measuring and modelling the airflow rate, the most common models and measuring methods to assess the airflow rates in naturally ventilated buildings are provided, together with their main advantages and disadvantages. However, this thesis mainly focuses on assessing the airflow rate using the direct measurement method using anemometers in the vents in an animal mock-up building and a semi-commercial dairy barn Regression is selected as model

approach and applied for prediction of airflow rates through the building and velocity distribution in the vents.

The step-by-step approach towards a reduced measurement protocol is described in the outline of this thesis, in chapter 1. This approach starts from a previously developed direct measurement method of Van Overbeke et al. (2016). Van Overbeke et al. (2016) developed and validated an accurate measuring method in a naturally ventilated animal mock-up building with a ridge and two side vents. This measuring method is conducted by direct velocity measurements in the side vents. Continuously moving sensors measure a detailed grid resulting in the velocity distribution over the vent. A platform was created for measuring airflow rates with a relative error of $(8 \pm 5)\%$ thus largely remaining within 20% error measured under a large variety of external conditions. This technique was found unique because it can generate a dataset of detailed airflow rates to test the accuracy of reduced measuring methods against detailed measurements. Notwithstanding the great value of this technique, simplification of the method was still necessary to achieve a more practical, time-reduced, cost-effective and yet sufficiently accurate method.

Chapter 2 provides a first step towards a reduced measuring strategy by developing a fast, accurate and simple to use airflow rate model for the animal mock-up building. This fast assessment technique combines linear regression and local air velocity measurements obtained from a meteomast. This assessment technique was validated against detailed measurement results obtained by the measuring method of Van Overbeke et al. (2016). The total wind velocity $|\bar{U}|$, the velocity vector \bar{U} , the normal $|\bar{Y}|$ and the tangential velocity component $|\bar{X}|$ as measured at the meteomast were chosen as input variables for the regression models. The airflow rates were split in one group where only uni-directional flows occurred at vent level (no opposite directions of \bar{Y} present in the airflow distribution of the opening), and a second group where bi-directional flows occurred (the air goes simultaneously in and out of the opening). The models for the airflow rates with uni-directional flows yielded the most accurate results with the input variables \bar{U} and $|\bar{Y}|$. For this reason, it was also suggested to use the $|\bar{Y}|$ instead of $|\bar{U}|$ in ASHRAE's formula $Q = E \times A \times |\bar{U}|$. For bi-directional flows a multiple linear model was suggested where input variables $|\bar{X}|$ and $|\bar{Y}|$ gave the best results to assess the airflow rate. This chapter suggested successfully a simple to use model to assess the airflow rate accurately, combined with only one sensor (using 2

velocity components) on a meteomast. However, to build such a model, it is still necessary to measure the velocity pattern in order to link the airflow rate through the vents with the velocities measured at the meteomast.

Chapter 3 provides insights in the velocity distribution in the openings of the animal mock-up building in order to look for reduced sampling strategies. The velocity distribution is important for many reasons. Firstly, only by knowing this velocity distribution, a selection of the optimal sampling locations can be achieved to measure the airflow rate accurately. Secondly, emission measurements using the product of the differential pollutant concentration and the airflow rate, is a challenge: quickly changing wind conditions induce high spatial and temporal variations in the velocity distribution at vent level. Thus, knowing the air velocity distribution is the first important step towards an accurate airflow rate and emission measuring method in naturally ventilated buildings.

In order to assess the predictability of the airflow rate distribution in vents, linear regression was applied to velocity measurements in the vents using velocities measured at a meteomast. Again, the detailed airflow rate measurements of Van Overbeke et al. (2016) were used as a to validate the statistical models. Results showed that the velocity distribution in the ridge vent could be modelled accurately and precisely for all wind directions ($R^2 > 89\%$). Models showed also that the predictability for the side vent was high for uni-directional flows ($R^2 > 92\%$). Models for bi-directional flows showed a good correlation for flows at the windward side going in the same direction as the outside wind ($R^2 > 88\%$), but showed less good results for flows in vents at the leeward side and for flows going the opposite direction. For all models and wind directions, the perpendicular velocity component measured at the meteomast was the most important input variable. The importance of the parallel velocity component increased near the edges of the vent when the vent was at the windward side, but still did not reach the weight of the perpendicular component. Results confirmed the importance of different models for uni- and bi-directional flows in order to obtain accurate airflow rate assessments.

As stated earlier, the distribution in the vents was important for selecting optimal sampling locations to measure the airflow rate. This is important because simplification of airflow rate measurements is mostly effectuated by lowering sampling density.

Chapter 4 focuses on the application of different sampling densities for the direct measuring method and the tracer gas method in the naturally ventilated animal mock-

up building. Different sampling densities were applied for both the direct and the tracer gas method and again compared with the direct measurement method of Van Overbeke et al. (2016). The results obtained by the reference method indicated that using only sampling locations in the middle of the side openings overestimated the airflow rate. In view of wind variations, better accuracy, precision and lower coefficients of variation were obtained with a higher number of sampling locations. The coefficients of variation varied between 5% for the reference using 48 sampling locations and 29% using only one sampling location in the side outlet. In the ridge opening, only one middle sampling location was sufficient for an accuracy of $\pm 2\%$ and a precision of $\pm 3\%$ of the maximum value. The spatial pattern of sampling locations was also found to be very important resulting in different accuracies for a given sampling density. The indirect tracer gas method gave irregular results mainly attributed to non-perfectly homogeneously mixed tracer/air. These varying concentrations gave large confidence intervals resulting in non-significantly different measurement results between the different sampling strategies.

The detailed measuring method of Van Overbeke et al. (2016) could be used as a reference to find possibilities to reduce sampling methods to measure the airflow rate in an animal mock-up building without obstructed surroundings. **Chapter 5** aims to check whether conclusions to improve the feasibility of reducing sampling methods tested on the animal mock-up building could be applied on a naturally ventilated commercial animal house. Experiments took place in more complex surroundings with obstacles inside and outside the building and with varying curtain configurations. Also, installing a moving sensor for velocity sampling was not feasible in the large vents. Therefore, two experiments were performed using detailed measurements to obtain a vertical and horizontal velocity profile, respectively. The meteomast was still able to correlate velocities in the side vents using linear regression combined with the tangential and normal velocity wind component for fully opened curtain configurations (R^2 -values $>70\%$). Using wind screens weakened correlations. Also, the accuracy was tested of reduced sampling of the velocity profiles (horizontal and vertical) by comparing the reduced against the detailed measurements. It was found that differences remained under 20% (predefined criterion) provided that two requirements were fulfilled. Firstly, a normal velocity profile for cross ventilation at the outlet should be expected (the opposite vent not fully closed) and secondly, velocities in the openings had to be larger than 1 m/s. These requirements were only met for 15% of

the data of the full dataset. Predicting good wind conditions (vent velocity > 1 m/s) could only be possible after calibrating the vents with measurement in order to determine the velocity profiles for the different wind conditions. Finally, **chapter 6** offers a discussion of the results found within this thesis together with some future perspectives. Firstly, the achievements in the mock-up building were discussed and how the findings were applied in the commercial animal house. The development of a general reduced measurement technique was not feasible for direct measurements in the side vents of a commercial dairy house using local sampling points. Improvements to obtain a better view on the velocity distribution were suggested e.g. by applying the tomography technique. Conclusions on the uncertainties in measurements were also applicable for the CO₂ mass balance method and were also discussed. Additionally, the advantages of the use of mechanistic models combined with measurements closer to the emitting sources (e.g. floor and manure pit level) are discussed with regard to emission measurements. Finally, some considerations are suggested to increase representative processing of the measured data.

Samenvatting

Dit doctoraatsonderzoek bestudeerde de haalbaarheid van een gereduceerde meettechniek om het natuurlijk ventilatiedebiet in stallen te bepalen, gebruik makend van directe metingen in de openingen. De mogelijkheid om gebruik te maken van eenvoudige (regressie-) modellen om het staldebiet en de snelheidsdistributie door de openingen te bepalen, werd bestudeerd. Inzichten werden verworven over de accuraatheid en precisie van de debietsmetingen t.o.v. gereduceerde meetlocaties en variërende windomstandigheden.

Het ventilatiedebiet meten in natuurlijk geventileerde stallen is een uitdaging door sterk variërende windomstandigheden. Debietsmetingen zijn moeilijk uit te voeren door plaats- en tijdsafhankelijke variaties van de snelheidsdistributie in de opening en in het gebouw. Niettegenstaande de sterke nood aan een referentiemeetmethode, is er momenteel nog steeds geen onbetwistbare referentie beschikbaar.

Hoofdstuk 1 geeft achtergrondinformatie over het belang van de ontwikkeling van een accurate gereduceerde meetstrategie. Dit, in de context van dierenwelzijn en voor emissiemetingen die van belang zijn i.v.m. de NEC-richtlijn en de actuele PAS (Programmatische Aanpak Stikstof) dat kadert binnen het Natura 2000-programma in Vlaanderen. De meest voorkomende modellen en meetmethoden voor het bepalen van het debiet in natuurlijk geventileerde stallen worden weergegeven, samen met hun voor- en nadelen. Deze thesis zal echter voornamelijk focussen op directe meetmethoden in de ventilatieopeningen, gebruik makend van ultrasone anemometers. Regressiemodellen werden geselecteerd als modelvorm en toegepast om het debiet door de stal en de snelheidsdistributie in de openingen te bepalen. Hoofdstuk 1 beschrijft ook de stap-voor-stap aanpak naar een mogelijk gereduceerd meetprotocol. De ontwikkeling start bij de eerder ontwikkelde meetmethode van Van Overbeke et al. (2016). De laatstgenoemden ontwikkelden en valideerden een accurate meetmethode in een natuurlijk geventileerde testconstructie met nok- en zijopeningen. De meetmethode gebruikt directe snelheidsmetingen door toepassing van bewegende snelheidssensoren in de zijopeningen. Zodanig kon het snelheidsprofiel continu bemeten worden en werd een platform gecreëerd om debieten te meten met een relatieve fout van $8 \pm 5\%$. Deze meetfout bleef binnen de vooropgestelde 20% meetfout, dit voor het grootste deel van data gemeten onder sterk variërende meetomstandigheden. Deze techniek werd uniek bevonden omdat het de mogelijkheid biedt een gedetailleerde dataset te genereren om de accuraatheid van

gereduceerde meetmethoden te testen. Niettegenstaande de grote waarde, is vereenvoudiging van deze techniek toch noodzakelijk voor een meer praktische, tijdsgereduceerde en kostenefficiënte, voldoende accurate meetmethode.

Hoofdstuk 2 beschrijft de eerste stappen naar een gereduceerde meetstrategie door het ontwikkelen van een snelle, accurate en eenvoudig te gebruiken model voor het bepalen van het debiet in een testconstructie. De testconstructie bestaat uit een sectie van een varkensstal zoals regelmatig gebouwd in Vlaanderen indien natuurlijke ventilatie toegepast is. Deze snelle techniek om het debiet te bepalen, combineert lineaire regressie en lokale luchtsnelheidsmetingen gemeten aan een meteomast. Deze techniek werd vergeleken met gedetailleerde metingen bekomen door toepassing van de meettechniek van Van Overbeke et al. (2016). De totale windsnelheid $|\bar{U}|$, de snelheidsvector \bar{U} , de normaal- $|\bar{Y}|$ en tangentiële snelheidscomponent $|\bar{X}|$ gemeten aan de meteomast, werden geselecteerd als inputvariabelen voor de regressievergelijkingen. De debieten werden gesplitst afhankelijk van de aard van de wind: bidirectioneel (wind gaat tegelijk binnen- of buiten) of unidirectioneel (de wind gaat maar in één richting door de opening). De modellen voor debieten met unidirectionele luchtstromen leverde de meest accurate resultaten met inputvariabelen \bar{U} en $|\bar{Y}|$. Voor deze reden werd voorgesteld $|\bar{Y}|$ als input te gebruiken i.p.v. $|\bar{U}|$ in ASHRAE's formule $Q = E \times A \times |\bar{U}|$. Voor bi-directionele luchtstromen werd een lineair model voorgesteld waarbij input variabele \bar{U} de meest accurate debieten voorspelde. Dit hoofdstuk stelde met succes een eenvoudig te gebruiken vergelijking voor om het debiet te voorspellen gecombineerd met een sensor geïnstalleerd op een meteomast. Echter, om dergelijk model te bouwen is eerst een gedetailleerde kalibratie van het debiet door de openingen noodzakelijk.

Hoofdstuk 3 geeft inzichten in de snelheidsdistributie in de openingen van de testconstructie om een gereduceerde techniek te kunnen ontwikkelen. De snelheidsdistributie is belangrijk om verschillende redenen. Eerst en vooral, enkel door kennis van de snelheidsdistributie kunnen optimale meetlocaties voor een accurate debietsmeting geselecteerd worden. Ten tweede, bepaling van emissies door toepassing van het product van het verschil tussen concentraties van de binnen- en buitengaande lucht, en het debiet is een uitdaging: snel veranderende windomstandigheden veroorzaken plaats- en tijdsafhankelijke variaties in de snelheidsdistributie ter hoogte van de opening. Zodoende is kennis over de

snelheidsdistributie een eerste belangrijke stap naar een accuraat debiets- en emissiemeetmethode in natuurlijk geventileerde stallen. Om de voorspelbaarheid van de snelheidsdistributie in de openingen te bepalen, werd lineaire regressie toegepast tussen de snelheden in de openingen en snelheden gemeten aan de meteomast. Opnieuw werden de resultaten van de statistische modellen vergeleken met de gedetailleerde meetresultaten door toepassing van de meetmethode van Van Overbeke et al. (2016). Resultaten toonden aan dat met deze methode de snelheidsdistributie in de nok accuraat en precies kon bepaald worden ($R^2 > 89\%$). Modellen toonden ook aan dat de voorspelbaarheid van de snelheidsdistributie in de zijopeningen hoog was voor unidirectionele luchtstromen in de openingen ($R^2 > 92\%$). Voor de modellen met bidirectionele luchtstromen werd de beste correlatie gevonden voor luchtstromen in de opening aan de loefzijde die dezelfde richting hadden van de wind ($R^2 > 88\%$). Luchtstromen in de opening aan de lijzijde hadden minder goede resultaten, net als luchtstromen die de tegenovergestelde windrichting hadden van de buitenwind. De normaal windcomponent gemeten aan de meteomast, was voor alle modellen en windrichtingen de belangrijkste inputvariabele. Het belang van de parallelle windsnelheidscomponent verhoogde voor locaties dicht bij de rand van de opening aan de loefzijde, echter bleef de normaalcomponent steeds belangrijker. Resultaten bevestigden het belang van verschillende modellen voor uni- en bidirectionele luchtstromen om een accurate debietsbepaling uit te voeren.

Eerder werd reeds aangehaald dat snelheidsdistributie in de openingen belangrijk was voor selectie van de optimale meetlocaties om debietsmetingen uit te voeren. Dit is van belang omdat vereenvoudiging van de debietsmetingen voornamelijk uitgevoerd wordt door verlaging van de meetdichtheid. **Hoofdstuk 4** focust op de toepassing van verschillende meetdichtheden voor directe meetmethoden en de tracer gasmethode in een natuurlijk geventileerde testconstructie. Verschillende meetdichtheden werden toegepast op allebei de directe en de tracergas methode en vergeleken met de gedetailleerde meetmethode van Van Overbeke et al. (2016) als referentie. De resultaten verworven met de referentiemethode duiden aan dat het gebruik van enkel 1 meetlocatie in het midden van de zijopening de snelheid overschatte. Een verhoging van het aantal meetsensoren verbeterde de accuraatheid en precisie t.o.v. de windvariaties. De variatiecoëfficiënt varieerde aan de uitlaat tussen 5% voor de referentie (48 meetlocaties) en 29% bij gebruik van 1 meetlocatie. In de nok was enkel 1 meetlocatie voldoende voor een nauwkeurigheid door afwijking van enkel $\pm 2\%$ en

een precisie van $\pm 3\%$ t.o.v. van de meetwaarde. Het patroon van de meetlocaties werd ook belangrijk gevonden. Verschillende patronen resulteerden in verschillende meetaccuraatheid voor eenzelfde hoeveelheid sensoren. De indirecte tracergasmethode gaf onregelmatige resultaten voornamelijk toegeschreven aan een niet perfect homogene mixing van de tracer en de lucht. Deze variërende concentraties gaven hoge betrouwbaarheidsintervallen die resulteerden in niet significant verschillende meetresultaten tussen de verschillende meetstrategieën.

De gedetailleerde meetmethode van Van Overbeke et al. (2016) kon gebruikt worden als referentie om verschillende mogelijkheden te bestuderen om debietsmeetmethoden in natuurlijk geventileerde testconstructie te reduceren. Echter waren geen obstructies aanwezig in de omgeving van de testconstructie. **Hoofdstuk 5** heeft o.a. als doel om na te gaan of de conclusies om de debietsmethode te reduceren uit de vorige hoofdstukken kunnen worden toegepast op een semi-commerciële melkveestal. Experimenten werden uitgevoerd in een meer complexe omgeving met interne en externe obstructies in de melkveestal en variërende gordijnconfiguraties. Installatie van een bewegende sensor was niet realiseerbaar in de grote openingen. Daarom werden 2 experimenten uitgevoerd waarbij ultrasone sensoren gedetailleerd meten ter hoogte van horizontale en verticale lijnen. De snelheden in de openingen konden nog steeds goed lineair gecorreleerd worden met de tangentiële en normale snelheidscomponent gemeten aan de meteomast. De R^2 -waarden waren $>70\%$ voor open gordijnstanden en verlaagden als gordijnen toegepast werden. Ook de accurateheid van gereduceerde metingen voor de (horizontale en verticale) snelheidsprofielen werden getest door vergelijking met de gedetailleerde metingen. Relatieve verschillen bleven onder de vooropgestelde meetfout van 20% indien aan 2 voorwaarden werden voldaan. Ten eerste moet een normaal windprofiel verwacht worden (het tegenoverstelde gordijn mocht niet volledig dicht zijn) en ten tweede, de snelheden in de opening moeten groter zijn dan 1 m/s . Aan deze vereisten werd enkel voldaan voor 16% van de volledige dataset. Het voorspellen van goede windomstandigheden (voor snelheden in de opening $> 1 \text{ m/s}$) kan enkel mogelijk zijn na een voorafgaande kalibratie van het snelheidsprofiel in de opening, door gebruik te maken van de voorgestelde correlaties.

Tenslotte biedt **hoofdstuk 6** een discussie aan van de gevonden resultaten binnen dit onderzoek samen met enkele toekomstige perspectieven. Eerst worden de verwezenlijkingen besproken uit de experimenten in de testconstructie en hoe de

bevindingen werden toegepast in de melkveestal. Het werd niet haalbaar geacht om een algemene gereduceerde meettechniek te ontwikkelen met gebruik van lokale meetlocaties in de zijopeningen van een semi-commerciële melkveestal. Verbeteringen a.d.h.v. tomografie werden voorgesteld om een betere meting te kunnen uitvoeren om de snelheidsdistributie in de opening vast te stellen. De conclusies voor de directe meetmethode uit deze studie waren ook van toepassing op de CO_2 massabalans methode en werden ook besproken. Ook werden de voordelen van het gebruik van mechanistische modellen besproken gecombineerd met metingen dicht bij emitterende oppervlakken. Ten laatste werden sommige overwegingen aangegeven om een meer representatieve verwerkingen van de meetdata mogelijk te maken;

1

Introduction

This work focuses on the development of reduced measuring strategies to assess the ventilation rate in naturally ventilated animal houses. To have a background on why (reduced) measuring the airflow rate is important, the introduction will expand on the importance of the indoor climate in animal houses. Further, more extra information is given on how the airflow rate is mostly assessed using measurement and modelling techniques. This chapter ends with the problem statement, overall objective and a thesis outline.

1.1 Importance of the indoor climate

1.1.1 Ventilating livestock buildings

A well-designed ventilation system is essential to ensure optimal animal production in agricultural buildings (Bartzanas et al., 2007). This, because animal welfare is strongly related to the quality of the air in animal houses (Algers et al., 2007). Ventilation controls the indoor air quality by replacing the air in an enclosed space (Khan et al., 2008) and thereby removes odours, dust, airborne bacteria, etc. Ventilation provides sufficient oxygen (Bartzanas et al., 2007) and makes sure there is no accumulation of hazardous gases that impacts the health of animals and humans (Calvet et al., 2014). For livestock and humans (care takers), these hazardous gases are mainly ammonia NH_3 and carbon dioxide CO_2 (Bartzanas et al., 2007).

Control of the ventilation rate, the volumetric flow rate of outside air that is introduced into the building, can be based on the indoor temperature, humidity, and/or the level of carbon dioxide CO_2 (Shen et al., 2016) and to control the level of other gases as e.g. NH_3 and CH_4 . A minimal ventilation rate is required for health reasons (Bruce, 1978) as it reduces risks of respiratory diseases (Kiwani et al., 2013; Saha et al., 2013). For a minimal ventilation, it is required to control the maximum level of CO_2 or humidity. This minimal airflow rate is derived from the CO_2 mass balance. The maximum capacity of the ventilation rate is derived from the heat balance. A maximal ventilation rate is important to limit investment costs of fans on hot summer days with low temperature differences between the in- and outside of the barn. It is not only the air exchange rate of the airflow that is important, but also the air distribution in the building

that has a great influence on providing optimal conditions for animals and humans (Bartzanas et al., 2007). Also, the air distribution is important to protect animals of exposition to high velocities under windy conditions (Morsing et al., 2002).

1.1.2 **Efficient ventilation towards emission control**

Beside controlling the quality of the indoor air, airflow (rate) assessment is also important to estimate the emissions of hazardous gases as e.g. NH_3 and CH_4 from the buildings. Measuring emissions has gained in importance since the awareness to the effect of NH_3 on the environment increased. These gases, mainly NH_3 , not only affect the animals inside the building, but also the outdoor environment after emission. Gases such as methane CH_4 and nitrous oxide N_2O (CIGR, 2010) contribute significantly to global greenhouse gas emissions (Jacobson et al., 2008) which affect climate change (Barrancos et al., 2013). Other atmospheric pollutants as NO_2 , SO_2 and especially NH_3 , as one of the major pollutants (Ulens et al., 2015), are associated with acidification of soils and eutrophication of ecosystems (Bluteau et al., 2009). Ammonia is mainly the result of conversion of urea in urine, or uric acid but also of manure and feed for cattle (Angrecka et al., 2014). The ammonia emission process has many influencing factors as the activity of livestock (Saha et al., 2014), or the variability in N-feed conversion efficiency into animal products (Gay et al., 2004), the type of flooring and temperature of the building (Bjerg et al., 2013c) among others. Ventilation as well has a great influence on emissions (Morsing et al., 2008) since decreasing the air velocity and/or turbulence intensity over the ammonia emitting surface and decreasing the temperature can reduce NH_3 emission (Bleizgys et al., 2016). Therefore it is important to improve ventilation in the barn, and limit ventilation over the ammonia sources as especially the manure pit.

In recent years, several regulations have been issued to reduce emissions as e.g., the Kyoto Protocol, European Ceilings Directive (Calvet et al., 2014). This, due to accumulation of these gases in the environment and the concerns over the negative environmental impact from livestock farming, (Bjerg et al., 2013c; Loyon et al., 2015) These regulations may affect the design and operation of livestock buildings (Herrero et al., 2011) and the aspect of ventilation in animal housing. Due to the strong correlation of emissions and ventilation, it has become more important to control the

air distribution and the airflow rate. For example, to decrease ammonia emission by avoiding airflows over the manure surface in the pit, or to prevent cases of over-ventilation to minimise ammonia release without compromising indoor air conditions (Shen et al., 2016).

1.1.3 *Natural vs. mechanical ventilation*

Ventilation in barns can be mechanical or natural. Both systems have their advantages and disadvantages. Mechanical ventilation has the advantage to be more predictable (Rong et al., 2016). The combination of mechanical ventilation with an automatic control system can enhance control precision (Choi et al., 2010). Natural ventilation is potentially the most sustainable way to accomplish a proper indoor climate for production: its driving force is not mechanical, but considered to be mainly pressure differences due to thermal buoyancy and due to wind (Demmers et al., 2001). It has therefore lower primary investment costs (no expensive fans) and less energy costs, and the reduced noise level is another advantage for animals and farmers is.

The application of natural ventilation is still limited due to the lack of a reliable measuring and control technique for the ventilation rate. As a result of restricted control, natural ventilation is hardly applied anymore in intensive pig and poultry production in countries as Belgium and the Netherlands. However, since the oil crisis in the 1970s, natural ventilation is an intensive research field for development of the technique due to its potential energy savings and the complexity of natural ventilation systems (Rong et al., 2016). It is more difficult to determine airflow rates of naturally ventilated livestock buildings than of mechanically ventilated livestock buildings (Bjerg et al., 2013c; Wu et al., 2012a). Both methods differ considerably (Calvet et al., 2013; Rong et al. 2013). Errors for measured ventilation rates tend to be higher in naturally ventilated buildings (Rong et al., 2016) because they are more impacted by local weather conditions as wind velocity and wind incidence angle (Joo et al., 2015; Ngwabie et al., 2014). Other factors influencing the airflow rate and increasing measurement uncertainties are: building envelope geometry, presence of external architectural structures and size of opening surfaces (Cui et al., 2016), internal obstacles (Chu et al., 2013), surrounding buildings (López et al., 2011b) and others. Beside these factors, the airflow rate is also adapted by manipulating e.g. vent

arrangements (Bartzanas et al., 2004; Hoff, 2001) and the ventilation opening height (Brockett et al., 1987; Bruce, 1978). All these factors together are challenging for scientists and policy makers to measure the airflow rate with a sufficient reliability.

1.2 Assessing the airflow rate in naturally ventilated buildings

To gain knowledge for optimising ti and emission control, application of modelling and measuring techniques are necessary. For an optimal climate in the animal house, the design of the building is of primordial importance. Models can help expert designers making decisions to enhance the efficient use of the natural wind and buoyancy forces in the building. After the building is constructed, the ventilation of naturally ventilated buildings can only be adjusted by (automatic) control systems to adjust the ventilation opening size or possibly even the airflow pattern Van Overbeke et al. (2015b). A good control system can avoid under- or overventilation which also may influence emission rates. To aid these control systems, measurements of the air velocity, wind direction or temperature measured outside and/or inside can be of great importance. A good choice of location for these measurements is crucial for its representativeness to adequately control the indoor climate. Models can help finding the most optimal measurement location(s) (Shen et al., 2013). Multiple locations can be necessary depending on the complexity of a system, however these can make the model complex and expensive (Shen et al., 2013). Finally, measurements are also important to assess the emission rates for determining emission factors of animal housing systems and to gain knowledge on the efficiency of mitigation techniques. Assessing emission rates is currently extra challenging as measurement techniques should be able to detect emission changes in the range of percentages in commercial animal barns (Laubach et al., 2005).

The following paragraphs will provide an overview of the most important modelling and measurement techniques which are currently used for naturally ventilated animal houses. Thorough studies have been performed on the modelling and measuring of the airflow rates in naturally ventilated buildings. For further information is referred to the publications in the special issue of Biosystems Engineering: *Emissions from naturally ventilated livestock buildings* (Bjerg et al., 2013a, 2013b, 2013c; Ogink et al., 2013a).

1.2.1 *Measuring techniques*

Measuring the airflow rate in naturally ventilated buildings, especially with (very) large openings, is not straightforward. As stated in §1.1.3, the airflow rate is greatly influenced by wind conditions. Varying wind conditions are an important source of variability in the airflow rate. The measurement of the airflow rate is therefore characterised by uncertainties due to instability of meteorological conditions (Kiwani et al., 2013). Air movement is complicated by rapidly fluctuating pressure differences produced by buoyancy or wind (Lule et al., 2014). Measurements are even more complicated by interactions of considerable effects of wind speed, wind direction, temperature differences, air inlet and outlet constructions, as well as the roof inclination angle on the air movement inside the building or the surrounding topography (Takai et al., 2013b). Beside the instability of the wind changing over time during the experiments, measurements in large openings (the size of windows, doors or larger) are also complicated because of the non-uniform airflow distribution over the ventilation openings (Etheridge, 2012). Large spatial and temporal variations are expected in these type of vents (Mendes et al., 2015b; Ogink et al., 2013a). Additional problems for selecting sampling points can occur because the flow through the opening is not necessarily uni-directional: the opening can simultaneously act as an inlet and outlet (Etheridge, 2015).

All these factors have challenged the accurate measurement of the airflow rate due to the above mentioned potential error sources resulting in a high uncertainty. Calvet et al. (2013) believe that for many measurements a standard uncertainty of more than 50% is present and doubt that an uncertainty of less than 20% can be achieved. Until now, no reference technique exists to measure the airflow rate in naturally ventilated buildings, mainly due to problems with handling the spatial and temporal variations in the openings (Edouard et al., 2016; Kiwani et al., 2013; Ogink et al., 2013a). Notwithstanding the fact that there is no reference, different measurement techniques are available. However, due to the lack of a reference technique, it is not possible to determine the accuracy of these different measurement techniques. Without a reference, the evaluation of a method can be performed in two other ways Van Overbeke et al. (2015a): (1) by comparing different methods under the same conditions (Kiwani et al., 2013); (2) or by using a mass balance method. However, the selected

method could still fail to give the actual airflow rate if this method is also used to measure the in- and outflow. Similar errors could occur for both sides while applying equal methods (López et al., 2011a; Molina-Aiz et al., 2009). Therefore the choice and number of sampling locations is very important to obtain results that are representative of the actual airflow rate.

The suitability of a measurement technique depends on many factors (Joo et al., 2014). These factors can be the fulfillment of the assumptions to apply a technique, but also the aim of the measurements: indoor climate control or emission measurement. These two aims require a different approach because the optimal frequency of the measurements can differ. The measurement system will be installed permanently for control purposes and will need real-time measurements at least e.g. every few minutes (Van Overbeke et al., 2015a) or every 15 min. (Hoff, 2004) to react adequately to changing wind conditions (Shen et al., 2013). On the contrary, hourly, diurnal or daily measurements can be sufficient for emission measurements. Both aims also have different requirements concerning accuracy. The accuracy for measurements for controlling purposes can be different compared to the specific needs of the animals: cows have a larger tolerance for differences in ventilation than pigs. When measurements for the quantification of emission rates are performed, the element of bias is of special importance as it can be used for measuring yearly emissions, the efficiency of mitigation techniques or the draft of new, or the enforcement of existing legislation (Calvet et al., 2013; Van Overbeke, 2015a).

Many techniques exist for measuring the airflow rate in naturally ventilated full scale buildings (wind tunnel measurements are not discussed). The following paragraphs describe the (dis)advantages, uncertainties and the techniques itself for tracer gas tests, pressure difference methods and airflow velocity measurements respectively.

1.2.1.1 Tracer gas methods

Tracer gas methods use a natural or artificial tracer to measure the airflow rate indirectly. Three different methods exist to measure the airflow rate with tracer gas: the decay method (Bartzanas et al., 2007; Boulard et al., 1995), the constant injection method (Sandberg et al., 1985) and the constant concentration method (Sherman,

1989). For the decay method, a tracer gas is injected in the building. After injection, the decay rate in concentration is measured. For the constant concentration method, an initial gas rate is injected. This gas rate is continuously adjusted to maintain a constant concentration in the building. The airflow rate is estimated based on the injection rate of the tracer. For the constant injection method a known concentration of a tracer is injected at a constant rate, while the airflow rate is estimated by measuring the dilution of the tracer. The latter method is most frequently used in practice.

The tracer gas techniques can only be applied accurately when certain assumptions are fulfilled. These techniques require complete mixing of the air space and steady wind conditions (Kiwani et al., 2012; Wu et al., 2012a). These requirements limit their applicability in naturally ventilated buildings due to the spatial and temporal variations of the airflow (Joo et al., 2014). Other error sources or experimental design choices that influence error sources are: identification of the inlet and outlet, number of the sampling points, location of these sampling points, location of tracer injection points and how the tracer is released (Calvet et al., 2013). However, the release of the tracer can be conducted very accurately using critical orifices to keep the volume rate constant. The use of artificial tracers has its limits for long term measurements due to the amount of tracer necessary to release for the duration of the experiments (Joo et al., 2014).

This limitation could be overcome by using the natural tracer CO_2 , produced by the animals, named CO_2 balance method (Kim et al., 2008). However, modelling the release rate of CO_2 has its own uncertainties because the release of CO_2 depends on physiological changes (Samer et al., 2011b). Uncertainties can occur in e.g. assumption of emission of CO_2 from manure or calculation of the metabolic energy which varies as a function of animal weight, productivity and pregnancy.

The places and number of sampling locations are of primordial importance for tracer gas tests when sampling a reference mean tracer concentration and for sampling the background concentration. Ngwabie et al. (2009) found that multi-locations increased the representativeness of the results of the sampling points for short-term measurements. Many studies have already been executed to find the most representative location for the sampling locations in tracer gas tests. Van Buggenhout

et al. (2009) found that large differences could be found up to 86%, using single-point measurements, due to non-perfect mixing of the tracer in the air. He also found that the most representative sample was found near the outlet of the building with the best accuracy (less than 10% error). The sampling positions near the air outlets showed the lowest errors, which was confirmed by Demmers et al. (2000). Both experiments used highly controlled forced ventilation. In naturally ventilated dairy barns with large vents, the possibility of bi-directional flows in the (outlet) opening exists, which makes it difficult to provide in representative tracer sampling. (Zhang et al., 2010) found differences as much as 40% difference in the determination of the tracer concentration due to different sampling locations in naturally ventilated respiration rooms for cows. Errors over 200% were found by Lefcourt et al. (2002) due to the incorrect selection of sampling positions. (Wang et al., 2016) compared the CO_2 mass balance method against a direct measurement method and found no significant difference between the airflow rates over a time of 24h. Shorter periods measured (1, 2, and 12 h) resulted in significantly different airflow rates.

1.2.1.2 Pressure difference methods

Another approach to determine the airflow rate is to measure the pressure difference over an opening. It is a direct local measurement method based on determining the airflow rate by measuring the pressure difference over openings between the air inside and outside the building.

However, applying this technique is difficult due to a non-uniform distribution of the pressure differences over the opening in space and time (Joo et al., 2014; Ogink et al., 2013a). Also, the pressure differences in very large openings are low and difficult to measure. The measured airflow rates in and out through all openings in the building can fail to balance due to wrong assumptions because of a lack of knowledge of the discharge coefficients (Demmers et al., 2001). Calvet et al. (2013) stated that this method is less accurate than tracer gas tests and uncertainties probably exceed 50%. The method is not considered reliable to estimate the airflow rate (Ogink et al., 2013a).

1.2.1.3 Methods using direct velocity measurements

Air velocity measurements in the opening can be combined with the respective surface

area to determine the airflow rate. It is the most straightforward method to monitor airflow rates (Molina-Aiz et al., 2009). The choice of type of anemometer is important because the sensor should be able to determine the normal velocity to the opening in the vent, especially because the direction of the airflow changes depending on the outdoor wind conditions. Ultrasonic sensors can measure this normal velocity, and are robust and suitable for field measurements (Van Overbeke, 2015a). The main drawback of this method is the high variation of the velocity profile in the ventilation openings, which is important because a local velocity measurement should be able to represent the mean velocity of a predefined surface area of the opening. Uncertainties in airflow measurements in the vent are caused not only by the high spatial and temporal variations of the velocities in the opening, but also due to the choice of sampling locations. The difficulty of measuring the airflow rate with local measurement points is that the optimal sampling position(s) may change when curtain configurations or wind conditions change. Shen et al. (2012c) stated that it is therefore necessary to determine the sampling positions independent of the opening states and wind directions. Increasing the number of sampling locations may overcome this problem, because the more heterogeneous the velocity profile is, the more sensors will be needed to give a correct airflow rate (Ogink et al., 2013a). Joo et al. (2014) stated that the challenge of this method is not to compromise the accuracy by establishing the minimum number of sampling locations to obtain a reasonable cost. Bartzanas et al. (2007) confirmed that measuring velocities to predict the airflow rate is very expensive in terms of time and money.

To overcome measurement uncertainties due to spatial and temporal variability in the opening, Van Overbeke et al. (2016, 2015b, 2014a, 2014b) developed a detailed direct measurement method to determine natural ventilation rates in an animal mock-up building. This method, using a linear guiding system to scan the openings continuously with an ultrasonic anemometer was validated first under conditions of mechanical ventilation in a wind tunnel before testing and validating under outside weather conditions. The results showed a relative error between inflow and outflow of $(8 \pm 5)\%$ as an estimated bias. The detailed data generated by the experiments using this method, can be used to test the airflow rate on accuracy and precision when reducing the number of measuring locations (Van Overbeke, et al., 2014b). Joo et al. (2014) measured differences of 12% and 19% less for the air outflow rates compared to the

air inflow rates in two different barns, respectively. Wu et al. (2012a) performed a study to evaluate a method for determination of air exchange rates in a naturally ventilated dairy cattle building. They compared three measurement techniques and chose the direct measurement method as the reference to compare with, because it was the direct way to obtain ventilation rates.

1.2.2 *Modelling techniques*

When airflow rates through buildings are difficult or expensive to measure, applying models for airflow rate assessment can be a solution. Airflow rates in naturally ventilated buildings are influenced by many factors as wind conditions and surrounding obstacles. Therefore these models need to be very detailed with integration of the majority of influencing parameters or a less complex statistical model is applied combined with initial or limited measurements. A choice of modelling approach is to be decided on the purpose of the airflow rate determination as e.g. for design purposes or for emission measurements.

Many theoretical models, as the orifice equation, have been developed to assess the airflow rate in mechanically ventilated buildings. Although natural ventilation differs from mechanical ventilation, due to its higher dependency on changing weather conditions, models sometimes are applied assuming steady flow conditions (i.e. slowly varying conditions) (Etheridge, 2015). Modelling airflow rates of natural ventilated buildings is difficult. It involves unpredictable variables as the weather and the physical driving forces are complicated (Etheridge, 2012). The following parameters influence the airflow rate: wind velocity, wind direction, surroundings, unsteadiness of the wind, internal and external obstacles, heat production of the animals, radiation of the sun, type of vent openings, air leakage of the building, different zones in the building. The prediction of airflow rates in naturally ventilated buildings is difficult because of the involvement of a large number of variables, as mentioned earlier, and their interactions (Riffat, 1991). Also, specifying some of these parameters can be difficult due to uncertainty of determining or measuring their values.

A common practice is therefore to apply a degree of simplification within a model to

reduce the presentation of the complexness of the interaction of all influences of the natural airflow rate. Therefore, in the following paragraphs, models will be classified regarding the type of simplification or the amount of details known from the processes of the models. The terms black and white models, and the shades in between, are used to specify the knowledge of the model: the reference of a white box is used when all processes within the model are known, and a black box is used when no information is known. A grey model is used for models in between black and white models.

Similar to the measurement methods, the choice of the modelling approach of a white, grey or black box model depends on the purpose of assessing the airflow rate. The airflow pattern can be important for emission prevention to decrease the velocity over the ammonia surface, or for health control, to manipulate the airflow pattern to avoid direct high air velocities on animals. For control purposes, it can also be important to have a fast responding model to detect sudden changes of wind conditions. Another reason to choose a specific model is due to the available budget as e.g. *CFD* requires a large investment.

However, building a solid model is not the only challenge. Validation of this model against reliable data that represent the variations in weather conditions is one major challenge (Bjerg et al., 2013c). The focus of the short modelling review will lay on the ability to assess the airflow rates in a naturally ventilated building with large vents. Parallel, the (dis-) advantages of the detailed representation or the simplification of the processes in the model, will be discussed compared to the potential to obtain accurate results.

1.2.2.1 White box approaches

White box modelling has a structure fully based on physical, chemical and/or biological laws (like deterministic models) where no assumptions are made (Frausto et al., 2003). Few white models exist to describe the airflow rate, because when an assumption is made, the models will change to a grey model. Computational fluid mechanics (*CFD*) is close to a white model. It uses physical equations in a highly detailed way. *CFD* is a powerful tool that solves Navier-Stokes equations, which are based on treating the fluid as a continuum. This means that the properties (as e.g. the velocity) are determined

at several points. *CFD* can solve equations that arise in mathematical models of ventilation and cannot be solved analytically (Etheridge, 2012). It divides the zone of study into subzones and for each zone, the mass, momentum and energy conservation equations are solved (Rong et al., 2015).

CFD has already been applied for natural ventilation purposes. It is “a very powerful technique” in predicting air movement and airflow rates (Asfour et al., 2007). It has a great potential for the study of how airflow distribution and ventilation rate are influenced by the design of the housing and the surroundings (Bjerg et al., 2013a). However, the formulation of the equations and the associated assumptions and approximations are needed and can have an impact on the solutions obtained (Etheridge, 2012). Bartzanas et al. (2007) stated that one of the important aspects in *CFD* modelling is to choose a proper turbulence model. As a consequence, applications of characteristics for human occupancy and agricultural buildings are not necessarily the same in terms of scale because livestock buildings are typically large and single zoned (the building exists of one room) (Bjerg et al., 2013a). Norton et al. (2007) stated that in order to be able to design the required ventilation system correctly, it is necessary to understand the principles of air motion. However, the fact that assumptions are made for these configurations is the reason why *CFD*, by definition, is actually no white box model.

The method has been questioned by the challenge of the simplification of governing equations (continuity, momentum and energy equations) and definition of boundary conditions, necessary to be verified and validated with experimental results (Shen et al., 2013). Another disadvantage can be that the building of models is time-consuming and may not be cost-effective. Application of *CFD* for real-time or event-based solutions is difficult to perform. For example, for the ammonia release from full scale naturally ventilated livestock buildings (Bjerg et al., 2013b) as from the manure pit. Practically, applications like this would require very large computational capacity to develop and operate the model. An advantage of *CFD* is the ability to integrate spatial distribution in models, in contrast to lumped models.

The accuracy of *CFD* models depends on the requirements for implementation of the design of the model. The accuracy of applications of the building geometry and

surrounding environments (e.g. insect screens or curtains) are associated with the implementation by the modeller (Norton et al., 2007). They should reflect realistic conditions as accurately as possible (Bjerg et al., 2013a). The accuracy of the meteorological micro-scale is coupled strongly to the description of the flow regime and boundary layer conditions, by choices made by the modeller (Bjerg et al., 2013a; Norton et al., 2007). Also, as stated in the introduction of §1.2.2, building a solid model is not the only challenge. Validation of this model against reliable data that represent the variations in weather conditions is a major challenge (Bjerg et al., 2013c). Currently, *CFD* is mostly applied to improve design of ventilation systems and less to have a better understanding in the mechanisms involved in wind-induced cross ventilation through large openings in livestock buildings (Rong et al., 2016). However, *CFD* can be used in many ways. Wu et al. (2012a) performed a study to evaluate methods for determining air exchange rate in a naturally ventilated dairy cattle building with large openings using computational fluid dynamics. He validated the air exchange rate with CO_2 measurements, with a relative difference smaller than 5% between the tracer measurements and the *CFD* results.

1.2.2.2 Black box approaches

Black box models are purely data driven models. They describe what happens with a given input over a limited range: the range of data provided to the model. This implies that they are fully based on empiricism (Frausto et al., 2003). Examples of applications of black boxes are the use of artificial neural networks (*ANN*) (Faggianelli et al., 2015a; Kalogirou et al., 2003) and response surface methodology (*RSM*) (Ayata et al., 2007, Shen et al., 2012, 2013).

Black boxes have also been applied for modelling natural ventilation. Shen et al. (2012c) used the *RSM* modelling technique to optimise the selection of sampling positions. They found the most optimal sampling position close to the centre of the building at approximately 30% of the barn height. They also investigated the use of *RSM* to model the airflow rate in naturally ventilated buildings and found this technique to be effective. The response values of the experimental setups were calculated by *CFD* simulations (Shen et al., 2012a).

Artificial neural networks *ANN* can also be utilized as an efficient tool for learning, training and predicting indoor air velocity distributions for natural ventilation (Ayata et al., 2007). It has more flexibility in analysing natural ventilation modelling challenges compared to *CFD* (Asfour et al., 2007). *ANN* are information processing systems that can 'learn' a relationship between input and output variables by studying given data (Haykin, 2005). Through a process of 'learning' *ANN* are able to perform computations. *ANN* already proved to be efficient for assessing natural ventilation (Faggianelli et al., 2015a) or validation of numerical models (Nikolopoulos et al., 2012).

Advantages of black boxes are that they do not require explicit evaluation of coefficients or model formulations (Frausto et al., 2003) and they have a superior power compared to traditional approaches (Olden et al., 2002).

Disadvantages of black boxes are that they require a large amount of training data and they provide little explanatory insight into the influence of the variables in the prediction process (Olden et al., 2002). The latter can be a problem when knowledge of the relationship of the cause is of interest. Because network models learn from the environment (provided data), it is of primordial importance to feed the models with quality data to maintain accurate results. Therefore, prior measurements in the building are unavoidable. Another disadvantage of black boxes is that the modelling results should be limited to the boundaries of the used input data. Applying this data beyond these boundaries could result in unreliable output data.

1.2.2.3 Grey box approaches

Grey box models combine a theoretical structure, like physical properties, with data to complete the model. Because assumptions are integrated in almost all models, most of the models are grey boxes. These grey boxes are simplified models where easily available information can be utilised to improve the simplified models and so reduce the number of parameters to be identified. Advantages of grey models are the conservation of a physical meaning and a more simplified application of the method than for white boxes. It is a compromise between complexity and accuracy (Faggianelli et al., 2015b). The choice of degree of complexity ('shade of grey' box) depends on e.g. the application and number of parameters or the degree of assumptions made. In

practice, analytical models are only used for simple geometries and almost entirely for single-zone geometries (Zhai et al., 2015).

The empirical equation most commonly used to describe the airflow through an opening, is the orifice equation (or pressure coefficient method) based on Bernoulli's assumption of steady incompressible flow (Chu et al., 2014; Karava et al., 2004). The airflow rate is proportional to the square root of the pressure difference across the opening. These envelope flow models are commonly used in the design of naturally ventilated buildings. They are based on discharge coefficients. However, these values are obtained from laboratory tests under still-air conditions and may not be appropriate for measurements under real wind conditions with fluctuations (Chiu et al., 2007). Also, the underlying problem is that obtaining accurate measurements under known conditions is technically difficult, very time-consuming and expensive for full scale buildings (Etheridge, 2015). These empirical models are often proposed to calculate the airflow rate with a minimum of information. However, due to the parameters (discharge and pressure coefficients) that are difficult to evaluate, high uncertainties are present (Faggianelli et al., 2015b). Rong et al. (2016) and Zhai et al. (2015) stated that highest accuracy of these models is achieved for cases with small openings, Demmers et al. (2001) found overestimations of more than 50%. ASHRAE (2009) suggests a similar practical formula [1] including the opening effectiveness, to be used for large vents as well.

$$Q = EFF \times A \times V \quad [1]$$

Q = the airflow rate (m³/s)

EFF = the opening effectiveness of the ventilation opening (dimensionless)

A = representing surface area of the velocity component (m²)

V = reference velocity (m/s)

EFF values can be found in literature (ASHRAE, 2009) for different incidence angles of the wind or in an expression. Besides an absolute value, *EFF* is also presented as a function of other parameters as e.g. the wind incidence angle, ratio between height and length of the opening or the slope of the roof (Nääs et al., 1988).

Ogink et al. (2013a) stated that combining local measurements with modelling of airflow patterns in vents is how improvement for airflow rate assessment can be reached. Hempel et al. (2015) also stated that accurate assessment of the complex flow characteristics can only be achieved by combining measuring and modelling methodologies.

Bjerg et al. (2013b) argued that statistical modelling has the ability to document how the airflow rate is affected by easily determined parameters based on data. However, the concern is to collect reliable data for validation of the models that aim to predict the airflow rate (Bjerg et al., 2013b).

1.3 Problem statement

The airflow in naturally ventilated buildings and openings is characterized by a highly varying velocity distribution in time and space. At the moment, no reference method is available (Edouard et al., 2016), although the availability of a reference method is needed to ensure the quality climate control or for measurement reports. The latter, for scientists and engineers to understand the results and for policy makers to understand the data to make policy decisions (Calvet et al., 2013).

Measuring airflow rates in commercial livestock buildings is complex and time-consuming (Calvet et al., 2014) because it is difficult to find the optimal sampling locations due to changing wind conditions or application of different curtain configurations. Finding these optimal sampling location(s) is challenging and may decrease the large uncertainties which depend on the wind conditions (Shen et al., 2012b). Identification of these measurement uncertainties is important to improve the quality of the measurements (Calvet et al., 2013). At the moment, measurement uncertainties in approaches to measure the airflow rate with a strongly reduced number of anemometers in the openings (Joo et al., 2014) are not known because the methods are not tested against any reference method. However, a reference is necessary to know in how far measurements can be simplified without giving in on a predefined accuracy. Therefore, it is important to perform detailed experiments to measure the uncertainties (defining the accuracy) resulting from assessing the airflow rate with reduced strategies.

Calvet et al. (2010) stated that “identification of the uncertainty sources is the most effective way to enhance the quality in ventilation measurements”.

1.4 Overall objective and thesis outline

The focus of this PhD thesis lays on the reduction of the measurement techniques for natural ventilation in animal houses, especially in the context of determination of emission factors and mitigation efficiencies. The overall objective of this thesis is:

**Development of reduced measuring strategies in vents
to assess ventilation rates
in naturally ventilated animal houses**

The method of Van Overbeke et al. (2016) could be used to test the actual accuracy of reduced measuring strategies. The knowledge to reduce the complexity of measuring methods learned from the experiments in the mock-up building will be further applied and tested in a semi-commercial building.

The overall objective of this study was split in **five research questions**: three were examined in the animal mock-up building, two in a semi-commercial animal barn.

The main objective for the experiments in the mock-up building was to find a reduced measuring strategy for the natural ventilation rate. This, in the presence of the previously developed detailed measuring method, used as a reference for the airflow rate. **The research questions conducted in the animal mock-up building are:**

1. Is it possible to find an easy to use correlation between the airflow rate through the building and the velocities measured at the meteomast, taking into account uni- and bi-directional airflow rates?
2. Is it possible to predict the airflow rate distribution in the vents using the velocities measured at the meteomast?

3. Is it possible to measure the airflow rate in the vents with a reduced number of sampling locations maintaining an accuracy of $\pm 20\%$?

Similarly to the mock-up building, the aim for the semi-commercial animal barn was to find a reduced measuring strategy for the natural airflow rate. However, because the number of sensors was limited compared to the dimensions of the vents, the results of the experiments were used as a proof of principle.

The research questions conducted in the semi-commercial animal barn were:

4. Can the correlations as found in the mock-up building still give accurate results in the animal barn taking into account many extra factors as e.g. the presence of animals and surrounding buildings?
5. Is it possible to measure velocity profiles in the vents with a reduced number of sampling locations maintaining an accuracy of $\pm 20\%$?

A fast, accurate and simple to use airflow rate model for the animal mock-up building is developed in chapter 2. A fast algorithm is combined with local air velocity measurements collected on a meteoromast. The assessment technique is tested for airflow rates of both uni- and bi-directional flows occurring in the side opening and evaluated to the commonly used formula of ASHRAE. Artificial Neural Networks (*ANN*) are applied to evaluate the input variables before applying linear algorithms in order to find existing correlations. The algorithms are validated against detailed airflow rates obtained by the measuring method of Van Overbeke et al. used as a reference.

Chapter 3 offers a study to assess the predictability of the airflow rate distribution over the vents of a naturally ventilated building. This is done by detailed sampling of the air velocities in the vents and by statistically modelling all in and outgoing airflow rates through the ridge and side vents of a naturally ventilated animal mock-up building. The spatial and temporal distribution of uni- and bi-directional airflow rates are analysed.

In **chapter 4**, a study is performed to determine the effects of the sampling density on

the uncertainty of airflow rate measurements in a naturally ventilated animal mock-up building. Both a direct measurement method using anemometers and a tracer gas method are compared against the reference method of Van Overbeke et al. (2016).

The multiple linear regressions (as found in chapter 2 and 3), are applied to correlate the velocities in the vents with the velocity components at the meteoromast in **chapter 5**. In this chapter, the experimental conditions are not only focused on different wind conditions, normal practice activity happened during the experiments and different screen positions were applied.

The ultimate goal was to find whether it is possible to measure the airflow rate in the vents of the animal barn with a reduced number of measurement locations. However, because the side vent dimensions are over 70 m width and 4 m height, it is chosen to focus on assessing the horizontal and vertical velocity profile in the vent in anticipation of the airflow rate. Again, the experiments in the side and ridge vent are performed under different wind conditions, using different screen positions.

Chapter 6 offers a discussion and final considerations and conclusions, besides discussing future perspectives.

2 Experiments in an animal mock-up building: assessing airflow rates*

*Adapted from De Vogeleer G., Van Overbeke P., Brusselman E., Mendes L.B., Pieters J.G., Demeyer (2016) P. Assessing airflow rates of a naturally ventilated animal mock-up building using a fast and simple algorithm supported by local air velocity measurements. *Building and Environment*. 10.1016/j.buildenv.2016.05.006.

Van Overbeke et al. (2016) developed an accurate technique for airflow rate measurements in a naturally ventilated animal mock-up building. Chapter 2 focuses on developing a reduced sampling strategy for easy airflow rate prediction. The first challenge in this chapter was to handle occurrence of both uni- and bi-directional airflow rates, where airflows enter and/or leave a vent simultaneously. The second challenge was to find a simple algorithm that was still able to predict the airflow rate with high precision. Artificial neural networks were applied to evaluate the input variables for regression. Also, proposed models were compared to the commonly used formula of ASHRAE to calculate the airflow rate.

2.1 Introduction

An accurate assessment of ventilation rates of animal houses is important with regard to, among others, the quantification of the related emissions. However, measuring ventilation rates in commercial animal houses is difficult in practice, due to significant uncertainties in measurements (Calvet et al., 2010).

Currently there is no standardized reference method available for measuring the ventilation rate in naturally ventilated animal housing (Özcan et al., 2009).

Van Overbeke et al. (2015a) developed and validated an accurate measuring method for the airflow rate of a naturally ventilated animal mock-up building with continuous direct velocity measurements using moving sensors (more details are given in §2.2.2.2). However, simplification is still necessary to achieve a more practical, time-reduced, low-cost and yet sufficiently accurate method. Combining modelling techniques with local air velocity measurements could be of interest to develop such a method (Calvet et al., 2013; Ogink et al., 2013a; Takai et al., 2013a). Additionally, the aim is to simplify and speed up the assessment of the ventilation rate and to result in real time determination of the ventilation rate. In this respect, the method of Van Overbeke et al. (2015a) can serve as an excellent starting point since it provides detailed information on the velocity profiles in the vents.

The conventional envelope model that describes how the air enters and leaves a building, is the Bernoulli equation as a simplification of the Navier-Stokes equations.

This so-called 'orifice equation' [2] is the most general relation describing the airflow rate through large intentional openings (Chu et al., 2010; Etheridge, 2012; Karava et al., 2011; Karava et al., 2004). It is written as:

$$Q = C_D \times A \times \sqrt{\frac{2 \times |\Delta Pr|}{\rho}} \quad [2]$$

Where

- Q = Airflow rate (m³/s)
- C_D = Still-air discharge component (dimensionless)
- A = Surface area of the opening (m²)
- ΔPr = Pressure difference across the opening (Pa)
- ρ = Air density (kg/m³)

This equation applies a still-air discharge coefficient for a typical small opening but it fails for large openings as the main assumptions are not fulfilled (e.g. pressure and velocity distributions are not constant in the opening (Heiselberg et al., 2004) and changes in weather conditions can cause unsteadiness for measuring or estimating the parameters in the formula (Heiselberg, 2006; Nääs et al., 1988). On top of these difficulties, (very) large openings (as typically found in dairy cow houses) would make it even more challenging to sample air volumes using the orifice equation due to the increased probability of bi-directional flows (Q_{bi}) in the openings where opposite directions of air velocities normal to the opening are present. This possibility for bi-directionality makes it also difficult to couple (ammonia) concentration measurements to velocity measurements to obtain emission values. Models for airflow rates with uni-directional flows (Q_{uni}) in vent openings give less accurate results when applied to bi-directional flows (Calvet et al., 2013; Etheridge, 2012). Also, measurement methods as e.g. tracer gas tests commonly used in mechanically (Cui et al., 2015) and naturally ventilated constructions (Belleri et al., 2014; Chao et al., 2004; Demmers et al., 2000; Samer et al., 2012), perform poorly in accuracy and precision under naturally ventilated circumstances (Calvet et al., 2013; Etheridge, 2012) due to variations in airflow rate and concentration of the tracer.

Etheridge (2012) expressed the airflow rate (Q_{uni}) r very large openings in a formula [1] in non-dimensional terms.

$$\frac{Q}{A \times V} = f(\phi) \quad [1]$$

Where

V = reference velocity (m/s)

f = ventilation function

ϕ = wind direction

ASHRAE (2009) suggests a similar practical formula [2] including the opening effectiveness.

$$Q = EFF \times A \times V \quad [2]$$

EFF = the opening effectiveness of the ventilation opening (dimensionless)

Different values for EFF are given depending on the wind incidence angle to the opening. For perpendicular winds it varies between 0.5 to 0.6 and for winds diagonal to the ventilation opening between 0.25 and 0.35 (ASHRAE, 2009).

Many studies were found for field measurements presenting linear fits between the airflow rate and the total velocity, for greenhouses (Campen et al., 2003), between the airflow rate and perpendicular velocity component, for dairy barns (Joo et al., 2014) and multi-zone test building (Lo et al., 2012). These references show that a considerable amount of information has been found in the peer reviewed literature assessing natural ventilation with simple statistical correlations, but it is not always clear which input variables result in the most accurate airflow rates, or which statistical correlation to use for airflow rates with bi-directional flows. Especially there is little information in the literature on the accuracy of the respective proposed models. Of course this is not unexpected because of the lack of a reference method for airflow rate measurements. In order to estimate the accuracy of a model, some studies (Boulard et al., 1996; Chu et al., 2014) based the reference airflow rate on pressure differences in the opening. However the uncertainty is high due to large fluctuations relative to the low measured pressure difference over large vents. Therefore, it cannot be used in the formula of uni-directional airflow rates. When direct measurements are carried out, single measurements are mostly assumed to represent the mean velocity for a large surface area in the opening, usually without prior calibration of the single

velocity measurement to the mean velocity of the represented area. For these experiments without calibration, it is possible to calculate the precision of the method used, but not the accuracy of the method. Because the method of Van Overbeke et al. (2015a) scans the surface area with an ultrasonic anemometer moving step-by-step in the opening, it creates the opportunity to find a better estimation of the real airflow rates and thus the accuracy and precision of a simplified method where limited velocity measurements are used.

The objective of this chapter was to develop a fast, accurate and simple to use airflow rate assessment technique for a naturally ventilated animal mock-up building combining a fast statistical correlation with a limited number of air velocity measurements collected on a meteoromast. The assessment technique is tested for airflow rates of both uni- or bi-directional flows occurring in the side opening evaluated to the commonly used formula of ASHRAE to calculate the airflow rate. Artificial neural networks were applied to evaluate the input variables before applying linear correlations in order to find existing correlations. The statistical correlations were validated by comparison to detailed airflow rates obtained by the measuring method of Van Overbeke et al. (2015b, 2014a, 2014b) as a reference.

2.2 Materials and Methods

2.2.1 *Animal mock-up building and instrumentation*

The animal mock-up building was situated on a site of the Institute for Agricultural and Fisheries Research in Merelbeke, Belgium (+50° 58' 38.56" N, +3° 46' 45.68" E; A on Figure 1). The building was located in a rural area and was oriented such that the side openings faced *NE* and *SW*, the latter being the dominant wind direction in Flanders.

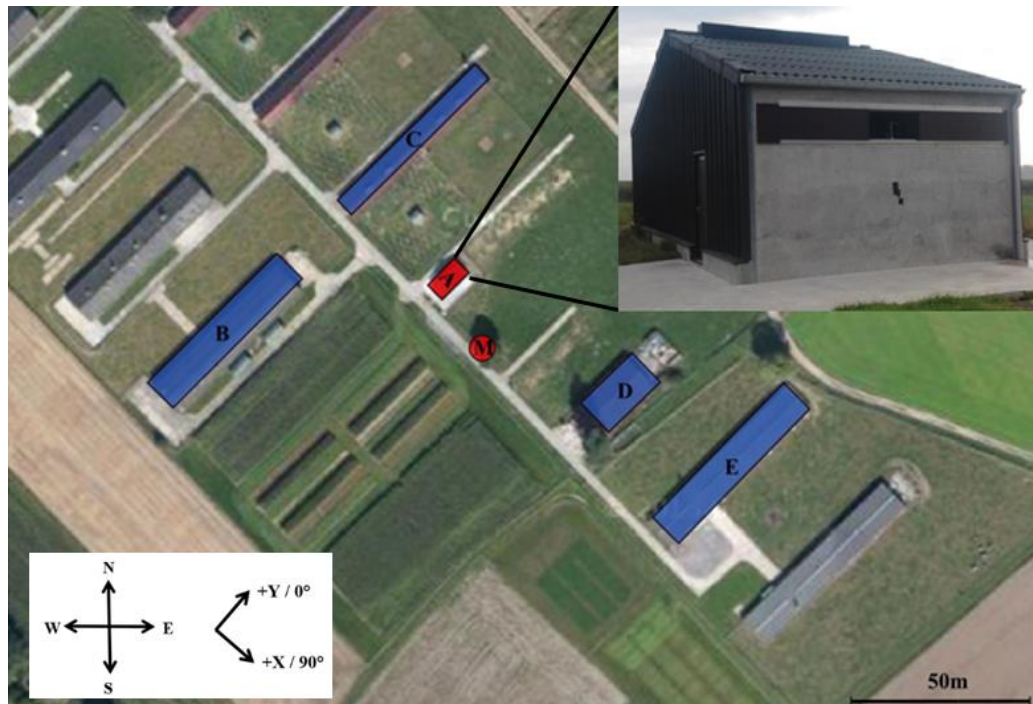


Figure 1: Site and building of the experimental set-up. The surrounding buildings were located at a distance of 50m from the animal mock-up building. (A) animal mock-up building (B-C-D-E) neighbouring buildings (M) meteomast

The animal mock-up building represented a section of a naturally ventilated pig house as commonly found in Flanders (Belgium). The internal dimensions of the animal mock-up building were 12.0 m length, 5.4 m width and 4.9 m ridge height. Its internal volume was 251 m³ (Figure 2). The two opposite concrete sidewalls had a ventilation opening adjusted with metal plates from 4.5 m to 3.0 m and had a height and depth of 0.5 m and 0.2 m, respectively. The ridge vent was 4.0 m by 0.35 m and could be closed and sealed when desired. A door and a gate were present in the animal mock-up building. They were always kept closed during the experiments.

A meteomast equipped with a 2D ultrasonic anemometer (Thies®, Göttingen, Germany) was installed to measure the wind velocity components (tangential component $|\bar{X}|$ - and normal component $|\bar{Y}|$ to the ventilation opening), wind direction and temperature with a frequency of 1Hz, at a standard height of 10m above field level (5 m above the top of the animal mock-up building). In the animal mock-up building, eight 2D and two 3D ultrasonic sensors (Thies®, Göttingen, Germany) were installed. Each of the two side openings was equipped with a 3D ultrasonic sensor installed on a 2D-linear guiding system (Figure 2), that transported the sensor to pre-set places

across the window openings where air velocities were automatically scanned following the sampling strategy developed by Van Overbeke et al. (2015a). The ridge vent was equipped with eight 2D ultrasonic sensors equally distributed along the opening (the second sensor starting from the NW, malfunctioned during the experiment). Velocity and temperature were measured at a frequency of 50Hz and 33Hz for the 2D and 3D sensors, respectively, and stored as 1s averages in a central logger (dataTaker® DT85M, Australia) via a serial interface (RS422).

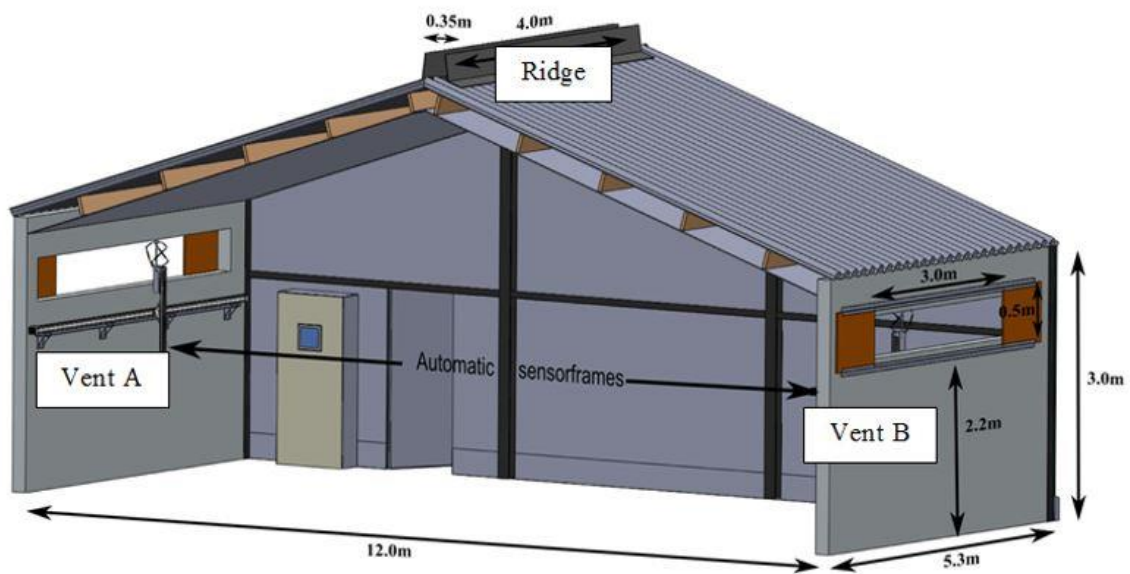


Figure 2: A 3D sketch of the animal mock-up building at the Institute for Agricultural and Fisheries Research in Merelbeke

The measurement system described above was activated for continuous monitoring, day and night over several months (December 2014 through March 2015) in order to cover a wide range of outdoor wind conditions.

The design of the animal mock-up building was almost completely symmetrical, except for the placement of the (closed) doors and the central electrical unit (with the wiring, datalogger, soft- and hardware).

2.2.2 Data Collection and Model Development Methods

2.2.2.1 General approach

Detailed airflow rate calculations were executed using the method of Van Overbeke et al. (2014a, 2014b, 2015), as described in detail in section 2.2.2.2. Data was collected for different experimental setups during periods of variable outside weather conditions. Different input variables were tested for their appropriateness using Artificial Neural Networks (ANN), which are able to detect (non-) linear correlations easily. Depending on the results of the ANN, the input variables were selected for further processing and used within a linear correlation to determine the airflow rates. Finally, methods for analysing the results, regression analysis and Bland Altman analysis were described. These methods will be described in more detail in the next paragraphs and is presented in Figure 3. All data processing, filtering, ANN and statistical analyses mentioned in this study were performed using the software Matlab ® R2013a.

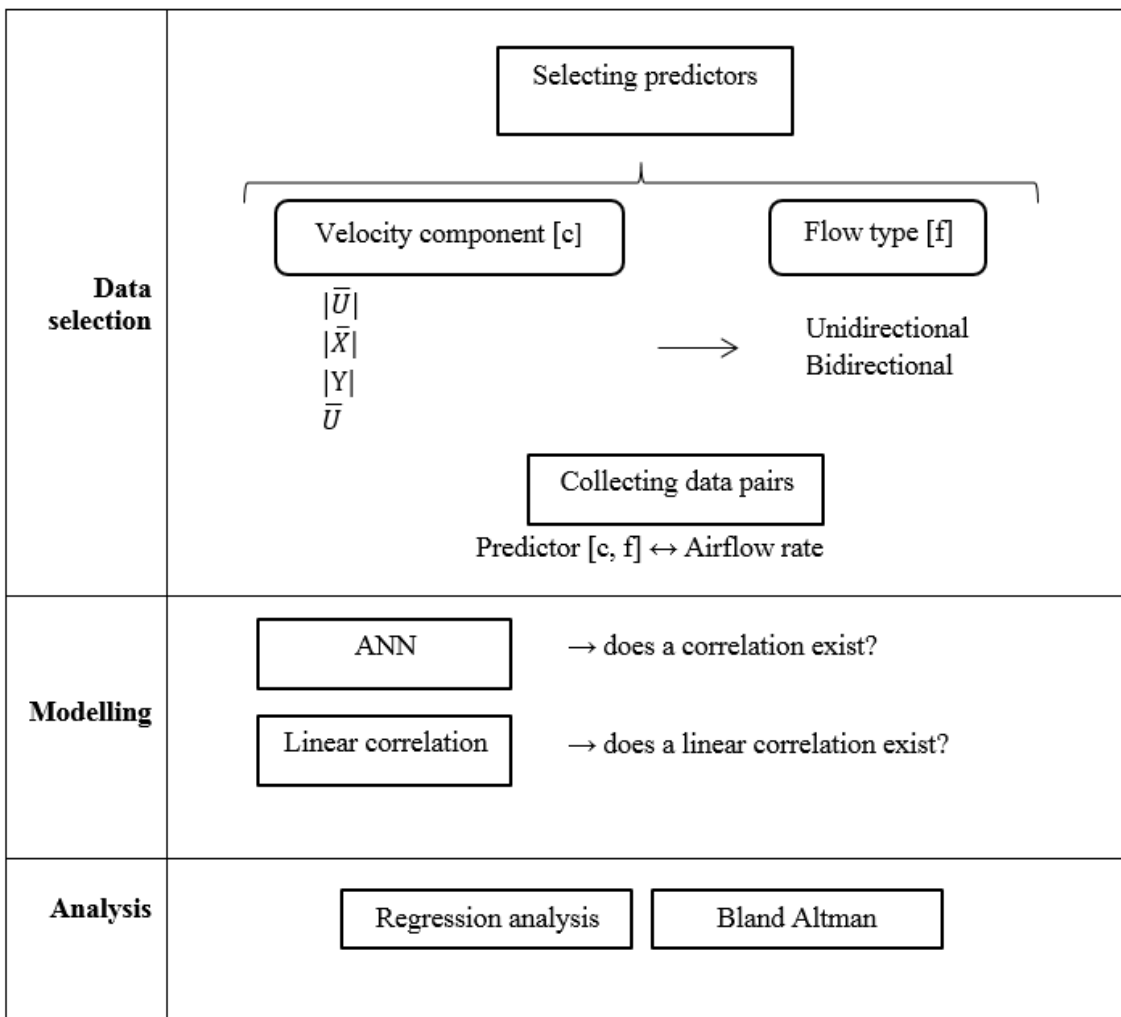


Figure 3: schematic presentation of the general approach to find simple statistical correlations for the airflow rate in the mock-up building

2.2.2.2 Reference airflow rate measurements

Detailed airflow rate measurements were conducted in the animal mock-up building, using the method proposed by Van Overbeke et al. (2015a) with moving sensors for the side vents and a method with fixed sensors to sample the ridge vent.

Air velocities were measured in the side vents by a moving sensor in each side opening. The spatial variation of the airflow pattern in the side openings was measured by sampling the full surface of the opening, divided in 48 measurement places. Every measuring place was sampled for 10×1 s before moving to the next sampling place. When all 48 places were sampled, the sensor started a new measuring round. To measure the total airflow rate, ten measuring rounds were repeated. The air velocity per measuring place was calculated by taking the mean of the 10 rounds of 10×1 s. All these measured mean air velocities were used to calculate the airflow rate with formula [3]. The measurement of one unique airflow rate took 1h and 40 min which was further referred to as approximately 1.5 h. The temporal variation of the airflow pattern was minimized because of this averaging over 1.5h. The temporal variation of velocity at the sampling locations was logged semi-continuously by the moving sensors. Furthermore, the metemast continuously logged the actual wind conditions in order to account for temporal variations over the full length of the measurements. For each replicate of scanning the opening (48 measuring places, each 10 min approximately), a new moving average of the total airflow rates could be calculated. One of the major advantages of the method was that it was able to measure the full airflow rate pattern, so that when bi-directionality occurred, this could be quantified in detail.

The velocities in the ridge vent were measured by eight fixed sensors (equally spread over the length; one sensor failed during the measurements). The mean velocities were calculated over the same period, 1.5 h, as the velocities in the openings. Every time a new measuring round started for the sensor in the side opening (approximately every 15 min.), a moving average was calculated in the ridge opening.

The principle to calculate the airflow rate was the same for the side and the ridge openings. The partial airflow rates through equal areas or partitions (A_k) in the window opening were summed to form the total airflow rate (Q_{tot}) [3]. The partial airflows were obtained by multiplying the locally measured perpendicular air velocity component $|\overline{Y_{ms}}|$ with the partial opening area (A_k). The airflow rate results of this method were used as a reference to compare the airflow rates resulting from the application of the simplified statistical correlations.

$$Q_{tot} = \sum_{k=1}^n (|\overline{Y_{ms}}|_k \times A_k \times 3600) \quad [3]$$

Where:

Q_{tot} = mean airflow rate through the mock-up building over a period of approximately 1.5h (m^3/h)

k = sampling location

$|\overline{Y_{ms}}|_k$ = mean perpendicular air velocity over a period of approximately 1.5h in measurement surface k (m/s)

A_k = surface area of sampling location k (m^2)

n = total number of surfaces in de side or ridge vents

2.2.2.3 Preliminary data analysis

Different velocity components were tested to use as input variables to determine the airflow rate. These input variables were the perpendicular $|\overline{Y_{MM}}|$ and parallel $|\overline{X_{MM}}|$ component, the total velocity $|\overline{U_{MM}}|$ and the velocity vector $\overline{U_{MM}}$ (that represents both $|\overline{X_{MM}}|$ and $|\overline{Y_{MM}}|$) all measured at the meteomast. Because an ultrasonic 2D anemometer was used, the $|\overline{X_{MM}}|$ -, $|\overline{Y_{MM}}|$ -component and $\overline{U_{MM}}$ were immediately available, the $|\overline{U_{MM}}|$ was derived from the measurements as in formula [4].

$$|\overline{U_{MM}}| = \sqrt{|\overline{X_{MM}}|^2 + |\overline{Y_{MM}}|^2} \quad [4]$$

$|\overline{U_{MM}}|$ = total velocity measured at the meteomast (m/s)

$|\overline{Y_{MM}}|$ = normal wind velocity component measured at the meteomast (m/s)

$|\overline{X_{MM}}|$ = parallel wind velocity component measured at the meteomast (m/s)

Previous research showed that models for airflow rates with uni-directional flows gave less accurate results when applied to bi-directional flows (Calvet et al., 2013;

Etheridge, 2012). For this reason, the data was split in a group where bi-directional flows and a group where only uni-directional flows occurred. The flow pattern of the data set was categorized as bi-directional when at least one normal velocity component in the side opening had a different sign (opposite direction) compared to the other normal components in the same opening. To rule out the effect of variations or short term fluctuations in the opening, only the mean velocity and not the separate measurements were taken into account to evaluate the bi-directionality in the openings.

Before applying a simple statistical correlation, Artificial Neural Networks (*ANN*) were used to extract or identify the most promising input variables. *ANN* are information processing systems that can 'learn' a relationship between input and output variables by studying given data (Haykin, 2005). Overall, the evaluation of the network results indicated that the *ANN* approach can be utilized as an efficient tool for learning, training and predicting indoor air velocity distributions for natural ventilation (Ayata et al., 2007). *ANN* already proved to be efficient for assessing natural ventilation (Faggianelli et al., 2015a). The work flow for the neural network has seven primary steps: collect data, create the network, configure the network, initialise weights and biases, and at last train, validate and use the network. This model placed the neurons in several layers. The first and last layers represent input and output, respectively. The output layer gives the results that are evaluated by the network. The most common model used for function fitting problems is the feedforward model (Haykin, 2005) where the input information only moves in one direction (from input nodes to hidden and output nodes). This was used with this research. The dataset was split in 70% training, 15% testing and 15% validation data. For every input variable, 8 different networks were tested. This was performed with different iterations of an *ANN*-script generated from the Matlab *ANN*-toolbox. The iterations differed from each other by different properties of the learning rate, the amount of neurons or the momentum rate.

The different input variables of the wind velocities $|\overline{U_{MM}}|$, $|\overline{Y_{MM}}|$, $|\overline{X_{MM}}|$ and $\overline{U_{MM}}$ were used as inputs for the network. The reference airflow rates of the barn, obtained using the method of Van Overbeke et al. (2015a) and calculated with formula [4], were introduced as targets for the model. The evaluation of the network results were based on R^2 -values. *ANN* were only used to establish whether a strong correlation existed

between the input variables and the airflow rates and to make a further selection of potential predictors of the airflow rates.

2.2.2.4 Simple statistical correlations

After testing the correlations with *ANN*, (multiple) linear regression modelling was applied to find fast and simple correlations to assess the airflow rates for uni- and bi-directional flows. The airflow rate was used as the dependent variable and the candidate input variables as the independent variables. Simple linear regression [5] was applied to assess the airflow rate Q_{tot} with respective input variables $|\overline{U_{MM}}|$, $|\overline{Y_{MM}}|$ and $|\overline{X_{MM}}|$. Multiple linear regression [6] was used when $\overline{U_{MM}}$ was implemented.

$$Q_{tot}(x) = j_1 \times x_1 + c + \varepsilon \quad [5]$$

$$Q_{tot}(x) = j_1 \times x_1 + j_2 \times x_2 + c + \varepsilon \quad [6]$$

where:

- Q_{tot} = airflow rate through the mock-up building (m^3/h)
- $j_{1,2}$ = coefficients (m^2)
- $x_{1,2}$ = input variables (m/s)
- c = constant (m^3/s)
- ε = error component (m^3/s)

The agreement between the modelled and the reference data was assessed using regression parameters and Bland Altman analysis. Because the experiments were performed under almost isothermal conditions (no extra heat was added), the assumption was made that no ventilation would occur with the absence of wind (measured on the meteomast). Therefore the intercept of the models was set to zero. The accuracy of the linear regression models was tested with two different methods: (1) the coefficient of determination and the regression coefficient; (2) the Bland Altman method (Bland et al., 2010), with which the respective absolute differences between the modelled and experimental results are related to the average of the modelled and reference results. The agreement between model results and experimental results is analysed with the slope β_0 and the intercept β_1 (formula [7]). Ideal models will result in coefficients close to zero. All statistical modelling was performed in Matlab (version 8_6). The coefficients a , b , c , β_0 and β_1 of the multiple regression models and the regression analysis were determined by applying curve fitting codes ('fit' and 'polyval'). The normality of the error distribution was checked with QQplots (residual plot) and

95% confidence intervals were calculated using the 'confint'-code.

$$(MR - RR) = \beta_0 \times \frac{MR+RR}{2} + \beta_1 \quad [7]$$

Where:

$MR - RR$ = difference between the modelled airflow results (MR) and the reference (measured) results (RR) (m^3/h)

$\frac{MR+RR}{2}$ = average of the modelled airflow results and the reference results

β_0 = coefficient of performance (dimensionless)

β_1 = intercept (m^3/h)

2.2.3 Experimental data

The measured airflow rates were split into 2 groups based on the uni- or bi-directional character of the flows. In total, 5953 uni-directional airflow rates and 1477 bi-directional airflow rates moving averages of airflow rates were calculated. An example of a bi-directional flow in a side vent A is presented in Figure 4. In this case, Vent A served as the main inlet opening, with part of the opening functioning as an outlet. The split between the opposite wind direction zone appeared vertical in the cases of bi-directional flows formed due to the wind (not to be confused with bi-directional flows formed by the stack-effect).

1.87	1.30	1.27	1.12	0.98	0.90	1.19	1.11	1.07	0.90	0.18	-0.07
2.09	1.96	1.83	1.60	1.50	1.54	1.57	1.66	1.57	1.11	0.27	-0.10
2.13	1.82	1.89	1.78	1.74	1.72	1.79	1.68	1.34	0.84	0.14	-0.09
2.02	1.61	1.48	1.29	1.50	1.42	1.48	1.53	1.29	0.86	0.04	-0.10

Figure 4: Measured average velocities (m/s) for each sampling place of Vent A with wind direction 47°; wind velocity 3 m/s measured at the meteomast; the scale intensity of colours (hot to cold) is related to the magnitude of the velocity

The uni-directional airflow rate values ranged between 1 612 m^3/h and 36 546 m^3/h , whereas the bi-directional airflow rate values varied between 1 455 m^3/h and 26 792 m^3/h . The magnitude of the airflow rates were influenced only by the outside weather conditions as temperature, wind direction and wind velocity. The wind roses and wind distribution profiles obtained from the data from the meteomast during the measurements are presented in Figure 5 and Figure 6 respectively. In Figure 6,

the positioning of the building to the wind directions is presented together with the notation of the term incidence angle'. The mean and standard deviation of the incidence angles of the uni- and bi-directional airflow rates were $(66 \pm 15)^\circ$ and $(33 \pm 18)^\circ$, respectively. As seen in Figure 7, distinction between uni-directional and bi-directional flows was found to depend mainly on the wind direction. Overall, the uni-directional flows occurred for wind directions between $(272 \text{ and } 83)^\circ$ and $(93 \text{ and } 264)^\circ$, bi-directional flows occurred for wind directions between $(4 \text{ and } 157)^\circ$ and $(201 \text{ and } 355)^\circ$. It was seen that the airflow rates with uni-directional flows not only occurred as expected for winds normal or diagonal to the opening and the airflow rates with bi-directional flows occurred not only for side winds. The unexpected results, as normal wind that produced a bi-directional flow, were mainly caused under circumstances of low wind velocities and probably in non-isothermal conditions.

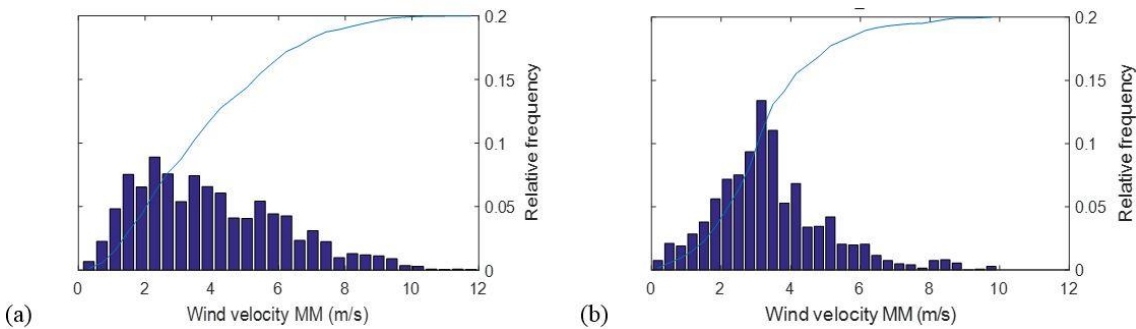


Figure 5: Wind profile distribution and cumulative relative frequency graph of the total velocity at the meteomast for the airflow rates with occurring (a) uni-directional and (b) bi-directional flows

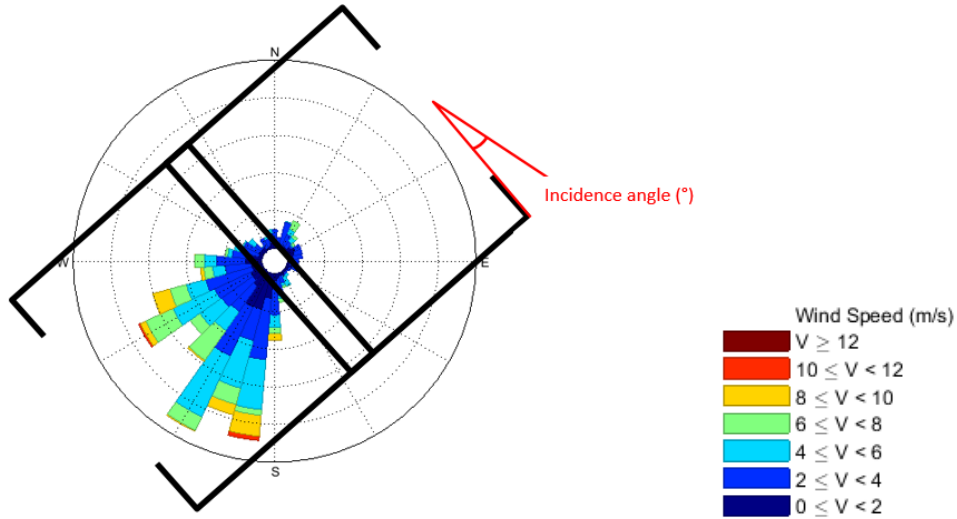


Figure 6: top view of the mock-up building projected on the wind rose of the experiments, together with the legend and indication of determination of the incidence angle, V_{MM} = wind velocity (m/s), circles indicating a frequency of occurrence in steps of 3%

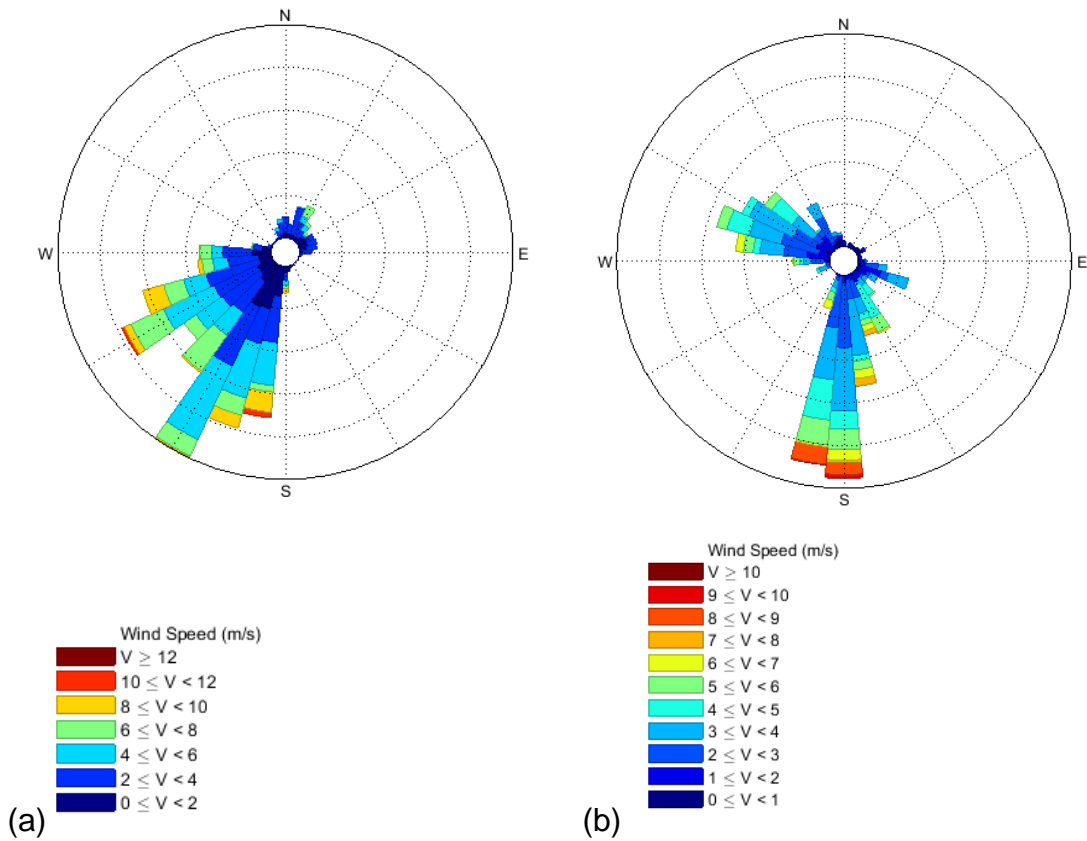


Figure 7: Wind rose with data of airflow rates with (a) uni-directional flows series and (b) bi-directional flows series in the side openings of the animal mock-up building, circles indicating a frequency of occurrence in steps of 3%

2.3 Results

2.3.1 Assessing the airflow rate for uni-directional flows in the side vents

2.3.1.1 Preliminary data analysis with ANN

The data of the airflow rates with uni-directional flows in the side vents were applied to ANN. The input variables $|\overline{U_{MM}}|$, $|\overline{Y_{MM}}|$, $|\overline{X_{MM}}|$ and $\overline{U_{MM}}$ measured at the metemast were used as input, the airflow rates as output. Table 1 shows the mean R^2 -values and their standard deviations of the relation between the reference Q_{tot} and the results of the ANN with different configurations. The R^2 -values for the total velocity $|\overline{U_{MM}}|$, perpendicular velocity $|\overline{Y_{MM}}|$, and velocity vector $\overline{U_{MM}}$ gave very high results above 98%. The standard deviation between the 8 different ANNs were very small so there was no need to look for the best configuration of ANN as these three input variables all resulted in good correlations. The parallel velocity component $|\overline{X_{MM}}|$ gave lower R^2 -values compared to the other input variables, Therefore this component was left out for further processing.

Table 1: Mean and SD of the R^2 -values for the measured and modelled data for different input variables (%)

Input	Mean R^2	SD R^2
$ \overline{U_{MM}} $	98.12	0.15
$ \overline{Y_{MM}} $	98.28	0.07
$ \overline{X_{MM}} $	55.49	4.63
$\overline{U_{MM}}$	99.40	0.08

2.3.1.2 Modelling and analysis of simple airflow rate correlations

Table 2 presents model parameters and the analysis results from the linear curve fitting of the candidate input variables for the uni-directional flows. The parameters showed that the coefficient for input variable $|\overline{Y_{MM}}|$ stayed approximately the same for models with inputs variables $|\overline{Y_{MM}}|$ and $\overline{U_{MM}}$. The results for the regression analysis showed that the $|\overline{U_{MM}}|$, $|\overline{Y_{MM}}|$ and $\overline{U_{MM}}$ input variables yielded good linear correlations with the airflow rate data for uni-directional flows. However, the Bland-Altman analysis (Table 3) showed that the $|\overline{Y_{MM}}|$ - and $\overline{U_{MM}}$ -models had slightly better results than the total velocity $|\overline{U_{MM}}|$. The $|\overline{Y_{MM}}|$ -component appeared to be the most important contributor in the correlation because the results for the $|\overline{Y_{MM}}|$ -model, with only the perpendicular

velocity component as input variable, were comparable to $\overline{U_{MM}}$. The results with the $|\overline{Y_{MM}}|$ and $\overline{U_{MM}}$ -input variables lay in the same range, with the latter slightly higher for the regression correlation and lower for the Bland Altman correlation. The graphs (Figure 8) confirm the good agreements for the reference and modelled airflow rates. Only small differences can be seen between the graphs, depending on the different input variables used. A possible explanation is that all graphs include modelled data using the most important contributor $|\overline{Y_{MM}}|$ -velocity component in different forms (integrated as $|\overline{U_{MM}}|$, $|\overline{Y_{MM}}|$ and $\overline{U_{MM}}$). Because these data concerned uni-directional flows mainly coming from winds more normal to the vent, the $|\overline{Y_{MM}}|$ -velocity component (perpendicular) was mostly larger than the $|\overline{X_{MM}}|$ -component (parallel). Also, the regression coefficient was lower for models using solely the input variable $|\overline{X_{MM}}|$.

The observations with small velocities in Figure 8 show a deviation for the data to the regression line. Possibly some stack-effect occurred (due to the presence of the sun and low wind velocity) and could have affected the model based on the wind effect. All three proposed models could identify the true airflow values consistently and had good estimation performances, with $|\overline{Y_{MM}}|$ and $\overline{U_{MM}}$ as the best input variables for the models. Input variable $|\overline{Y_{MM}}|$ had preference of choice over $\overline{U_{MM}}$ because one component less was needed to obtain similar modelling performance.

Table 2: Model parameters of the airflow rate related to an input variables (x_1 and x_2): coefficient of variable ($j_{1,2}$) and constant (c); regression analysis results for the modelled and measured total Q_{uni} : slope (a), intercept (m^3/h) (b) and coefficient of determination (R^2)

x_1	x_2	j_1	c	j_2	a	b	R^2
$ \overline{U_{MM}} $		3267	0	-	0,92	1234	0,96
$ \overline{Y_{MM}} $		3588	0	-	0,95	673	0,96
$ \overline{Y_{MM}} $	$ \overline{X_{MM}} $	3346	0	653	0,94	866	0,97

Table 3: Bland Altman results for the comparison of modelled to measured uni-directional flows with coefficients β_0 and β_1 ; all values were significantly different from 0

<i>Input</i>	β_0	β_1
$ \overline{U_{MM}} $	0.07	-1033
$ \overline{Y_{MM}} $	0.03	-457
$\overline{U_{MM}}$	0.05	-722

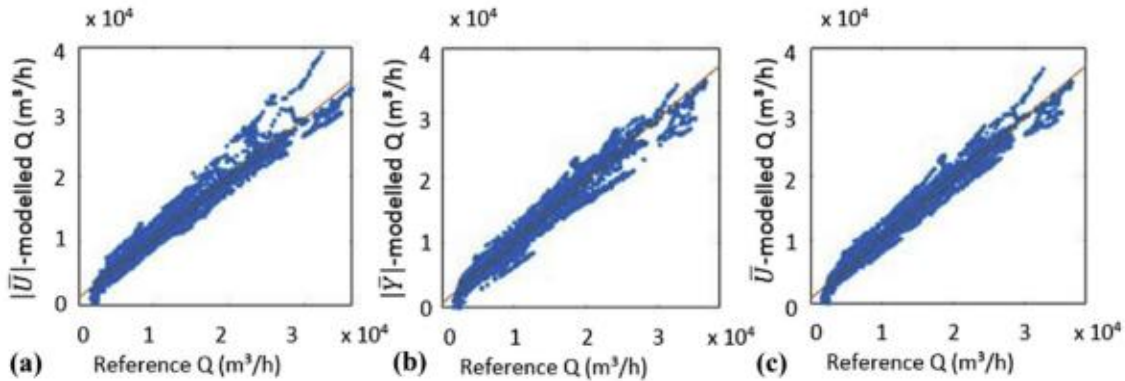


Figure 8: (Linear) correlation between the reference and the modelled uni-directional flows for input variables (a) total velocity $|\overline{U_{MM}}|$; (b) perpendicular velocity $|\overline{Y_{MM}}|$; (c) velocity vector $\overline{U_{MM}}$

2.3.1.3 Ventilation opening effectiveness

ASHRAE (2009) proposed a formula to calculate the airflow rate with the opening effectiveness EFF through the inlet opening (Formula [2]). This formula was applied to the data of the reference airflow rates to determine the EFF -values. Figure 9 shows a boxplot of the EFF -values calculated for each reference airflow rate. The median EFF was 0.59 and the 25- and 75-percentiles were 0.53 and 0.64 respectively. Outliers were found below 0.36 and above 0.78. Not all outliers were given on the boxplot as some even got up to 6. The EFF -values plotted against total wind velocity in Figure 10 (b) showed that these outliers were only appearing for low velocities smaller than 1 m/s. These outliers were not used in the following calculations.

Earlier it was found that the $|\overline{Y_{MM}}|$ was a good predictor to assess the airflow rate. ASHRAE's formula applies the wind velocity $|\overline{U_{MM}}|$. Hence, the EFF was expected to correct for this parameter using a coefficient related to the incidence angle. R^2 -values of 0.23 and 0.13 were found for the correlation between the EFF -factor and the incidence angle and the wind velocity, respectively. Although the mean EFF -factor

found with the available data had a value similar as given by ASHRAE (0.6), these low R^2 -values showed that the wind velocity $|\overline{U_{MM}}|$ was not a precise predictor.

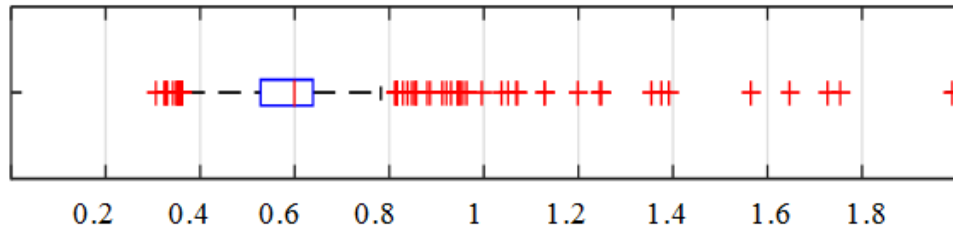


Figure 9: Boxplot EFF -factor for airflow rates with uni-directional flows

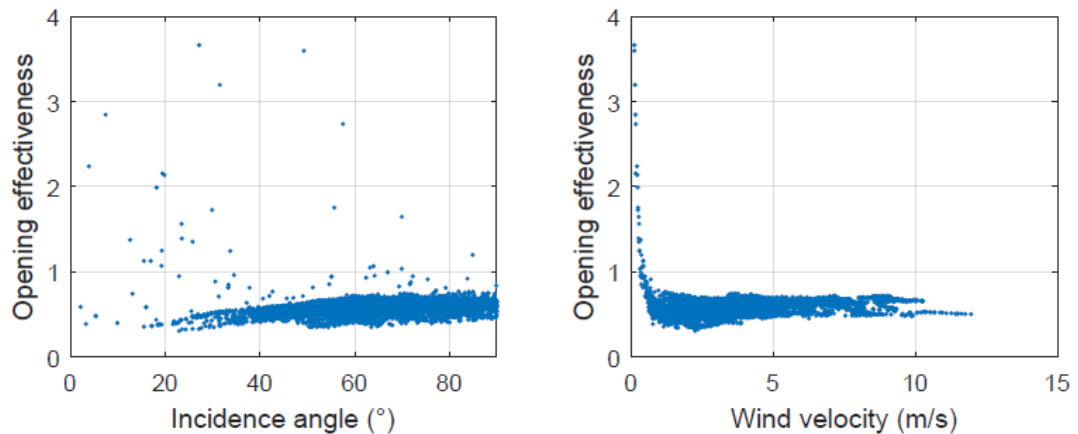


Figure 10: EFF -values (opening effectiveness) for uni-directional flows plotted against the (a) incidence angle of the wind ($^{\circ}$) and (b) the wind velocity (m/s)

2.3.2 Assessing the airflow rate for bi-directional flows in the side vents

2.3.2.1 Preliminary data analysis with ANN

Table 4 presents the mean and standard deviations of the R^2 -values between the measured and the ANN modelled bi-directional airflow rates for different input variables. The input variables $|\overline{Y_{MM}}|$ and $\overline{U_{MM}}$ gave highest correlations and therefore showed best potential to find a good fit with bi-directional airflow rates. The perpendicular component $|\overline{Y_{MM}}|$ still showed to be a very important factor to assess the airflow rate, even for bi-directional flows occurring for mainly diagonal and parallel winds. The tangential component was for this dataset still the worst predictor for the airflow rate, but it became a more important determination factor for the airflow rate correlation compared to the results for uni-directional flows, probably due to the character of the wind (diagonal to parallel). Because of the lower results compared to

the other input variables, $|\overline{X_{MM}}|$ was left out for further processing. The total velocity $|\overline{U_{MM}}|$ resulted in lower results for the R^2 -values than found for the uni-directional flows. An explanation could be that the bi-directional flows have larger $|\overline{X_{MM}}|$ -components compared to $|\overline{Y_{MM}}|$. This can result in a large total velocity, but as seen for the input variable $|\overline{X_{MM}}|$, it will not necessarily result in a good correlation with the airflow rates.

Table 4: Mean, standard deviation (SD) of the R^2 -correlation coefficients (%) between measured and ANN modelled Q_{bi} for different input variables

Input	Mean	SD
$ \overline{U_{MM}} $	88.21	1.82
$ \overline{Y_{MM}} $	96.76	0.70
$ \overline{X_{MM}} $	64.87	4.92
$\overline{U_{MM}}$	98.74	0.88

2.3.2.2 Modelling and analysis of simple airflow rate correlations

Table 5 shows the model parameters and the results of the correlations of the models built for the bi-directional flows. Table 6 gives the results of the Bland Altman analysis. Both input variables $|\overline{U_{MM}}|$ and $|\overline{Y_{MM}}|$ applied to the models for bi-directional airflow rates gave lower regression coefficients and Bland Altman correlations as applied to the models for uni-directional airflow rates. These showed that applying input variable $|\overline{Y_{MM}}|$ alone gave insufficient information to assess the airflow rate with bi-directional flows. Input variable $\overline{U_{MM}}$ gave a very good correlation, ANN showed that $|\overline{X_{MM}}|$ alone was insufficient for assessing the bi-directional airflow rates, however gave satisfying results in combination with $|\overline{Y_{MM}}|$ (input variable $\overline{U_{MM}}$). The regression and Bland Altman results were high for input variable $\overline{U_{MM}}$ compared to the other variables. The graphs on Figure 11 show that the total velocity $|\overline{U_{MM}}|$ gave the worst correlation for the modelled and reference bi-directional airflow rates. The input variable $|\overline{Y_{MM}}|$ alone improved the results, which could indicate that $|\overline{Y_{MM}}|$ is more important than $|\overline{X_{MM}}|$ to assess the ventilation rate. Though the modelling weight of $|\overline{X_{MM}}|$ is less than the weight of $|\overline{Y_{MM}}|$, $|\overline{X_{MM}}|$ is still of great importance for the accuracy of the model to find the best results for the bi-directional airflow rates. The results of the models for bi- and uni-directional flows showed that it was important to use separate models for these respective flows to maintain accurate prediction rates.

Table 5: Model parameters of the airflow rate related to an input variable (x_1, x_2): coefficient of variable ($j_{1,2}$) and constant (c); regression analysis results between the modelled and measured total Q_{bi} : slope (a), intercept (m^3/h) (b) and coefficient of determination (R^2)

x_1	x_2	j_1	c	j_2	β_0	β_1	R^2
$ \overline{U}_{MM} $		2164	0	-	0,69	2410	0,76
$ \overline{Y}_{MM} $		3597	0	-	1.10	-1354	0,92
$ \overline{Y}_{MM} $	$ \overline{X}_{MM} $	2736	0	808	0,97	174	0,96

Table 6: Results of the Bland-Altman analysis for bi-directional airflow rates with coefficients β_0 and β_1 ; *: not significantly different from 0

Input	β_0	β_1
$ \overline{U}_{MM} $	0.25	-1988
$ \overline{Y}_{MM} $	-0.14	1595
\overline{U}_{MM}	0.01*	-29*

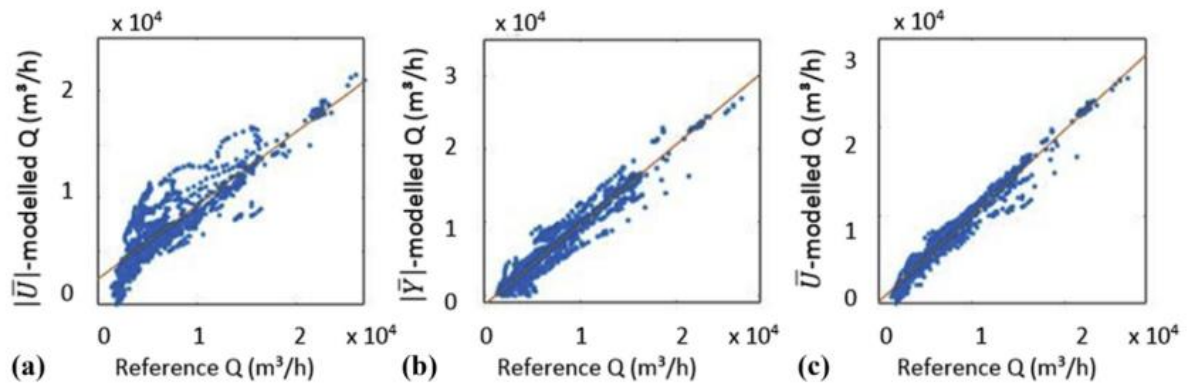


Figure 11: (Linear) correlation between the reference and the modelled Q_{bi} for input variables (a) total velocity $|\overline{U}_{MM}|$; (b) perpendicular velocity $|\overline{Y}_{MM}|$; (c) velocity vector \overline{U}_{MM}

2.3.2.3 Ventilation opening effectiveness

Similar to results of the uni-directional airflow rates, the *EFF*-values for the bi-directional airflow rates were also calculated. Figure 12 shows a boxplot of the *EFF*-values for bi-directional airflow rates. The median value was 0.41, the 25- and 75-percentile were 0.31 and 0.47 respectively. The outliers were found above 0.70. Similar to the *EFF*-values of the uni-directional airflow rates, high *EFF*-values appeared for low wind velocities (Figure 13). Similar to the data for the uni-directional flows, the outliers seen in Figure 11 are appearing only for low wind velocities (<1 m/s). Correlations were calculated for the data without these outliers. The *EFF*-values increased with increasing incidence angle, a regression coefficient of 0.0051 and R^2 -value of 0.65 were found for the regression line. No clear relation was found with the total wind

velocity measured at the metemast, the R^2 -value was found to be small (5×10^{-4}). The opening effectiveness showed the same behaviour compared to the perpendicular $|\overline{Y_{MM}}|$ and parallel velocity components $|\overline{X_{MM}}|$ as seen for the total velocity: small velocity components gave high values and velocity components above approximately 1 m/s gave did not give extra information as the opening effectiveness.

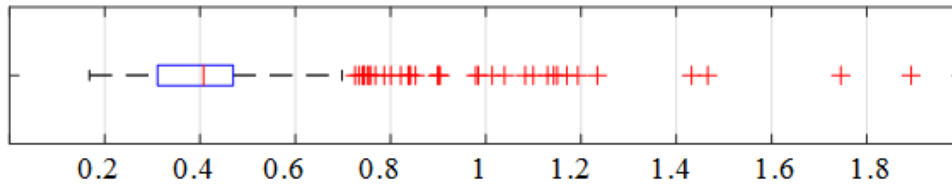


Figure 12: Boxplot *EFF*-factor for airflow rates with bi-directional flows

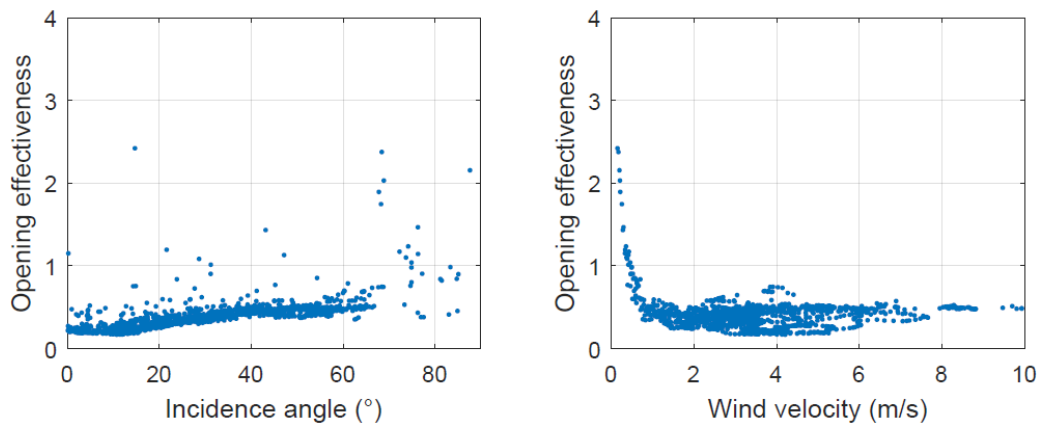


Figure 13: *EFF*-values (opening effectiveness) for bi-directional airflow rates plotted against the (a) incidence angle of the wind ($^{\circ}$) and (b) the wind velocity (m/s)

2.4 Discussion

Relatively simple models developed to assess the naturally ventilated airflow rates are widely available in literature. Chu et al. (2015), Choinière et al. (1992) already found linear correlations between the total velocity and the airflow rates in naturally ventilated greenhouses, Nääs et al. (1988), Verlinde et al. (1998), Yu et al. (2002) in test rooms in wind tunnels, ASHRAE (1981) and Etheridge (2012) for naturally ventilated buildings. Other researchers as Joo et al., (2014) and Lo et al., (2012) suggested a linear fit between the perpendicular component $|\overline{Y}|$ and velocities in the opening in a large dairy barn and a multi-zone test building respectively.

In this chapter, the input variables $|\overline{U_{MM}}|$, $|\overline{Y_{MM}}|$, $|\overline{X_{MM}}|$ and $\overline{U_{MM}}$ were tested to find the best input variable in a simple linear model for airflow rate assessment for both uni-directional and bi-directional airflows. For uni-directional flows, $\overline{U_{MM}}$ and $|\overline{Y_{MM}}|$ were found to be the most accurate input variables, where $|\overline{Y_{MM}}|$ was the most practical input variable because only one velocity component was needed. For 2D or 3D ultrasonic anemometers both the tangential and normal velocity component are available, which makes the input variable $\overline{U_{MM}}$ most accurate and practical for all wind directions.

In literature it is on average not clearly specified whether the proposed models can be applied for uni- and bi-directional flows. Though, if specified, it is mostly stated that these were proposed for uni-directional flows and when used for bi-directional flows, the accuracy will be low (Calvet et al., 2013; Etheridge, 2012). No specific models were found in literature for assessing airflow rates based on direct measurements with occurring bi-directional flows caused by the wind effect (not to be confused with models for bi-directional flows due to temperature differences). Our study suggested to use a multiple linear model where the tangential and perpendicular velocity components ($\overline{U_{MM}}$) are both included.

Though $\overline{U_{MM}}$ was found to be a good input variable for both uni-directional flows and bi-directional flows it was not suggested to use the same parameters for both models due to the differences in character of the flow pattern.

EFF is assumed to be a constant depending on the wind direction, [0.5-0.6] for perpendicular winds and [0.25-0.35] for diagonal winds (ASHRAE, 2009). The median opening effectiveness of 0.59 for the reference airflow rates was found to lay within these ranges. But values of percentile 75 and above (outliers), lay within the range between 0.64 and 0.78. Another explanation for the higher values of *EFF* found in this study might be that no obstructions were present in the animal mock-up building during measurements. The suggested *EFF* values in literature of 0.5-0.6 are given for practical use in naturally ventilated barns where animals and the arrangement of pen equipment, short partition walls and obstacles inside the buildings can affect the efficiency of the ventilation (Chu et al., 2014).

In literature, the reference velocity to calculate the opening effectiveness EFF is the total velocity $|\overline{U_{MM}}|$. Nääs (1988) and Yu et al. (2002) confirmed the wind angle of incidence is the most important factor influencing opening effectiveness. Our study suggested to use $|\overline{Y_{MM}}|$ instead of $|\overline{U_{MM}}|$ within the formula, due to the results where $|\overline{Y_{MM}}|$ correlated better with uni-directional flows. The suggested values of the opening effectiveness (EFF) should be checked in another study for its appropriateness with this new parameter.

The situation for bi-directional flows was different. The results of these experiments showed that the perpendicular velocity component $|\overline{Y_{MM}}|$ had a major influence on the resulting airflow rates, but the tangential component $|\overline{X_{MM}}|$ had also an important contribution to the airflow rate. This means that applying $|\overline{Y_{MM}}|$ as suggested for bi-directional flows would give less accurate results because no contribution of the tangential component was present. The use of $|\overline{U_{MM}}|$ could also lead to less accurate results, because this parameter does not allow for a differentiation in the magnitude of $|\overline{Y_{MM}}|$ or $|\overline{X_{MM}}|$. For bi-directional flows it is suggested not to use the formula with the opening effectiveness as $|\overline{U_{MM}}|$ or $|\overline{Y_{MM}}|$ are not giving accurate results to assess the airflow rate. In this situation the multiple linear regression with $\overline{U_{MM}}$ should be used for accurate results.

Further research should focus on commercial animal houses with large openings (dairy barns) to validate the model findings of this study.

2.5 Conclusions

In order to find a fast and simple airflow rate assessment technique for a naturally ventilated animal mock-up building, a linear model was applied using velocity measurements on a meteor mast of 10m height. Different combinations of velocity components were tested to find the most accurate input variable to assess the airflow rate. The total velocity $|\overline{U_{MM}}|$, the perpendicular $|\overline{Y_{MM}}|$ and the tangential velocity component $|\overline{X_{MM}}|$ and the velocity vector $\overline{U_{MM}}$ of the air velocity were tested as input variables. The calculated airflow rates were compared to the reference airflow rates measured by the detailed method developed by Van Overbeke et al., 2015a.

In addition, the data for modelling the airflow rates was split in uni- and bi-directional flows (opposite directions are present in the airflow pattern of an opening).

For uni-directional flows, $|\overline{Y_{MM}}|$ and $\overline{U_{MM}}$ yielded the most accurate airflow rates with R^2 -values of 96 and 97%, respectively. Although $|\overline{Y_{MM}}|$ being the easiest input variable because only one velocity component was needed to model the airflow rates. For this reason, it was found to give the best correlation using $|\overline{Y_{MM}}|$ in ASHRAE's formula of $Q=EFF \times A \times |\overline{U_{MM}}|$.

A multiple linear model was suggested for airflow rates with bi-directional flows. The $\overline{U_{MM}}$ -input variable was found to be the best input variable with an R^2 -value of 96%. Though the wind velocity component $|\overline{Y_{MM}}|$ was found to have the highest contribution within the models. $|\overline{X_{MM}}|$ was found to be an important contributor too for an accurate estimation of the airflow rate for bi-directional flows.

3 Experiments in an animal mock-up

building: assessing airflow

distribution in vents

In order to find a reduced measuring method for airflow rates in naturally ventilated buildings, a simple regression model to assess the airflow rate in an animal mock-up building was developed in chapter 2. A regression model was suggested with both the tangential and normal velocity components of the wind velocity measured at the meteoromast as input variables for bi-directional flows. These proposed model designs are used in chapter 3 to predict the behaviour of the airflow distribution in the vents for different wind conditions of uni- and bi-directional flows.

3.1 Introduction

Assessing emissions is important to determine emission factors of animal houses and to know the efficiency of mitigation techniques. Emission calculated as the product of differential pollutant concentration and airflow rate is suggested as one of the main measurement concepts (Ogink et al., 2013a). However, especially for naturally ventilated livestock buildings, measuring emission is not straightforward in practice due to uncertainties that are largely unknown (Calvet et al., 2010; Samer et al., 2011a). Uncertainties related to measuring emissions from these buildings are mostly a consequence of high spatial and temporal variations in the velocity distribution in the vents due to constantly changing weather conditions (Ogink et al., 2013a; Seifert et al., 2006), especially for very large openings. Furthermore, these large openings can even act as in- and outlets at the same time (so called 'bi-directional flows') (Demmers et al., 2000; Etheridge, 2015; Özcan et al., 2009; Wu et al., 2012a; Zhang et al., 2005). The direction of the flows in the opening can change between different parts of an opening and this within a short time frame.

When measuring the airflow rate with direct measurements the uncertainty of the method is inversely proportional to the number of measuring points in the vents (Joo et al., 2014). The less measurement points are used, the more information on the flow is lost. Depending on the measurement location, different information will be available on the spatial distribution (Kiwan et al., 2012; Saha et al., 2013; Van Buggenhout et al., 2009).

In most studies with direct measurements, sensors are equally spread over the surface area of the vents (Boulard et al., 1998; Teitel et al., 2005a; Joo et al., 2014) or a sensor

is traversed over the opening in time steps (Faggianelli et al., 2015a; López et al., 2011b; Van Overbeke et al., 2015a). Sampling locations in the openings are typically determined as a compromise to the availability of sensors (Faggianelli et al., 2015a). As a consequence, monitoring flow distribution is very important for design and efficiency purposes of measuring methods. However, research in the field of airflow or velocity distribution in the openings is scarce. In greenhouses (Wang et al., 1999a, 1999b; Teitel et al., 2008; Lopez et al., 2011a), ventilated rooms in civil buildings (Nielsen, 2015) and for dairy barns (Fiedler et al., 2011; Norton et al., 2009; Wu et al., 2012a), experiments were performed on velocity patterns inside buildings. Although many experiments exist with velocity measurements located in the vents (De Vogeleer et al., 2016; Joo et al., 2014, 2015; Molina-Aiz et al., 2009; Wang et al., 2016), most of the measurement results were used to calculate the total airflow rate through the building but not to study the behaviour of the velocity distributions of uni- and bi-directional flows in the openings for different wind conditions. Only few experiments have been performed at opening level in animal barns in outside weather conditions to study the behaviour of inlet and outlet flows (direction of the velocity), the velocity distribution (velocity gradients) and the steadiness or fluctuations of the airflows.

Multiple studies conducted in greenhouses already demonstrated that the in- or outlet behaviour of vents is dependent on the wind incidence angle (Boulard et al., 2002; López et al., 2011; Shilo et al., 2004; Teitel et al., 2008). Choinière et al. (1994) introduced a 'critical incidence angle' for which the flow direction can change in an opening, this study was performed on a mock-up swine building in a wind tunnel. Other theoretic studies (Li et al., 2000; Wang et al., 2012) focused also on the bi-directionality in the openings due to the buoyancy effect (with a horizontal neutral plane). Choinière et al. (1994) and Teitel et al. (2008) found that wind perpendicular to the opening provided the most uniform airflow rate patterns in vents and inside buildings. Kiwan et al. (2012) studied the effect of positioning of the sensors in the vent opening in naturally ventilated barns. He assumed that it is more important to measure the air velocity at different points within an opening to obtain representative data for the whole opening than to measure at a high number of openings which are located in very similar positions.

To obtain efficient sampling of the airflow rates or emissions by measuring in the vents,

still a lot of research is needed to have an in depth understanding about the velocity distribution in the vents and the factors influencing them.

The objective of this research was to assess the predictability of the airflow rate distribution over the vents of a naturally ventilated building. This is done by detailed sampling of the air velocities in the vents and by statistically modelling all in and outgoing airflow rates through the ridge and side vents of a naturally ventilated animal mock-up building. The spatial distribution of uni- and bi-directional airflow rates was analysed.

3.2 Materials and Methods

Different steps were taken to assess the predictability of the velocity distribution in the vents of a naturally ventilated building. Firstly, detailed sampling of the air velocities in the vents was performed to have a dataset of the velocity distribution for several wind conditions. Secondly, the vents were virtually divided in 4 different partitions. These partitions contained detailed velocity measurements and related partition airflow rates. For every partition, statistical models were built to assess the different in- and outgoing flows. Distinction was made between uni- and bi-directional flows. Analysis of the statistical models per partition gives an indication of the possibility of predicting the velocity distribution in the vents.

3.2.1 *Animal mock-up building, instrumentation and experimental setup*

A description of the animal mock-up building, instrumentation and experimental set-up can be found in the previous section §2.2.1.

3.2.2 *Reference airflow rate measurements and calculations*

The airflow rate measurements were conducted using the method of Van Overbeke et al. (2014b, 2015a, 2015b, 2016) based on direct measurements in the openings using ultrasonic anemometers. For every sampling location, an average velocity was sampled. The locations in the ridge opening were sampled continuously because fixed anemometers were installed in the ridge opening. The locations in each side opening

were sampled with an automatically moving sensor for 10s at 1 Hz. Measuring all locations (one measurement round) took approximately 10 minutes. For each measurement place, a mean velocity was calculated from observations over 10 measurement rounds. Every new measurement round, a new moving average was calculated over the last 10 measurement rounds (approximately 1.5h). The mean velocity measurements per sampling location resulted in a detailed sampling grid of the vents of the animal mock-up building. These data can be used to evaluate the airflow distribution on building level, vent level or in different partitions (groups of sampling locations) of the openings.

3.2.2.1 Airflow rate at sampling location level

The grid of the sampling locations in the side opening was determined by the size of the sensor head. The sensor head had dimensions of approximately 0.25 m × 0.125 m which was applied as the surface area per sampling location. These dimensions resulted in a matrix of 4 rows and 12 columns within the opening (48 sampling locations).

The ridge vent was equipped with eight fixed anemometers giving surface areas of 0.35 m × 0.5 m per sampling location. One anemometer failed during the experiments, the respective velocities were replaced by the mean of the two neighbouring sensors. Each sampling location was defined by a magnitude (m/s) and a direction of the flow. The direction of the flow could be subdivided in con-current and counter-current flows according to the direction of the airflow compared to the outside wind direction (Figure 14).

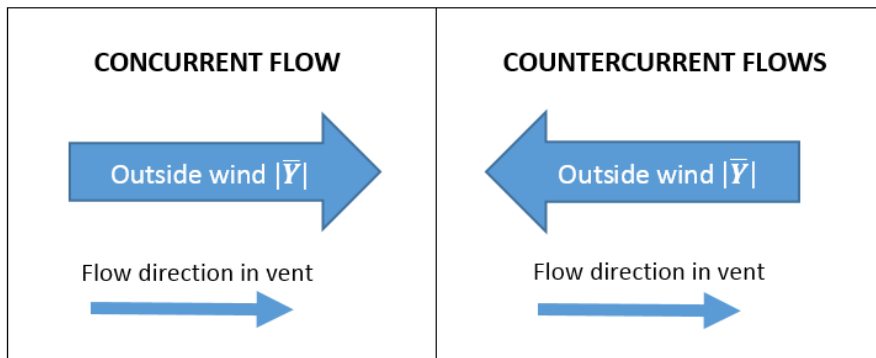


Figure 14: Flow directions of the outside wind ($|\bar{Y}_{MM}|$) and the airflow in the vent for (left) con-current and (right) counter-current airflows

3.2.2.2 Airflow rate at partition level

Within this study, the openings were divided in different partitions to facilitate modelling of the airflow distribution. For all openings (ridge and side), four partitions were chosen. The ridge opening had two different measurement locations within a partition. The side opening had twelve different measurement locations each (4 rows and 3 columns) (Figure 15). Due to the dimensions of the opening, the opening had a width larger than the height, only horizontal and no vertical virtual partitions were assigned in the side opening. Vertical partitions were not of interest because no extra heat was added, so isothermal conditions were assumed (a maximum of 1°C was measured between in- and outlet) and no stack effect was expected (De Vogeleeer et al., 2016), also due to the limited height of the vents and building, no effects of the boundary layer were expected.

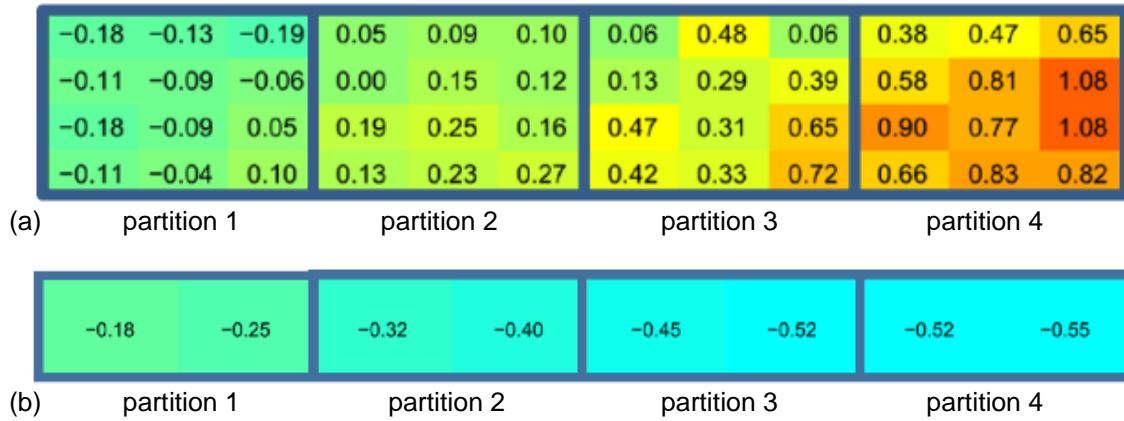


Figure 15: Measuring locations in 4 partitions for a measurement example in (a) the side vent and (b) the ridge vent; the values represent mean velocities over 1.5h. The gradient of the colours varies from blue (large negative velocity/going out the vent) to red (large positive velocity/going in the barn)

For each partition in the opening a (partition) airflow rate was calculated. Summing the partition airflow rates then gives the total airflow rate through the opening.

These partition airflow rates were calculated using the velocities per measurement location by summing the products of the surface areas with the local velocity measurements of their location [8].

$$Q_{part} = \sum_{j=1}^n (|\bar{V}_{ms}|_j \cdot A_j \cdot 3600) \quad [8]$$

Where

Q_{part} = partition airflow rate (m^3/h)

ms = measurement surface

$|\bar{V}_{ms}|_j$ = mean perpendicular velocity component in measurement surface j (m/s)

A = surface area (m^2)

n = total number of sampling locations within a partition (i.e. 12 for a side vent, 2 for a ridge vent partition)

j = sampling surface

The airflow rates were given a sign according to their direction towards the building. A positive direction was attributed to air inflows (+Q), while a negative direction indicated an air outflow (-Q) from the animal mock-up building. For each partition, the in- and outgoing airflow rates were calculated by taking the sum of the positive or negative airflow rates, respectively, at the measurement locations of the respective partition.

3.2.2.3 Airflow rate at building level

Using the data of all sampling locations, it was also possible to calculate the in- and outflow rates on the level of the opening or the animal mock-up building. The airflow rates were calculated using a similar formula as for the partitions [9].

$$Q_{tot} = \sum_{k=1}^n (|\bar{Y}_{ms}|_k \cdot A_k \cdot 3600) \quad [9]$$

Where

Q_{tot} = mean airflow rate through the building over a period of approximately 1.5 h (m^3/h)

ms = measurement surface

$|\bar{Y}_{ms}|_k$ = mean normal velocity component over a period of approximately 1.5 h in measurement surface k (m/s)

A_k = surface area of sampling location k (m^2)

n = total number of sampling locations in the side or ridge vents (i.e. 48 for a side vent, 8 for a ridge vent).

Simultaneously with the calculation of the in- and outflows for each vent, the total surface area representing these in- and outflows was calculated. Because the animal mock-up building was symmetrical over the vertical plane through the ridge (similar results were expected), only one side opening (facing SW) and the ridge opening were examined for airflow distribution.

3.2.3 Data collection and model development

3.2.3.1 Data selection

Airflow rate models were built for every partition in the vent. The data per partition was first split into groups with airflows directed inwards or outwards the building. For this, all measurements were split in a perpendicular component, Y_+ for winds coming from 90-270° (sector 1) and Y_- for winds coming from 270° to 360° and from 0° to 90° (sector 2) (Figure 16).

Secondly, distinction was made on partition level between the character of the flow pattern, uni- or bi-directional. Partitions were determined as bi-directional when at least one velocity measurement in that partition had a different sign (Figure 14) than the

other measurements. The sign of the flow distinguished whether the flow was con- (mainstream) or counter-current (against mainstream) in case of bi-directional flows (Figures 14 and 16).

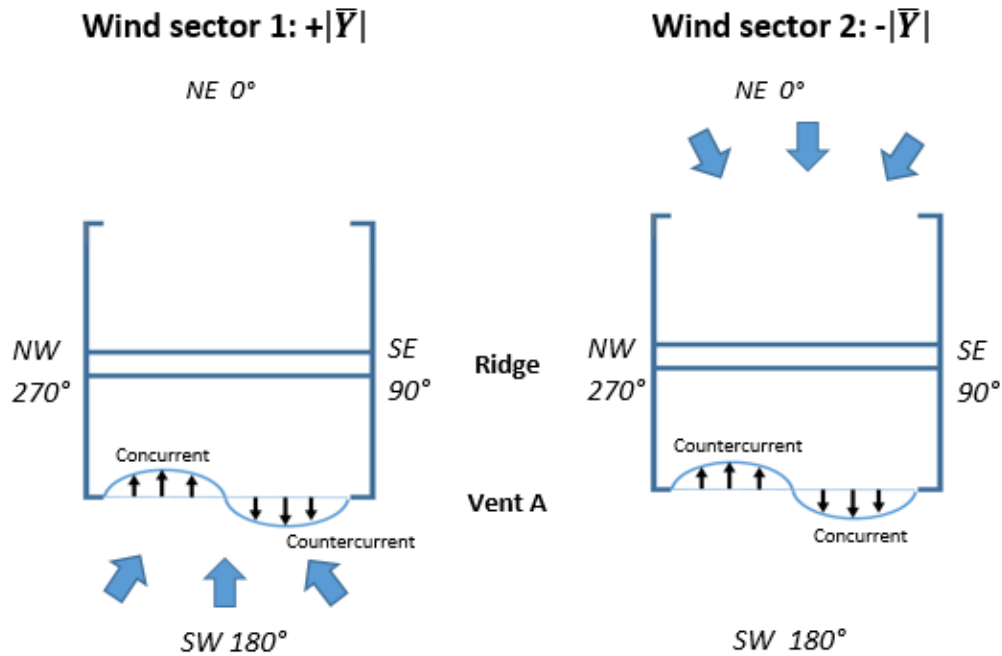


Figure 16: Definition of con- and counter-current flows for the SW-opening of the mock-up building for (left) Wind sector 1 with a positive wind component $|\bar{Y}_{MM}|$ and for (right) Wind sector 2 with a negative wind component $|\bar{Y}_{MM}|$

3.2.3.2 Statistical models

Multiple linear regression [10] was used to model the partition airflow rates at partition level as used in De Vogeleer et al. (2016). These statistical models gave information on how to model the (partition) airflow rates in the openings with data measured at the meteoromast and are given the name of distribution models in sections 3.3.2 and 3.3.3 of the results.

The $|\bar{X}|$ - and $|\bar{Y}|$ -velocity components measured at the meteoromast were used as independent variables, the airflow rate at partition level as dependent variable [10]. All statistical modelling was performed in Matlab (version 8_6). The coefficients a , b and c of the multiple regression model and regression analysis were determined by applying curve fitting codes (fit and polyval). The normality of the error distribution was checked with QQplots (residual plot) and 95% confidence intervals were calculated

using the confint-code. All modelled partition airflow rates [11] were compared to all measured partition airflow rates using single linear regression [12].

Determination of the coefficients of the statistical model [10]

$$Q_{measured,part} = a_{part} \times |\bar{X}_{MM}| + b_{part} \times |\bar{Y}_{MM}| + c_{part} + \varepsilon_{part}$$

Determination of the modelled airflow rates [11]

$$Q_{modelled,part} = a_{part} \times |\bar{X}_{MM}| + b_{part} \times |\bar{Y}_{MM}| + c_{part}$$

Comparing modelled and measured airflow rates [12]

$$Q_{measured,part} = z \times Q_{modelled,part} + c_{part}$$

where:

$ \bar{X}_{MM} $	= tangential wind velocity component (m/s)
$ \bar{Y}_{MM} $	= perpendicular wind velocity component (m/s)
<i>part</i>	= index referring to partition
<i>a, b</i>	= coefficients (m^2)
<i>c</i>	= coefficient (m^3/h)
ε	= error component of the statistical model (m^3/h)
<i>z</i>	= constant (dimensionless)
$Q_{measured}$	= measured airflow rates at partition level (m^3/h)
$Q_{modelled}$	= modelled airflow rates at partition level (m^3/h)

Measurements were executed over approximately 5 months time. However, not enough observations were available of all wind directions to be separated as a dataset for validation. Therefore the same measured dataset was used for validation and for building the models.

The agreement between the modelled and the reference airflow rates was assessed using two different methods: regression, as described above, and Bland Altman analysis. These methods are described in the previous chapter 2.

3.2.4 **Experimental data**

Measurements were executed continuously over the period December 2014 through March 2015.

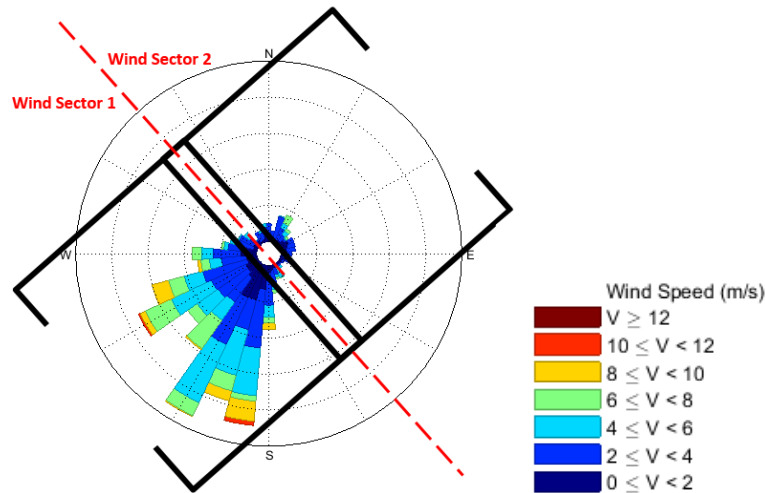


Figure 17: Top view of the mock-up building projected on the wind rose, together with the legend and indication of wind sector 1 and 2, V = wind velocity (m/s), circles indicating a frequency of occurrence in steps of 3%

The wind conditions during the measurements were representative of the typical wind in Flanders. The typical wind speed was 2-3 m/s. On the wind rose it can be seen that more data points (5998 measured airflow rates of ± 1.5 h each) were measured for wind sector 1 (Figure 17) than for sector 2 (1172 airflow rates). Wind speeds went up to 12 m/s, with the highest peaks recorded in wind sector 1.

3.3 Results & discussion

3.3.1 Characterisation of the airflow rates through the vents

Figure 18 c and d, show that the ridge opening was acting mainly as an outlet only, independently from the wind direction (positive or negative $|\bar{Y}_{MM}|$). Figure 18 a and b show the fractions of the surface areas acting as inlet and outlet. Only for about 1% of the measured airflow rates, air also entered the animal mock-up building through the ridge opening. The side opening was acting as an inlet and/or an outlet depending on the wind direction. The ratio of the in- and outgoing flows (Figure 18) was not necessarily equal to the ratio of the surface area of the in- and outgoing flows because of spatial variations in the velocity distribution in the openings. Although the counter-current airflow rates through the side opening were very small, the relative surface area was larger than proportionally expected, which could be of great importance for emission and/or airflow rate measurements.

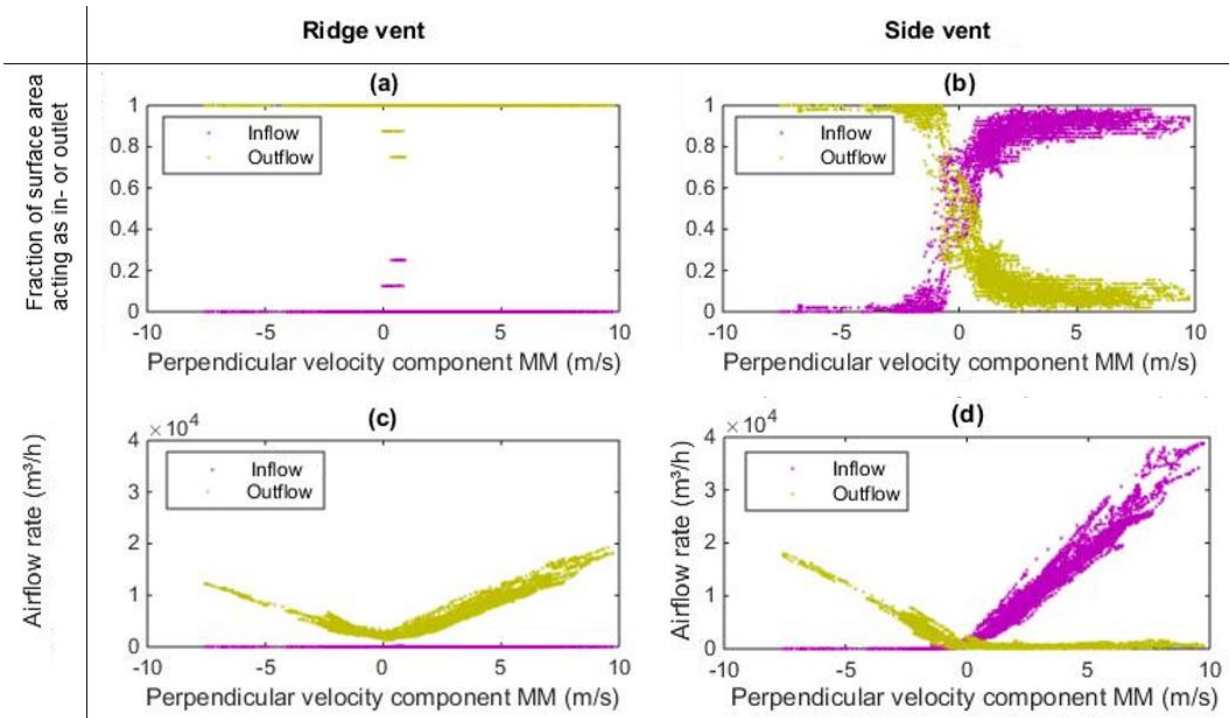


Figure 18: Fraction of vent surface area acting as in- or outlet and airflow rates through the vents as a function of the perpendicular velocity component $|\bar{V}_{MM}|$ for (a) the ridge opening; (b) the side opening; Absolute airflow rate values (m³/s) for the in- and outlet rates through the vents as a function of the perpendicular velocity component $|\bar{V}_{MM}|$ for (c) airflow rate in the ridge opening; (d) airflow rate in the side opening

The maximum outgoing airflow rate for the ridge opening was 19 254 m³/h and 12 253 m³/h with wind speeds coming from wind sectors 1 and 2, respectively. The maximum inflow and outflow rates for wind from sector 1 in the side opening were 38 975 m³/h and 2 224 m³/h, respectively. For sector 2, these were 17 987 m³/h and 1 755 m³/h, respectively. Airflow rates for wind sector 1 were mainly higher than those for sector 2 as expected, based on the measured wind conditions during the experiment and as seen in the wind rose (Figure 17).

3.3.2 Distribution models for the ridge vent

The experiments in the animal mock-up building showed that the ridge opening acted almost always as uni-directional outlet. In both wind sectors 1 and 2, some airflow rates acted bi-directionally (0.01% and 0.001% respectively), but these were so few in number and so little in magnitude that these were omitted from the modelling. The coefficients shown per sector in Figure 19, can be used as input for a multiple linear regression model to assess the airflow rate through each partition in the ridge opening.

The error bars of the coefficients are so small (high number of observations) that they are almost not detectible on the graph. This was confirmed with a slope of nearly 0 and a low intercept (compared to the maximum airflow rate) for the Bland Altman analysis in Table 7. For all cases, regression analysis gave slopes of 1 and intercepts that were not significantly different from zero. This means that the models for the ridge opening were very accurate and precise (high R^2 -values, Table 7).

Because the animal mock-up building was almost symmetrical, it was expected that the coefficients would be comparable for both wind sectors. Differences of coefficients b and c between the wind sectors could result from the dissimilarity in landscape on each wind sector side of the animal mock-up building or because wind sector 2 did not have a data set in the same wide range of velocities as wind sector 1. Parallel wind components $|\bar{X}_{MM}|$ seemed to have only a small effect on the airflow rate through the partitions of the ridge opening (small a coefficient). The coefficients b for input variable $|\bar{Y}_{MM}|$ were the highest in number for both sectors, which made this one the most important input variable to assess the airflow rate. Only in wind sector 2, the intercept c lay in the same range as b , but when the perpendicular velocity component $|\bar{Y}_{MM}|$ increased, this intercept decreased in importance.

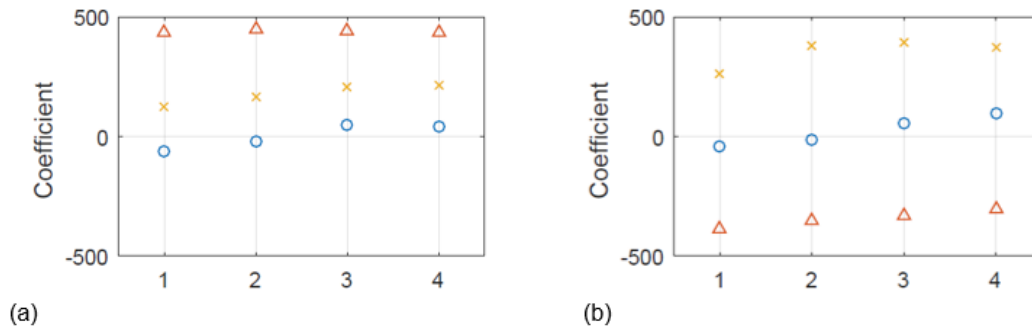


Figure 19: Coefficients of multiple linear regression for uni-directional flows in the ridge vent with confidence intervals of 95% as error bars for (a) wind sector 1 and (b) wind sector 2 with coefficients: a (m^2) as \circ ; b (m^2) as \triangle and c (m^3/h) as \times

Table 7: Analysis results per sector for each partition in the ridge opening: regression analysis (R^2), Bland Altman analysis (β_0, β_1), the maximum airflow rate through the partition (m^3/h) and number of data points (n), *: not significantly different from zero

Part	sector 1					sector 2				
	R^2	β_0	β_1	max	n	R^2	β_0	β_1	max	n
1	0.95	-0.03	-43	-5001	5961	0.92	-0.04	-47	-3245	1171
2	0.95	-0.03	-44	-4970	5998	0.89	-0.06	-63	-3122	1172
3	0.94	-0.03	-53	-4760	5998	0.92	-0.04	-45	-3052	1172
4	0.93	-0.03	-60	-4737	5998	0.94	-0.03	-32	-2835	1172

3.3.3 Distribution models for the side vent

3.3.3.1 Uni-directional flows

The model coefficients of the uni-directional flows in the different partitions of the side vent are shown in Figure 20. Error bars of the coefficients are so small that they are almost not detectable on the graph (this was probably due to the high number of observations). Overall, $|\bar{Y}_{MM}|$ is the most important coefficient, but coefficient b of the variable $|\bar{Y}_{MM}|$ was larger for wind sector 1 than for sector 2. This is because for wind sector 1, the side opening is the main inlet opening. Whereas for sector 2, the side vent is a shared outlet with the ridge vent. For winds coming from wind sector 2 both the ridge and the side vent had similar b coefficients, i.e. approximately 400 and 600 m^2 . This implies that they were both important outlet vents.

Generally, the $|\bar{X}_{MM}|$ -velocity component had little influence. For wind sector 2, this little influence, compared to the other components, was steady over all partitions. As the opening lay at the leeward side for wind sector 1, a uniform velocity pattern was expected as seen in Figure 20. For the outermost partitions (1 and 4) in sector 1, when the opening was on the windward side, the influence of the $|\bar{X}_{MM}|$ -velocity component increased highly.

The intercept c (constant) was of the same magnitude for both wind sectors, 100-150 m^3/h . This value became negligible for higher wind velocities, especially for a higher $|\bar{Y}_{MM}|$ -variable, which has a coefficient of $\pm 1000 m^2$.

It was seen that as the opening was a main inlet (sector 1), coefficients b and c

remained steady over all partitions, and only *a* was affected by the side walls of the opening.

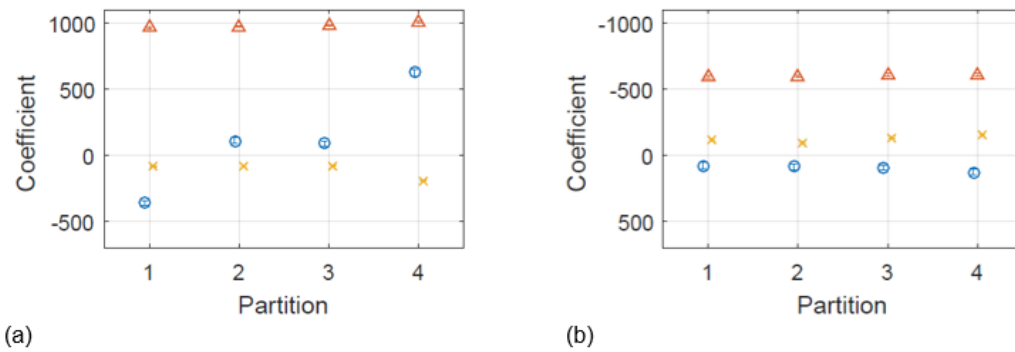


Figure 20: Coefficients of multiple linear regression for uni-directional flows in the side vent with confidence intervals of 95% as error bars for airflow data related to (a) sector wind 1 and (b) wind sector 2 with coefficients: *a* (m²) as \circ ; *b* (m²) as Δ and *c* (m³/h) as \times

Table 8: Analysis results per wind sector for each partition in the side opening for uni-dir. flows: regression analysis (R^2), Bland Altman analysis (β_0, β_1), the maximum of minimum airflow rate through the partition (m³/h) and number of data points (*n*), all values were significantly different from zero

Part	Sector 1					Sector 2				
	R^2	β_0	β_1	<i>max</i>	<i>n</i>	R^2	β_0	β_1	<i>min</i>	<i>n</i>
1	0.98	-0.01	43	11443	5553	0.92	-0.04	-48	-4733	1040
2	0.96	-0.02	69	10055	5863	0.96	-0.02	-27	-4335	1028
3	0.97	-0.02	51	9972	5922	0.96	-0.02	-24	-4505	1023
4	0.95	-0.03	86	12326	5274	0.95	-0.03	-34	-4583	1014

Comparable to the results for the ridge vent, the slope and intercept of the airflow rate models for uni-directional flows through the side vent were close to 1 and nearly 0, respectively. The coefficients of determination (Table 8) showed that for both wind sectors, the variance of the airflow rates for uni-directional flows through the partitions could be explained almost entirely with the $|\bar{X}_{MM}|$ - and $|\bar{Y}_{MM}|$ - input variables. The Bland Altman coefficients showed that the results of the models followed the same trend as the results of the reference airflow rates. These results showed that good agreement was found between modelled and measured airflow rates. It was possible to have an accurate and precise model to predict the distribution in the opening with the $|\bar{X}_{MM}|$ - and $|\bar{Y}_{MM}|$ - input variables measured at the meteomast.

3.3.3.2 Bi-directional flows

Data for airflow rates of bi-directional flows were separated for wind sectors (12% of the data for wind sector 1 and 13% for wind sector 2) and based on the direction of the airflow compared to the outside wind (con- or counter-current flows). Figure 21 shows the model coefficients for the airflow rates of the side vent with bi-directional flows, with in the columns the coefficients per wind sector and in the rows the coefficients per con- or counter-current flow, respectively. The regression results of the modelled and the experimental airflow rates for all bi-directional flows, gave promising results with a slope of 1 and an intercept of nearly 0. This stated that the models of all partitions and wind sectors of the bi-directional flows are very accurate. To see whether the models are precise, the results of the variance and the residual plots of Bland Altman are given in Table 9 and Table 10.

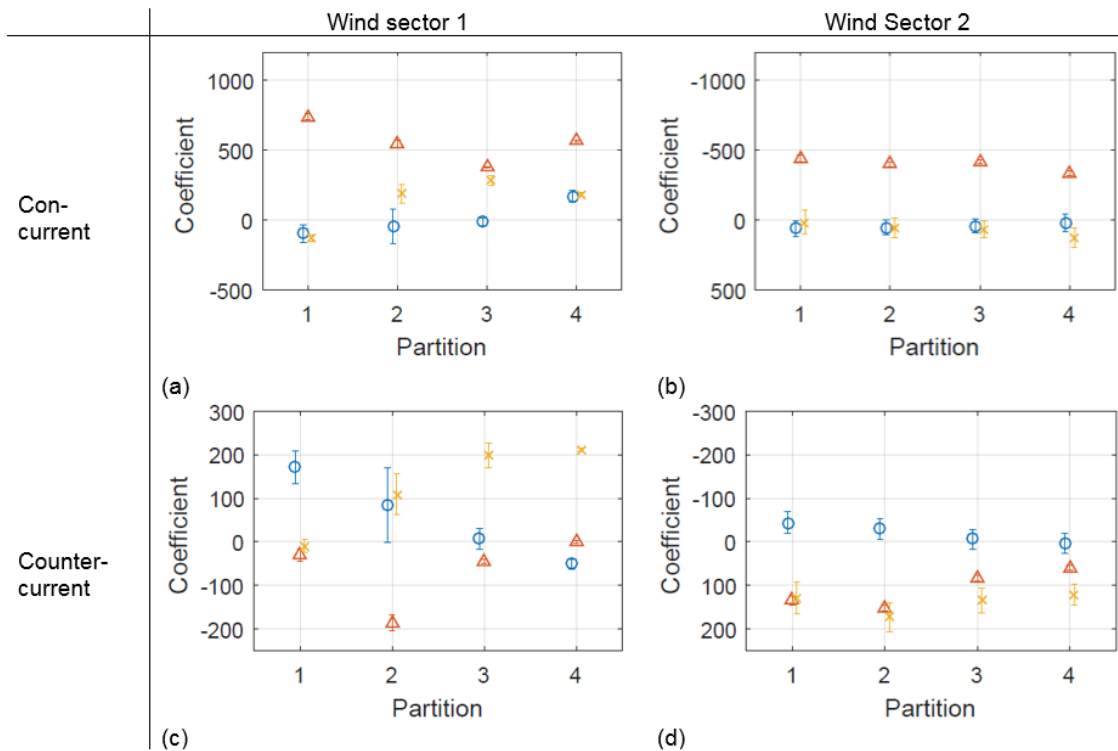


Figure 21: Coefficients of multiple linear regression of airflow rates for bi-directional flows in the side vent with confidence intervals of 95% as error bars for (a) con-current flows of wind sector 1, (b) con-current flows of wind sector 2, (c) counter-current flows of sector 1, (d) counter-current flows of sector 2 with coefficients: a (m²) as ○; b (m²) as ▲ and c (m³/h) as ×

Table 9: Analysis results per sector for each partition in the side opening for con-current airflow rates of bi-dir. flows: regression analysis (R^2), Bland Altman analysis (β_0 , β_1), the maximum of minimum airflow rate through the partition (m^3/h) and number of data points (n), not significantly different from zero (*)

Part	Con-current flow									
	Sector 1					Sector 2				
	R^2	β_0	β_1	max	n	R^2	β_0	β_1	max	n
1	0.88	-0.07	41	3668	445	0.53	-0.37	117	870	132
2	0.79	-0.13	45	1628	135	0.47	-0.44	139	824	144
3	0.90	-0.05*	29*	1053	76	0.56	-0.32	110	1294	149
4	0.89	-0.06	75	3983	724	0.38	-0.58	229	1029	158

Table 10: Analysis results per sector for each partition in the side opening for counter-current airflow rates of bi-dir. flows: regression analysis (R^2), Bland Altman analysis (β_0 , β_1), the maximum of minimum airflow rate through the partition (m^3/h) and number of data points (n), not significantly different from zero (*)

Part	Counter-current flow									
	Sector 1					Sector 2				
	R^2	β_0	β_1	max	n	R^2	β_0	β_1	max	n
1	0.62	-0.27	114	1283	445	0.35	-0.64	37	506	132
2	0.71	-0.18	53	634	135	0.39	-0.56	46	405	144
3	0.29	-0.76	126	330	76	0.19	-1.02	80	476	149
4	0.67	-0.22	77	730	724	0.19	-1.02	69	456	158

Comparing partitions, the graphs for sector 2 (Figure 20) show more stable coefficients and smaller error bars than these for sector 1. This is probably the result of the airflow developing to a less turbulent flow when passing through the building.

The results for wind sector 1 varied considerably among partitions for both the con- and counter-current flows. This could result from the direct influence of the wind effects on the measurements, the flows have no guiding through the building first. This direct wind effect is also the reason why wind sector 1 contains more bi-directional airflow rate measurements for the outermost partitions, e.g. 724 measurements n (12%) for partition 4 and 76 for partitions 3 (1,2%), and the amount of measurements for sector 2 is relatively steady over all partitions (approximately 11% of all airflow rates of sector 2). Although wind sector 2 gave the most steady coefficients for the models with lower error bars, the R^2 -values are overall lower and the residuals (lower β_0 and β_1) are relatively larger for all partitions and for both con- and counter-current flows. This could

be a result of lower magnitudes of airflow rates compared to the inlet (the ridge mainly acts as an outlet). Similar to former results, it could be seen that the $|\bar{X}_{MM}|$ -velocity component had most influence on the outermost partitions for winds coming from sector 1 and less for the inner partitions of sector 1 and all partitions of sector 2.

Overall, it is seen that coefficient b for the $|\bar{Y}_{MM}|$ - input variables remained the largest component in weight. Compared to the models for uni-directional flows, however, the component a for the $|\bar{X}_{MM}|$ - input variable increased in importance with a higher value. The comparison of the results of the coefficients of the uni-directional and bi-directional con-current flows of wind sector 1 and 2 (counter-current flows are not present for uni-directional flows), showed that it was important to build separate models for airflow rates for uni- and bi-directional flows. This is not in line with the findings of Calvet et al. (2013), Etheridge et al. (2012), De Vogeleeer et al. (2016). Both sectors gave lower values for con-current flows (e.g. Figure 19 and Figure 21).

The counter-current flows gave models with a higher variance than the con-current flows. Also the results of Bland Altman analysis revealed larger deviations between modelled and experimental results for the counter-current flows compared to the con-current flows. Possibly other parameters indicating influences of surrounding obstacles, window sizes or turbulence should be considered.

Figure 22 shows examples of all bi-directional flows being both the con- and counter-current flows of wind sectors 1 and 2. The coefficients in Figure 21 show that the con-current flows gave larger airflows than the counter-current flows. It is also seen that the counter-current flows for wind sector 2 are scattered more which explains the low R^2 -value and disappointing results for the Bland Altman coefficients.

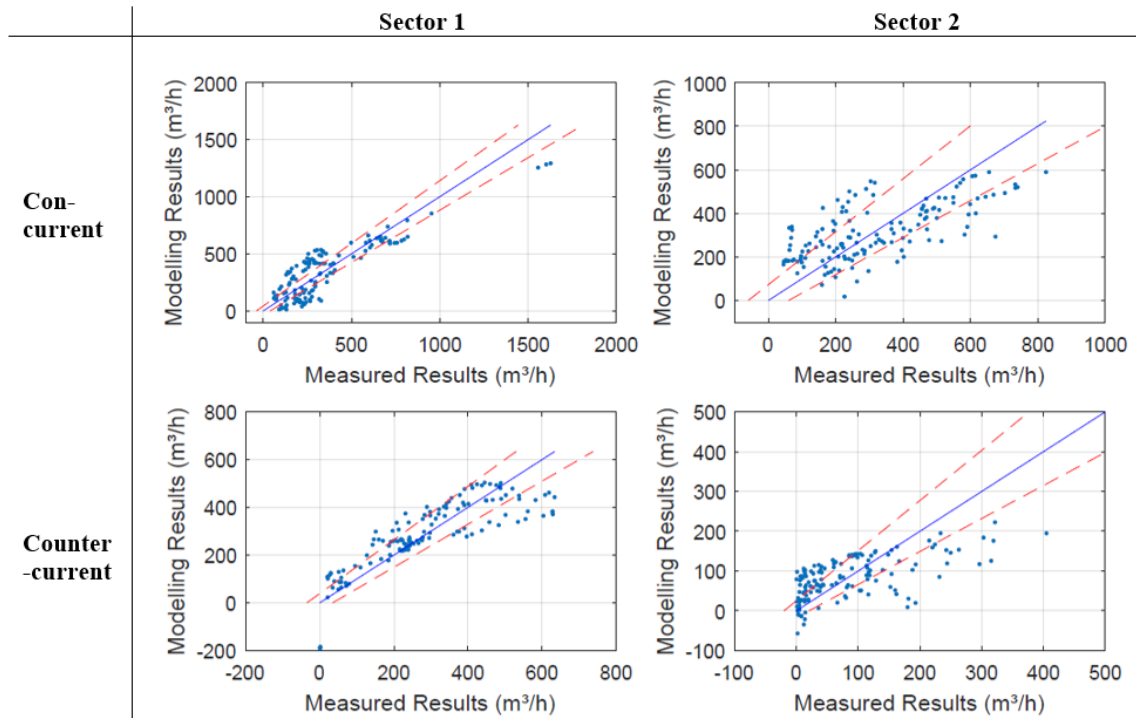


Figure 22: Typical examples of the models and partition airflow rate through the side vent partition 2 with --- : model line and - - - 95% confidence interval model line for (a) con-current airflow rates wind sector 1; (b) con-current airflow rates wind sector 2; (c) counter-current airflow rates wind sector 1; (d) counter-current airflow rates wind sector 2

3.4 General discussion

The experiments were executed without internal obstructions and without surrounding buildings in the immediate vicinity. Although these conditions were not entirely representation of commercial livestock buildings, the experiments were of great value because they involved very detailed (dens sampled) measurements in the openings of a real scale animal mock-up building and under outside wind conditions. These relatively simple circumstances (undisturbed environment) gave the opportunity to make a detailed study of modelling the partition airflow rates whilst investigating the influence of the known measured parameters.

The partition airflow rates in the ridge opening could be modelled accurately and precisely for both wind sectors. All airflow rates of the partitions of the side opening for uni-directional airflows could be modelled accurately and precisely for both wind sectors. For bi-directional flows however, only for con-current flows (app. 90% of the measurements) of wind sector 1 high R^2 -value between 79-90% were found. The models for the counter-current airflow rates or results for wind sector 2 were accurate

(giving a slope of nearly 1 and an intercept of nearly 0 comparing modelling and experimental results) but not precise (giving a low R^2 -value in a range of 19-71%). A possible explanation was that the airflow rates were relatively low (more sensitive to unsteady wind conditions). An extra input variable could give rise to better results, e.g. a local velocity measurement within the partition. For this experiment, the bi-directional flows were limited in number compared to the total amount of airflow rates. However, in naturally ventilated buildings such as dairy barns, these conditions can occur more frequently due to the very large vents (Calvet et al., 2013; De Vogeleer et al., 2016; Etheridge, 2015).

These findings are also important in relation to emission measurements of NH_3 or CO_2 concerning the effect of the airflow distribution on the local concentration measurements in the vents. Information concerning airflow distribution in the vent is of primordial importance for an efficient concentration measurement campaign. Especially as the airflow rate per surface area is not equal for all places in the opening, large airflow rates can go through a small part of the opening. This information can be used to choose the number and position of the sampling points.

As models for the con-current airflows were precise and accurate, it is expected that measurement campaigns can focus more on diversity in conditions of measurements, measuring under different wind conditions as many as possible, and less on measurement repetitions.

Further research should focus on buildings with large vents to validate the findings of this study. The challenge will be to calibrate the proposed models under real life conditions to a reference technique.

3.5 Conclusions

In order to make an analysis of the airflow rate distribution and its predictability in a naturally ventilated animal mock-up building, detailed measurements were executed in ventilation openings. Multiple linear regression was applied to this data, using velocity measurements at a meteoromast of 10 m height (De Vogeleer et al., 2016). The models were validated using detailed airflow rate measurement results of the side and

ridge opening, obtained under different wind conditions. The detailed airflow rate measurements were performed using the method of Van Overbeke et al. (Van Overbeke et al., 2015a). Models were built for different wind direction sectors and for the character of the flow at vent level, i.e. uni- or bi-directional. When the flow was bi-directional, con-current flows (flow going the same direction as outside wind) and counter-current flows (flows going the opposite direction of the outside wind) were modelled and discussed. The velocity components at the meteomast $|\bar{X}_{MM}|$ and $|\bar{Y}_{MM}|$ were used as input variables in a linear regression model to calculate the airflow rates. The airflow rates through all partitions in the ridge vent could be modelled accurately and precisely for both wind sectors ($R^2 > 89\%$). The coefficients for all partitions of the ridge vent were comparable and the coefficient for the $|\bar{Y}_{MM}|$ component was the most important input variable for the ridge vent. The ridge opening mostly behaved as an outlet opening, independently of the wind direction. The airflow rates in the side vent behaved differently depending on wind direction. Models showed that the predictability for the side vent was high for uni-directional flows ($R^2 > 92\%$). Models for bi-directional flows showed good results for flows going the same direction of the outside wind at the windward side ($R^2 > 79\%$), but lower results for flows in vents at the leeward side ($R^2 < 56\%$). The models for the counter-current flows showed larger deviations than those of the con-current flows. Possibly an extra input variable is needed for these types of models to improve precision.

The prediction of the airflow rate distribution in the vents of a naturally ventilated animal mock-up building was feasible using measurement data at a meteomast and simple linear models for consecutive sections of the vent.

**Experiments in an animal mock-up
building: effect of sampling density
on the accuracy of airflow rate
measurements**

Chapters 2 and 3 focused on developing a reduced sampling strategy for the airflow rate measurement technique of Van Overbeke et al. (2016). Simplification of airflow rate measurements is mostly effectuated by lowering sampling density. Therefore, chapter 4 will focus on the quantification of uncertainties on the airflow rates resulting from different sampling densities in the openings, with respect to reduced sampling strategies. In this chapter, different sampling densities were applied for both a direct and a tracer gas method and compared with the detailed sampling method of Van Overbeke et al. (2016) in the animal mock-up building.

4.1 Introduction

Ventilation in buildings is used for controlling indoor air parameters as temperature, relative humidity, velocity and chemical species concentrations (Chen et al., 2009). Measurement of the ventilation rate for naturally ventilated buildings is not always straightforward because naturally ventilated buildings have large spatial and temporal variabilities in velocity in the vents and in the building (Calvet et al., 2013; Etheridge, 2012; Ogink, et al., 2013a), especially for (very) large vents as for e.g. dairy barns (Ngwabie et al., 2009; Saha et al., 2013). Models are available to support measurements for airflow rates through naturally ventilated buildings, but only a few are applicable to buildings with large vents as they are often excluded when high accuracy is needed (Etheridge, 2015). Etheridge (2015) suggested models for naturally ventilated buildings, using a discharge coefficient for the openings. However, because the velocity distributions in large vents are not strictly uni-directional (all velocities go in or out the opening simultaneously), the method using a discharge coefficient is not appropriate. For the same reason of potentially changing directions in the opening, the pressure difference method is not reliable for large vents either (Ogink et al., 2013a). To measure natural airflow rates in livestock buildings, VERA (2011) suggests the tracer gas method. However, according to this protocol, the proposed measurement technique cannot be applied when vents of the building are too open to allow proper mixing of the tracer (high measuring uncertainty exists because the assumption of homogeneity is not fulfilled (Calvet et al., 2013; Joo et al., 2015; Wang et al., 2016)). The VERA-test protocol (2011, currently under revision) states that no adequate method exists to measure the airflow rate when there is no sufficient air mixing. In practice, most experiments to assess natural ventilation in buildings with

large openings use direct methods or tracer gas methods. A lot of these airflow measurements are conducted in the vents of a building. Especially when airflow rate measurements are combined with pollutant concentration measurement. The outlet which is normally considered the most representative sampling location for emission measurements (Ogink et al., 2013a). At the moment, tracer gas methods are mostly using the tracer gas ratio method for emission measurements because there is no need to estimate the airflow rate directly (Mendes et al., 2015b). To measure the airflow rate, direct measurements combine velocity measurements in the vents with the surface area of the openings. Tracer gas measurements are based on conservation of mass of the tracer, while the tracer can be artificial as nitrous dioxide, sulphur hexafluoride, krypton and others (Demmers et al., 2000; Cui et al., 2015) or natural (Edouard et al., 2016; Mendes et al., 2015b; Ngwabie et al., 2014; Samer et al., 2011a). A disadvantage of these tracers is that they are all air pollutants and/or greenhouse gases. CO₂, also a greenhouse gas, is still one of the least polluting tracers, even if artificially inserted and not natural available. For both direct and tracer techniques, air is locally sampled. Dense sampling of the full opening is recommended because of wind variations, but this approach is not realistic for large vents. So currently, the conventional way is to treat the velocity distribution of a vent as a mainly uniform profile using a limited sampling density (Lo et al., 2012), however, few or no calibration is conducted to compare this simplification to the true mean velocity over a surface. Choosing sampling locations that are representative of the full building or vent is crucial to obtain accurate measurements. The accuracy of a method is related to the number of measurement points used (Joo et al., 2014). However, not only the number of sampling locations, but also the positions of the sampling points have an impact on the accuracy. Kiwan et al. (2012) measured the velocity in the vent at three different heights and found that the velocity varied over the whole area of the opening and found the highest air velocities at the centre of the opening (Özcan et al., 2009). Not only air velocities, but also point concentrations of the tracer method are influenced by wind speed and wind direction (Saha et al., 2013). The choice of sampling locations could result in errors up to 86% for measurements inside a mechanically ventilated building (Van Buggenhout et al., 2009), so errors for naturally ventilated buildings could be expected to be higher due to effects of changing wind conditions.

Currently, for economical or practical reasons, measurement simplifications, mostly

carried out by sampling along a horizontal line in the side vents (Joo et al., 2014; López et al., 2011; Rong et al., 2015; Zhang et al., 2005) are applied without a prior study for determination of the accuracy against the actual airflow rate. Moreover, the airflow rates obtained by simplified methods, are being used as reference to test or calibrate proposed models. However, the main problem to determine uncertainties due to measurement reduction is the lack of a reference (Takai et al., 2013b; Van Buggenhout et al., 2009), especially when investigating the effect of using a limited number of sampling points on the uncertainties under changing wind conditions (López et al., 2011). Ogink et al. (2013a) stated that few scientific reports on field measurements can be found concerning the effect of high variation of the wind velocity in the openings and the fact that measurements are sampled only locally. Because no reference technique is available in buildings with very large openings, the accuracy of airflow rate measurements cannot be determined, only the precision of the measurements. Nevertheless, measurement conditions (e.g. wind unsteadiness) are of great impact on measurement results of airflow rates and results of uncertainty analyses should therefore always be noted (Calvet et al., 2013).

To overcome measurement uncertainties due to spatial and temporal variability in the opening, Van Overbeke et al. (2015a) developed a detailed direct measurement method to determine natural ventilation rates in an animal mock-up building. The detailed data generated by the experiments using this method, can be used to test accuracy and precision when reducing the number of measuring locations (Van Overbeke et al., 2014b).

The objective of this chapter is to determine the effects of sampling density on the uncertainty of airflow rate measurements in a naturally ventilated animal mock-up building. Both a direct measurement method using anemometers and a tracer gas method were compared against the reference method of Van Overbeke et al. (Van Overbeke et al., 2016).

4.2 Materials and Methods

4.2.1 *Animal mock-up building and experimental setup*

The animal mock-up building and its surroundings are described in detail in §2.2.1.

4.2.2 Airflow rate methods

4.2.2.1 Direct airflow rate measurements

Reference airflow rate measurements were obtained applying the technique developed by Van Overbeke et al. (2016) and also applied by De Vogeleer et al. (2016) using a high sampling density of direct wind velocity measurements (Van Overbeke et al., 2016). The velocities in the opening were densely measured using ultrasonic anemometers in the vent openings and the airflow rate was calculated as a result of the multiplication of the measured air velocities and the surface areas representing the respective air velocities [14].

$$Q_{tot} = \sum_{k=1}^n (|\bar{Y}_{ms}|_k \cdot A_k \cdot 3600) \quad [13]$$

Where

Q_{tot} = mean airflow rate through the mock-up building over a period of approximately 1.5 h (m^3/h)

k = measurement surface

$|\bar{Y}_{ms}|_k$ = mean normal velocity component over a period of approximately 1.5 h in measurement surface k (m/s)

n = total number of measurement surface areas in the side or ridge vents (in this case particularly 48 for a side vent and 8 for a ridge vent).

A = measurement surface area (m^2)

The ridge opening was equipped with 8 fixed *2D* ultrasonic anemometers (Thies®, Göttingen, Germany) equally spread over the length of the opening and mounted as close as possible to the axial symmetry of the ridge.

Each side opening was equipped with a single *3D* ultrasonic anemometer (Thies®, Göttingen, Germany) fitted in an automated linear guiding system to allow measurements at 48 predefined locations in the opening (4 rows and 12 columns). For this study solely the velocity components normal to the opening were analysed.

The sensor had a measuring speed of 250 Hz and every 1 second these measurements were averaged and logged. Each sampling location was sampled during 10 s before moving to the next one. One measuring round was obtained after measuring all 48 locations. In total 10 such measurement rounds were conducted sequentially. The velocities per sampling location were averaged over 10 measurement rounds.

Using this method, an accuracy of $(8 \pm 5)\%$ was obtained for in- and outgoing airflow rates through the building. Measurements were executed continuously day and night over a period starting from December 2014 through March 2015.

4.2.2.2 Indirect airflow rate measurements

The constant injection method was used to determine the airflow rate using tracer gas measurements. The method is based on mass conservation of the tracer. The tracer is injected into the building with a constant volume rate. The dilution of the tracer in the air is a measure for the airflow rate (formula [14]). The tracer, carbon dioxide CO_2 , also used in the method suggested by VERA (2011), was selected because it is one of the least polluting tracers and because it is non-toxic to humans in the concentrations used. The volume rate of the tracer was chosen so the concentration of the mixed air was easily detectable and at a level of normal CO_2 concentrations in a (dairy) barn.

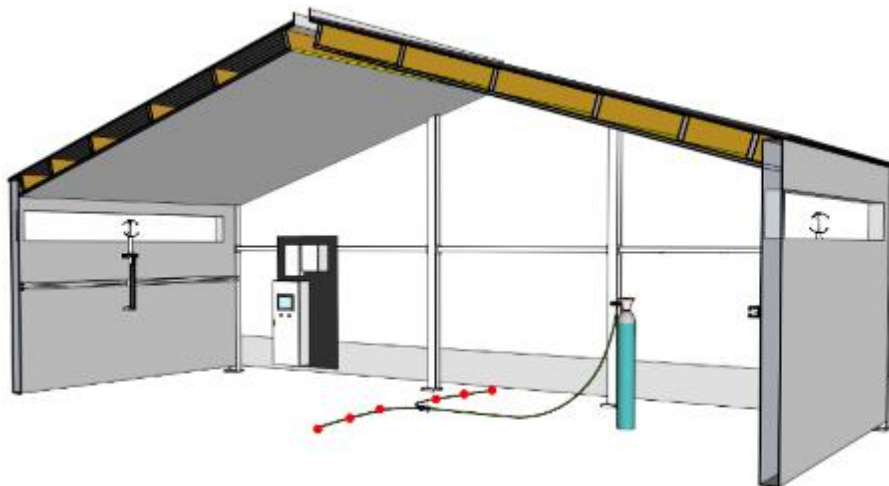


Figure 23: A 3D sketch of a section of the animal mock-up building at the Institute for Agricultural and Fisheries Research in Mellebeke with CO_2 gas bottle and CO_2 release locations (●) and anemometers in the opening mounted on linear guiding systems

The injection rate was set to a constant value during the complete experiment. The CO₂/air mixture was sampled by two Infrared Photoacoustic Detectors (multi gas monitor type INNOVA 1312 and 1314). The INNOVAs were calibrated within the year before and were tested against span gases to correct for possible drifting. The default configuration settings of the INNOVA were used for the chamber flushing time (10s) and tube flushing (13s), the measurement of the tracer gas was carried out every 1 min. All sampling tubes connected to the INNOVAs was made of polytetrafluoroethylene (PTFE), that had an internal diameter of 3.2 mm and a length of 15m.

Before starting the experiments, the temperature of the heating chambers of the INNOVAs were stabilised during 1 hour. The CO₂-background level of the air was measured during 10 minutes before releasing the tracer. The tracer was released from bottles of 20 kg CO₂. A gas pressure controller was used to lower the bottle pressure to a lower pressure. The actual CO₂ volume was released with a mass flowmeter (Bronckhorst) and logged by a GRANT Squirrel data logger. Temperature and air pressure data were obtained from the Royal Meteorological Institute weather measuring station in BE-Melle.

Uncertainties of the measurements are related to the number of observations and time basis of measurements, the choice of sampling points and the mixing of the tracer in the experimental house.

Selection of the number of observations and time basis of the experiment depended on the availability of 2 INNOVAs, the configurations and the possibility to release the gas at a constant rate. Generally five measurement locations were used in the side outlet, and three in the ridge opening. For winds parallel to the vents, three measurement locations in each side opening were sampled. Gas concentration measurements were performed continuously, all sampling points were measured twice before measuring the next point. The measurement values for each location were averaged over one hour to calculate the airflow rate with formula [14]. In order to maintain a constant flow from the CO₂ bottle, a 1 hour period was chosen as injection time. An hour was found to be a reliable averaging time to estimate the airflow with tracer gas measurements (Gao et al., 2009).

The first experimental choice was to place the sampling locations in the vents (and not

inside the building). Although this location was risking measurements with backflow, this was found to be the best choice because this was the most reliable place to measure all outgoing mixed air/tracer. The direct measurements using the anemometers were used simultaneously and were able to measure possible backflow. The second experimental choice was how to locate the sampling points with respect to the geometrics of the building and openings. All sampling locations were evenly distributed over the width of the opening and placed in the middle of the height of the opening. The concentration measurements were measured by two INNOVAs.

The choice of the release and mixing potential of the tracer is important for the homogeneity of the mixed air/tracer. The tracer was not released in the supposed inlet, but in the middle of the building. No mechanical mixing was applied so the natural airflow would not be disturbed. To enhance a homogeneous mixing, the tracer was injected at 6 different locations near ground level (Figure 23). The measurements started after 10 min. of tracer release.

Nine tracer gas tests were executed on 7 different days in March and in the period of August-September 2015. Simultaneously, the airflow rate measurements with the reference method took place.

$$Q_{tot} = EMR / ((CO_{2m} - CO_b) \times 10^{-6} \times \frac{MMass}{M} \times \frac{Pr}{Pr_{ref}} \times \frac{T_{ref}}{T}) \quad [14]$$

Q_{tot}	Airflow rate (m ³ /h)
EMR	CO ₂ injection rate (g/h)
CO_{2b}	Background CO ₂ concentration (ppm)
CO_{2m}	Measured CO ₂ concentration in outlet (ppm)
$MMass$	Molar mass CO ₂ (44,01 g/mol)
M	Molar volume for 0°C and 1 atmosphere (0,022414 m ³ /mol)
Pr	Air pressure measured during experiments (hPa)
Pr_{ref}	Reference air pressure (1013,25 hPa)
T	Measured internal air temperature (K)
T_{ref}	Reference temperature (273,15 K)

4.2.3 Sampling density reduction schemes

Simplified methods were introduced for both direct and indirect measurements. These were executed by reducing the sampling density. The simplified methods were compared against the detailed (dense sampled) measurements of the method of Van Overbeke et al. (2016) as the reference.

4.2.3.1 Direct airflow rate measurements

Different sampling densities for both the side and ridge vents were tested to study the effects on accuracy for the direct measurement method (Table 11). Reduction schemes for the side vent were divided in 3 different patterns: a chess pattern, a horizontal and a vertical line pattern. The ridge opening had only a horizontal line pattern due to its dimensions. In the width of the ridge opening, a simplification was already introduced in the reference method by multiplying the measured velocities with a pipe or reduction factor. This factor takes into account losses of contraction of the airflow through the ridge vent. More details can be found in the work of Van Overbeke et al. (2016).

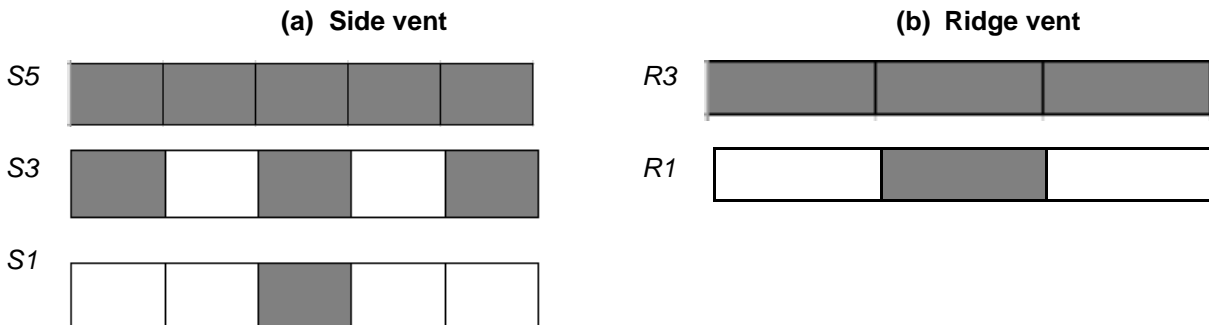
Table 11: Lowering the sampling density for the side vent using a chess pattern, horizontal and vertical line patterns; and for the ridge vent using a horizontal line pattern

Side opening			Ridge
<p>Chess pattern</p> <p>SC24</p> <p>SC12</p> <p>SC6</p> <p>SC3</p> <p>SC1</p>	<p>Horizontal line</p> <p>SH12</p> <p>SH6</p> <p>SH3</p> <p>SH2</p> <p>SH1</p>	<p>Vertical line</p> <p>SV4</p> <p>SV2a</p> <p>SV2b</p> <p>SV1</p>	<p>Horizontal line</p> <p>RH4 RH2 RH1</p>

4.2.3.2 Indirect airflow rate measurements

Due to the limited number of sampling points to measure tracer gas concentrations, only horizontal line simplification was conducted (Table 12).

Table 12: Simplification of the concentration measurements in (a) the side vent and (b) the ridge vent of the animal mock-up building



4.2.4 Analysis of the reliability of airflow rate measurements

Because uncertainties are of great importance to know the reliability of airflow rate data and because statistical terms are not always used within the right context, the uncertainties of emission measurements were discussed by Calvet et al. (2013). Natural ventilation is a challenging component, the former article is of great value for emission measurements using the method based on multiplication of the pollutant concentration and airflow rate (Ogink et al., 2013a). The statistical terms used in this study are clarified further in combination with Figure 24. To calculate the true errors on the measurements, the true airflow rate or velocities are to be known. The detailed method of Van Overbeke et al. (2016) proved to have an accuracy of $(8 \pm 5)\%$ and could therefore be used as a reference.

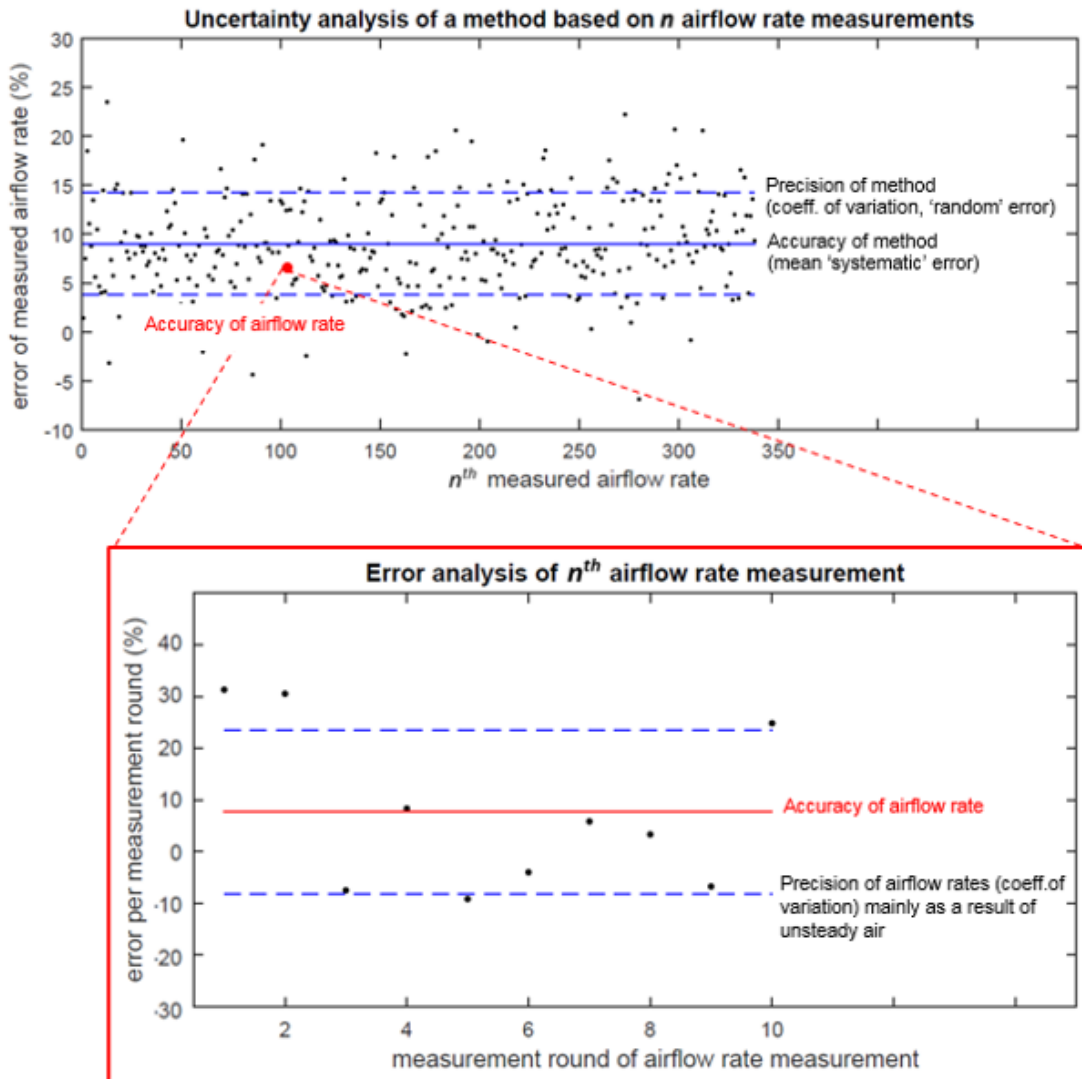


Figure 24: Explanation of statistical terms concerning the uncertainty of a measurement method and the errors on the airflow rate measurements

Distinction is made between the uncertainty of a method (applying different sampling densities) and the error on a single airflow rate measurement. The error analysis will characterize the nature and magnitude of the errors of the single airflow rate measurements based on 10 sampling and measurement rounds within each measurement cycle. The uncertainty of a method aggregates all errors of all respective single airflow rate measurements (Calvet et al., 2013). The spread of all errors of the single airflow rate measurements is a measure for the precision of the measurement method, and the mean of all errors is an estimate for its systematic error. Statistically, a constant environment is needed for the determination of these parameters. However, in a natural environment, unsteadiness of the wind has an influence on the

measurements. Consequently, the unsteadiness of the wind is integrated in the results of the accuracies. The terms “accuracy, systematic error and precision” are used to describe both the reliability of the measurement method (uncertainty analysis) and of the ‘single’ airflow rate measurements (error analysis). The accuracy is understood as the closeness of agreement between the measured airflow rate (or method) and the reference airflow rate (or method) (BIPM et al., 2008) and is expressed by the systematic error and precision. The systematic error was determined by calculating the (relative) difference between the airflow rates obtained by the tested sampling density and the reference (plotted in the following graphs Figure 27 to 30 as red points and error bars). The systematic error of both the method and single airflow rate measurements are determined by comparing the simplified (reduced sampling locations) and detailed measurement techniques. The precision is a measure for the repeatability of the airflow rate measurement (or method) and is expressed as the relative standard deviation (or coefficient of variation) of the airflow rate measurement (or method) (BIPM et al., 2008). During the experiments, the precision of the measurements is affected by the continuously changing variation of the airflow rate due to changing wind conditions. Both the systematic error and the precision are given as an absolute and a relative number.

To avoid outliers in the dataset, it was chosen to leave out all airflow rates for a normal wind velocity <1 m/s for further processing. Still 83% airflow rates of the full dataset remained.

For these experiments, the uncertainty analysis gives information of whether a method gives systematic errors. The accuracy of the airflow rate measurements was mainly the result of the air unsteadiness in the opening, the number and places of sampling locations and random errors. To find correlations between the precision and accuracy of the airflow rates and the influencing factors, a sensitivity analysis was executed in §4.3.1.1 where the coefficients of variation were plotted against the incidence angle and the wind velocity.

The accuracy of the ultrasonic anemometer (0,1 m/s for values ≤ 5 m/s) and the INNOVA (2,5% of the measured value) was significantly smaller than the accuracies found in the results and were not mentioned further.

4.2.4.1 Experimental conditions

In total, 833 airflow rates were experimentally determined for different wind conditions as shown in Figure 25. Winds coming from South West (main wind direction) dominated the dataset. One side vent was directed towards the SW as plotted in Figure 25a. Winds parallel to the ridge and side vents were least represented. Maximum airflow rates went up to 36 603 m³/h, which resulted in an air exchange rate of approximately 145 h⁻¹.

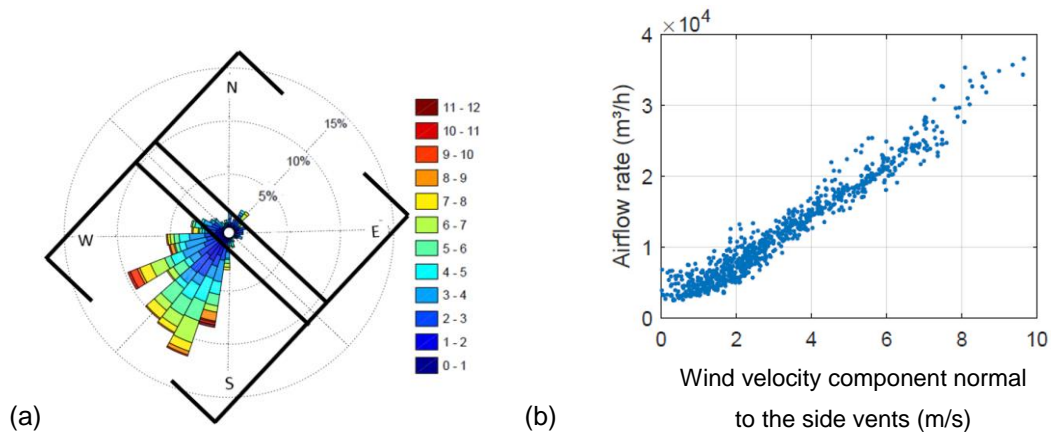


Figure 25: (a) Wind rose: wind conditions during airflow rate measurements with a floor map of the animal mock-up building; (b) Mean airflow rates against the wind velocity normal to the side vents

The measurement method of Van Overbeke et al. (2016) performed measurements of a detailed pattern in the openings. These measurements could give information whether flows in the opening were in- and/or outgoing, which is important information for the tracer gas experiments. Bi-directional flows in the vents were mainly the result of low wind velocity or low incidence angle of the wind as found in previous research using the same animal mock-up building (De Vogeleer et al., 2016). The counter- and con-current flows of the bi-directional flows were calculated by summing all airflow rates going in or out the vent. Occurrence of bi-directional flows was predicted best in the mock-up building with the wind component normal to the side vents (De Vogeleer et al., 2016). Figure 26 shows (a) the counter-current flow rate relative to the mainstream flow rate and (b) the absolute counter-current flow, both against the wind component normal to the side vents. Only results of the inlet are shown, those for the outlet vents were similar. The graph shows some high ratios between the in- and outgoing air, but absolute values show that these flows are still small compared to the

maximum airflow rates in Figure 25.

The ridge opening acted almost always as an outlet only (De Vogeleer et al., 2016) except for 1% of the dataset. This 1% data was left out due to a low number of measurements.

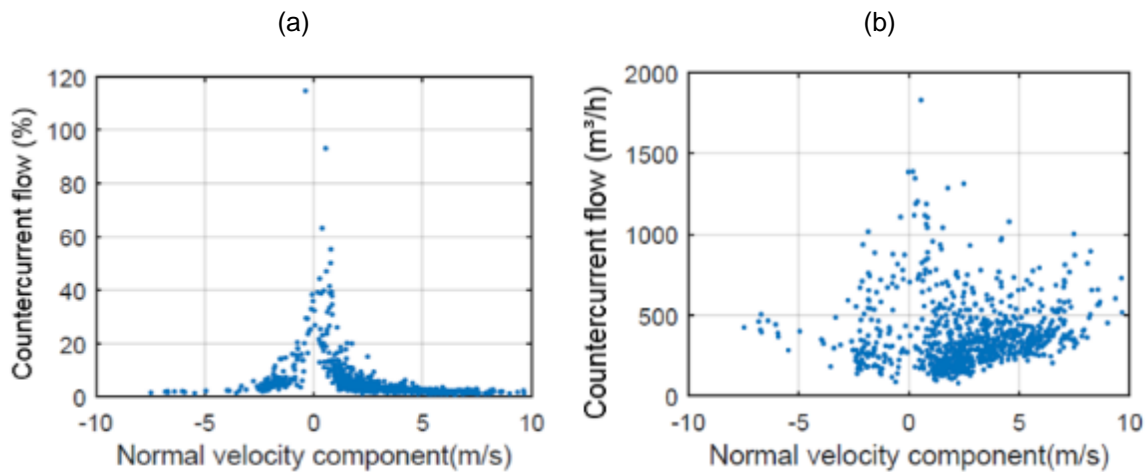


Figure 26: Counter-current flows in the inlet side opening related to the normal wind component for (a) the ratio of the outgoing airflow rates on the mean airflow rate (b) the absolute airflow rates

4.3 Results and discussion

4.3.1 *Direct airflow rate measurements*

4.3.1.1 Effect of sampling density on the reliability of the airflow rate measurements

The errors on the measured airflow rates and the uncertainties of the method were determined for both the ridge and side vents (inlet and outlet) and for all sampling patterns (vertical, horizontal, or chess pattern).

4.3.1.1.1 *Uncertainty analysis*

The inaccuracy of all methods with different sampling density for the side openings were plotted for both in- and outlets in Figure 27. The mean accuracies using the simplified method were plotted as dots, the coefficients of variation of these accuracies were plotted using error bars.

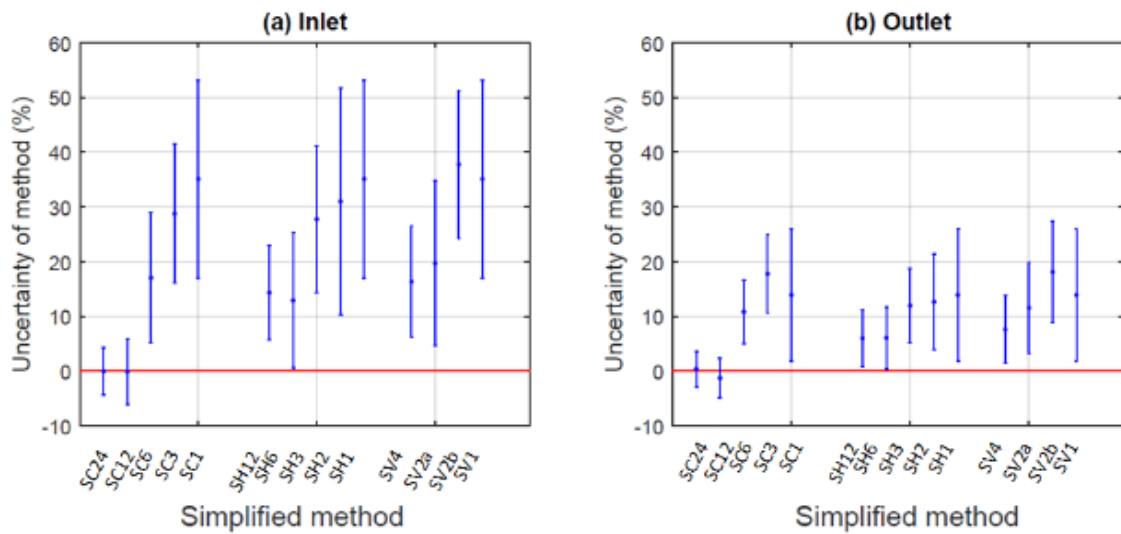


Figure 27: Uncertainty of different methods: for the reference (red line) and different sampling densities for the side openings for (a) the inlet and (b) the outlet, respectively with • the mean error of the measured value (systematic difference) and the error bar as the coefficient of variation of the measured value (precision)

Overall, the results showed a positive deviation for the simplifying methods, meaning an overestimating of the airflow rate through the side vent. Compared to the reference method, the chess pattern gave very good values for both halves of the maximum measurement places SC24 and a quarter of the measurement places SC12. No significant difference was found. For the pattern SC6 approximately $(17 \pm 12)\%$ and $(11 \pm 6)\%$ uncertainty were calculated for the inlet and outlet, respectively. Less sampling locations gave rise to lower accuracy. When measurement reduction was applied over a horizontal line, the maximum sampling locations SH12, still had a deviation of $(14 \pm 9)\%$ and $(6 \pm 5)\%$ for inlet and outlet, respectively. Reducing the number of measurement places to 50%, gave similar results, but further reductions gave larger deviations. When a vertical line of locations in the middle of the vent was used to determine the airflow rate, an overestimation of $(16 \pm 10)\%$ was found. Further reduction of locations using the middle 2 locations or the combination of a middle and a location, gave higher errors compared to all vertical locations. However, the mean deviations between these similar configurations with 2 locations were not significantly different from each other.

These results confirm literature findings that the middle of the opening is less subjected

to friction near the edges of the opening (Etheridge, 2012). Consequently, measurements in the middle give higher values than the mean velocity in the opening. Comparing the different patterns of the side vents, it was seen that although the same number of sensor locations was used for two different configurations, the pattern SC12 gave a better accuracy for the inlet (0 ± 6)% and outlet (1 ± 4)% of the measured value, compared to the pattern SH12 with (14 ± 9)% for the inlet and (6 ± 5)% of the measured value for the outlet. These results show that measuring at equally distributed locations over the whole vent opening area, is giving a more representative result and better accuracies than measuring at horizontally or vertically restricted areas in the vent. Comparing measurements in the ridge opening gave very steady variation results (Figure 28), a better precision and systematic error of the results was found. Measuring the airflow rate through the ridge vent with only one sampling location did not have a significantly different result from the reference using all locations. Measurements using only one sampling point had a deviation of (2 ± 3)%.

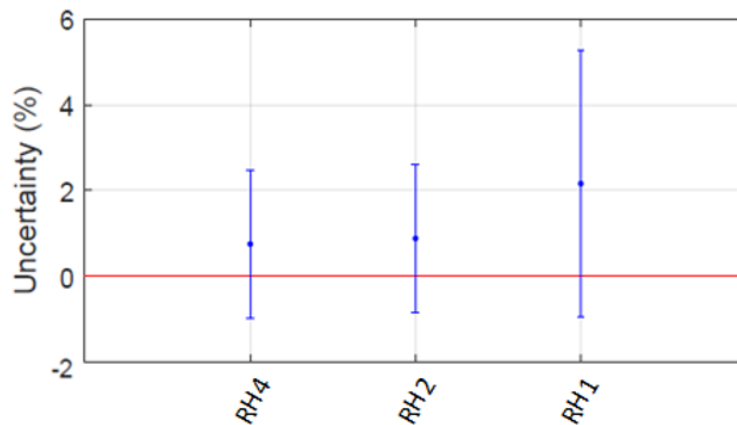


Figure 28: Uncertainties for the reference method (red line) and the methods with different sampling densities for the ridge opening with • the mean error of the measured value (systematic difference) and the error bar as the coefficient of variation of the measured value (precision)

4.3.1.1.2 Error analysis

Overall results of the errors on single airflow rate measurements showed that lowering the sampling density resulted in lower precision and higher relative standard deviations (Figure 28 and Figure 29). This could be explained statistically by the uncertainty calculation where more available measurements within one measurement cycle tend to lower the uncertainty. The results of the coefficients of variation for the airflow rates of the side opening are presented in Figure 29. The coefficients of variation for the inlet

and outlet airflow rates lay within the same range. The reference method had a coefficient of variation of $(5 \pm 1)\%$ for both the inlet and the outlet. The highest uncertainties were found when using only one sampling location, for which the coefficients of variation were $(28 \pm 12)\%$ for the inlet and $(29 \pm 10)\%$ for the outlet.

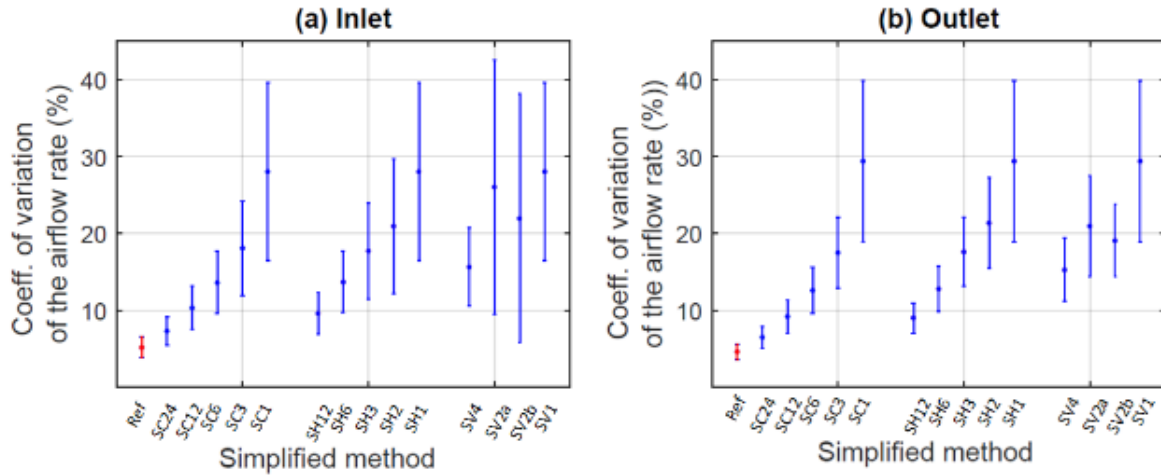


Figure 29: Coefficients of variation of the airflow rates for the reference airflow rates (marked in red) and the different sampling densities for the side openings acting as (a) an inlet and (b) an outlet with • the mean coefficient of variation of the measured value and the error bar explaining its own variation

Error analysis for the ridge opening (Figure 30) showed an error of $(10 \pm 4)\%$ for the use of all sensors and an error of $(26 \pm 11)\%$ when only the middle sensor was used. Comparison of all uncertainties using only one sensor in the vent showed that the velocities in the ridge opening were significantly not different from each other. Measurements of one sensor in the ridge vent gave an uncertainty of $(26 \pm 11)\%$ compared to the uncertainty of the side openings of $(29 \pm 11)\%$.

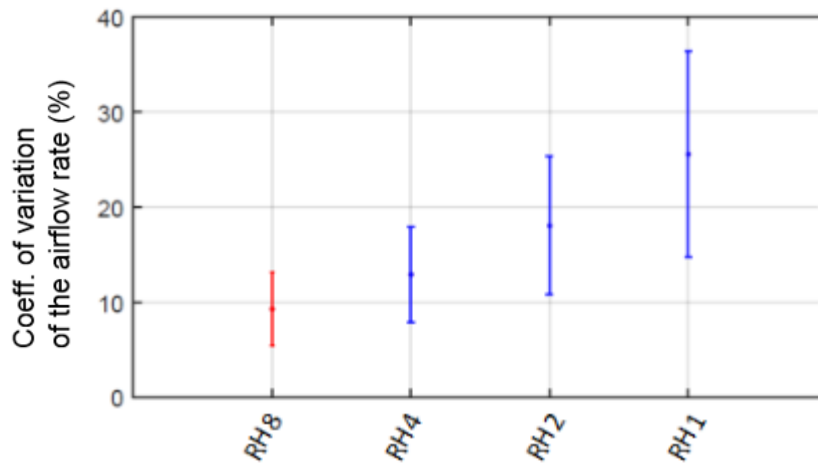


Figure 30: Coefficient of variation for the reference (RH8) and the different sampling densities (RH4-2-1) for the ridge vent with • the mean coefficient of variation of the measured value and the error bar

4.3.1.1.3 Sensitivity of variations in measurements in the side vent due to (mainly) the wind effect

The coefficients of variation for the airflow rates in the side vents were given. In Figure 29. To investigate whether these results were constant or correlated with wind components, the results for sampling density SH12 were plotted against the incidence angle and the normal wind component (Figure 31). The plot with the errors on the airflow rates against the incidence angle shows similar results between 50 and 90° (normal to the vent) incidence angle. The results for the incidence angles under 40° were not plotted because there were too little measured airflow rates (<10). The wind component normal to the side vent seemed to have a large influence on the errors. The coefficient of variation decreased for higher incidence angles and a higher normal wind velocity component. This means that the steadiness of the wind increased for higher incidence angles and for winds normal to the vents.

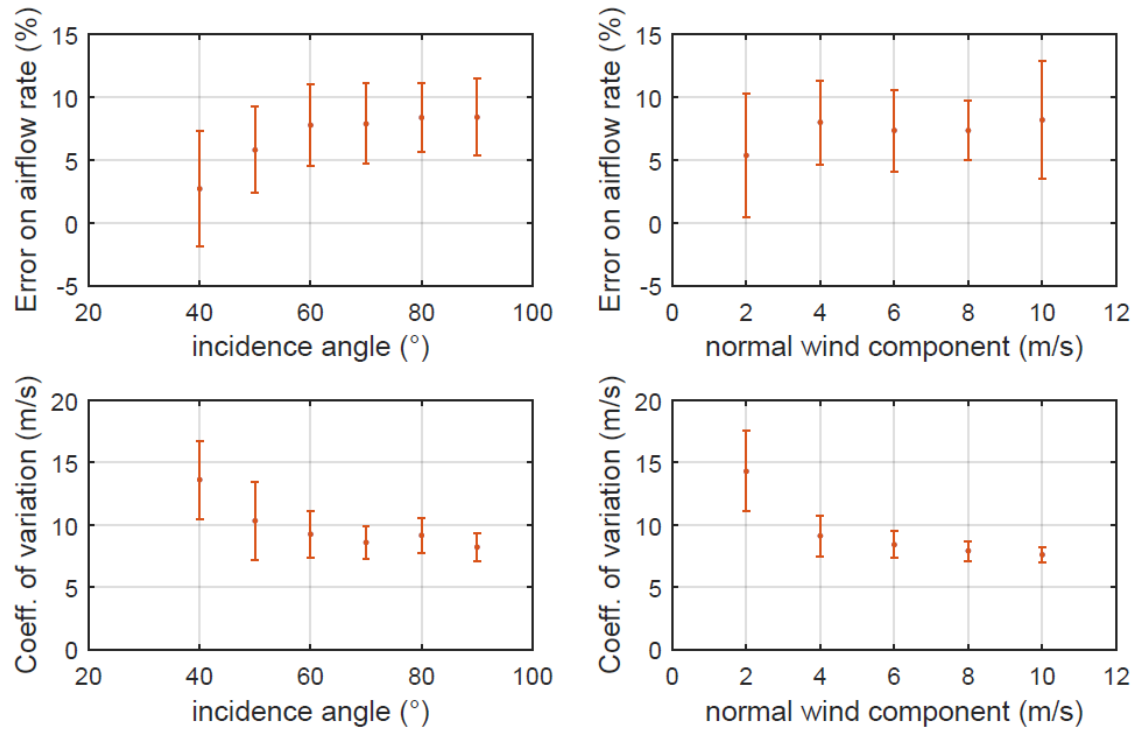


Figure 31: Errors on the airflow rate against (a) the incidence angle (°) and (b) the wind component normal to the side vents; the coefficients of variation (m/s) for (c)) the incidence angle (°) and (b) the wind velocity component normal to the side vents

4.3.2 Indirect airflow rate measurements

4.3.2.1 Experimental conditions

Nine different tracer gas experiments were performed (Table 13). A first analysis of the wind conditions showed varying wind direction and wind velocity, as was expected for natural ventilation. The estimated average airflow rates using the tracer gas method (Table 15) had errors because the actual airflow rates were not constant. Previously, this was already found by (Sherman, 1990).

Table 13: Information tracer gas experiments: experiment number, date, injection rate *EMR* (CO₂ l/min), wind direction (°) with the incidence angle *IA*, total velocity *MM* (m/s), temperature (°C)

Exp.	Date	<i>EMR</i> (CO ₂ l/min)	Wind direction (°)			Total velocity (m/s)		Normal veloc. (m/s)	Temp. (°)
			Mean	SD	IA	Mean	SD		
1	13/03/2015	20	73	19	73	3,6	0,9	3,4	12,2
2	16/03/2015	40	15	27	15	2,5	0,9	2,4	7,1
3	17/03/2015	30	49	20	49	2,1	0,6	1,3	6,3
4	17/03/2015	35	22	40	22	1,6	0,7	1,5	8,9
5	20/03/2015	30	342	37	18	2,9	0,7	2,7	9,0
6	3/08/2015	35	197	18	17	3,6	1,1	3,4	26,3
7	13/8/2015 (a)	35	44	13	44	4,8	0,9	3,4	25,0
8	13/8/2015 (b)	35	40	13	40	5,6	1,0	4,3	30,5
9	11/09/2015	35	52	-	52	6,3	-	3,9	17,1

The airflow rate was determined by measuring the dilution rate of the tracer in the air. Bi-directional flow cannot be detected with the tracer gas method, but it can cause large errors in the measurements. Flows going in and out the opening, can give a larger dilution of the tracer and can give faulty larger airflow rates (Kiwani et al., 2012). It is therefore in general not recommended to place sampling locations in the vent opening plane. Table 14 shows the relative airflow rate of the flow with opposite direction to the main wind direction, measured using the reference technique of Van Overbeke et al. (2016). It showed that for low incidence angles, the counter-current flow ratio (against the mean airflow rate) increased. Also, for these incidence angles, the outlet is a little less subjected to bi-directional flows than the inlet vent.

Table 14: Relative airflow rate at vent level with opposite direction to the flow of the main wind flow in the opening

Experiment	IA	Ratio countercurrent flow/main flow (%)		
		Side Inlet	Side Outlet	Ridge
1	73	1,3	2,9	0
2	15	10,6	9,5	0
3	49	31,5	13	0
4	22	1,1	3,5	0
5	18	1,2	2,4	0
6	17	0,7	3	0
7	44	1,1	3,9	0
8	40	21,3	10,8	0
9	52	28,1	12,8	3,1

4.3.2.2 Effect of sampling density on the reliability of the airflow rate measurements

The uncertainty analysis of the tracer gas method was difficult to perform because only a limited number (nine) of single airflow rate measurements was available to support the analysis. However, comparing the results of the separate tests (Table 15) allows to see large variation in the errors for the different sampling densities. Similar to the results of the direct measurements, it was seen that high variations occurred for lower normal wind components, although these were not below 1 m/s as premised earlier as outlier limit for the direct method.

For both in- and outlet openings, the airflows through the side vents were not perfectly uni-directional, meaning that (small) opposite airflows were present. These flows cause errors in the airflow determination because (a small) part of the inlet is used as outlet or vice versa. For small ratios, these errors/uncertainties, though difficult to determine exactly, stay limited. But for unsteady bi-directional flows, the assumptions of avoidance of re-entrainment are not fulfilled. As a result, the errors became as large as 147% and 572% for case 2 and 3, respectively. Therefore, knowledge of the airflow rate distribution in the vents is necessary to know when to apply this method for naturally ventilated buildings.

The accuracy of the indirect single airflow rate measurements is difficult to compare exactly with those of the direct measurement method because the sampling time (before averaging) was not identical for both methods. Still, higher coefficients of variation were found in a range of (8.3 – 34)% compared to direct measurements. A possible reason could be that the airflow rate was averaged over less single measurements (frequency of measurements was lower), but also non perfect mixing could be a source of the unsteady results. Still, the tracer was released at different points within the animal mock-up building, but because of the natural ventilation and the lack of natural breathing impulse of animals, mixing could not be controlled and was expected to be non-perfect. This non-perfect mixing attributes to the inaccuracy of the method (Sherman, 1989). Also, the averaging of the varying concentrations concerning unsteadiness of the wind could give a biased estimate of the airflow rate (Sherman, 1990).

Simplified sampling methods were investigated on the tracer gas tests too. The methods depended on the combination of sampling locations used in the vents. Five sampling locations in the outlet and three in the ridge vent were referred to as 5S-3R. These simplified methods gave irregular results. It was expected that the less measurement points were used, the lower the accuracy or precision would be. However, this was not observed in the results. These unexpected results could be explained by the high standard deviations of the measurements of the single sampling locations so no significant differences could be found. Variation in the concentration measurements and the occurrence of bi-directional flows were important limitations to measure the airflow rate with the tracer gas method.

Table 15: Error analysis of tracer gas tests: reference airflow rate; absolute and relative error (systematic difference and precision); standard deviation and relative standard deviation, for the different test cases

Meth.	Q (m ³ /h) REF	Systematic diff. (m ³ /h)			Systematic diff. (%)			Precision (m ³ /h)			Precision (%)			
		5S-3R	3S-3R	1S-1R	5S-3R	3S-3R	1S-1R	5S-3R	3S-3R	1S-1R	5S-3R	3S-3R	1S-1R	
1	8 648	-85	-1 331	218	-1,0	-15,4	2,5	1123	1143	2157	13,1	13,5	24,3	
2	2 575	3 767	3 214	4 248	146,3	124,8	165,0	1439	1498	1285	22,7	24,3	18,8	
3	1 172	6 714	5 141	6 178	572,7	438,5	527,0	2678	3037	2758	34,0	37,8	37,5	
4	8 224	-	- 429	- 578	-	-5,2	-7,0	-	986	1942	-	12,7	25,4	
5	9 412	179	364	975	1,9	3,9	10,4	959	1075	1956	10,0	11,2	18,8	
6	14 349	-2	131	-2 344	-1 058	-14,8	-16,3	-7,4	910	989	1569	7,5	8,5	11,8
7	11 893	-394	-2 072	813	-3,3	-17,4	6,8	959	1003	2094	8,3	9,1	16,5	
8	5 550	-	851	2 064	-	15,3	37,2	-	848	1041	-	13,6	13,7	
9	6 647	-	12	25	-	191,4	382,3	-	838	2952	-	8,0	17,7	

4.4 General discussion

Evaluations of systematic errors are especially of importance for emission purposes. Still, to our knowledge, only few studies are available on the accuracy of (simplified) measuring methods. Therefore comparison of results on the uncertainties on airflow rate measurements in naturally ventilated buildings to literature was difficult.

For the direct measurement method, Joo et al. (2015) performed measurements with a simplified technique using only sampling locations in one horizontal plane in the vents. They recognized the limitations of this approach and simultaneously performed

a vertical velocity profile measurement with 3 sensors. It was mentioned that obstacles such as structural members of the barn, may cause non-uniform vertical and horizontal gradients in downwind openings. However, no more attention was given to the vertical profiles because these were subjected to large uncertainties since relative instrument precision was low for the range of measured velocities.

Comparing the results with literature for the indirect measurement is less applicable because of our specific setup related to the size of the building and duration of the experiments. However the experiments confirm results of other studies stating that the positioning of the sampling locations is of great importance and that it is in general not recommended to place sampling points in the vent opening plane. The results also confirmed the large sensitivity of the tracer gas method to wind variations (place and time), bi-directional flows and/or mixing difficulties (VERA 2011).

A (spatial) simplification of a measurement method without giving in on accuracy implies not only reducing the number of sampling locations, but carefully choosing the remaining locations. Choosing the pattern of sampling locations greatly affects the representativeness of the airflow measured in the opening. The most commonly used simplification of the measurement method for experiments on buildings with large vents is to apply a horizontal line of equally spaced sampling locations to measure the natural ventilation through a vent. This configuration is known to lead to overestimation of the measured airflow rates (Kiwani et al., 2012; Van Overbeke et al., 2016). An overestimation of 14.9% was found for the in- and outlet of the animal mock-up building, respectively. These inaccuracies might decrease for larger openings compared to those of the animal mock-up building. Applying a reduction or pipe factor as suggested by American Society of Heating, Refrigerating and Air-Conditioning Engineers, (2009) is of interest for many experiments. Of course, these factors need to be calibrated before application. Further research should focus on reliable calibration data.

Although bi-directional flows were found to be small in magnitude and number, knowledge of the airflow rate distribution was of great importance for interpreting tracer gas and direct methods results. For direct measurements, it is important to know the uni- or bi-directional pattern with respect to sampling location selection. For tracer gas

measurements, misidentifying the in- and outlet zones can lead to great errors (dilution of the tracer) or tracer may leave in unexpected zones of an opening where no sensors are installed. The knowledge of flow distribution is especially important for natural ventilation as the wind conditions can alter unexpectedly. Precision for measuring the airflow rate with tracer in this experiment was found to be low, mainly due to not perfectly mixed tracer/air and changing wind conditions and positioning of the tracer sampling locations.

The experiments for this study focused on spatial simplification. Further research should focus on the impact of temporal simplification because choosing longer periods for averaging measurements can be favourable to minimize unsteady measurements due to fluctuations (increase precision). Contrarily, choosing a period that is too long, may lead to a decrease in precision due to changes in wind conditions (Van Overbeke et al., 2015a).

This research was conducted from airflow measurements of naturally ventilated buildings, but all results are also of interest for emission measurements where the key issue is to measure the airflow rate to quantify the gaseous emissions when using the direct measurement method (Ogink et al., 2013a; Samer et al., 2011a).

All results within this study were conducted in ideal situations, under circumstances with no large obstructions in or around the animal mock-up building. Extra research should be executed to find the impact of disturbing factors on real scale livestock housing with large openings.

4.5 Conclusions

Measuring natural ventilation in buildings with large vents with high accuracy is not evident due to high spatial and temporal variability in the velocity distribution in the openings of the building. Although no reference is available to measure natural ventilation for buildings with large vents, for economic reasons, simplification of methods is mostly applied by reducing the number of sampling locations in the vents. Because distribution of the velocities in the vents changes with wind conditions,

selecting the number and places of sampling locations in the opening is crucial to obtain accurate results.

- Simplifications of a direct and a tracer gas method were applied and compared with the method of Van Overbeke et al. (2016) as the reference. For both methods, highest uncertainties (and the presence of bi-directional flows) were found for low velocities normal to the vent.
- A simplification of the reference method in the side vent of the test facility was feasible by using only a quarter of the measurement locations using the chess pattern without giving in on accuracy (<2%). Whereas for the same amount of locations placed on a horizontal line, a deviation of 15% was found. This proved the distribution of the sampling locations over the vent to be at least as important as the number of sampling locations used.

Generally, reduced measurement strategies applied at the ridge opening gave very satisfying results. Only one middle sampling location was sufficient for an accuracy of 2% and a precision of 3%. However, the coefficient of variation due to wind unsteadiness was only slightly lower than those for the side vents. For the direct measurement method, simplification was tested with different patterns of sampling density in the side vents. It was found that not representative selected sampling locations could lead to systematically over- or underestimation of the airflow rates.

Generally, it was found that better accuracy was obtained with a higher number of sampling locations. A 2D spread pattern (not all on 1 line) and accuracies for outlet vents gave better results than for inlet vents.

The tracer gas method gave high uncertainties. These were attributed probably due to non-perfectly homogeneous mixed tracer/air, positioning of the sampling locations in the vent and time basis of the measurements. The varying measured concentrations gave high confidence intervals resulting in not significantly different measurement results between the sampling locations.

The use of direct measurements for determining natural ventilation rates clearly has

the advantage that it allows to measure ingoing and outgoing flows. Reducing sampling locations was possible but knowledge of the velocity distribution in the opening and choosing representative sampling locations was found to be crucial for maintaining the accuracy of the measurements.

In practice this implies a prior calibration of the opening before choosing measurements locations, or choosing a sampling location strategy depending on the dimensions of the opening and the building.

**Experiments in a dairy barn:
effect of sampling density on the
accuracy of airflow rate
measurements and correlations
between the sampling points in the
vent and at the meteo mast**

Chapter 4 focused on the identification and quantification of the uncertainties when measuring the airflow rates in the openings of an animal mock-up building, with respect to reduced sampling locations. Chapter 5 will focus on testing the findings of the previous chapter in a commercial dairy building and investigating the predictability of the velocity patterns in the vents with velocity data of the meteomast. The accuracy of measuring a velocity profile along horizontal and vertical lines with a reduced number of sampling locations was determined by comparing to detailed measurements.

5.1 Introduction

Airflow rates are often calculated using the multiplication of the measured air velocities and the surface areas representative for the respective air velocities (Van Overbeke et al., 2016). The challenge for this method is not to compromise the accuracy of the measurement by limiting the number of sampling locations to obtain a reasonable cost (Joo et al., 2014).

Research has already been performed on the effect of surroundings or obstructions on the airflow rate distribution in the opening, such as the influence of buildings (van Hooff et al., 2010), size of the ventilation opening (De Paepe et al., 2012) (Norton et al., 2010), internal obstacles (Chu et al., 2013), screens (Rigakis et al., 2015; Teitel, 2007) and canopy (Rong et al., 2015) on the airflow rate or airflow rate distribution in buildings. All these factors have an important impact on the local velocity and ventilation performance of the building (Passe et al., 2015) and can lead to deviations from the airflow rates predicted by models (Cui et al., 2016). However, limited research has focused on the accuracy of reduced measuring strategies for airflow rates, with or without surrounding obstacles. In chapter 4, the accuracy and precision of airflow rate measurements applying spatially reduced measuring strategies was investigated. This research found that it was possible to reduce the number of sampling locations and still measure the airflow rate accurately. However, care has to be taken choosing the number and the location of these sampling points to avoid under- or overestimation of the airflow rates. The results of this study were specific for the mock-up building. Measurements in the ridge vent were steady and sampling locations could be reduced to only 2 point without giving in on measurement accuracy. The research in this chapter

will be conducted in a semi-commercial dairy barn.

The objective of this chapter is to measure the effect of reduced measurement strategies for airflow rate assessment through the vents of a semi-commercial dairy barn. This was conducted by

- (a) determining the accuracy of airflow rate measurements when reducing the number of sampling locations in the side and ridge vents. Because detailed measurements as in the mock-up building were not feasible, it was chosen to determine the accuracy of measurements with reduced number of sampling locations along a horizontal and vertical line (profile) in the side vent. Conducting this experiment could determine the feasibility of predicting (vertical and horizontal) velocity profiles with reduced measurements and whether generalisation of these conclusions is possible for different wind conditions and screen positions.
- (b) determining the predictability of the velocity pattern in the vents by correlating velocities to the wind conditions measured on a metemast.
- (c) comparing the different measurement results of the airflow rates through the side and ridge vent.

The experiments were executed for different curtain configurations. The curtains were adapted to maintain a comfortable environment for the animals as a function of actual weather conditions.

5.2 Materials and Methods

Section 5.2.1 describes the site and building used for the experiments. Section 5.2.2 describes the experimental set-up and section 5.2.3 the data processing. The relation of the methods to the formerly defined objectives is given. All the processing was performed using Matlab® (Mathworks, USA).

5.2.1 *Site and building description*

Measurements were carried out in a naturally ventilated commercial dairy barn situated on a site of the Institute for Agricultural and Fisheries Research in Merelbeke, Belgium (+50° 98' 48.44" N. +3° 77'86.31" E: Figure 32). The surroundings of the dairy barn are shown in Figure 32. The building is sited next to an open grassland (*SW* and *SE* of the building). The height of the clamp silos for ensilage roughage *E*, sited to the North of the dairy barn, is approximately 2m. Because this storage is installed at a lower base, the clamp silos only has a height of approximately one meter compared to the base of the ventilation openings of the dairy building (Figure 32). To the *NE* of the building, at 15 m distance of the dairy barn, an stanchion barn *F* with roof height of 6 m is situated. Next to this building *F*, an old young stock barn *G* and a beef cattle house *H* are present. At a distance of approximately 100 m, there is a row of trees (*I*) with a height of 15 m (in Figure 32). To the *SW* of the building, in front of the side vent a long open structure with a roof for measuring cow lameness (a gaitwise) is installed (Maertens et al., 2011).

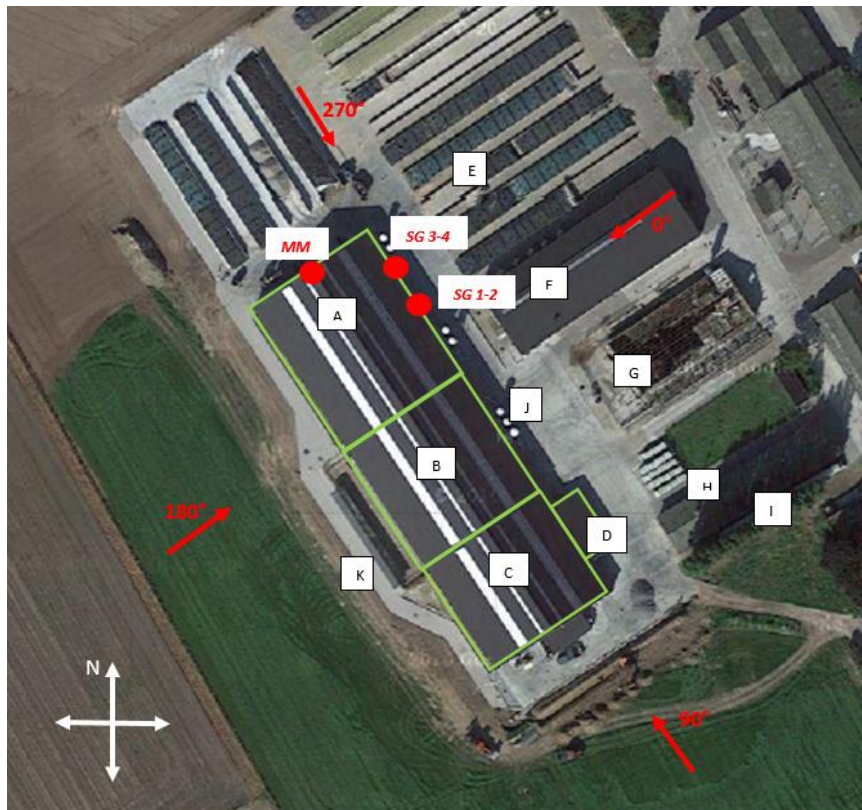


Figure 32: Site and building of the experimental set-up barn; ● sampling locations meteomast *MM*, Sensor groups *SG1*, *SG2*, *SG3* and *SG4* (also place for horizontal experiments); *A*: nutritional research part, *B*: management research part, *C*: care section, *D*: technical room, *E*: clamp silos for ensilage roughage, *F*: stanchion barn, *G*: old young stock barn, *H*: beef cattle house, *I*: trees, *J*: silos, *K*: gaitwise system, wind rose with indication of the north and arrows pointing out the wind direction

The barn has 164 cubicles installed, but only approximately 120 cows occupied the cubicles during the experiments. The building (Figure 33) has dimensions of 114.6 m length, 36.6 m width and a height of 12.0 m and a 0.5 m wide ridge vent with wind deflectors of a height of 0.35 m installed on both sides of the ridge decreasing its width to approximately 0.15 m. The narrowing of the wind deflectors combined with the wind above the deflectors causes a venturi effect to enhance ventilation.

The building was built for commercial use, but was also designed for research purposes. It was designed with a cow walking alley of 2 m width in the middle of the barn and on each side of the ventilation openings a feeding alley of 4 m to enable passage with a tractor. The dairy building had less animal places than normally expected for the size of the building due to the cow walking alleys and because the surface area of the cubicles had to be larger than in a commercial barn.

The roof has integrated see-through roof parts to have optimal natural light, and is insulated to avoid condensation. The building is divided into three main sections: a nutritional (*A*) and management (*B*) research part and a care part (*C*). The care section has a ridge 1 m lower than the other parts of the building. Inside the building, between the feeding alley and part *A*, automatic feed troughs of 1.3 m height were installed for feeding trials in the nutritional part. They reached 1 m above the lowest point of the vents. The other building parts were occupied with feeding rail barriers.

The ventilation openings have lengths of 30 m in part *B* and 34 m in part *A*. All vents have heights of 4 m. The vents in part *C* have dimensions of approximately 10 m at the *NE*-side and 30 m at the *SW*-side. All side vents are equipped with a lattice bird protection (mesh of 0.05 m). Two other types of screens can overlap this bird protection: a wind curtain ($\pm 2\%$ porosity) or wind break net ($\pm 50\%$ porosity). A detail of the full side opening seen from the *NE* is found in Figure 36. The gates in the gables were normally closed, but were used frequently for normal farm practices.

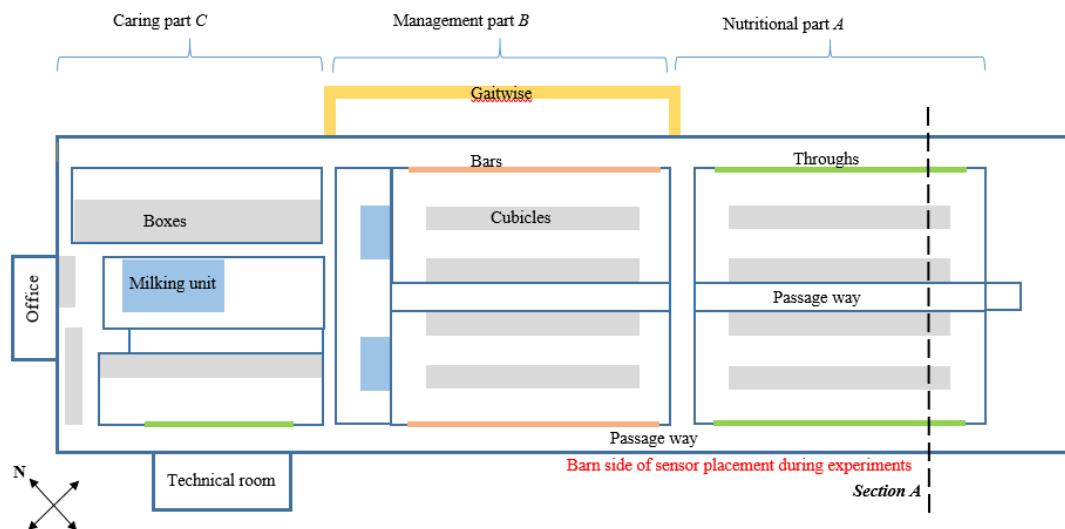


Figure 33: floor map of the dairy building: ■ boxes and cubicles; ■ gaitwise; ■ feeding troughs; ■ bar/rail barriers; ■ milking units; wind rose with indication of the north

5.2.2 Experimental set-up

This section describes the experimental set-up used to obtain results for the objectives. In section 5.2.2.1, the equipment is discussed. Section 5.2.2.2 handles the experimental procedures: the management of the screens (curtain configurations), the

surrounding obstacles, the sampling locations for the different experiments and the frequency of measurements during the experiments.

5.2.2.1 Equipment used

Air velocities in the vents and on the meteor mast were measured with *2D* or *3D* ultrasonic sensors (Thies®, Göttingen, Germany). Only the normal and/or tangential velocity component was measured for both type of sensors. Therefore, the selection of the type of sensors in the vents was of no importance. The ultrasonic anemometers had an accuracy of 2% full span. However, when the velocities were lower than 5 m/s, the accuracy was ± 0.1 m/s. Outside wind conditions were measured using a *2D* ultrasonic anemometer placed on a meteor mast which was installed on the edge of the roof of the barn 0.25 m above the highest point of the building. Temperature was measured using the ultrasonic anemometers in the side vent and ridge vent and on the meteor mast. Because the temperature measured by the ultrasonic sensors could be overestimated due to humidity (e.g. produced by the livestock), an extra thermistor (probe type CT-UU-VL15-0 Grant) was installed in the ridge vent to measure the temperature differences in- and outside the building. All sensors measured continuously day and night, although occasionally some data was missing due to hardware malfunctioning as e.g. signal loss. All data was logged simultaneously using a logger (Delphin Expert version 100).

5.2.2.2 Experimental procedures

In order to investigate the possibility of reduced sampling strategies, different experiments were conducted. Performing a detailed airflow rate experiment as in the mock-up building was not feasible in the (very) large side vents of the dairy barn due to insufficient availability of the amount of sensors for dense measuring. Therefore, for the side vents, experiments were set up as a proof of concept where detailed velocity measurements were conducted along horizontal and vertical lines.

5.2.2.2.1 Management of the screens

The experiments were conducted in a (semi-) commercial dairy stable. Therefore, wind screens were used to protect the animals and adapted to the weather conditions. The sections below describe the curtain positions used during the experiments and their

randomisation in time during the period of measurements.

5.2.2.2.1.1 Curtain configurations

Velocity measurements took place in the openings of part *A*. Curtains of part *A* and part *B* were always manipulated identically. The curtains of part *C* were held closed with the wind stop curtain during the experiments and were only opened occasionally to improve the climate for the livestock. Five curtain configurations were selected for application (Figure 34):

- *CC1*: all curtains open
- *CC2*: wind break nets in the vents on both sides of the barn
- *CC3*: a wind stop curtain placed in the lower half of the *SW*-vent opening, while the *NE*-vent stayed open
- *CC4*: the wind stop curtain was used to close the vent on the *SW*-side, while the wind break net was used for the *NE*-side
- *CC5*: the *SW*-side of the barn was fully closed with the wind break net, the *NE*-side was fully opened
- *CC6*: the *SW*-side of the barn was half closed with the wind break net, the *NE*-side was fully opened
- *CC7*: the *SW*-side of the barn was fully opened, the *NE*-side was half closed with the wind stop curtain
- *CC8*: the *SW*-side of the barn was fully closed with the wind break net, the *NE*-side was half closed with the wind break net.

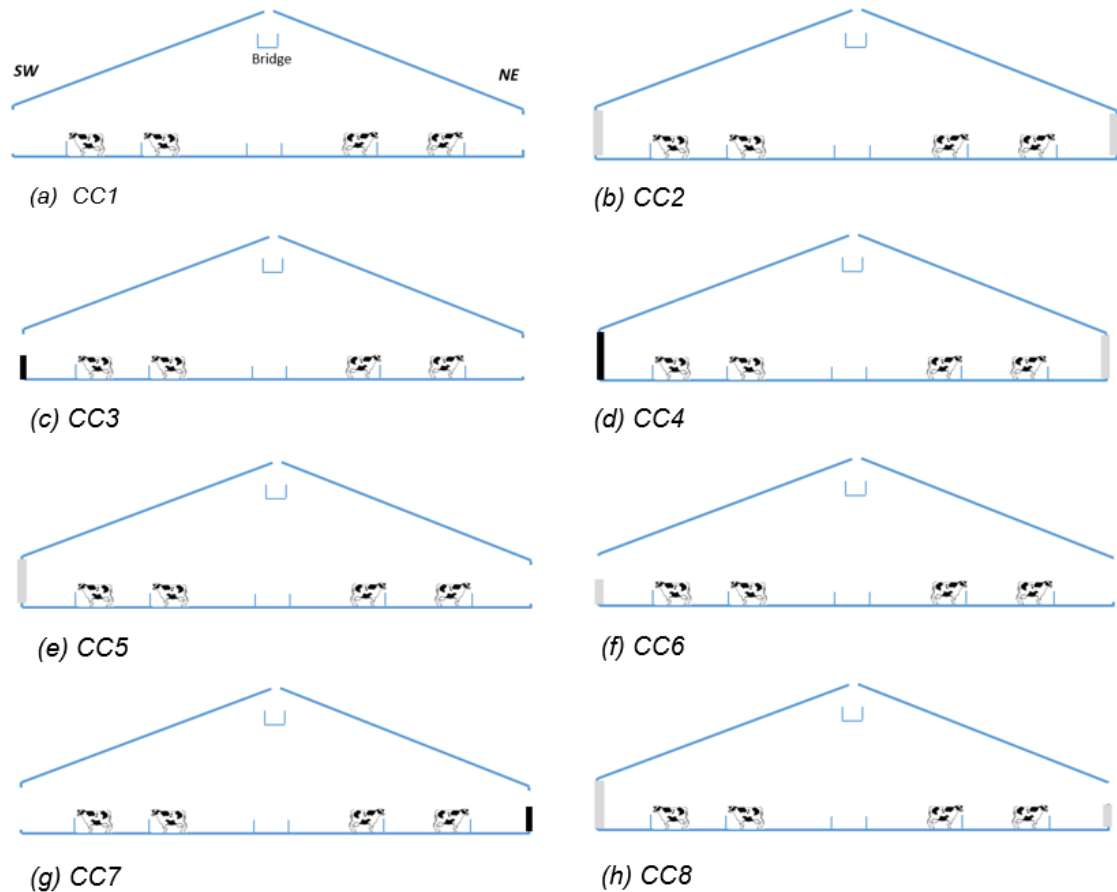


Figure 34: Section A (Figure 33) of the barn with configurations of the curtain positions in the vents during the experiments (a) CC1, (b) CC2, (c) CC3, (d) CC4, (e) CC5, (f) CC6, (g) CC7, (h) CC8; ■: wind stop curtain; ■: wind break net

5.2.2.2.1.2 Randomisation in time of curtain configurations

The application of the type of curtain configuration was selected as a function of the weather conditions to maintain the comfort of the animals. The application of certain types of curtain configurations was not manipulated in favour of the experiments. The curtain configurations during the experiments were therefore representative of the weather conditions during the period of measurements. Figure 35 shows a timescale for the curtain configurations as used during the different experiments in the ridge and side vents. Not all curtain configurations were used for every experiment. All changes in position of the curtains were carried out and logged manually by the caretakers.

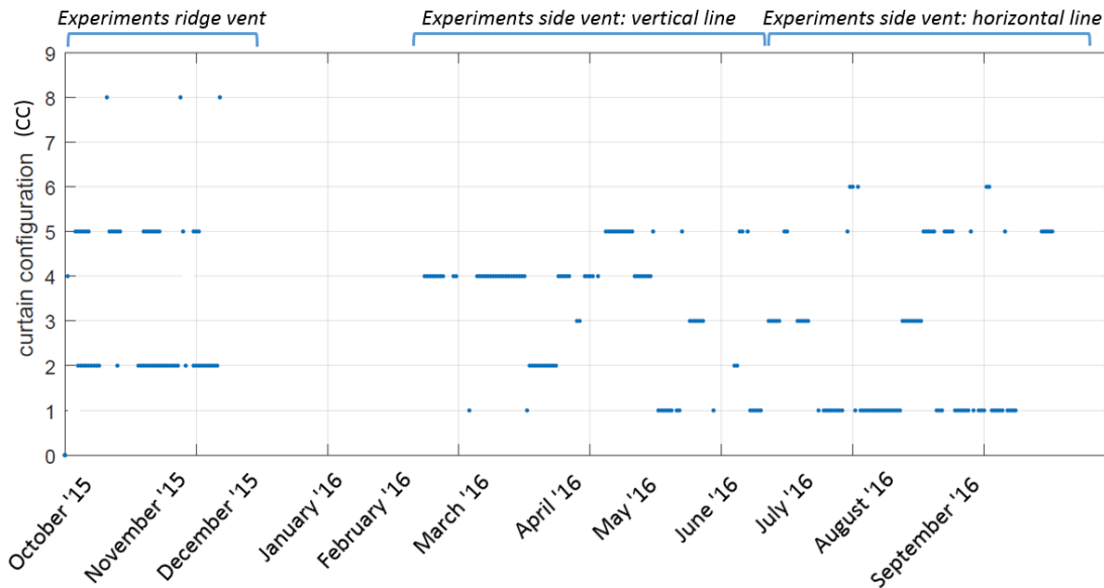


Figure 35: Timescale of the curtain configurations applied during the experiments in the ridge vent and the side vent (sensors placed on a vertical and horizontal line)

5.2.2.2.2 Sampling locations and wind conditions during experiments

5.2.2.2.2.1 Vertical velocity profile in a side vent

Four sensor groups (*SG1*, *SG2*, *SG3* and *SG4*), each consisting of three vertically aligned anemometers, were placed in the *NE*-side vent: two groups in the middle and two near the side edge of the vent (Figure 36). Sensor groups *SG1-4* were installed at a distance of 15 m, 14 m, 5 m and 4 m from the side of the *NE*-opening, respectively. For each group, the sensors were installed at a height of 1 m, 2.25 m and 3.25 m to establish vertical velocity profiles. The middle sensor was installed 0.25 m higher than the middle of the opening because for a closed wind break net, a pipe partially carrying the screen structure hang at the middle of the opening (Figure 36a). Each separate sensor was named with different indexes, the first number being the sensor group and the second number being the row number as showed in Figure 36a.

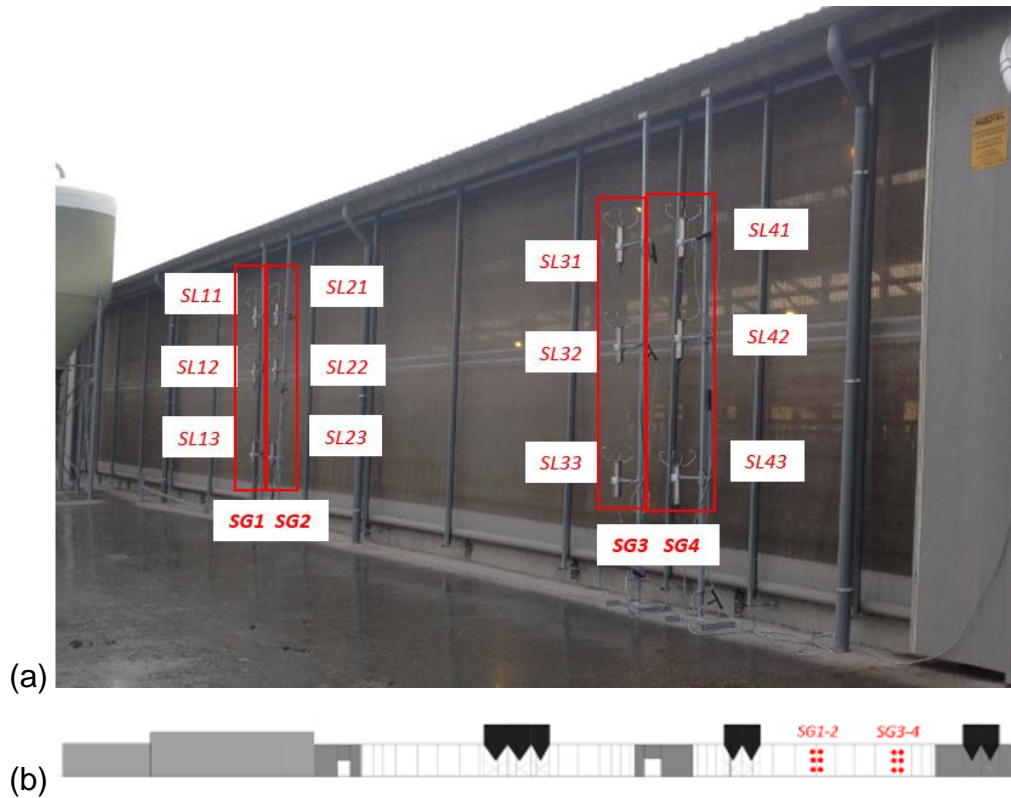


Figure 36: (a) detail picture of sensor groups and single sampling locations, (b) placement of sampling locations of sensor groups SG1-4 on the NE side of the barn

The wind conditions during the experiments with curtain configurations CC1, CC2, CC3 and CC4 are plotted in wind roses in Figure 37. For these configurations, 195, 118, 66 and 406 one hour means of the velocities were sampled, respectively.

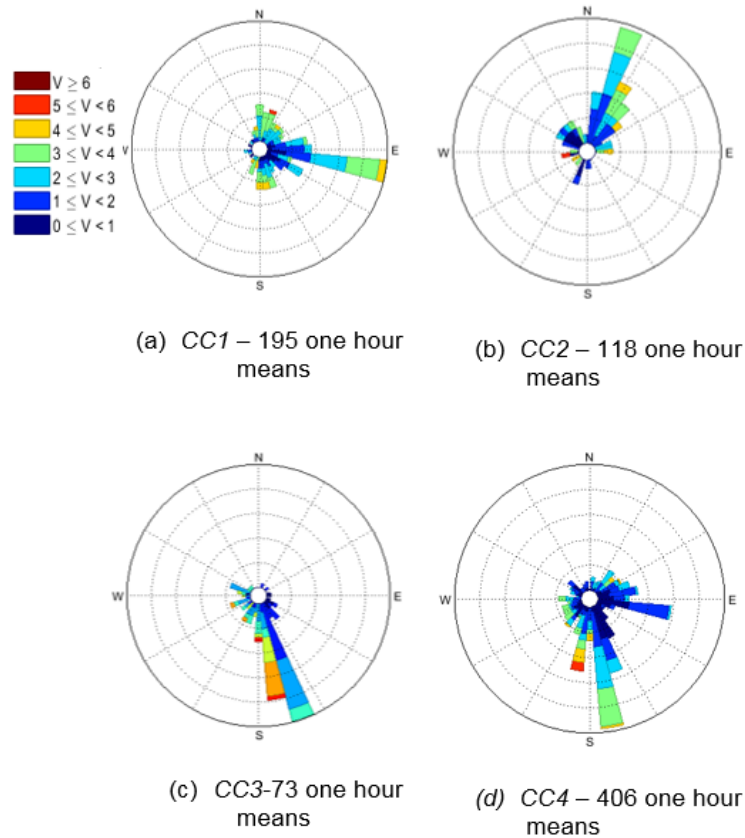


Figure 37: Wind roses and legend for the experiments with wind velocity V measured at the metemast in m/s: (a) CC1, (b) CC2, (c) CC3, (d) CC4; circles indicating frequency of 5%

5.2.2.2.2 Horizontal velocity profile in a side vent

Twelve anemometers were placed along a horizontal line in the side vent at the *NE*-side of the dairy barn (Figure 38) to establish a horizontal velocity profile. The sensors were all mounted at a height of 2.75 m and were equally spaced over the length of the two openings of part *A* and part *B* of the dairy barn. The sensors were placed approximately every 6m in the vent, therefore the sampling density was 1 sensor per $\pm 25\text{m}^2$. The vertical position of the sensors was chosen considering the expected disturbance by the silos on the one hand (lower placement) and lower velocities due to the profile of the boundary layer and disturbance effects of surroundings of feeding troughs, temporarily parked tractors or other vehicles (higher placement). The latter could not always be avoided or controlled because the measurements took place over a period of months and 24/24h. The air velocities measured by all sensors were logged simultaneously. However, due to hardware problems not all velocities could be logged continuously. Data transmission problems sometimes occurred for the sensors furthest away of the logger. Because too many malfunctions occurred for data transmission of

sensor *hSL1*, it was chosen to duplicate the data of *hSL1* by measurements of *hSL2*. The results for *hSL1* that were successfully measured (approximately 3000 velocities of 10s means for different wind directions) were in the same low range (placed side-by-side and next to the wall of the technical room of the barn) and showed the same velocity behaviour as for the *hSL2*.

Figure 39 presents the names of the sampling locations, projected on the side view of the *NE*-side of the dairy barn. Also, five strategies with reduced number of sampling locations are presented using 6, 4, 3, 2 and 1 sampling location(s) which were named *6RSL*, *4RSL*, *3RSL*, *2RSL* and *1RSL*, respectively.



Figure 38: Photo of the *NE*-side of the dairy barn with anemometers on a horizontal line (marked with red circles), equally spaced over the openings

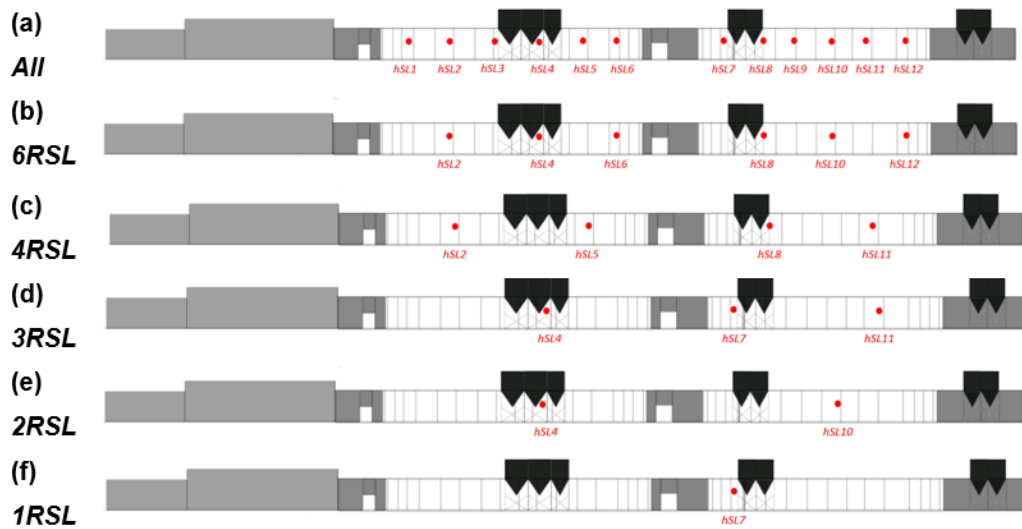


Figure 39: Sampling locations (a) all sampling locations *hSL1-12*; reduced sampling strategy: (b) *6RSL* (c) *4RSL* (d) *3RSL* (e) *2RSL* (f) *1RSL*

The wind conditions during the experiments with curtain configurations *CC1*, *CC3* and *CC5* are plotted in wind roses in Figure 40. For these configurations, 214, 72 and 63 one hour means of the velocities were sampled, respectively. The experiments with the different curtain configurations were spread over the months of July, August, September and October 2016.

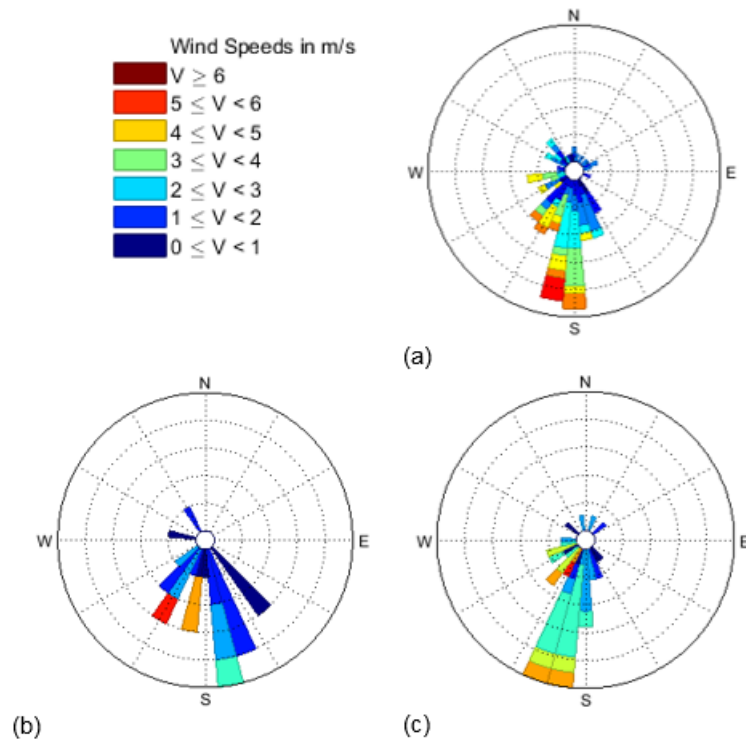


Figure 40: Wind roses for experiments with curtain configuration: (a) CC1, (b) CC3, (c) CC5, circles indicating a frequency of 5%

5.2.2.2.2.3 Velocity measurements in the ridge vent

Eight sensors were mounted in the ridge vent to conduct the detailed measurements. During the experiments in the side vents (horizontal and vertical profiles), only four sensors were mounted in the ridge vent. Their positions are presented in Figure 41b and c, respectively. A walking-bridge under the ridge vent (Figure 41a) was installed in part A and B of the building. Due to the easy access, the anemometers were installed all above this bridge (approximately 2/3th of the ridge vent).

No detailed measurements were performed to determine the pipe factor in the ridge vent. The mounting of the sensors in the ridge vent within this experiment was different from the one in the experiment of Van Overbeke et al. (2016) so the value of the pipe factor could not be introduced in the calculation of the airflow rate of this experiment. The sensor heads measured the velocity over a distance of 0.25 m. Approximately 3/5th of the actual width of the ridge was measured. Therefore, the velocity measured by the anemometer was used as an estimate of the actual velocity in the vent. No pipe factor was taken into account because the aim was to give an estimate of the airflow rate of the ridge and the side vent.

Wind direction and speed during the experiments are plotted in Figure 42.



Figure 41: (a) Pictures of the bridge under the ridge vent and an example of a mounted sensor, (b) Sampling locations for the detailed measurements ridge vent (*DR8*), (c) Reduced sampling locations ridge vent with 4, 2 and 1 locations, respectively specified as *RR4*, *RR2* and *RR1*

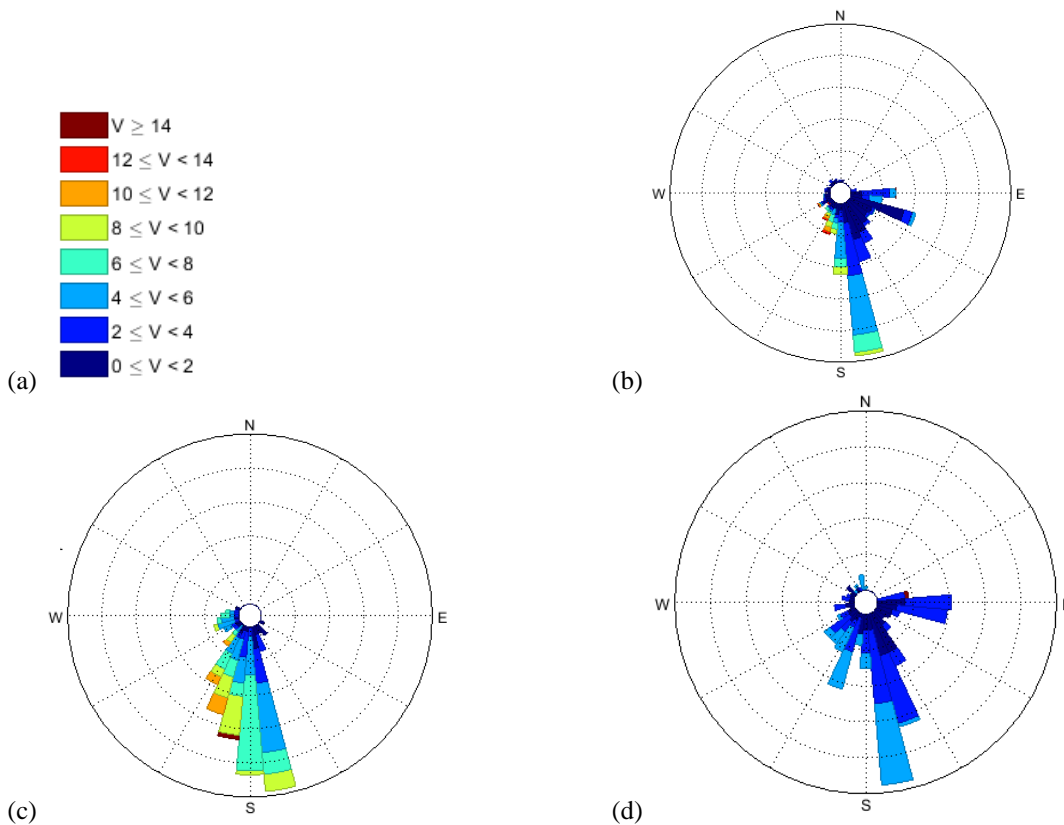


Figure 42: (a) Wind roses for the experiments during the application of different curtain configurations for *CC2* (b), *CC4* (c), *CC8* (d); *V* indicating the velocity measured at the meteomast (m/s), circles indicating frequency of 5%

5.2.2.2.3 Surrounding obstacles

Velocities in the vents were not only the result of the wind conditions and the screen positions, but also from surrounding obstacles. The magnitude and variation of the velocity on a specific location in the vent can be influenced by e.g. a nearby building or silo. To be able to make better interpretation of the results, panorama views taken on the locations of SG1 and SG3 is presented in Figure 43. This figure shows obstacles for the airflow for different wind directions.



Figure 43: View with surrounding obstacles for (a) SG3 and (b) SG1, projected on a scale of degrees referring to the wind direction

5.2.2.2.4 Frequency of measurements

The experiments were conducted continuously day and night during the months of January until July 2016. Every 10s, a ten second mean of the normal velocity component read by the anemometers was transferred to the datalogger. The 10s mean was calculated by the ultrasonic anemometer that stored mean velocities (measured at 250Hz) every second in its internal memory.

This raw data was processed to one minute and one hour means (when at least 80% of the data of one hour was available) for further analysis. The one minute and one hour averages were selected in order to make an analysis for the different time scales of the measurements for controlling or (emission) measuring purposes.

5.2.3 Data processing

The data processing sections are sorted per objective: processing of the velocity data, calculation of the uncertainty of the velocity measurements due to unsteadiness of the wind, calculation of the accuracy of velocity measurements due to reduction of the sampling locations, calculation of correlations between velocities measured at the meteomast and on sampling locations in the vents and estimation of the airflow rates through the measured vents.

5.2.3.1 Predictability of velocity profiles using reduced number of sampling locations in the vents

The effect of the reduction of the number of sampling locations on the accuracy of velocity measurements was determined. In this way it was possible to investigate whether the velocities of reduced sampling locations were good predictors for the velocity profiles in the vents. The accuracy of measurement was given by calculating the relative difference between the velocities measured with the reduced and detailed sampling locations [15]. The detailed measurements were used as the reference.

$$\text{Relative difference (\%)} = \frac{|\overline{Y_{ms, \text{reduced sampling}}}| - |\overline{Y_{ms, \text{detailed sampling}}}|}{|\overline{Y_{ms, \text{detailed sampling}}}|} \times 100 \quad [15]$$

$|\overline{Y_{ms}}|$ = mean perpendicular velocity in measurement surfaces in the vent (m/s)

Because high relative differences can be found for low values, outliers were avoided by excluding data lower than 0.1 m/s from the dataset. To separate good predictors from bad predictors, a criterion of 20% relative difference was deemed acceptable between the velocities of the reduced and detailed sampling locations. In other words, the mean velocities should not differ from each other with more than 20%. This criterion was set at 20% as a compromise between the expected variability of the velocities due to wind unsteadiness and between the needed accuracy for ammonia flux calculations from barns and to assess the efficiency of mitigation techniques.

To give a measure to the precision of measurements, the standard deviation *SD* and coefficient of variation *CV* of the measurements on the sampling locations were determined. This precision uncertainty was caused not only by the surrounding

obstacles, but also by the unsteadiness of the wind.

5.2.3.2 Correlations between velocities of the meteomast and of local sampling locations

Multiple linear regression was applied to find correlations between the wind velocity components at the meteomast and the normal velocity component in the sampling locations at the side vent. Multiple linear correlations were chosen, with both the tangential and normal component of the meteomast data (De Vogeleer et al., 2016). Before applying a regression analysis, the dataset was split in a group where the vent was the main inlet (wind direction $>270^\circ$ or $\leq 90^\circ$) and a group where the vent was the main outlet (wind direction $>90^\circ$ and $\leq 270^\circ$) (De Vogeleer et al., 2016).

The proposed correlations were based on the assumption that the airflow rate was wind driven. However, the buoyancy effect could affect correlations between the velocities in the vents and the velocity components measured at the meteomast. Therefore, the velocities were compared for experimental measurements where the inside and outside temperature was higher and lower than 2°C . The group with temperature differences higher than 2° consisted only of 20% of the data and even a smaller group within with actual wind velocities $<2\text{m/s}$. The two different groups did not show different behaviour in velocity patterns, therefore the data was not split for further analysis.

The tangential and normal velocity components measured at the meteomast were used as the independent variables, the normal velocity component measured on a sensor location in the side vent as the dependent variable [16]. The modelled velocities were compared to the measured velocities using single linear regression.

$$RV_{ms} = a_{ms} \times |X_{MM}| + b_{ms} \times |Y_{MM}| + c_{ms} \quad [16]$$

where:

a, b	coefficients (dimensionless)
c	constant (m/s)
ms	measurement surface in the vent
RV	(reference, measured) velocity component perpendicular to the vent (m/s)
$ X_{MM} $	tangential velocity component measured at the meteomast (m/s)
$ Y_{MM} $	perpendicular velocity component measured at the meteomast (m/s)

Agreement between the modelled and the reference velocities in the sampling locations was assessed using regression parameters and Bland Altman analysis. The accuracy of the linear regression models was tested with the Bland Altman method (Bland et al., 2010). For this analysis, absolute differences between the modelled and experimental (reference) velocities are related to the average of the modelled and reference velocities. The agreement between modelled and experimental velocities [18] is analysed with the slope (β_0) and the intercept (β_1) [18]. Ideal models will result in coefficients close to zero.

$$RV_{ms} = p_{ms} \times MV_{ms} + c_{ms} \quad [17]$$

$$(MV_{ms} - RV_{ms}) = \beta_0 \times \frac{MV_{ms} + RV_{ms}}{2} + \beta_1 \quad [18]$$

Where:

MV	modelled velocity component normal to the vent (m/s)
RV	detailed (reference) velocity component measurements normal to the vent (m/s)
ms	index referring to the measurement surface
β_0	coefficient of performance (dimensionless)
β_1	intercept (m/s)
p	slope (dimensionless)

5.2.3.3 Airflow rate estimation

Estimated airflow rates were calculated to compare the airflows through the ridge and NE-side vent. The partial airflow rates were summed after multiplying the local velocities with their related partial surface area in the vent [19]. This formula was comparable to the other chapters, however, the airflow rate was estimated with a

limited number of measurements (compared to the size of the vents) and not with detailed measurements. Therefore, the airflow rate could only be defined as estimate.

$$Q_{tot} = \sum_{k=1}^n (|\bar{Y}_{ms}|_k \cdot A_k \cdot 3600) \quad [19]$$

Where:

Q_{tot} = mean airflow rate over a period of approximately 1 h (m^3/h)

$|\bar{Y}_{ms}|_k$ = mean normal velocity component over a period of approximately 1.5 h in measurement surface k (m/s)

A_k = surface of partial opening area k (m^2)

ms = measurement surface

n = total number of partial opening areas in the side or ridge vents (i.e. 12 for the side vent, 8 for a ridge vent).

5.3 Results and discussion

5.3.1 Velocities of reduced sampling locations as predictors for the velocity profile

5.3.1.1 Vertical velocity profile in the side vent

The vertical profile was measured on 4 locations SG1-4. The measurements of the paired groups of SG1-2 and SG3-4, that were placed only 1m apart (per pair), gave similar results. Therefore only the results for SG1 and SG3 are discussed and plotted. For every curtain configuration, three graphs are plotted: The upper graphs show data plots with one hour mean velocities for SG1, SG3 and outside wind velocity v against wind direction. The middle graphs show the absolute differences between the middle point velocity and the velocity average of the reference vertical profile in the vent. The lower graphs in the third row show the respective relative differences, with the criterion of 20% as a red line. Additional to the graphs, tables are presented with the mean and standard deviation of the relative differences. The two upper graphs are plotted to have better understanding of the lower graph with the relative differences between the velocities. Although measurements for the different sensor groups were carried out simultaneously, the amount of one hour means was not equal for groups SG1 and SG3 due to occasional hardware malfunctioning. The graphs as described before are plotted for curtain configurations CC1, CC2, CC3 and CC4 in Figures 44 to 47, respectively. Discussions of the graphs are not executed in detail.

High relative differences, exceeding the criterion of 20%, occurred between the mean velocities of the reduced and the detailed measurements. This can be the result of **low absolute velocities** measured at the vents which result in not significantly different velocities. Or importantly, because the middle location is **not a good predictor** for average of the 3 vertically aligned measurements. The latter can be a result of disturbing influence of its surroundings of e.g. neighbouring buildings, silos, cows, side gables, screen positions or inside furniture of the dairy barn itself.

When **comparing results per sensor group** it can be seen that different patterns occur for the relative differences. The middle point predictors can over- or underestimate the velocity depending on the wind direction measured at the MM. These different patterns can be the result of the surroundings influencing the vertical velocity profile. These disturbances of surrounding can be large due to the presence of nearby buildings, or 'smaller' due to nearby poles.

When **comparing results between sensor groups**, it is seen that the patterns of their relative differences are not similar to each other. For a specific wind direction, the disturbance of surroundings is not always equal and has different influences on the velocity profile resulting in different relative differences.

When comparing results per curtain configurations, it is seen that the relative differences between velocities measured with the reduced and detailed method have a different pattern for each curtain configuration.

All these results showed that the velocity profile was influenced by the wind direction, surrounding obstacles, sensor place in the vent. Therefore, the overall conclusion was that generalisation of one measured vertical profile for the vertical profile of an entire opening was not a possible simplification method to reduce sampling locations in a vertical section of the opening. Therefore one should be careful when using only horizontally placed sensors to measure the airflow rate through a side vent.

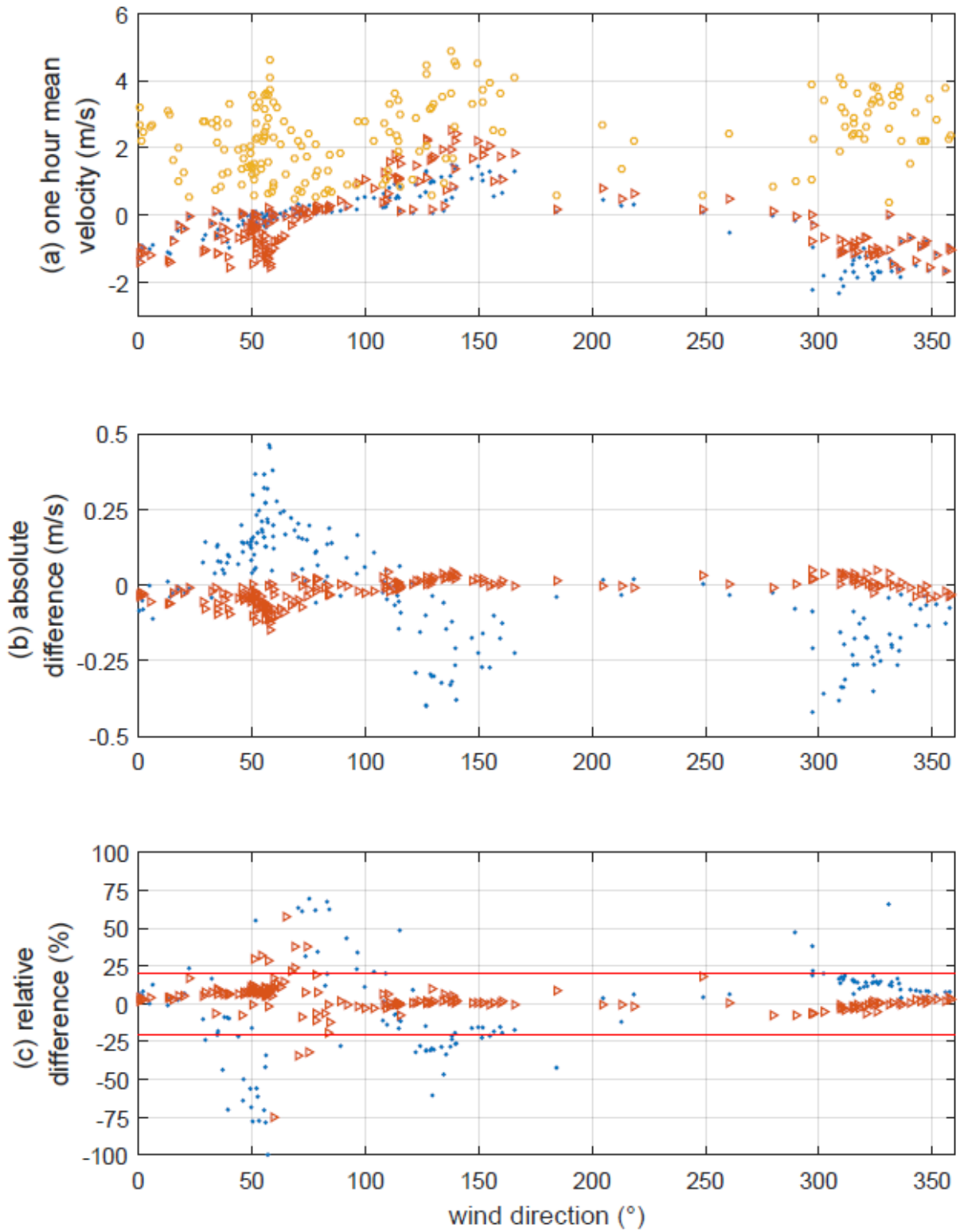


Figure 44: Results for experiments with (reduced) vertical profile measurements for CC1; a) one hour averaged velocity measurements; b) absolute and c) relative differences between the measurements with a reduced and detailed method; ● SG1, ▲ SG3, ○ MM velocity;

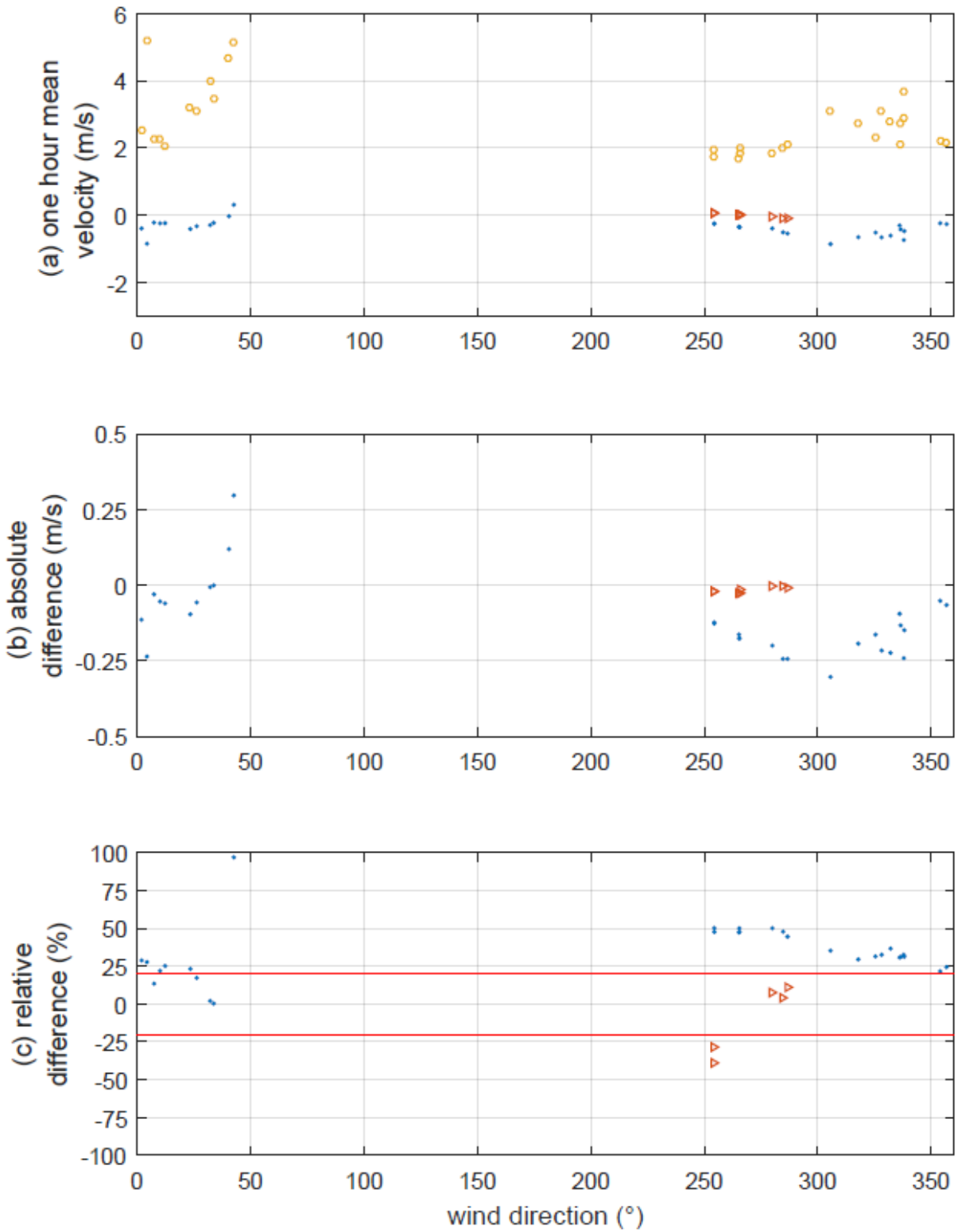


Figure 45: Results for experiments with (reduced) vertical profile measurements for CC2; a) velocity measurements; b) absolute and c) relative differences between the measurements with a reduced and detailed method; ● SG1, ▲ SG3, ○ MM velocity

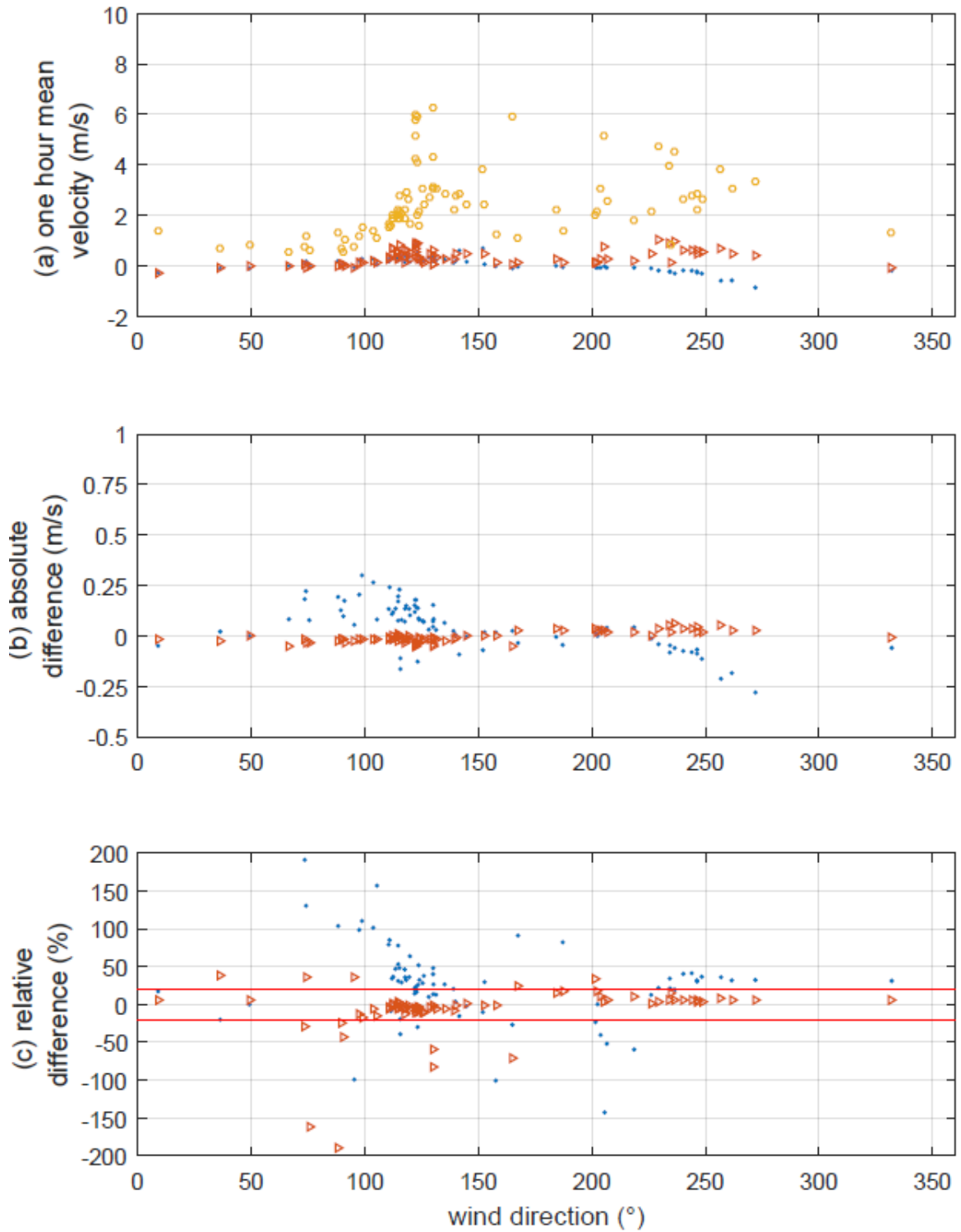


Figure 46: Results for experiments with (reduced) vertical profile measurements for CC3; a) velocity measurements; b) absolute and c) relative differences between the measurements with a reduced and detailed method; ● SG1, ▲ SG3, ○ MM velocity

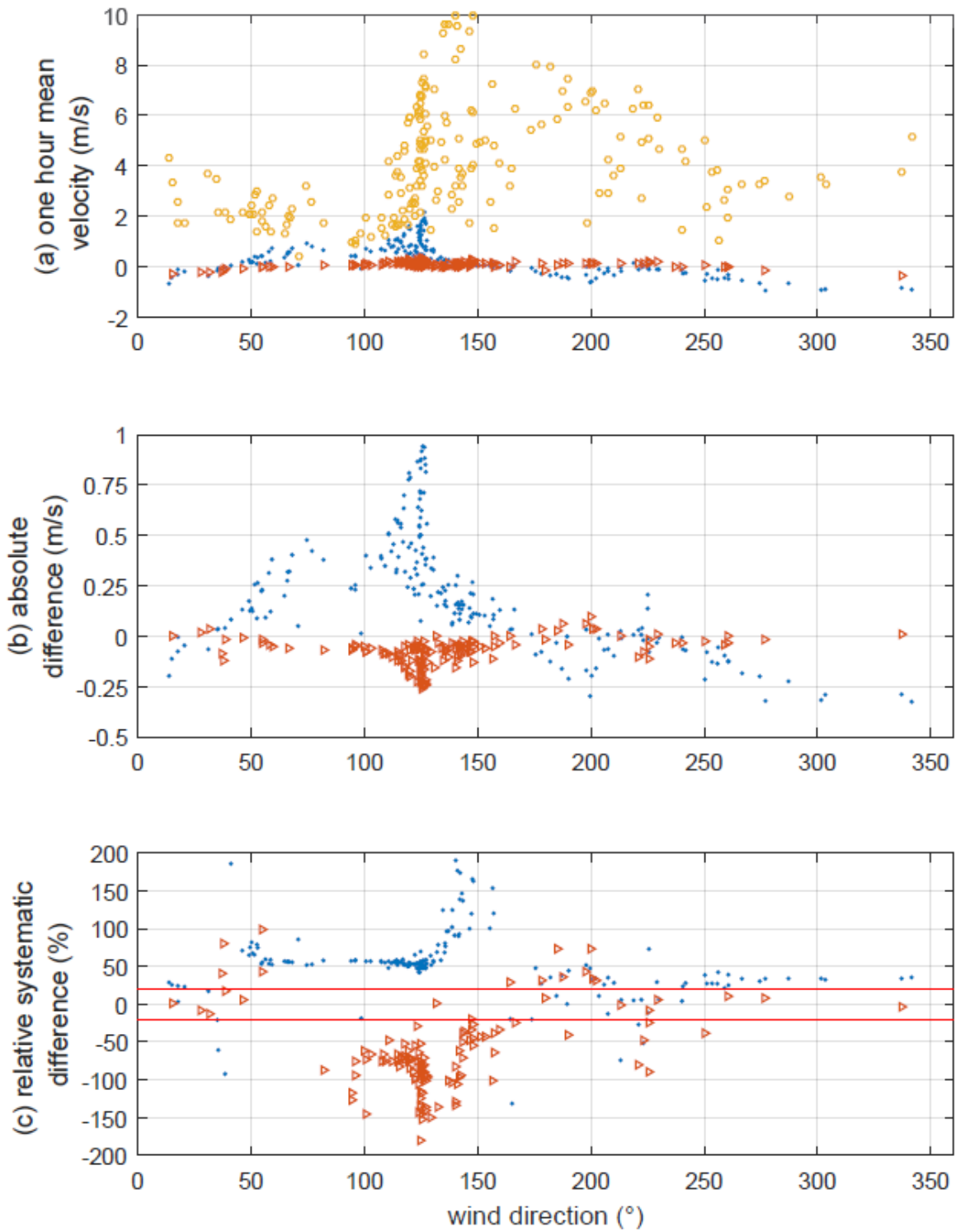


Figure 47: Results for experiments with (reduced) vertical profile measurements for CC4; a) velocity measurements; b) absolute and c) relative differences between the measurements with reduced and detailed method; ● SG1, ▲ SG3, ○ MM velocity

Figures 44 to 47 show that the relation of the relative difference between the velocity measured with the reduced and detailed method was dependent on the wind direction, curtain configuration and surrounding obstacles. Figure 48 shows the same data of relative differences but plotted against the normal wind velocity component in the vent and the wind velocity measured at the metemast. It shows that high relative differences are not necessarily related to the wind velocity. However, a more clear relation was found for the relative difference against the normal velocity in the vent. Here was seen that high relative differences could be related to low velocities in the vents. These low velocities were not necessarily related to low wind velocities, but were probably also influenced by surrounding obstacles. It was seen that if the velocity pattern was not disturbed by curtains (as for *CC4*), the predefined criterion of 20% relative difference was met when the velocity in the vents was higher than 1 m/s.

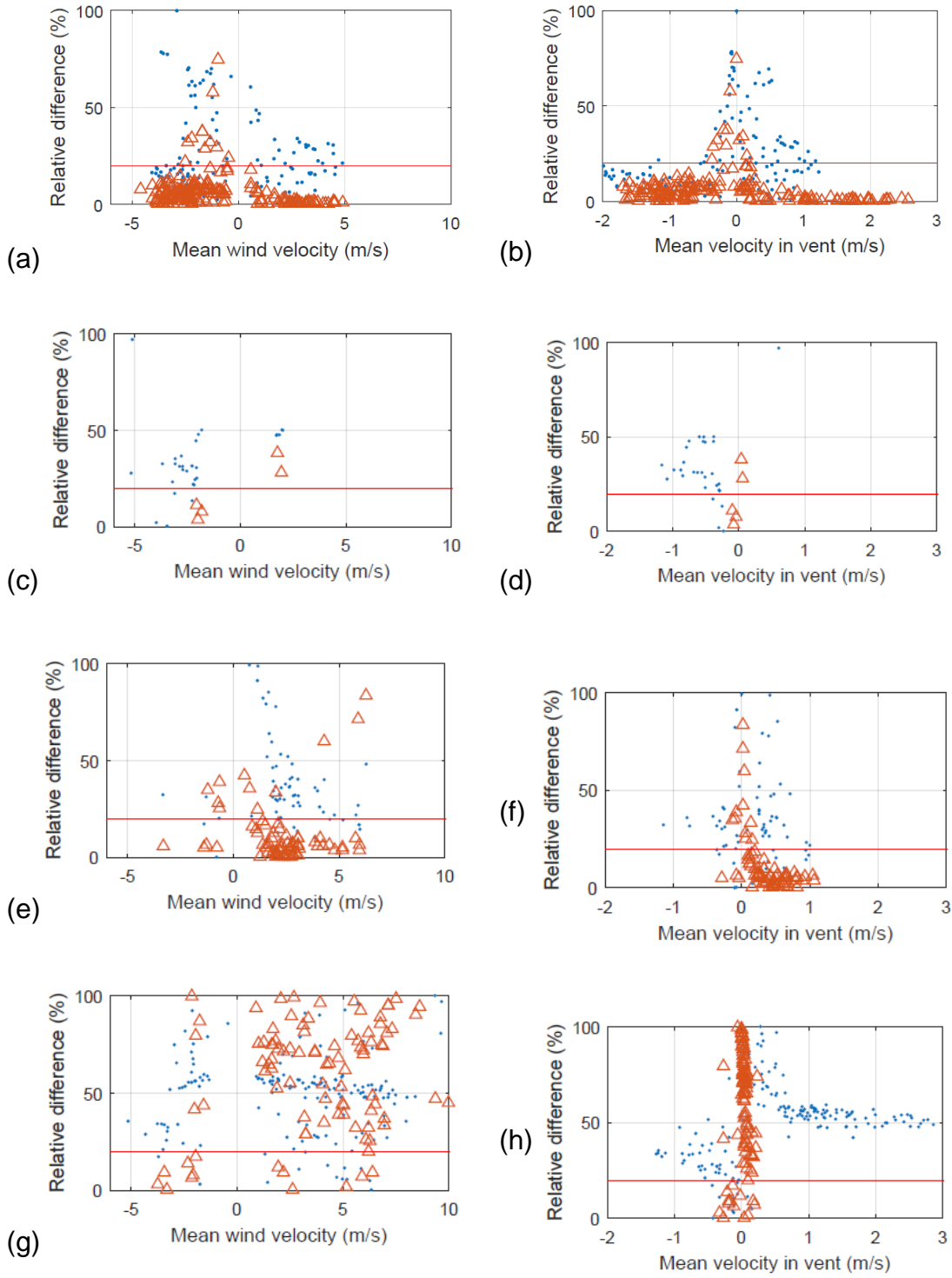


Figure 48: Relative difference against the wind velocity (left column) and normal velocity in the vent (right column), for curtain configurations *CC1* (a and b); *CC2* (c and d); *CC3* (e and f) and *CC4* (g and h)

5.3.1.2 Horizontal velocity profile in the side vent

The results of the experiments of the horizontal profiles were plotted similarly to the results for the experiments with the vertical profiles: for every curtain configuration, 3 subgraphs are plotted. The upper graphs show data plots with the mean velocities for *6RSL*, *4RSL*, *3RSL*, *2RSL*, *1RSL* and the outside wind velocity v against the wind direction. The middle graphs show the absolute differences between the velocities measured with the reduced and detailed methods. The lower graphs in the third row show the respective relative differences.

The graphs as described before are plotted for curtain configurations *CC1*, *CC3*, *CC5* and *CC7* in Figures 49 to 52, respectively.

It was difficult to draw conclusions from the measurements of the experiments with horizontal profiles. The variety in wind direction was limited, so general conclusions were not applicable.

Notwithstanding these conditions, some conclusions could be drawn. Similar to the results for the experiments with vertical profiles, low velocities in the vents resulted mostly in high relative differences. Another conclusion was that in general it is seen that using more sensors increase the capacity to predict the horizontal profile. Selecting representative sampling locations is therefore most important. In general, using more sensors decrease the relative importance of disturbing influences of obstacles. It seen that for 180° , wind direction normal to the *SW*-vent of the barn is a certain kind of turning point where an overestimation of the velocity profile could swap to an underestimation or vice versa.

Results show that care is to be taken when reducing sampling locations to measure the horizontal profile. Selecting too few sampling locations can cause over- or under estimation of the velocity profile.

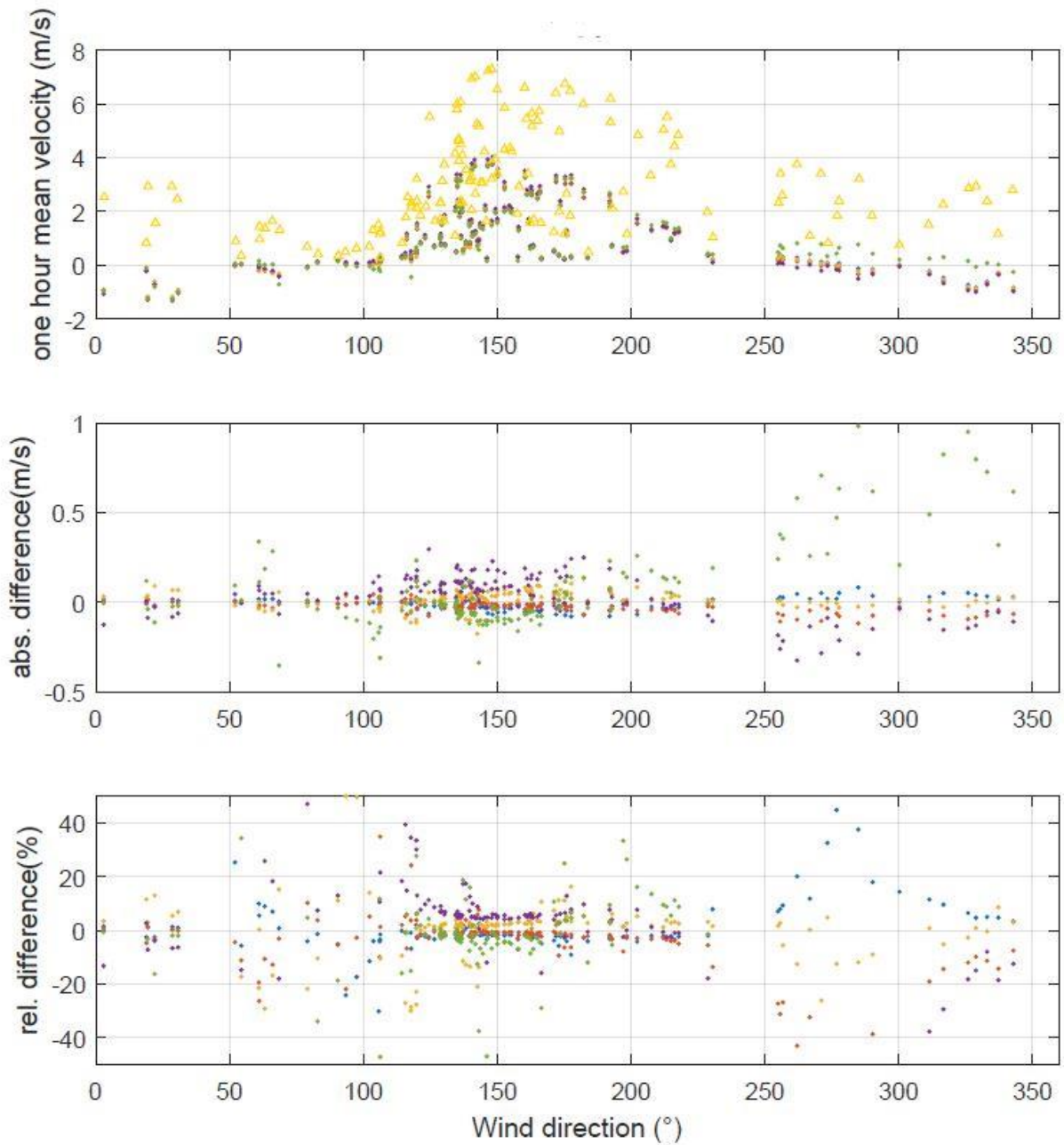


Figure 49: Results for experiments with (reduced) horizontal profile measurements for CC1; a) velocity measurements; b) absolute and c) relative differences between the measurements with a reduced and detailed method; ● 1RSL; ● 2RSL; ● 3RSL; ● 4RSL; ● 6RSL; ▲ MM velocity

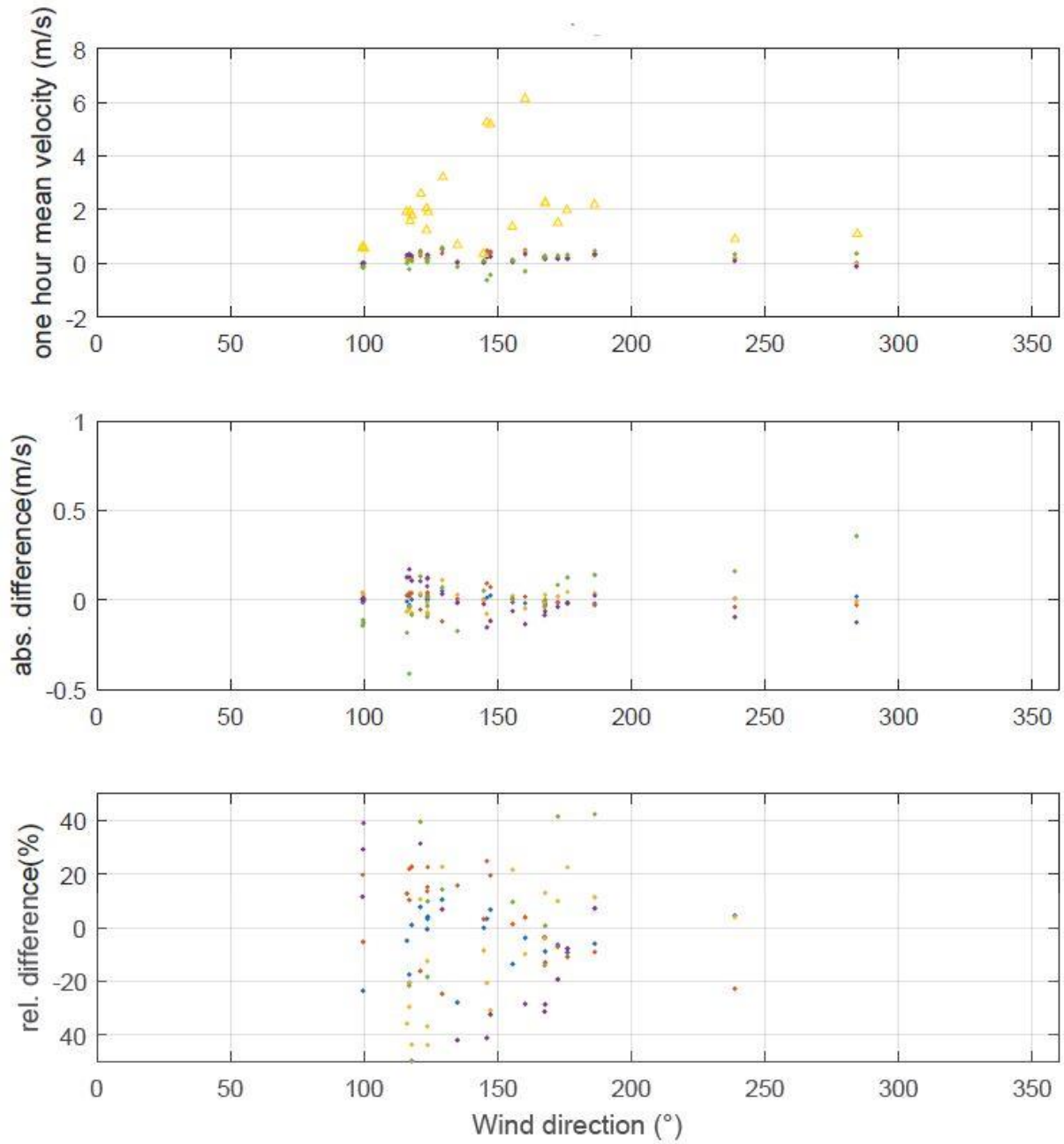


Figure 50: Results for experiments with (reduced) horizontal profile measurements for CC3; a) velocity measurements; b) absolute and c) relative differences between the measurements with a reduced and detailed method; ● 1RSL; ● 2RSL; ● 3RSL; ● 4RSL; ● 6RSL; ▲ MM velocity

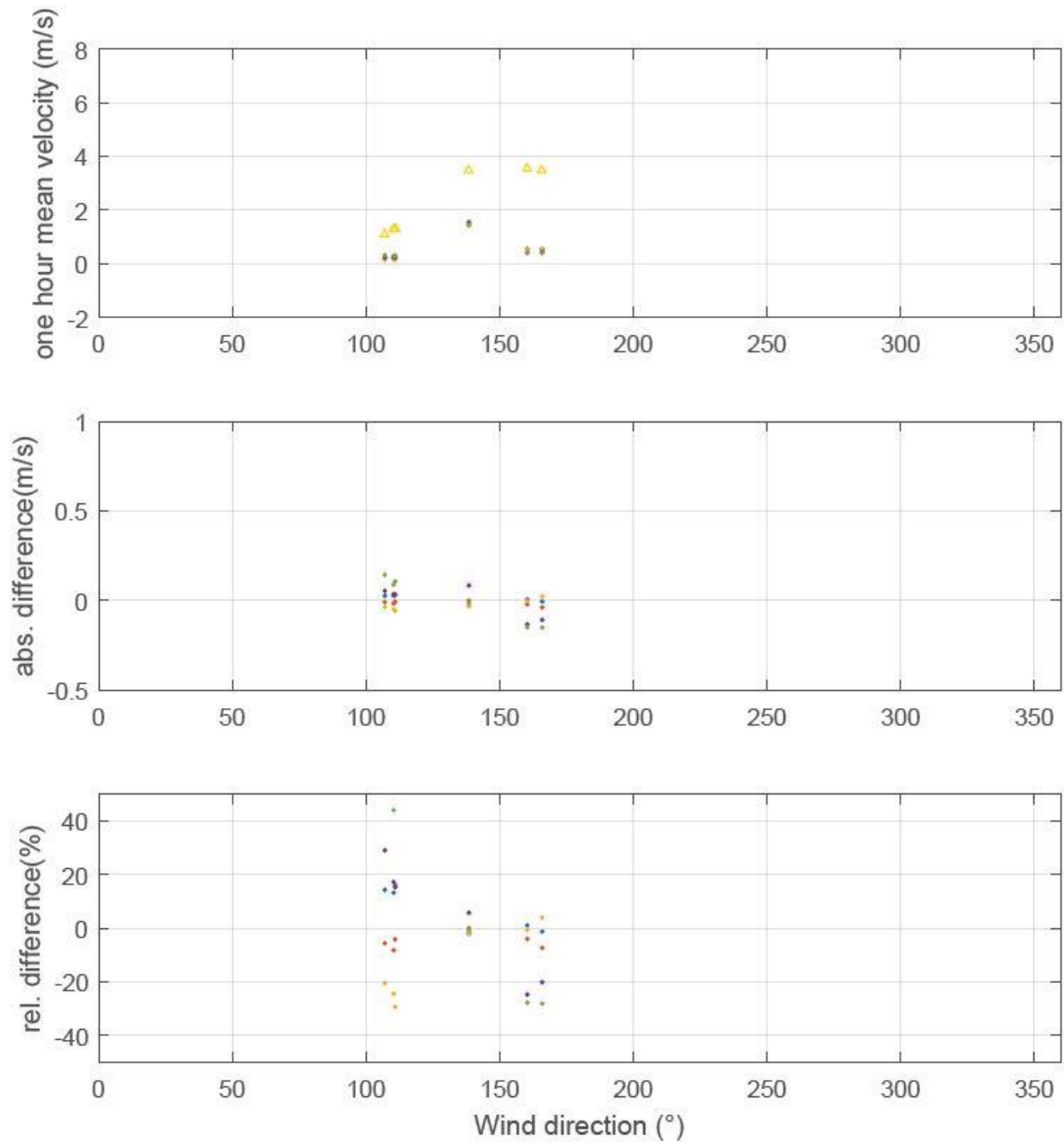


Figure 51: Results for experiments with (reduced) horizontal profile measurements for CC5; a) velocity measurements; b) absolute and c) relative differences between the measurements with a reduced and detailed method; ● 1RSL; ● 2RSL; ● 3RSL; ● 4RSL; ● 6RSL; ▲ MM velocity

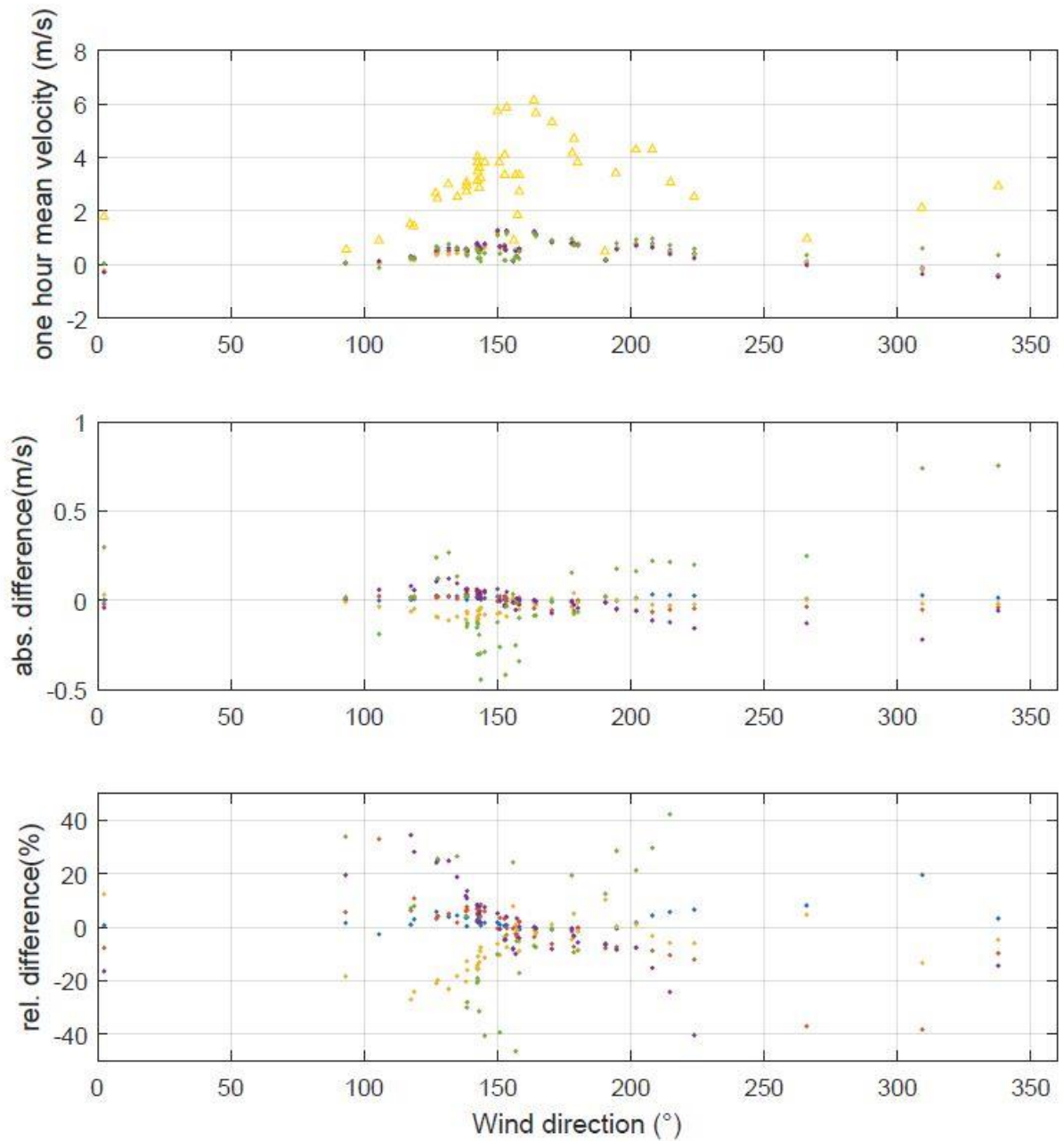


Figure 52: Results for experiments with (reduced) horizontal profile measurements for CC7; a) velocity measurements; b) absolute and c) relative differences between the measurements with a reduced and detailed method; ● 1RSL; ● 2RSL; ● 3RSL; ● 4RSL; ● 6RSL; ▲ MM velocity

5.3.1.3 Velocity profile in the ridge vent

The results of the experiments in the ridge vent were plotted in a similar way as to the results for the experiments with the vertical and horizontal profiles: for every curtain configuration used during the period of measurements, 3 subgraphs are plotted. The upper graphs show data plots with the mean velocities for *RR4*, *RR2*, *RR1* and the outside wind velocity v against the wind direction. The middle graphs show the absolute differences between the reduced velocity measurements and the reference horizontal velocity profile in the vent. The lower graphs in the third row show the respective relative differences, with the criterion of 20% in a red line. Results are plotted in Figures 53 to 55 for *CC2*, *CC4* and *CC8*, respectively.

The figures for all curtain configurations show that using half (4) or a quarter (2) of the number of sampling locations was enough to predict the mean of the detailed velocities in the ridge vent: these results were similar for all wind directions and all wind velocities within the criterion of $\pm 20\%$ relative difference. Although using one sensor gave mostly good results, the relative difference exceeded the criterion for some wind conditions. Reducing sampling locations to only 2 in the ridge vent was found feasible for 1) constant accurate results and 2) a relative difference within the predefined criterion of 20%.

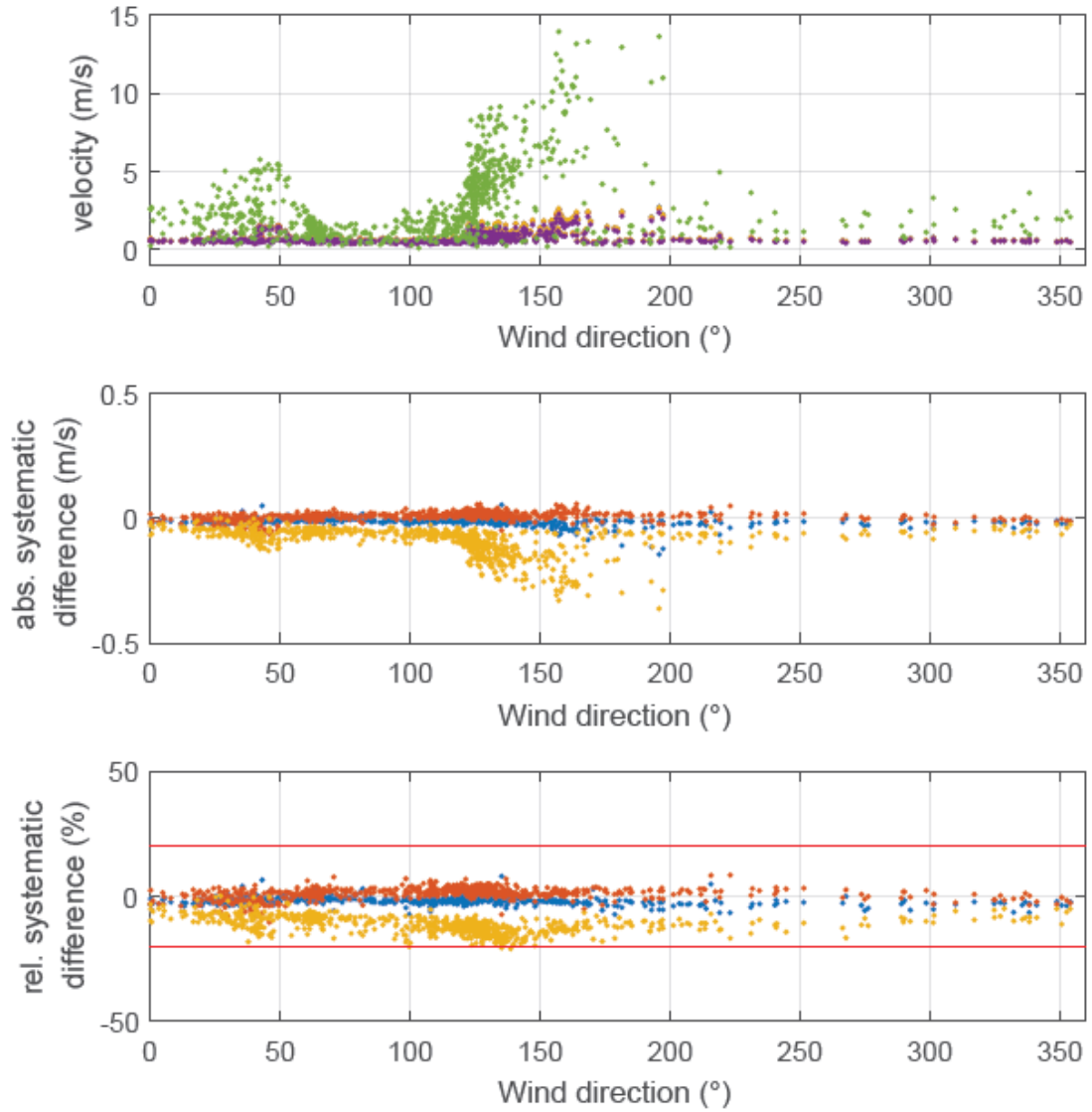


Figure 53: Results for experiments with (reduced) profile measurements in the ridge vent for CC2; a) velocity measurements; b) absolute and c) relative differences between the measurements with reduced and detailed method; ● RR4, ● RR2, ● RR1, ● MM, — ±20% criterion

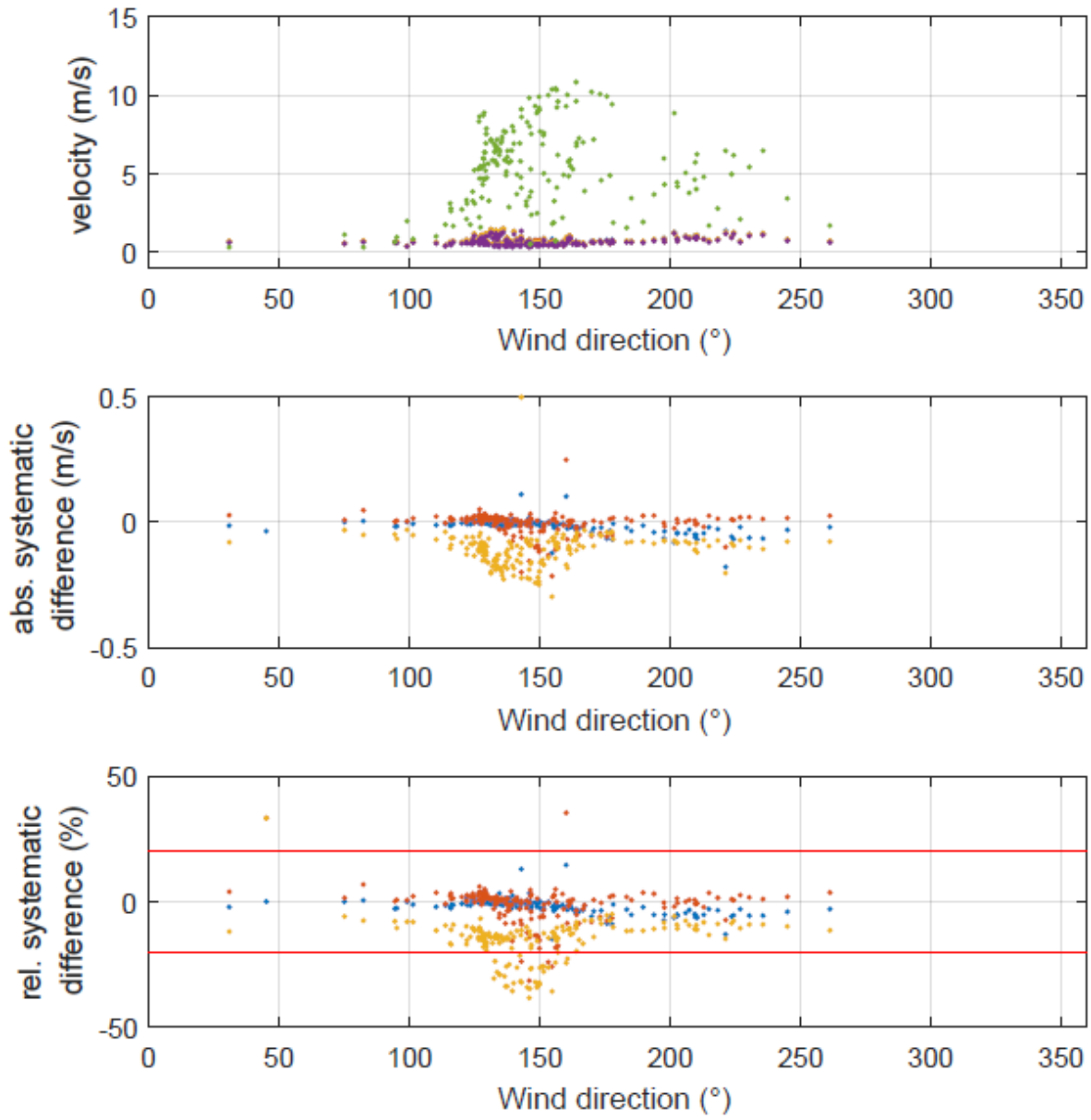


Figure 54: Results for experiments with (reduced) profile measurements in the ridge vent for CC4; a) velocity measurements; b) absolute and c) relative differences between the measurements with reduced and detailed method; ● RR4, ● RR2, ● RR1, ● MM, - ±20% criterion

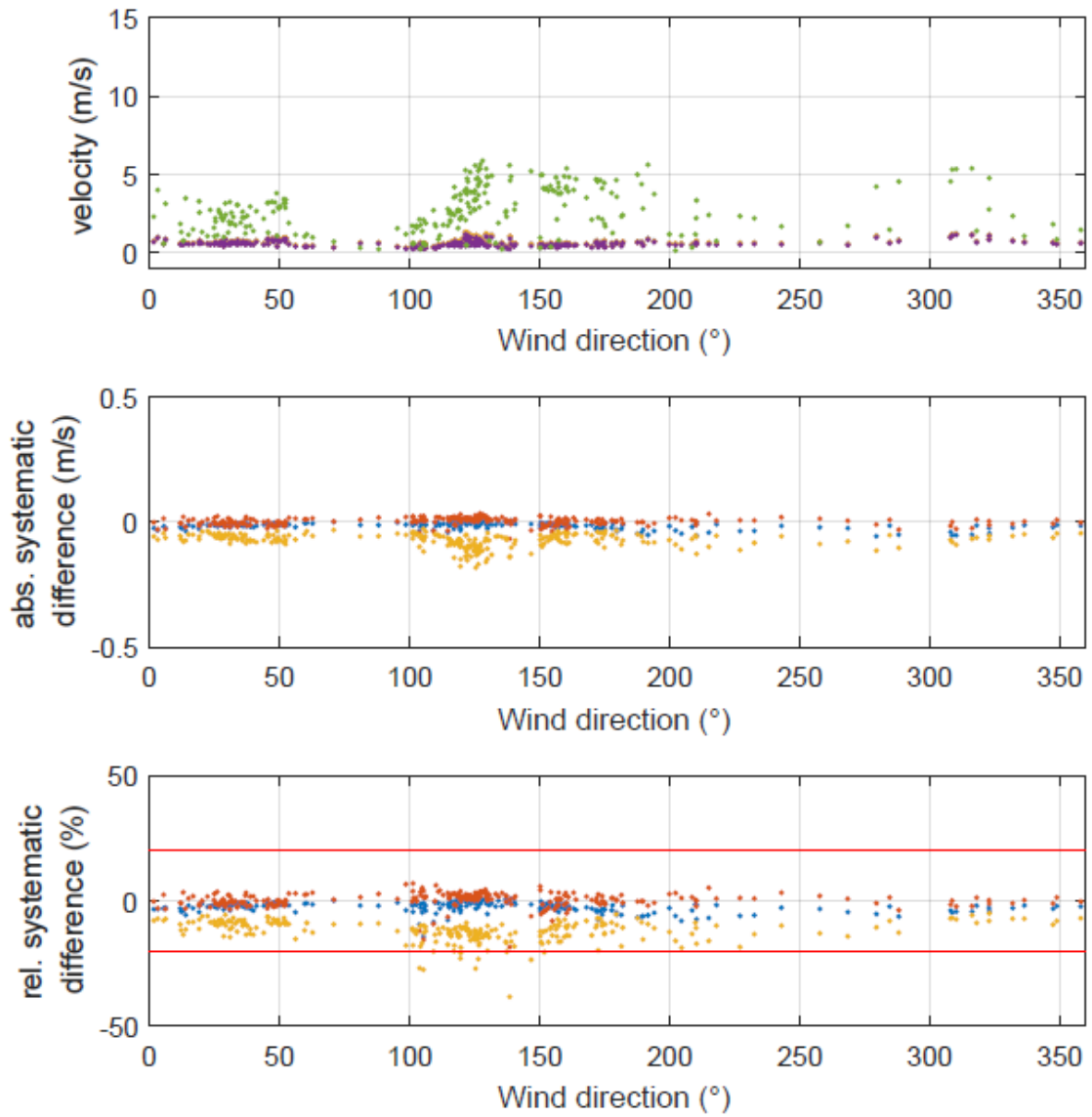


Figure 55: Results for experiments with (reduced) profile measurements in the ridge vent for CC8; a) velocity measurements; b) absolute and c) relative differences between the measurements with reduced and detailed method; ● RR4, ● RR2, ● RR1, ● MM, — ±20% criterion

5.3.2 **Predictability of the velocity pattern in the vents**

5.3.2.1 Side vents

Multiple linear models were applied to predict the mean velocities. This was done for the single sampling locations, as well as for the sensor groups with reduced measurement strategies. The correlations for the multiple linear models and Bland Altman of the one minute and one hour means were compared. These results were very similar. Therefore all results were given for the one hour means, but only the R^2 results for the one minute means.

Tables 16-21 give the results for the correlations between the sampling locations in the *NE*-side vent and the wind velocity components measured at the metemast for different curtain configurations: regression coefficients a , b , c , and Bland Altman coefficients β_0 and β_1 , minimum and maximum velocity values and the number of velocities measured and the R^2 -values.

Highest R^2 -values were found where highest velocities are expected:

- 1) in the upper rows of the vents;
 - 2) at the inlet side;
 - 3) when least obstruction is present for the airflow e.g. no to curtains or no silos.
- Bland Altman results confirmed that the correlations were accurate.

This resulted in the highest R^2 -values, >83%, when no curtains were used (*CC1*) for the sampling locations of the vertical profile experiments and >71% for the horizontal profile experiments. The difference in results for the R^2 -values for correlations for the experiments with horizontal and vertical profile show that care should be taken with interpretation of the results due to a different dataset of wind conditions.

The other experimental cases gave results lower than those with conditions without many obstacles. The decrease in R^2 -values was dependent of the three points as described above.

Both the normal and tangential component were important input variables for the correlation and changed in mutual importance depending on the curtain configuration or in- or outlet side.

It could be concluded that it was possible to predict the velocity pattern in the side vents with the use of the normal and tangential velocity components measured at the meteomast. However, surrounding obstacles decreased the R^2 -value of the correlations and correlations were specific per sensor location and per curtain configuration.

Table 16: Results in the *main outlet side* for the correlations between the velocity measured at the sampling locations in the *NE-side vent* and the wind velocity components measured at the meteomast for different curtain configurations: regression coefficients *a*, *b* and *c*

>90 and <270° Main outlet	<i>a</i>					<i>b</i>					<i>c</i>				
	CC1	CC2	CC3	CC4	CC5	CC1	CC2	CC3	CC4	CC5	CC1	CC2	CC3	CC4	CC5
SL11	-0,11	-	-0,14	-0,23	-	0,16	-	0,04	-0,13	-	0,06	-	0,05	0,65	-
SL12	-0,15	-	-0,17	-0,25	-	0,20	-	0,00	-0,15	-	0,04	-	0,06	0,68	-
SL13	-0,26	-	-0,10	-0,03	-	0,51	-	0,02	-0,04	-	-0,16	-	-0,07	-0,01	-
SG1	-0,17	-	-0,13	-0,17	-	0,29	-	0,02	-0,11	-	-0,02	-	0,01	0,44	-
SL21	-0,13	-	-0,13	-0,19	-	0,21	-	0,04	-0,09	-	0,07	-	0,11	0,57	-
SL22	-0,15	-	-0,15	-0,22	-	0,24	-	0,01	-0,12	-	0,04	-	0,08	0,59	-
SL23	-0,26	-0,06	-0,11	-0,03	-	0,50	0,06	0,01	-0,05	-	-0,12	-0,11	-0,02	-0,02	-
SG2	-0,18	-	-0,13	-0,15	-	0,32	-	0,02	-0,08	-	0,00	-	0,06	0,38	-
SL31	-0,25	0,02	0,00	-0,03	-	0,45	0,06	0,08	0,02	-	0,20	0,03	0,45	0,13	-
SL32	-0,27	-	0,03	0,01	-	0,42	-	0,08	0,01	-	0,17	-	0,31	0,01	-
SL33	-0,29	-	0,01	0,00	-	0,39	-	0,08	0,01	-	0,11	-	0,23	0,00	-
SG3	-0,27	-	0,02	-0,01	-	0,42	-	0,08	0,01	-	0,16	-	0,31	0,07	-
SL41	-0,26	0,01	0,04	0,00	-	0,43	0,05	0,09	0,02	-	0,22	0,02	0,46	0,08	-
SL42	-0,25	0,01	0,04	-0,01	-	0,40	0,06	0,09	0,02	-	0,19	0,00	0,37	0,07	-
SL43	-0,30	-0,02	0,05	0,02	-	0,41	0,07	0,10	0,02	-	0,12	-0,04	0,25	-0,12	-
SG4	-0,27	-	0,05	0,01	-	0,41	-	0,09	0,02	-	0,18	-	0,32	0,02	-
hSL2	-0,08	-	-0,17	-	-0,05	0,43	-	0,10	-	0,17	-0,08	-	-0,09	-	0,11
hSL3	-0,10	-	-0,50	-	-0,03	0,57	-	-0,02	-	0,22	-0,12	-	-0,65	-	-0,06
hSL4	-0,08	-	-0,08	-	-0,02	0,42	-	0,07	-	0,15	-0,07	-	0,01	-	0,10
hSL5	-0,10	-	-0,08	-	-0,09	0,48	-	0,06	-	0,16	-0,10	-	0,12	-	0,09
hSL6	-0,10	-	0,10	-	0,02	0,45	-	-0,04	-	0,17	-0,04	-	0,23	-	0,10
hSL7	-0,09	-	0,10	-	0,07	0,51	-	0,13	-	0,22	-0,11	-	0,06	-	-0,01
hSL8	-0,22	-	-0,05	-	-0,05	0,43	-	0,07	-	0,18	-0,13	-	-0,01	-	-0,02
hSL9	-0,26	-	-0,06	-	-0,12	0,44	-	0,08	-	0,19	-0,12	-	0,00	-	-0,05
hSL10	-0,24	-	0,02	-	-0,07	0,42	-	0,09	-	0,20	-0,01	-	0,04	-	0,02
hSL11	-0,21	-	0,10	-	-0,05	0,38	-	0,13	-	0,21	0,09	-	0,07	-	0,05
hSL12	-0,16	-	0,07	-	0,01	0,40	-	0,20	-	0,26	0,15	-	0,03	-	0,08
6RSL	-0,16	-	-0,04	-	-0,03	0,46	-	0,07	-	0,18	-0,08	-	0,05	-	0,05
4RSL	-0,17	-	-0,06	-	-0,05	0,46	-	0,08	-	0,18	-0,10	-	0,03	-	0,05
3RSL	-0,16	-	0,02	-	-0,01	0,48	-	0,09	-	0,19	-0,09	-	0,06	-	0,02
2RSL	-0,17	-	-0,07	-	-0,11	0,47	-	0,07	-	0,18	-0,11	-	0,06	-	0,02
1RSL	-0,09	-	0,10	-	0,07	0,51	-	0,13	-	0,22	-0,11	-	0,06	-	-0,01

Table 17: Results in the *main inlet side* for the correlations between the velocity measured at the sampling locations in the NE-side vent and the wind velocity components measured at the meteomast for different curtain configurations: regression coefficients a, b and c

Main inlet	a					b					c				
	CC1	CC2	CC3	CC4	CC5	CC1	CC2	CC3	CC4	CC5	CC1	CC2	CC3	CC4	CC5
SL11	-0,40	-0,26	-0,32	-0,36	-	0,45	0,18	0,25	0,31	-	-0,03	-0,02	-0,06	0,25	-
SL12	-0,39	-0,27	-0,37	-0,39	-	0,48	0,18	0,33	0,32	-	-0,01	-0,07	-0,03	0,26	-
SL13	-0,03	-0,02	-0,07	-0,06	-	0,46	0,08	0,04	0,06	-	0,01	-0,04	-0,18	-0,10	-
SG1	-0,27	-0,18	-0,25	-0,27	-	0,46	0,15	0,20	0,23	-	-0,01	-0,04	-0,09	0,13	-
SL21	-0,38	-0,24	-0,30	-0,34	-	0,50	0,21	0,28	0,32	-	0,01	-0,01	-0,02	0,22	-
SL22	-0,37	-0,26	-0,34	-0,37	-	0,51	0,21	0,32	0,33	-	0,01	-0,04	-0,03	0,21	-
SL23	-0,09	-0,04	-0,12	-0,07	-	0,51	0,06	0,08	0,06	-	0,02	-0,12	-0,17	-0,11	-
SG2	-0,28	-0,17	-0,25	-0,26	-	0,50	0,16	0,23	0,24	-	0,01	-0,05	-0,08	0,10	-
SL31	0,04	-0,03	0,07	-0,04	-	0,63	0,12	0,45	0,12	-	0,31	0,07	0,27	0,05	-
SL32	0,08	-	0,11	-0,03	-	0,63	-	0,35	0,10	-	0,25	-	0,10	-0,04	-
SL33	0,05	-0,02	0,10	-0,02	-	0,52	0,10	0,28	0,09	-	0,12	-0,01	0,00	-0,04	-
SG3	0,06	-	0,09	-0,04	-	0,61	-	0,36	0,12	-	0,24	-	0,12	0,01	-
SL41	0,10	0,00	0,14	-0,01	-	0,62	0,12	0,40	0,10	-	0,33	0,03	0,25	0,06	-
SL42	0,09	-0,01	0,11	-0,03	-	0,63	0,16	0,37	0,11	-	0,25	0,00	0,12	0,00	-
SL43	0,12	0,01	0,17	0,01	-	0,48	0,05	0,22	0,06	-	0,13	-0,08	-0,02	-0,07	-
SG4	0,10	-	0,14	-0,02	-	0,59	-	0,33	0,09	-	0,25	-	0,11	-0,02	-
hSL2	0,12	-	-	-	0,08	0,37	-	-	-	0,15	0,02	-	-	-	0,01
hSL3	0,17	-	-	-	-	0,38	-	-	-	-	-0,08	-	-	-	-
hSL4	0,17	-	-	-	0,23	0,30	-	-	-	0,10	0,13	-	-	-	0,09
hSL5	0,23	-	-	-	0,33	0,39	-	-	-	0,15	0,11	-	-	-	0,08
hSL6	0,23	-	-	-	-	0,34	-	-	-	-	0,26	-	-	-	-
hSL7	0,12	-	-	-	-0,06	0,36	-	-	-	0,08	0,02	-	-	-	-0,04
hSL8	-0,12	-	-	-	-0,21	0,42	-	-	-	0,23	-0,09	-	-	-	-0,06
hSL9	-0,15	-	-	-	-0,15	0,50	-	-	-	0,33	-0,10	-	-	-	-0,05
hSL10	-0,09	-	-	-	-0,03	0,56	-	-	-	0,35	0,03	-	-	-	0,01
hSL11	0,00	-	-	-	0,10	0,55	-	-	-	0,28	0,11	-	-	-	0,06
hSL12	0,13	-	-	-	0,17	0,55	-	-	-	0,34	0,19	-	-	-	0,17
6RSL	0,05	-	-	-	-	0,42	-	-	-	-	0,09	-	-	-	-
4RSL	0,02	-	-	-	0,08	0,44	-	-	-	0,21	0,05	-	-	-	0,02
3RSL	0,05	-	-	-	0,06	0,41	-	-	-	0,18	0,05	-	-	-	0,02
2RSL	0,02	-	-	-	0,09	0,45	-	-	-	0,24	0,02	-	-	-	0,01
1RSL	0,12	-	-	-	-0,06	0,36	-	-	-	0,08	0,02	-	-	-	-0,04

Table 18: Results for the correlations between the velocity measured at the sampling locations in the NE-side vent and the wind velocity components measured at the metemast for different curtain configurations for the *side vent acting as a main outlet*: minimum and maximum velocity values $|\bar{V}|$ and the number of velocities measured

>90 and <270° Main outlet	min					max					n				
	CC1	CC2	CC3	CC4	CC5	CC1	CC2	CC3	CC4	CC5	CC1	CC2	CC3	CC4	CC5
SL11	-0,42	-	-0,67	-0,65	-	1,01	-	0,96	3,13	-	52	-	72	158	-
SL12	-0,56	-	-0,80	-0,92	-	1,23	-	1,00	3,19	-	52	-	72	160	-
SL13	-0,60	-	-0,31	-0,46	-	2,41	-	0,85	0,14	-	52	-	72	160	-
SG1	-0,53	-	-0,59	-0,63	-	1,50	-	0,84	2,16	-	52	-	72	158	-
SL21	-0,33	-	-0,59	-0,58	-	1,25	-	1,04	2,79	-	52	-	72	160	-
SL22	-0,48	-	-0,67	-0,68	-	1,38	-	1,00	2,93	-	52	-	72	160	-
SL23	-0,53	-0,32	-0,37	-0,55	-	2,41	0,24	0,87	0,15	-	52	18	72	167	-
SG2	-0,44	-	-0,54	-0,52	-	1,65	-	0,93	1,95	-	52	-	72	158	-
SL31	0,19	0,04	0,10	-0,05	-	2,68	0,38	1,36	0,78	-	52	18	72	235	-
SL32	0,13	-	-0,11	-0,15	-	2,57	-	1,05	0,23	-	51	-	66	134	-
SL33	0,01	-	-0,23	-0,17	-	2,37	-	1,11	1,52	-	52	-	72	238	-
SG3	0,14	-	-0,08	-0,03	-	2,54	-	1,01	0,32	-	51	-	66	126	-
SL41	0,17	0,03	0,07	-0,04	-	2,67	0,32	1,32	0,53	-	52	18	72	148	-
SL42	0,12	-0,01	-0,10	-0,09	-	2,50	0,31	1,23	0,42	-	52	18	72	192	-
SL43	-0,01	-0,07	-0,27	-0,46	-	2,48	0,36	1,18	0,21	-	52	18	72	241	-
SG4	0,11	-	-0,10	-0,06	-	2,55	-	1,19	0,27	-	51	-	66	126	-
hSL2	-0,23	-	-0,10	-	-0,01	3,18	-	1,11	-	1,17	131	-	41	-	45
hSL3	-0,05	-	0,13	-	-0,05	4,05	-	0,80	-	1,39	104	-	9	-	13
hSL4	-0,23	-	-0,33	-	-0,12	3,15	-	1,59	-	1,09	126	-	48	-	49
hSL5	-0,17	-	-0,10	-	-0,02	3,84	-	1,17	-	1,65	142	-	64	-	52
hSL6	-0,45	-	-0,63	-	-0,12	3,77	-	0,56	-	1,21	116	-	24	-	45
hSL7	-0,11	-	-0,05	-	-0,02	4,21	-	0,95	-	1,69	190	-	71	-	59
hSL8	-0,63	-	-0,27	-	-0,25	4,07	-	0,57	-	1,26	214	-	71	-	63
hSL9	-0,71	-	-0,15	-	-0,30	4,22	-	0,88	-	1,37	169	-	69	-	53
hSL10	-0,29	-	-0,10	-	-0,18	4,26	-	0,97	-	1,40	211	-	71	-	63
hSL11	-0,07	-	-0,12	-	0,02	4,02	-	1,03	-	1,41	211	-	70	-	63
hSL12	-0,11	-	-0,04	-	0,04	4,04	-	1,27	-	1,66	201	-	71	-	50
6RSL	0,03	-	-0,04	-	0,05	3,73	-	0,54	-	1,24	113	-	24	-	42
4RSL	-0,12	-	-0,04	-	0,05	3,76	-	0,67	-	1,21	120	-	41	-	45
3RSL	0,00	-	0,00	-	0,03	3,87	-	0,84	-	1,22	126	-	48	-	49
2RSL	-0,10	-	-0,03	-	-0,03	4,03	-	0,91	-	1,40	140	-	64	-	52
1RSL	-0,11	-	-0,05	-	-0,02	4,21	-	0,95	-	1,69	190	-	71	-	59

Table 19: Results for the correlations between the velocity measured at the sampling locations in the NE-side vent and the wind velocity components measured at the meteomast for different curtain configurations for the side vent acting as a main inlet: minimum and maximum velocity values $|\bar{V}|$ and the number of velocities measured

<90° or >270° Main inlet	min					max					n				
	CC1	CC2	CC3	CC4	CC5	CC1	CC2	CC3	CC4	CC5	CC1	CC2	CC3	CC4	CC5
SL11	-2,68	-1,13	-1,03	-1,17	-	0,53	0,58	0,33	1,36	-	139	25	11	37	-
SL12	-2,71	-1,17	-1,15	-1,27	-	0,52	0,60	0,39	1,40	-	140	25	11	40	-
SL13	-1,60	-0,45	-0,42	-0,41	-	0,23	-0,10	-0,13	0,02	-	140	25	11	40	-
SG1	-2,33	-0,86	-0,87	-0,95	-	0,32	0,31	0,19	0,92	-	139	25	11	37	-
SL21	-2,69	-1,17	-0,94	-1,31	-	0,51	0,34	0,32	1,21	-	140	25	11	40	-
SL22	-2,69	-1,24	-1,04	-1,37	-	0,51	0,42	0,35	1,28	-	140	25	11	40	-
SL23	-1,92	-0,54	-0,55	-0,44	-	0,23	-0,15	-0,05	0,01	-	140	55	11	37	-
SG2	-2,43	-0,91	-0,84	-1,01	-	0,36	0,16	0,21	0,83	-	139	25	11	37	-
SL31	-2,21	-0,54	-0,24	-0,91	-	0,44	-0,01	0,46	0,26	-	143	55	11	151	-
SL32	-1,70	-	-0,30	-0,33	-	0,45	-	0,42	0,01	-	131	-	11	15	-
SL33	-2,03	-0,48	-0,31	-0,85	-	0,47	-0,08	0,30	0,11	-	143	50	11	156	-
SG3	-1,64	-	-0,28	-0,34	-	0,44	-	0,39	0,08	-	131	-	11	15	-
SL41	-1,68	-0,18	-0,22	-0,43	-	0,49	0,01	0,63	0,15	-	140	8	11	26	-
SL42	-1,75	-0,35	-0,30	-1,08	-	0,42	-0,05	0,46	0,09	-	140	8	11	60	-
SL43	-1,74	-0,45	-0,29	-0,71	-	0,53	-0,07	0,50	-0,08	-	143	55	11	150	-
SG4	-1,71	-	-0,27	-0,28	-	0,48	-	0,53	0,02	-	131	-	11	15	-
hSL2	-1,12	-	-	-	-0,57	0,24	-	-	-	0,09	43	-	-	-	11
hSL3	-1,33	-	-	-	-	0,36	-	-	-	-	19	-	-	-	-
hSL4	-0,93	-	-	-	-0,48	0,57	-	-	-	0,51	40	-	-	-	11
hSL5	-1,42	-	-	-	-0,73	0,53	-	-	-	0,41	51	-	-	-	24
hSL6	-1,27	-	-	-	-	0,78	-	-	-	-	34	-	-	-	-
hSL7	-1,29	-	-	-	-0,58	0,16	-	-	-	0,00	94	-	-	-	26
hSL8	-1,58	-	-	-	-1,54	0,17	-	-	-	0,09	119	-	-	-	26
hSL9	-1,61	-	-	-	-1,82	0,20	-	-	-	0,04	73	-	-	-	26
hSL10	-1,54	-	-	-	-1,54	0,18	-	-	-	0,04	119	-	-	-	26
hSL11	-1,56	-	-	-	-0,81	0,17	-	-	-	0,02	119	-	-	-	26
hSL12	-1,55	-	-	-	-0,86	0,53	-	-	-	0,12	95	-	-	-	26
6RSL	-1,23	-	-	-	-	0,12	-	-	-	-	31	-	-	-	-
4RSL	-1,24	-	-	-	-0,55	0,12	-	-	-	-0,03	37	-	-	-	11
3RSL	-1,18	-	-	-	-0,48	0,11	-	-	-	-0,02	40	-	-	-	11
2RSL	-1,33	-	-	-	-0,74	0,16	-	-	-	-0,04	48	-	-	-	24
1RSL	-1,29	-	-	-	-0,58	0,16	-	-	-	0,00	94	-	-	-	26

Table 20: Results for the correlations between the velocity measured at the sampling locations in the NE-side vent and the wind velocity components measured at the meteomast for different curtain configurations for the side vent acting as a main outlet. Bland Altman coefficients β_0 and β_1 and R^2 -values for the one hour and one minute means

>90 and <270° Main outlet	β_0					β_1					R^2 hourly means					R^2 minutely means				
	CC1	CC2	CC3	CC4	CC5	CC1	CC2	CC3	CC4	CC5	CC1	CC2	CC3	CC4	CC5	CC1	CC2	CC3	CC4	CC5
SL11	0,06	-	0,11	0,32	-	-0,03	-	-0,03	-0,21	-	89	-	81	57	-	44	30	62	47	-
SL12	0,04	-	0,10	0,27	-	-0,02	-	-0,02	-0,18	-	92	-	82	62	-	63	38	63	49	-
SL13	0,02	-	0,38	0,27	-	-0,02	-	-0,02	0,03	-	95	-	52	62	-	84	2	16	28	-
SG1	0,01	-	0,12	0,29	-	-0,01	-	-0,02	-0,12	-	98	-	80	60	-	77	27	53	52	-
SL21	0,03	-	0,15	0,38	-	-0,02	-	-0,04	-0,24	-	93	-	75	52	-	71	32	58	37	-
SL22	0,03	-	0,14	0,31	-	-0,02	-	-0,03	-0,20	-	95	-	77	58	-	70	32	59	43	-
SL23	0,01	0,04	0,29	0,30	-	-0,02	0,00	-0,03	0,03	-	97	93	59	58	-	86	75	46	38	-
SG2	0,01	-	0,16	0,33	-	0,00	-	-0,03	-0,13	-	99	-	75	55	-	83	31	59	46	-
SL31	0,03	0,06	1,43	0,67	-	-0,03	-0,01	-0,81	-0,15	-	95	89	9	33	-	84	50	11	7	-
SL32	0,02	-	1,26	0,73	-	-0,03	-	-0,50	-0,02	-	95	-	13	30	-	80	42	13	3	-
SL33	0,03	-	1,58	1,78	-	-0,03	-	-0,53	-0,05	-	95	-	6	3	-	81	39	8	0	-
SG3	0,02	-	1,36	1,22	-	-0,03	-	-0,55	-0,13	-	95	-	11	14	-	83	51	11	2	-
SL41	0,03	0,04	1,25	0,96	-	-0,04	0,00	-0,70	-0,14	-	94	92	13	21	-	83	78	12	2	-
SL42	0,03	0,09	1,24	0,97	-	-0,03	-0,01	-0,57	-0,14	-	95	85	13	21	-	82	65	13	7	-
SL43	0,03	0,07	1,27	0,56	-	-0,04	0,00	-0,47	0,05	-	94	87	12	39	-	78	12	12	13	-
SG4	0,03	-	1,02	0,75	-	-0,04	-	-0,43	-0,05	-	94	-	19	29	-	81	52	18	3	-
hSL2	0,05	-	0,09	-	0,17	-0,05	-	-0,03	-	-0,10	91	-	84	-	73	-	-	-	-	-
hSL3	0,06	-	0,07	-	0,05	-0,09	-	-0,03	-	-0,04	90	-	88	-	90	-	-	-	-	-
hSL4	0,07	-	0,76	-	0,22	-0,08	-	-0,21	-	-0,11	87	-	29	-	67	-	-	-	-	-
hSL5	0,10	-	0,89	-	0,22	-0,12	-	-0,32	-	-0,13	83	-	24	-	67	-	-	-	-	-
hSL6	0,14	-	1,03	-	0,33	-0,19	-	-0,07	-	-0,18	77	-	19	-	56	-	-	-	-	-
hSL7	0,19	-	0,08	-	0,06	-0,23	-	-0,01	-	-0,03	71	-	86	-	89	-	-	-	-	-
hSL8	0,15	-	0,22	-	0,09	-0,17	-	-0,05	-	-0,05	75	-	66	-	85	-	-	-	-	-
hSL9	0,13	-	0,37	-	0,02	-0,17	-	-0,10	-	-0,01	78	-	53	-	95	-	-	-	-	-
hSL10	0,17	-	0,65	-	0,08	-0,20	-	-0,13	-	-0,05	73	-	34	-	85	-	-	-	-	-
hSL11	0,18	-	0,22	-	0,08	-0,22	-	-0,04	-	-0,06	72	-	67	-	85	-	-	-	-	-
hSL12	0,17	-	0,15	-	0,04	-0,22	-	-0,06	-	-0,03	73	-	75	-	92	-	-	-	-	-
6RSL	0,06	-	0,23	-	0,03	-0,08	-	-0,04	-	-0,02	89	-	66	-	94	-	-	-	-	-
4RSL	0,07	-	0,08	-	0,02	-0,09	-	-0,02	-	-0,01	87	-	86	-	95	-	-	-	-	-
3RSL	0,07	-	0,28	-	0,01	-0,09	-	-0,06	-	-0,01	88	-	60	-	97	-	-	-	-	-
2RSL	0,10	-	0,47	-	0,05	-0,13	-	-0,15	-	-0,03	82	-	45	-	91	-	-	-	-	-
1RSL	0,19	-	0,08	-	0,06	-0,23	-	-0,01	-	-0,03	71	-	86	-	89	-	-	-	-	-

Table 21: Results for the correlations between the velocity measured at the sampling locations in the NE-side vent and the wind velocity components measured at the metemast for different curtain configurations for the side vent acting as a main inlet. Bland Altman coefficients β_0 and β_1 and R^2 -values for the one hour and one minute means

<90° or >270° Main inlet	β_0					β_1					R^2 one hour means					R^2 one minute means				
	CC1	CC2	CC3	CC4	CC5	CC1	CC2	CC3	CC4	CC5	CC1	CC2	CC3	CC4	CC5	CC1	CC2	CC3	CC4	CC5
SL11	0,02	0,11	0,01	0,04	-	0,02	0,11	0,01	0,04	-	96	80	98	92	-	82	32	87	11	-
SL12	0,03	0,12	0,01	0,04	-	0,03	0,12	0,01	0,04	-	95	80	97	92	-	81	35	86	18	-
SL13	0,09	0,17	0,14	0,07	-	0,09	0,17	0,14	0,07	-	84	73	77	87	-	57	38	21	60	-
SG1	0,03	0,13	0,00	0,04	-	0,03	0,13	0,00	0,04	-	94	79	99	93	-	80	34	84	18	-
SL21	0,02	0,12	0,01	0,04	-	0,02	0,12	0,01	0,04	-	96	80	98	93	-	82	30	85	8	-
SL22	0,03	0,11	0,02	0,04	-	0,03	0,11	0,02	0,04	-	95	81	97	93	-	81	29	85	9	-
SL23	0,06	0,38	0,02	0,07	-	0,06	0,38	0,02	0,07	-	88	52	96	88	-	64	45	57	49	-
SG2	0,03	0,13	0,01	0,03	-	0,03	0,13	0,01	0,03	-	95	78	99	93	-	80	35	84	10	-
SL31	0,05	0,03	0,05	0,03	-	0,05	0,03	0,05	0,03	-	91	94	91	94	-	65	47	42	3	-
SL32	0,06	-	0,04	0,18	-	0,06	-	0,04	0,18	-	88	-	92	72	-	66	23	43	16	-
SL33	0,08	0,07	0,08	0,12	-	0,08	0,07	0,08	0,12	-	86	87	86	80	-	57	57	33	15	-
SG3	0,06	-	0,05	0,08	-	0,06	-	0,05	0,08	-	88	-	91	86	-	67	41	47	34	-
SL41	0,06	0,01	0,03	0,02	-	0,06	0,01	0,03	0,02	-	89	97	95	95	-	70	64	49	47	-
SL42	0,07	0,02	0,04	0,05	-	0,07	0,02	0,04	0,05	-	88	97	92	91	-	69	52	46	2	-
SL43	0,10	0,31	0,02	0,13	-	0,10	0,31	0,02	0,13	-	83	57	96	79	-	54	33	45	23	-
SG4	0,07	-	0,02	0,08	-	0,07	-	0,02	0,08	-	87	-	96	85	-	67	42	52	19	-
hSL2	0,05	-	-	-	0,26	0,02	-	-	-	0,07	91	-	-	-	63	-	-	-	-	-
hSL3	0,02	-	-	-	-	0,01	-	-	-	-	97	-	-	-	-	-	-	-	-	-
hSL4	0,05	-	-	-	0,09	0,01	-	-	-	0,01	91	-	-	-	84	-	-	-	-	-
hSL5	0,09	-	-	-	0,05	0,02	-	-	-	0,01	85	-	-	-	91	-	-	-	-	-
hSL6	0,16	-	-	-	-	0,01	-	-	-	-	74	-	-	-	-	-	-	-	-	-
hSL7	0,09	-	-	-	0,12	0,04	-	-	-	0,03	84	-	-	-	79	-	-	-	-	-
hSL8	0,13	-	-	-	0,07	0,05	-	-	-	0,04	79	-	-	-	87	-	-	-	-	-
hSL9	0,09	-	-	-	0,09	0,05	-	-	-	0,07	85	-	-	-	84	-	-	-	-	-
hSL10	0,07	-	-	-	0,08	0,03	-	-	-	0,06	87	-	-	-	86	-	-	-	-	-
hSL11	0,08	-	-	-	0,05	0,03	-	-	-	0,03	86	-	-	-	90	-	-	-	-	-
hSL12	0,05	-	-	-	0,03	0,02	-	-	-	0,02	90	-	-	-	93	-	-	-	-	-
6RSL	0,03	-	-	-	-	0,01	-	-	-	-	94	-	-	-	-	-	-	-	-	-
4RSL	0,03	-	-	-	0,02	0,01	-	-	-	0,01	94	-	-	-	96	-	-	-	-	-
3RSL	0,03	-	-	-	0,02	0,01	-	-	-	0,01	94	-	-	-	95	-	-	-	-	-
2RSL	0,07	-	-	-	0,10	0,03	-	-	-	0,04	88	-	-	-	83	-	-	-	-	-
1RSL	0,09	-	-	-	0,12	0,04	-	-	-	0,03	84	-	-	-	79	-	-	-	-	-

5.3.2.2 Ridge vent

Similarly to results for the side vents, correlations were built between the velocities of the meteomast and the velocities measured in the ridge vent. The regression and Bland Altman coefficients, R^2 -values, number of measurements and minimum and maximum of the results are given in Table 22 and Table 23. Results confirmed that the ridge vent acted at all times as an outlet. The minimum velocity measured was 0.19 m/s during the full period of measurements.

The main conclusion was that prediction of the velocities in the ridge vent with velocity data of the meteomast was not successful. Only for part of one experiment good results were found (when the airflow came through the NE-vent for CC2). A reason could be that the buoyancy effect has an important contribution in the correlation. Also, low correlation could be deduced from the Figures 53 to 55 because the velocity in the ridge vent remained quite steady for changing wind conditions.

In Figures 53 to 55 can be seen that the velocity through the ridge vent is quite steady and is not that much affected by the wind velocity or direction. Therefore, it could be seen visually that the velocities through the ridge vent were difficult to predict with a meteomast.

Table 22: Results for the correlations between the sampling locations in the ridge vent and the wind velocity components measured at the metemast for different curtain configurations: R^2 -values, minimum and maximum velocities $|\overline{Y}_{ms}|$ and the number of on hour mean velocities measured

Wind direction >90 and <270°	R ² hourly means			min			max			n		
	CC2	CC4	CC8	CC2	CC4	CC8	CC2	CC4	CC8	CC2	CC4	CC8
SR1	45	-	75	0,22	-	0,25	1,50	-	1,47	292	-	90
SR2	40	-	68	0,31	-	0,33	1,67	-	1,50	292	-	90
SR3	36	-	58	0,33	-	0,29	1,38	-	1,17	292	-	90
SR4	40	-	53	0,36	-	0,31	1,46	-	1,13	292	-	90
SR5	36	-	49	0,45	-	0,37	1,67	-	1,28	292	-	90
SR6	34	-	42	0,46	-	0,40	1,67	-	1,22	292	-	90
SR7	41	-	34	0,47	-	0,45	1,84	-	1,21	292	-	90
SR8	48	-	34	0,35	-	0,34	1,45	-	0,96	292	-	90
DR8	39	-	53	0,40	-	0,34	1,58	-	1,22	292	-	90
RR4	40	-	50	0,40	-	0,34	1,56	-	1,17	292	-	90
RR2	34	-	50	0,40	-	0,34	1,52	-	1,19	292	-	90
RR1	40	-	53	0,36	-	0,31	1,46	-	1,13	292	-	90
Wind direction >90 and <270°	R ² hourly means			min			max			n		
	CC2	CC4	CC8	CC2	CC4	CC8	CC2	CC4	CC8	CC2	CC4	CC8
SR1	86	49	25	0,28	0,18	0,19	3,43	1,90	1,22	496	175	166
SR2	84	31	19	0,33	0,19	0,20	3,39	1,84	1,28	496	175	166
SR3	83	12	16	0,33	0,18	0,13	2,62	1,28	1,15	496	175	166
SR4	83	3	20	0,29	0,31	0,23	2,36	1,34	1,15	496	175	166
SR5	84	0	24	0,41	0,39	0,31	2,82	2,18	1,41	496	175	166
SR6	85	3	27	0,40	0,43	0,32	2,84	1,71	1,46	496	175	166
SR7	85	19	35	0,39	0,43	0,35	2,95	1,87	1,59	496	175	166
SR8	84	40	44	0,26	0,18	0,25	2,20	1,43	1,28	496	175	166
DR8	85	1	23	0,36	0,39	0,28	2,73	1,48	1,29	496	175	166
RR4	84	0	26	0,34	0,39	0,27	2,58	1,46	1,29	496	175	166
RR2	84	1	22	0,38	0,34	0,29	2,70	1,50	1,31	496	175	166
RR1	83	3	20	0,29	0,31	0,23	2,36	1,34	1,15	496	175	166

Table 23: Results for the correlations between the sampling locations in the ridge vent and the wind velocity components measured at the meteorost for different curtain configurations: regression coefficients a , b and c and the Bland Altman coefficients β_0 and β_1

Wind direction >90 and <270°	a			b			c			α			β		
	CC2	CC4	CC8	CC2	CC4	CC8	CC2	CC4	CC8	CC2	CC4	CC8	CC2	CC4	CC8
SR1	0,39	-	0,40	0,00	-	-0,08	0,13	-	0,18	0,47	-	0,15	-0,27	-	-0,10
SR2	0,47	-	0,48	0,03	-	-0,07	0,11	-	0,17	0,55	-	0,21	-0,36	-	-0,15
SR3	0,44	-	0,45	0,04	-	-0,04	0,07	-	0,13	0,62	-	0,31	-0,36	-	-0,20
SR4	0,44	-	0,44	0,06	-	-0,03	0,07	-	0,13	0,55	-	0,36	-0,32	-	-0,23
SR5	0,54	-	0,54	0,07	-	-0,03	0,06	-	0,13	0,61	-	0,41	-0,43	-	-0,31
SR6	0,56	-	0,57	0,08	-	-0,03	0,05	-	0,12	0,66	-	0,51	-0,47	-	-0,38
SR7	0,60	-	0,62	0,11	-	-0,01	0,04	-	0,11	0,52	-	0,65	-0,40	-	-0,53
SR8	0,44	-	0,44	0,11	-	0,01	0,03	-	0,09	0,42	-	0,66	-0,25	-	-0,40
DR8	0,49	-	0,49	0,06	-	-0,03	0,07	-	0,13	0,56	-	0,36	-0,36	-	-0,25
RR4	0,48	-	0,48	0,07	-	-0,03	0,06	-	0,13	0,55	-	0,39	-0,35	-	-0,27
RR2	0,50	-	0,51	0,06	-	-0,03	0,06	-	0,12	0,65	-	0,40	-0,42	-	-0,28
RR1	0,44	-	0,44	0,06	-	-0,03	0,07	-	0,13	0,55	-	0,36	-0,32	-	-0,23
Wind direction >90 and <270°	a			b			c			α			β		
CC2	CC4	CC8	CC2	CC4	CC8	CC2	CC4	CC8	CC2	CC4	CC8	CC2	CC4	CC8	
SR1	0,40	0,61	0,41	-0,05	-0,08	-0,01	-0,17	-0,07	-0,07	0,08	0,41	0,85	-0,06	-0,29	-0,46
SR2	0,46	0,76	0,48	-0,02	-0,07	0,02	-0,17	-0,05	-0,06	0,09	0,72	1,04	-0,08	-0,56	-0,66
SR3	0,41	0,71	0,43	0,00	-0,04	0,03	-0,14	-0,01	-0,03	0,10	1,31	1,14	-0,07	-0,85	-0,63
SR4	0,39	0,67	0,39	0,01	-0,02	0,04	-0,12	-0,01	-0,03	0,10	1,79	0,99	-0,07	-1,17	-0,52
SR5	0,47	0,83	0,51	0,03	0,00	0,07	-0,15	0,00	-0,02	0,09	1,99	0,89	-0,08	-1,64	-0,59
SR6	0,49	0,86	0,50	0,04	0,02	0,07	-0,15	0,01	-0,03	0,09	1,80	0,79	-0,08	-1,55	-0,54
SR7	0,51	0,89	0,53	0,07	0,06	0,09	-0,15	0,02	-0,02	0,08	1,03	0,63	-0,09	-0,96	-0,46
SR8	0,37	0,61	0,37	0,07	0,07	0,09	-0,10	0,01	-0,01	0,09	0,54	0,48	-0,07	-0,39	-0,26
DR8	0,44	0,74	0,45	0,02	-0,01	0,05	-0,14	-0,01	-0,03	0,09	1,90	0,90	-0,07	-1,46	-0,55
RR4	0,43	0,72	0,44	0,03	0,00	0,06	-0,14	-0,01	-0,03	0,09	1,97	0,84	-0,08	-1,48	-0,50
RR2	0,45	0,78	0,46	0,02	-0,01	0,05	-0,14	0,00	-0,03	0,09	1,94	0,95	-0,08	-1,47	-0,58
RR1	0,39	0,67	0,39	0,01	-0,02	0,04	-0,12	-0,01	-0,03	0,10	1,79	0,99	-0,07	-1,17	-0,52

5.3.3 **Characterisation of airflow rates through side and ridge vent**

5.3.3.1 Measured airflow rates through openings

The estimated airflow rates through the ridge and *NE*-side vents show the behaviour of these airflow rates against the wind direction. These ratios give a better view of the relative importance of the measurements.

Figure 56 presents the estimated airflow rates in the barn. The air exchange rates (*AER*) were comparable to other studies with values going up to 100 *AER* per hour as e.g. *AER*-values up to 60 per hour measured by Wang et al., (2016). Wu et al. (2012a) found *AER* up to approximately 120. In the previous sections it could be seen that the magnitude of the velocities through the ridge and side vents lay in the same range. The airflow rates of the side vents were larger because the surface area of the *NE*-side vents (64m × 4m) were much larger than the surface area of the ridge vent (0.50m × 110m).

These results showed that the airflow rate through the side vents was very dependent on the wind velocity and wind direction. The airflow rates through the ridge vent stayed approximately steady during the time of measurements and were relatively small for large wind velocities perpendicular to the vents.

This could be the result of short-circuiting (Norton et al. 2009), when the air leaves the building before mixing with the indoor air. However, the anemometers were placed at vent level and not within the building, this could not be confirmed by measurements.

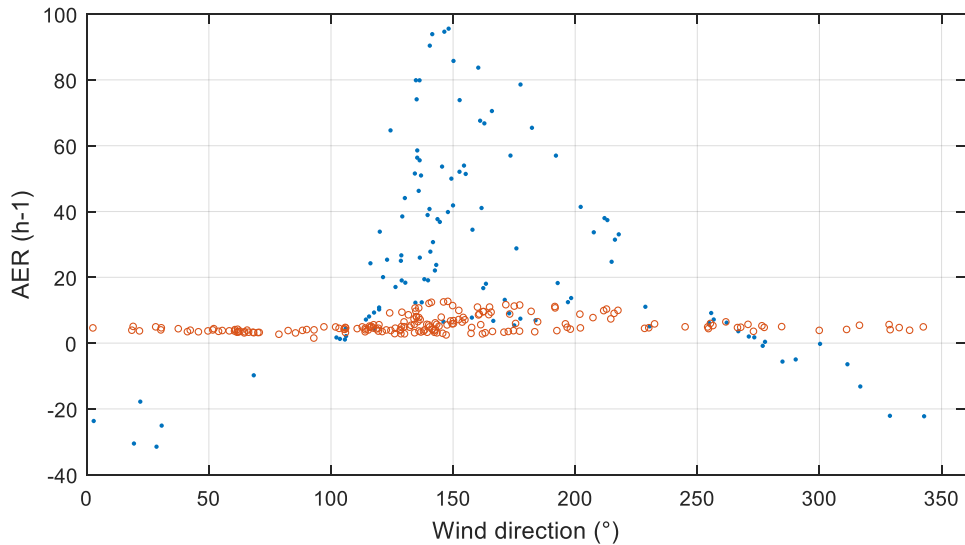


Figure 56: AER through the vents of the commercial animal house with open vents (CC1). ●: NE-side vent; ○ ridge vent

5.3.3.2 Uncertainty of measurements through different openings

The uncertainty of local velocity measurements in the vents were characterised by the unsteadiness of the wind, the accuracy of the ultrasonic anemometer used for the measurements and influences of surrounding obstacles. The uncertainty due to wind unsteadiness was much larger than the measurement uncertainty of the sensors for the majority of the measurements. Therefore, the latter was not taken into account.

Figure 57 and Figure 58 give measurement examples of the variability measured on sampling locations for CC1 and CC4, respectively. The variability is expressed as the standard deviation in the upper graphs of the figures. The variability is expressed as the coefficient of variation in the middle and lower graph against the wind direction and the local normal velocity, respectively.

Results were comparable for both curtain configurations. It can be seen that high variability on the measurements was present for all wind directions. However, the largest variability occurred mainly for low velocities. Only when plotting the coefficients of variation against the local (normal) wind velocity, a pattern is seen. For measurements below 0.5 m/s, very high coefficients of variation can be found. It is also seen that the variability of the measurements in the ridge vent was low compared to the results in the side vents. The uncertainty of the measurements in the ridge vent was independent of the local velocity. Unsteadiness comparable to these of the

velocities in the ridge vent could only be reached in the side vent for local velocities larger than approximately 1 m/s (Figure 57b). For velocities lower than 1 m/s, results varied even more than 50%.

These variations in measured velocities are high for some applications. When the velocities are used to measure the airflow rate for quantification of emissions, the variability is too high in the side vents. Increasing the number of sampling locations can consequently decrease the variation significantly.

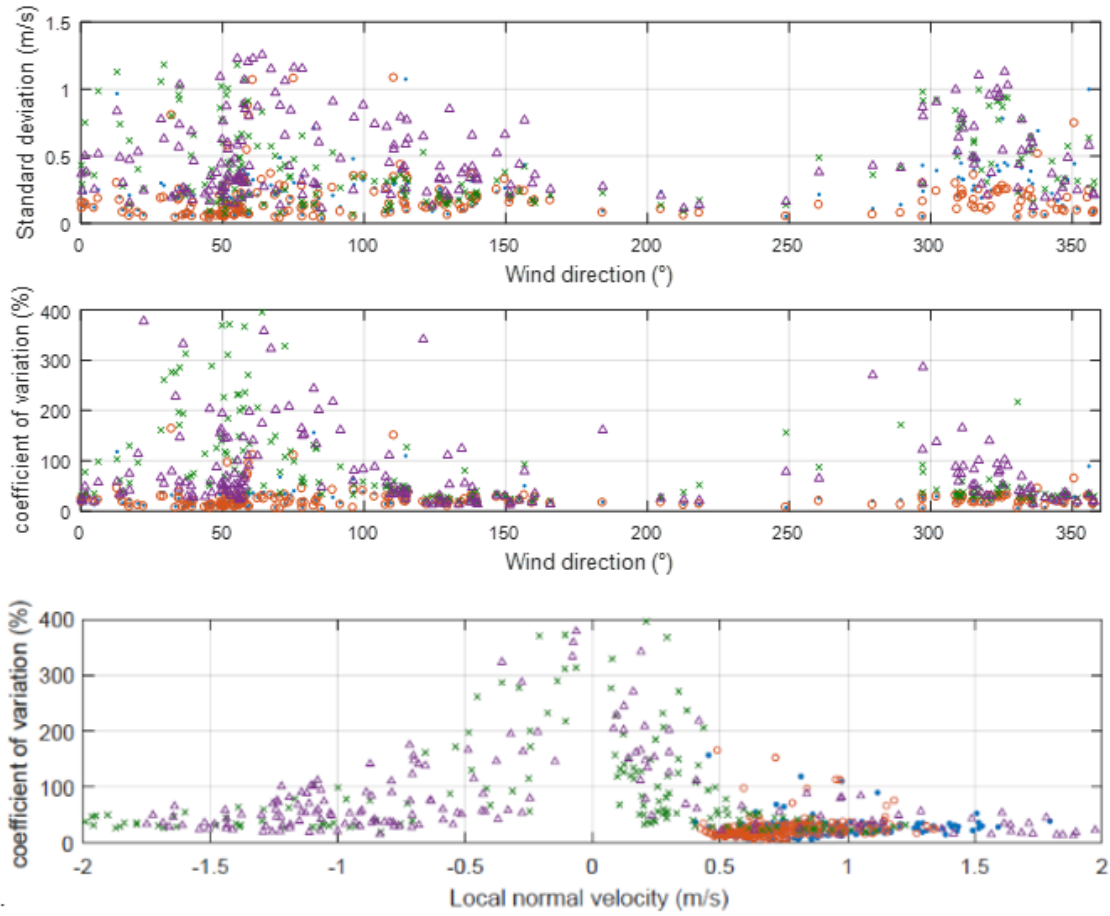


Figure 57: Results for the variability of the velocities in the vents for CC1: (a) Standard deviation of the local measured one hour mean velocity against the wind direction; (b) Coefficient of variation against the wind direction; (c) Coefficient of variation against the perpendicular velocity $|\overline{Y_{ms}}|$, negative velocities are used for inward airflows, positive values for outward airflows ○ Side of ridge vent; ● Middle of ridge vent; ▲ Middle of side vent; × Side of side vent

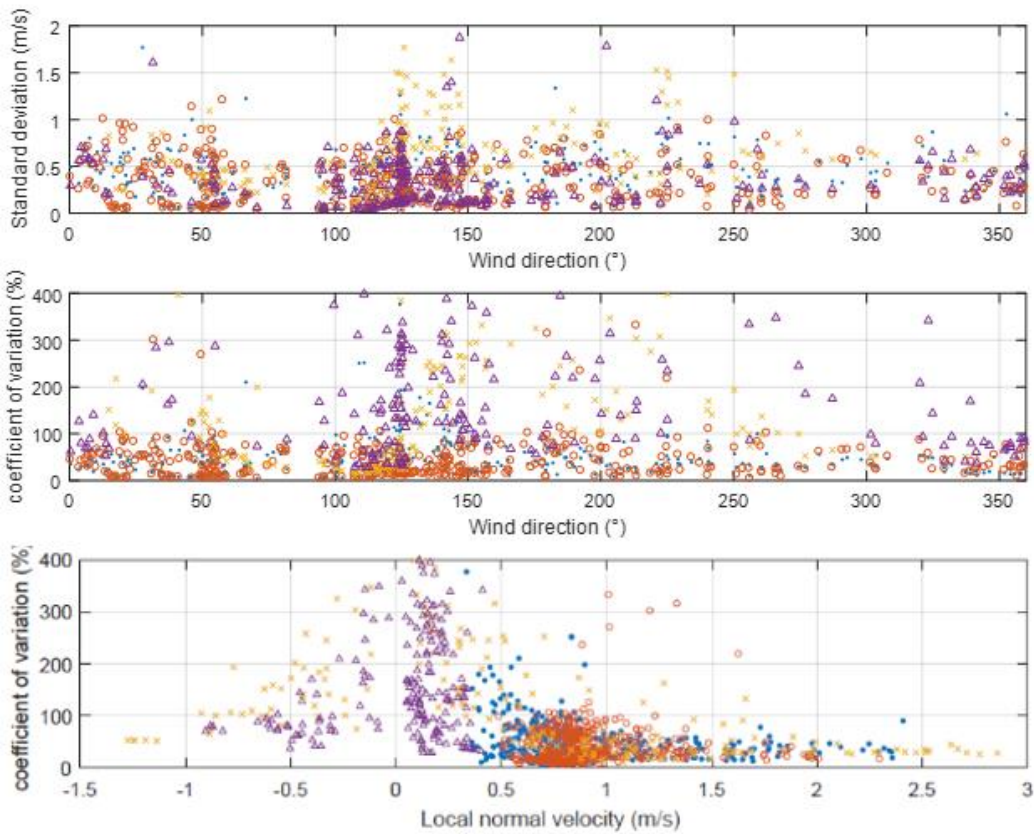


Figure 58: Results for the variability of the velocities in the vents for CC4: (a) Standard deviation of the local measured one hour mean velocity against the wind direction; (b) Coefficient of variation against the wind direction; (c) Coefficient of variation against the perpendicular velocity $|\overline{Y}_{ms}|$, negative velocities are used for inward airflows, positive values for outward airflows ○ Side of ridge vent; ● Middle of ridge vent; ▲ Middle of side vent; × Side of side vent

5.4 General discussion

Surroundings and internal obstructions can greatly affect or disturb the air distribution in the opening (Cui et al., 2016). The curtains not only decrease the air velocities with respect to the wind velocity in the open vents (Teitel et al., 2007) but also change the flow distribution. However, notwithstanding all surrounding obstructions, good correlations were found for the configuration with fully opened vents. For the different curtain configurations, the vertical airflow distribution per sensor group changed. This implies that the vertical profile must be calibrated for every different curtain configuration.

Previous studies have shown that the ridge vent can act as an inlet (Choinière et al., 1992; Van Overbeke, 2015a). The results of the experiments for different wind conditions showed that the ridge vent at all times acted as an outlet.

The experimental dataset was a result of the prevailing wind directions during the periods of measurements. Not all wind directions were measured per experiment. However, patterns were already visible to draw conclusions from.

Activities at the dairy barn as e.g. passing or temporarily parking of tractors in the neighbourhood of the sensors could influence measurements. These disturbing influences could decrease R^2 -values for the correlations with the meteomast or affect the predictor capacity of measurements with reduced sampling locations. The installation of a meteomast on the roof is normal practice for commercial dairy buildings using natural ventilation.

The meteomast was placed on the side of the roof of the dairy barn as for normal practice in Flanders when using automatic curtain control.

For certain cases, the standard deviation on the velocities (uncertainty due to wind unsteadiness) was larger than the absolute difference between the velocity of the middle sensor and the mean of the sensor group (difference). Precision could be increased by using more sensors so measurements can be precise enough to measure effects of mitigation techniques. However this was against the objective of reducing

sampling locations for practical reasons.

Although large differences could be found between the velocity of the one middle point velocity and the average vertical profile, the absolute velocity can be small. Notwithstanding the small velocity of the respective airflow rates, these measurements are still of importance when emission reduction of only a few percent should be detected to measure mitigation effects.

Joo et al. (2014) experienced the same conditions of low air velocities at the outlet side of the opening and therefore suggested an inflow-only approach of airflow modelling (regression using the normal wind velocity) because the low velocity (near zero) at outlet was inherent to uncertainties in the measurements. However, the author of this thesis thinks it is still necessary to be able to measure the airflow rates at the outlet vents to be able to combine them to emission measurements. Measurements were carried out under normal practice conditions, which means many unlogged disturbances could have taken place as e.g. tractors or milk collector trucks parked in front of the sensors, different cow locations in the barn, occasional opening of the side gable gates to allow tractor passage.

The results and conclusions are specific for the barn used within this research. The surroundings of the barn were quite representative of a dairy site in Flanders. The inside of the barn was specially built for research purposes. The feed troughs could have caused a larger change of the air movement, however in between the troughs and the measurements, there was the presence of a wide side alley. This alley increased a more homogeneous distribution because no obstructions were nearby to change the distribution. This situation may not be a reference situation, although a reference situation is difficult to define.

5.5 Conclusions

In summary we arrive at the following conclusions to reduce measurement strategies for natural ventilation in a dairy barn.

Reducing sampling locations for measuring the airflow rate in the vents:

- No general rule was found to reduce the number of sampling locations in order to measure the velocity profile (or airflow rate) and maintain accurate results. Differences between the reduced and detailed velocity measurements in the vents changed for different wind conditions, surrounding obstacles and for different curtain configurations. Reducing sampling locations without a prior calibration of the velocity pattern in the vent can lead to over- or underestimations of the airflow rate of more than 20%. Depending on the type of curtain configuration or wind direction, over- or underestimations exceeded 50%.
- For both experiments in the side vents, measuring the horizontal and vertical profile, it was found that measuring with reduced sampling locations was mostly feasible when the mean velocity in the vent was higher than approximately 1m/s. When the mean velocity was below 1m/s, the criterion of 20% was in many cases not met. The mean velocity in the vent was not clearly related to the normal or total wind velocity measured at the meteomast. It was assumed that the wind direction and the surrounding obstacles influenced the mean velocity.
- Reducing sampling locations in the ridge vent was found possible for measuring the velocity profile accurately. For all measured curtain configurations, using only 2 sensors was found feasible to meet the criterion of $\pm 20\%$ accuracy.

Predictability of the velocity pattern in the vents using wind data of the meteomast:

- For the NE-side vent, it was found that the velocity of single sampling locations could be correlated accurately (R^2 between 71-99%) for fully opened vents and

for all wind directions. When a certain curtain configuration was used, prediction of the sampling locations was still possible at the inlet vent. However, values were lower for velocities at outlet vents probably due to more complex distributions caused by curtains, internal obstacles and the occurrence of velocity values close to the accuracy level of the anemometer.

- Both the normal and tangential component were important input variables for the correlation and changed in mutual importance depending on the curtain configuration or in- or outlet side of the side vents.
- Correlating the velocities in the ridge vent with an acceptable accuracy was not possible using the velocity components measured at the meteoromast. R^2 -values were irregular and of low values.

Characterisation of the airflow rates through the vents:

- The airflow rate through the ridge vent was very steady and remained approximately the same magnitude for different wind conditions. Contrarily, the airflow rate through the side vents was immediately affected by the wind velocity and wind direction.
- Variability of velocity measurements in the side vent were very high (>100% coefficient of variation) for velocities smaller than 1 m/s. Velocities in the ridge vent were more steady and coefficients of variation were smaller than velocities measured in the side vent.

It was concluded that no general rule could be applied to reduce sampling locations in the side vents without exceeding an accuracy level of $\pm 20\%$. The airflow distribution in the vents changed too much depending on wind direction, velocity and obstacle surrounding. Results for the ridge vent were satisfying due to its more constant airflow pattern for different wind conditions.

Predicting the airflow distribution in the side vents was possible after calibration the velocities in the vent for different wind conditions. However, care should be taken for

complex distributions caused by curtains, internal obstacles and the occurrence of velocity values close to the accuracy level of the anemometer.

General discussion & perspectives

The overall goal of this PhD research was to study the feasibility of reduced measuring strategies to assess ventilation rates in naturally ventilated animal houses. The possibility of using simple regression models was investigated to predict both the airflow rate through the building and the velocity distribution in the vents. Insight was gained in the influence of reducing sampling locations and varying wind conditions on the accuracy and precision of airflow rate measurements. The results were discussed mainly against the background of ammonia emission measurements which is an important topic for the NEC-directive and concerning PAN (Programmatic Approach to Nitrogen), imposed by the Flemish government with regard to the EU NATURA2000 program.

5.6 Research questions

The focus of this PhD thesis lay on the measurement techniques for natural ventilation in animal houses, especially in context of determination of emission factors and mitigation efficiencies. The overall objective of this thesis was:

**Development of reduced measuring strategies in vents
to assess ventilation rates
in naturally ventilated animal houses**

The overall objective of this study was split in **five research questions**, three were examined in the animal mock-up building, two in the semi-commercial animal barn.

The research questions in the animal mock-up building were:

6. Is it possible to find an easy to use correlation between the airflow rate through the building and the velocities measured at the meteomast, taking into account uni- and bi-directional airflow rates? (**chapter 2**)

7. Is it possible to predict the airflow rate distribution in the vents using the velocities measured at the meteomast? (**chapter 3**)

8. Is it possible to measure the airflow rate in the vents with a reduced number of

sampling locations maintaining an accuracy of $\pm 20\%$? (**chapter 4**)

The research questions in the semi-commercial animal barn were:

9. Can the correlations as found in the mock-up building still give accurate results in the animal barn taking into account many extra factors as e.g. the presence of animals and surrounding buildings? (**chapter 5**)
10. Is it possible to measure velocity profiles in the vents with a reduced number of sampling locations maintaining an accuracy of $\pm 20\%$? (**chapter 5**)

In **chapter 2** it was concluded that it was possible to apply an easy to use correlation to assess the airflow rate using velocities measured at the meteor mast. For uni-directional flows, input variables $|\bar{Y}|$ and \bar{U} yielded the most accurate airflow rates with R^2 -values of 96 and 97%, respectively. Although $|\bar{Y}|$ being the easiest input variable because only one velocity component was needed to model the airflow rates. For this reason, it was found to give the best correlation using $|\bar{Y}|$ in ASHRAE's formula of $Q = EFF \times A \times |\bar{U}|$. The \bar{U} input variable was found to be the best input variable for bi-directional flows with an R^2 -value of 96%.

In **chapter 3** it was found possible to predict the airflow rate pattern in the different vents. The airflow rates of the predefined partitions in the ridge vent could be modelled accurately and precisely ($R^2 > 89\%$). Models showed that the predictability for the airflow rates in the side vent were high for uni-directional flows ($R^2 > 92\%$). Models for bi-directional flows showed good results for flows going the same direction of the outside wind at the windward side ($R^2 > 79\%$), but lower results for flows in vents at the leeward side ($R^2 < 56\%$). Possibly an extra input variable is needed for these types of models to improve precision.

In **chapter 4** measurement methods using reduced sampling locations were tested on reaching accuracy of $\pm 20\%$. Generally, it was found that better accuracy was obtained with a higher number of sampling locations. A 2D spread pattern (not all on 1 line) and accuracies for outlet vents gave better results than for inlet vents. A simplification of the reference method in the side vent of the test facility was feasible by using only a

quarter of the measurement locations using the chess pattern without giving in on accuracy (<2%). Whereas for the same amount of locations placed on a horizontal line, a deviation of 15% was found. Generally, reduced measurement strategies applied at the ridge opening gave very satisfying results. Only one middle sampling location was sufficient for an accuracy of 2% and a precision of 3%.

In **chapter 5** it was concluded that no general rule could be applied to reduce sampling locations in the side vents without exceeding an accuracy level of $\pm 20\%$. The airflow distribution in the vents changed too much depending on wind direction, velocity and obstacle surrounding. Results for the ridge vent were satisfying due to its more constant airflow pattern for different wind conditions.

Predicting the airflow distribution in the side vents was possible after calibration the velocities in the vent for different wind conditions. However, care should be taken for complex distributions caused by curtains, internal obstacles and the occurrence of velocity values close to the accuracy level of the anemometer.

5.7 Feasibility of reduced sampling strategies

5.7.1 *Reduced sampling strategies in the animal mock-up building*

Theoretically it was feasible to reduce measurement strategies in the animal mock-up building. A reduced number of sampling locations could be applied for measuring the airflow rate and a correlations could be determined to assess the airflow rate using velocity components measured at the meteomast. However:

- Earlier it was already found that the airflow distribution differed when the vent acted as an outlet or as an inlet. Compared to the outlet, a higher number of sampling locations should be applied to measure the airflow rate in the inlet. The velocity distribution at the inlet side of the building was influenced by the wind direction and wind velocity. These influences of wind conditions were weakened at the outlet side due to the air guidance between the side walls of the mock-up building.

- Correlations were not necessarily a simplification for airflow rate determination if used for short time measurements (e.g. measurements for a day/week). The time and financial investment of calibrating the vent to establish the correlations between the velocities in the vent and at the meteomast were high.
- Correlations needed to be determined for every new situation of surroundings, building, vent opening or other.
- A variety of wind conditions important to obtain a reliable correlation, more important than measuring duplicates of similar wind conditions (repetitions). This because a strong relation existed (R^2 -values >95%) between the velocity distribution and the velocities measured at the meteomast. Consequently, this can result in long periods of measurements as the wind conditions cannot be predicted on long terms or controlled for appearance.
- The velocity distribution at the inlet side of the building was influenced by the wind direction and wind velocity. These influences of wind conditions were weakened at the outlet side due to the air guidance between the side walls of the mock-up building. Therefore, a higher number of sampling locations should be applied to measure the airflow rate at the inlet compared to the outlet of the mock-up building.

5.7.2 **Reduced measurement strategies in a commercial animal house**

Generally it was found that accurate ($\pm 20\%$) reduced measurement strategies were only applicable depending on specific wind directions and wind velocities. These changing conditions for application of a reduced method makes it not practical for application in naturally ventilated barns:

- Measurement conditions to obtain results with an accuracy of $\pm 20\%$ were only found when the air velocity was higher than 1m/s in the vent. These measurement conditions were only measured during a time of 16% of the experimental period (Figure 59).

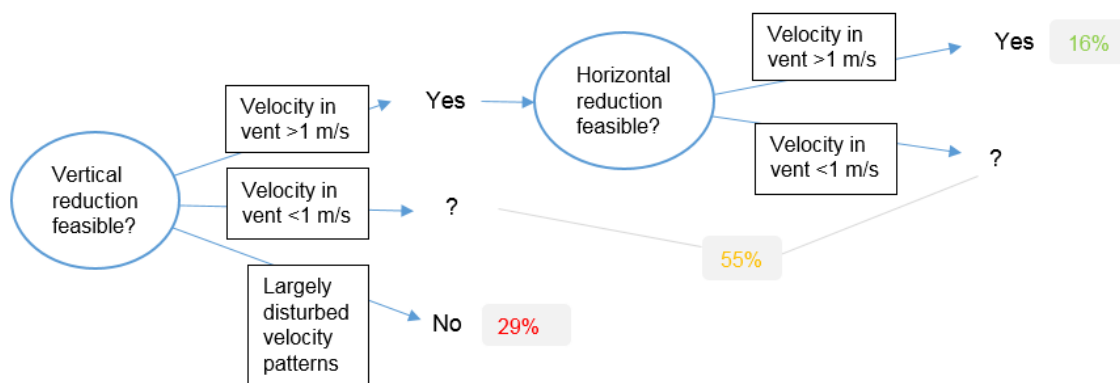


Figure 59: Diagram for applicability of sampling density reduction with the frequency of occurrence of each situation over all conducted experiments with different curtain configurations; percentages referring to measurement period of 8 months.

- These numbers are only an indication of occurrence of good measurement conditions because wind conditions and related curtain configurations during the measurements in the barn were not necessarily representative for a reference year (the measurements in this study were conducted between the months of January and September). However, they indicate that the appearance of good measurement conditions is low.
- Good measuring conditions were not only relatively rare, it was also not possible to predict when these conditions would actually occur. Prediction could be conducted by correlating the air velocity distribution in the vent with the wind velocity components measured on a metemast using a (simple) linear regression.
- Velocities lower than 1 m/s were difficult to correlate with measurements at the metemast. The buoyancy effect can affect the correlation. Temperature difference between in- and outside the building should be integrated in these correlations.
- Prior calibration of the velocity distribution in the vent is effective and can be a useful technique, however it is labour intensive. It was concluded that accurate measurements in the side vent are best performed by measuring the velocity profile on (a minimum of) three horizontal lines.

- Reducing sampling locations for airflow (rate) measurements in the vents is difficult due to the spatial and temporal variations. Tracer gas measurements as suggested by VERA (Verification of Environmental Technologies for Agricultural Production) however, deal with similar problems. Concentration profiles in the vent (or building) do not necessarily correlate with the velocity profiles in the vent (or building) (Mendes et al., 2015a) e.g. because of an unevenly spread number of cows over the floor of a barn. Therefore great care, and with the same precaution as for airflow measurements, must be taken when sampling concentrations to quantify the emissions.

5.7.3 ***Suggestions for an improved airflow sampling technique in the vents***

5.7.3.1 Tomography

Complex situations due to obstacles inside and outside (e.g. buildings, cows) increase the difficulty to measure the actual airflow rate. To obtain accurate measurements, a high number of sensors are needed to capture the more complex velocity distribution in the vents. However, practical considerations and costs are to be considered for experimental settings in field application. This local detailed sampling could be partially overcome by introducing ultrasonic tomography. It measures the mean of a velocity profile between two sensor heads placed over a predefined distance as e.g. installed over the width and the length of the opening:

- The velocity distribution in the vent can be measured when the approach is to measure a velocity grid.

Tomography technique has been tested by Ozcan et al. (2011) in a round duct with the intention of using this set-up in naturally ventilated buildings. A follow-up research is necessary to develop a ready-to-use tomography technique to apply in naturally ventilated buildings. However, this will require development time and investments.

Similarly, the heterogeneous nature of the concentration profile can be overcome by measuring the mean concentration profile instead of local concentrations. At the moment, open path lasers are available and tested to measure the mean concentration over a distance in naturally ventilated buildings (Mendes et al., 2015b). Advantages of

the open path laser are:

- a high frequency (range of a second) compared to local measurement techniques as infrared photo-acoustic analysers (range of a minute).
- A high accuracy to measure the ammonia concentration as it reaches (low) values in ranges of approximately (0.5-3) ppm in naturally ventilated buildings. The open path laser provides very accurate measurements (<0.1 ppm, Miller et al., 2014) as the accuracy of NH_3 measurements with INNOVAs decreases for concentrations under 2 ppm (Hassouna et al., 2013).

5.7.3.2 Relating uncertainties to the CO_2 mass balance method

Although no undisputed reference technique has been recognised for measuring natural ventilation, several authors or publications (Edouard et al., 2016; Ogink et al., 2013a; Samer et al., 2012; VERA, 2011) propose to use the CO_2 mass balance method to assess the airflow rate in naturally ventilated barns. The principles of this method are described shortly in the introduction (§1) and in detail in Phillips et al. (2001) and Mosquera et al. (2002). The choice of CO_2 as a tracer has the advantage that CO_2 is a free, easy to measure and constantly available tracer. Error sources for this method include unaccounted CO_2 (Wang et al., 2016). However, another disadvantage is the uncertainty of the measurement related to the number and positioning of the sampling locations (similarly to the direct measurement method, see introductions). Many findings of this study can be related to the CO_2 mass balance method:

- Mendes et al. (2015a) found that an average concentration of the tracer over a full barn length lead to more accurate airflow rates compared to using only one sampling location, even if placed at the centre of the barn. Similar as to the conclusions of their work and with respect to the direct measurements method in this study, it was also found that using more sampling locations leads to more accurate airflow rate measurements.
- Edouard et al. (2016) distinguished between measuring airflow rates in conventional situations (with restricted side inlets) and open situations. They

found that for conventional situations, measurements in the ridge vent should be preferred because of less influence by turbulence and the higher representativeness of the concentration for the barn average. The results for the measurements in all vents of the barn as presented in §5.3.3, confirmed that the ridge vent (velocity) measurements were more steady, compared to the measurements in the side vents. When curtains are applied, it is better to use the CO_2 mass balance method than the direct measurement method due to its statistically high variations for too low mean velocities (<1 m/s local velocity).

For very open situations, Edouard et al. (2016) found a high variability for the airflow rates using the CO_2 balance method (Mosquera et al., 2002; Ogink et al., 2013b). They stated that disturbed airflows can be derived from cross ventilation and may affect gas mixing. Also, larger velocities decrease the difference between the concentration in the vent and the background concentration leading to higher uncertainties. Wang et al. (2016) found that a minimum of 200 ppm difference in CO_2 concentration is needed to ensure the reliability of the CO_2 balance method because random and erratic variations were greater at these low concentrations.

- On the contrary, the best results for direct measurements in this study were found for very open situations. However, a strong reduction to only 4 sampling locations without exceeding $\pm 20\%$ accuracy of the measured value, was only found possible for 35% of the measurement period for fully opened vents. Also, in §5.3.3 it was found that the airflow rates through the side vents were directly affected by the changing wind conditions, whereas the airflow rate through the ridge vent remained quite constant. This indicated that the ridge vent might not be representative of the total airflow rate, but also that the air inside the building could be heterogeneously mixed.

Based on the measurements within this study, it was concluded that one of the main differences between the direct measurements method and the CO_2 balance method was found in their performance for conditions with different air velocities in the barn. Therefore, with the current knowledge of techniques, a choice of method depending on the curtain configurations could be considered to enhance reliability of the results, namely the CO_2 balance method for conventional ventilation methods (curtains mainly

closed) and the direct measurements in the vents for barns with very open vents. However, this approach would be unpractical and not economical.

5.8 Future perspectives

5.8.1 *Linking with mechanistic models describing ammonia release at source level*

In addition, several field experiments on ammonia emissions from naturally ventilated cattle building have documented that the release rate is affected by the wind speed measured near the site (Ngwabie et al. 2009; Zhang et al., 2005). It indicates that the convection release process above the floor region (e.g. air velocity above the release surface) may relate to the outdoor wind. Currently, there are very limited measurement data available from the literature. It is anticipated that the combination of field measurement and *CFD* methods can be a useful tool for generating such data, having made appropriate assumptions about internal structures and animal occupancy.

Uncertainties of airflow rates and emission measurements can be decreased by selection of a sufficient number of sampling locations and optimal positions as discussed in the previous paragraph. The quality of emission measurements can also be increased by measuring closer to the source of the emission. In dairy barns, ammonia is mainly emitted from puddles of cow urine and from the manure pit. Measuring the ammonia concentrations at source level gives the advantage of measuring less low concentrations. These higher ranges can facilitate measurements by an improved measurement accuracy. Of course, to quantify emissions, the air flux above the puddle surface are to be conducted simultaneously with the concentrations. Studies focused on release models of ammonia of puddles Snoek et al. (2014), free stall cubicle dairy cow houses (Monteny et al., 1998) or the manure pit under a slatted floor (Wu et al., 2012b). Saha et al. (2010) stated that increasing the wind velocity reduced (tunnel) outlet ammonia concentrations and increased emissions. Therefore, it can be important to integrate and combine measurements of the velocity in the barn or above the ammonia release surface in the modelling approaches.

Although there is still room for optimisation, mechanistic models are important tools to

gain knowledge on the release of ammonia and to find ways to prevent release. Recently, Mendes et al. (2016) developed a process-based emission model and applied it to quantify an ammonia reduction potential of several mitigation techniques. However, the authors stated that certain techniques, and the resulting emissions were not integrated due to the lack of empirical data to validate the model. Further experimental research should invest in specialised measurements to validate models and to relate the impact of airflow rates and airflow patterns to emissions. Also, for modelling as for normal practice in buildings, research is performed to extend the current mechanistic models of ammonia release as a single zone source to a representative surface as found in barns (Snoek et al., 2016). Understanding the impact of adapting curtains on the airflow patterns and the ammonia release is an obvious next step. This knowledge could enhance the development of smart control systems as ACNV (Automatically Controlled Natural Ventilation). In this way, the optimal compromise could be found between comfort or, the necessity of a healthy climate for the animals, and a minimized ammonia release.

Additionally, an improvement of knowledge on controlling airflows could enhance homogeneity of CO_2 in barns or homogeneity of velocity distributions in the vents to gain a better robustness and reliability of simplified measuring methods of calibration phases (determination of airflow rate using a detailed sampling method). A combined approach of experimental data from commercial animal houses, mechanistic modelling and applying *CFD* will be necessary due to the complex relation between all parameters involved. *CFD* could also help estimating parameters that are difficult to measure.

The use of modelling approaches has proven to be beneficial (Mendes et al., 2016). Again, it may be concluded that the combined approach of models and measurements may improve knowledge necessary to facilitate measurements and to reduce emissions (Ogink et al., 2013a). For example, a scoping modelling study can reveal the number and location of crucial or sensitive sampling points. Placing sensors at these places can increase accuracy and therefore reliability of the measurements.

5.8.2 **Representativeness of measurement conditions**

Assessing the airflow rate and pollutant concentrations is not the only challenge when determining emission factors from housing systems (usually expressed as kg NH_3 /animal place/year). Many parameters are of importance as they influence ammonia release or the determination of the ammonia emissions: measurement conditions as curtain configurations, manure management, measurement period, the size of the observation unit and others. During measurements, VERA already suggests applying general management practices. However, VERA only gives limited information on how to carry out measurements of the natural ventilation rate. Parameters influencing the measuring or release of ammonia should be described to enhance a representative determination of the actual ammonia release. Some suggestions for more measurement uniformity to improve determination of emission factors are provided within the context of this work:

- One of the suggestions is to use three rows of sampling points to be able to measure horizontal and vertical profiles. In practice, this method can result in more than 15 anemometers per side vent opening of a similar dairy barn as in this thesis. However, applying this high (minimum) number of anemometers is less expensive than applying too little sampling locations as unreliable results are the most expensive experiments.
- Simultaneously, the use of anemometers spread in the building can give information (magnitude and direction) about the presence of cross ventilation, especially for fully opened vents in dairy barns and give some information concerning air mixing. An updated version of the test protocol of VERA with extended information for applying the measurement methods is currently in progress.
- Previously, the relation between the velocity and ammonia release was discussed. It is suggested to apply normal practices for curtain configurations: due to the influence of the velocity on the ammonia release, curtains should not be adapted to facilitate measurements.

Cebecauer et al. (2015) stated that the input measurement data should be at least 10 years to reduce uncertainties from weather variability within a measurement year. This could also be related to measurements of annual emission factor. Although a higher temporal resolution is desirable to record the effect of short-term events (Schrade et al., 2012). This statement could be used for patterns over a one year period. However, this approach of measuring over a period of 10 years is economically not feasible and reduction of the measurement period is unavoidable. For naturally ventilated barns where no case-control method is possible, VERA (2011) suggests to measure 6 days evenly spread over a year to capture the variability over a year. Currently, measurements should at least be performed on 4 different locations. The obtained data is then extrapolated on an annual time base. These limited measurement days, and the lack of control of the wind conditions and temperature during the experiments, make it an extra challenge to extrapolate measurement data to a (reference) annual time base. Therefore, the way of processing these measurements for calculating year average emission factors is crucial to obtain representative emission factors. A strategy that considers weather variability, should include differentiation of geographical representativeness for wind conditions for a reference year. Also, it is important to give a representative weight to the influencing parameters to select measurement conditions that represent the variation of the parameters over the period of measuring as much as possible (e.g. a year) (Cebecauer et al., 2015).

References

- Al., K. et. (2008). A review on wind driven ventilation techniques. *Energy and Buildings*, 40(8), 1586–1604. <http://doi.org/10.1016/j.enbuild.2008.02.015>
- Algers, B., Bertoni, G., Oltenacu, P., & Rushen, J. (2009). Effects of farming systems on dairy cow welfare and disease Report of the Panel on Animal Health and Welfare. Annex to the EFSA Journal, (1143), 1–284.
- Algers, B., Blokhuis, H. J., Broom, D. M., Costa, P., Domingo, M., Guemene, D., ... Wooldridge, M. (2007). In relation to housing and husbandry Scientific Opinion of the Panel on Animal Health and Welfare. *EFSA Journal*, 564(September), 1–14.
- American Society of Heating, Refrigerating and Air-Conditioning Engineers, I. (2009). *ASHRAE Fundamentals* (Vol. 30329).
- Angrecka, S., & Herbut, P. (2014). The Impact of Natural Ventilation on Ammonia Emissions from Free Stall Barns. *Pol. J. Environ. Stud.*, 23(6), 2303–2307.
- Asfour, O. S., & Gadi, M. B. (2007). A comparison between CFD and Network models for predicting wind-driven ventilation in buildings. *Building and Environment*, 42(12), 4079–4085. <http://doi.org/10.1016/j.buildenv.2006.11.021>
- Ayata, T., Arcaklıoğlu, E., & Yıldız, O. (2007). Application of ANN to explore the potential use of natural ventilation in buildings in Turkey. *Applied Thermal Engineering*, 27(1), 12–20. <http://doi.org/10.1016/j.applthermaleng.2006.05.021>
- Barrancos, J., Briz, S., Nolasco, D., Melián, G., Padilla, G., Padrón, E., ... Hernández, P. a. (2013). A new method for estimating greenhouse gases and ammonia emissions from livestock buildings. *Atmospheric Environment*, 74, 10–17. <http://doi.org/10.1016/j.atmosenv.2013.03.021>
- Bartzanas, T., Boulard, T., & Kittas, C. (2004). Effect of Vent Arrangement on Windward Ventilation of a Tunnel Greenhouse. *Biosystems Engineering*, 88(4), 479–490. <http://doi.org/10.1016/j.biosystemseng.2003.10.006>
- Bartzanas, T., Kittas, C., Sapounas, a. a., & Nikita-Martzopoulou, C. (2007). Analysis of airflow through experimental rural buildings: Sensitivity to turbulence models. *Biosystems Engineering*, 97(2), 229–239. <http://doi.org/10.1016/j.biosystemseng.2007.02.009>
- Belleri, A., Lollini, R., & Dutton, S. M. (2014). Natural ventilation design: An analysis of predicted and measured performance. *Building and Environment*, 81, 123–138. <http://doi.org/10.1016/j.buildenv.2014.06.009>
- BIPM, IEC, IFCC, ILAC, ISO, IUPAC, IUPAP, OIML. (2008). *JCGM 200 : 2008 International vocabulary of metrology — Basic and general concepts and associated terms (VIM)* *Vocabulaire international de métrologie — Concepts fondamentaux et généraux et termes associés (VIM)*. International Organization for Standardization Geneva ISBN, 3(Vim), 104. [http://doi.org/10.1016/0263-2241\(85\)90006-5](http://doi.org/10.1016/0263-2241(85)90006-5)
- Bjerg, B., Cascone, G., Lee, I.-B., Bartzanas, T., Norton, T., Hong, S.-W., ... Zhang, G. (2013a). Modelling of ammonia emissions from naturally ventilated livestock buildings. Part 3: CFD modelling. *Biosystems Engineering*, 116(3), 259–275. <http://doi.org/10.1016/j.biosystemseng.2013.06.012>
- Bjerg, B., Liberati, P., Marucci, A., Zhang, G., Banhazi, T., Bartzanas, T., ... Norton, T. (2013b). Modelling of ammonia emissions from naturally ventilated livestock buildings: Part 2, air change modelling. *Biosystems Engineering*, 116(3), 246–258. <http://doi.org/10.1016/j.biosystemseng.2013.01.010>
- Bjerg, B., Norton, T., Banhazi, T., Zhang, G., Bartzanas, T., Liberati, P., ... Marucci, a. (2013c). Modelling of ammonia emissions from naturally ventilated livestock buildings. Part 1: Ammonia release modelling. *Biosystems Engineering*, 116(3), 232–245. <http://doi.org/10.1016/j.biosystemseng.2013.08.001>
- Bland, J. M., & Altman, D. G. (2010). Statistical methods for assessing agreement between two methods of clinical measurement. *International Journal of Nursing Studies*, 47(8), 931–936. <http://doi.org/10.1016/j.ijnurstu.2009.10.001>
- Bleizgys, R., & Bagdoniene, I. (2016). Control of ammonia air pollution through the management of thermal processes in cowsheds. *Science of The Total Environment*. <http://doi.org/10.1016/j.scitotenv.2016.05.017>

- Bluteau, C. V., Massé, D. I., & Leduc, R. (2009). Ammonia emission rates from dairy livestock buildings in Eastern Canada. *Biosystems Engineering*, 103(4), 480–488. <http://doi.org/10.1016/j.biosystemseng.2009.04.016>
- Boulard, T., & Draoui, B. (1995). Natural Ventilation of a Greenhouse with Continuous Roof Vents: Measurements and Data Analysis. *Journal of Agricultural Engineering Research*, 61(1), 27–35. <http://doi.org/10.1006/jaer.1995.1027>
- Boulard, T., Meneses, J. F., Mermier, M., & Papadakis, G. (1996). The mechanisms involved in the natural ventilation of greenhouses. *Agricultural and Forest Meteorology*, 79(1-2), 61–77. [http://doi.org/10.1016/0168-1923\(95\)02266-X](http://doi.org/10.1016/0168-1923(95)02266-X)
- Boulard, T., Kittas, C., Papadakis, G., & Mermier, M. (1998). Pressure Field and Airflow at the Opening of a Naturally Ventilated Greenhouse, 93–102.
- Boulard, T., & Wang, S. (2002). Experimental and numerical studies on the heterogeneity of crop transpiration in a plastic tunnel. *Computers and Electronics in Agriculture*, 34(1-3), 173–190. [http://doi.org/10.1016/S0168-1699\(01\)00186-7](http://doi.org/10.1016/S0168-1699(01)00186-7)
- Brockett, B. L., & Albright, L. D. (1987). Natural Ventilation in Single Airspace Buildings, (April 1986), 141–154.
- Bruce, J. M. (1978). Natural Convection Through Openings and its Application to Cattle Building Ventilation. *J. Agric. Engng Res.*, (January), 151–167.
- Calvet, S., Cambra-López, M., Blanes-Vidal, V., Estellés, F., & Torres, a. G. (2010). Ventilation rates in mechanically-ventilated commercial poultry buildings in Southern Europe: Measurement system development and uncertainty analysis. *Biosystems Engineering*, 106(4), 423–432. <http://doi.org/10.1016/j.biosystemseng.2010.05.006>
- Calvet, S., Gates, R. S., Zhang, G., Estellés, F., Ogink, N. W. M., Pedersen, S., & Berckmans, D. (2013). Measuring gas emissions from livestock buildings: A review on uncertainty analysis and error sources. *Biosystems Engineering*, 116(3), 221–231. <http://doi.org/10.1016/j.biosystemseng.2012.11.004>
- Calvet, S., Campelo, J. C., Estellés, F., Perles, A., Mercado, R., & Serrano, J. J. (2014). Suitability evaluation of multipoint simultaneous CO₂ sampling wireless sensors for livestock buildings. *Sensors (Basel, Switzerland)*, 14(6), 10479–96. <http://doi.org/10.3390/s140610479>
- Campen, J. ., & Bot, G. P. (2003). Determination of Greenhouse-specific Aspects of Ventilation using Three-dimensional Computational Fluid Dynamics. *Biosystems Engineering*, 84(1), 69–77. [http://doi.org/10.1016/S1537-5110\(02\)00221-0](http://doi.org/10.1016/S1537-5110(02)00221-0)
- Cebecauer, T., & Suri, M. (2015). Typical Meteorological Year Data: SolarGIS Approach. *Energy Procedia*, 69, 1958–1969. <http://doi.org/10.1016/j.egypro.2015.03.195>
- Chao, C. Y., Wan, M. ., & Law, A. K. (2004). Ventilation performance measurement using constant concentration dosing strategy. *Building and Environment*, 39(11), 1277–1288. <http://doi.org/10.1016/j.buildenv.2004.03.012>
- Chen, Q. (2009). Ventilation performance prediction for buildings: A method overview and recent applications. *Building and Environment*, 44(4), 848–858. <http://doi.org/10.1016/j.buildenv.2008.05.025>
- Chiu, Y.-H., & Etheridge, D. W. (2007). External flow effects on the discharge coefficients of two types of ventilation opening. *Journal of Wind Engineering and Industrial Aerodynamics*, 95(4), 225–252. <http://doi.org/10.1016/j.jweia.2006.06.013>
- Choi, H. L., Song, J. I., Lee, J. H., & Albright, L. D. (2010). Comparison of natural and forced ventilation systems in nursery Pig houses. *Applied Engineering in Agriculture*, 26(6), 1023–1033.
- Choinière, Y., Tanaka, H., Munroe, J. A., & Suchorski-Tremblay, A. (1992). Prediction of wind-induced ventilation for livestock housing. *Journal of Wind Engineering and Industrial Aerodynamics*, 44(1-3), 2563–2574. [http://doi.org/10.1016/0167-6105\(92\)90048-F](http://doi.org/10.1016/0167-6105(92)90048-F)
- Choinière, Y., & Munroe, J. A. (1994). A wind tunnel study of wind direction effects on airflow patterns in naturally ventilated swine buildings.

- Chu, C.-R., & Wang, Y.-W. (2010). The loss factors of building openings for wind-driven ventilation. *Building and Environment*, 45(10), 2273–2279. <http://doi.org/10.1016/j.buildenv.2010.04.010>
- Chu, C.-R., & Chiang, B.-F. (2013). Wind-driven cross ventilation with internal obstacles. *Energy and Buildings*, 67, 201–209. <http://doi.org/10.1016/j.enbuild.2013.07.086>
- Chu, C.-R., & Chiang, B.-F. (2014). Wind-driven cross ventilation in long buildings. *Building and Environment*, 80, 150–158. <http://doi.org/10.1016/j.buildenv.2014.05.017>
- Chu, C.-R., Chiu, Y.-H., Tsai, Y.-T., & Wu, S.-L. (2015). Wind-driven natural ventilation for buildings with two openings on the same external wall. *Energy and Buildings*, 108, 365–372. <http://doi.org/10.1016/j.enbuild.2015.09.041>
- Cui, S., Cohen, M., Stabat, P., & Marchio, D. (2015). CO₂ tracer gas concentration decay method for measuring air change rate. *Building and Environment*, 84, 162–169. <http://doi.org/10.1016/j.buildenv.2014.11.007>
- Cui, S., Stabat, P., & Marchio, D. (2016). Numerical simulation of wind-driven natural ventilation: effects of loggia and facade porosity on air change rate. *Building and Environment*. <http://doi.org/10.1016/j.buildenv.2016.03.021>
- De Paepe, M., Pieters, J. G., Cornelis, W. M., Gabriels, D., Merci, B., & Demeyer, P. (2012). Airflow measurements in and around scale model cattle barns in a wind tunnel: Effect of ventilation opening height. *Biosystems Engineering*, 113(1), 22–32. <http://doi.org/10.1016/j.biosystemseng.2012.06.003>
- De Vogeleeer, G., Van Overbeke, P., Brusselman, E., Mendes, L. B., Pieters, J. G., & Demeyer, P. (2016). Assessing airflow rates of a naturally ventilated test facility using a fast and simple algorithm supported by local air velocity measurements. *Building and Environment*, 104, 198–207. <http://doi.org/10.1016/j.buildenv.2016.05.006>
- Demmers, T. G. M., Burgess, L. R., Phillips, V. R., Clark, J. a., & Wathes, C. M. (2000). Assessment of Techniques for Measuring the Ventilation Rate, using an Experimental Building Section. *Journal of Agricultural Engineering Research*, 76(1), 71–81. <http://doi.org/10.1006/jaer.2000.0532>
- Demmers, T. G. M., Phillips, V. R., Short, L. S., Burgess, L. R., Hoxey, R. P., & Wathes, C. M. (2001). Validation of Ventilation Rate Measurement Methods and the Ammonia Emission from Naturally Ventilated Dairy and Beef Buildings in the United Kingdom. *Journal of Agricultural Engineering Research*, 79(1), 107–116. <http://doi.org/10.1006/jaer.2000.0678>
- Edouard, N., Mosquera, J., Van-Dooren, H. J. C., Mendes, L. B., & Ogink, N. W. M. (2016). Comparison of CO₂- and SF₆- based tracer gas methods for the estimation of ventilation rates in a naturally ventilated dairy barn. *Biosystems Engineering*, 149, 11–23. <http://doi.org/10.1016/j.biosystemseng.2016.06.001>
- Etheridge, D. (2012). *Natural Ventilation of Buildings*. John Wiley & Sons.
- Etheridge, D. (2015). A Perspective on Fifty Years of Natural Ventilation Research. *Building and Environment*. <http://doi.org/10.1016/j.buildenv.2015.02.033>
- Faggianelli, G. A., Brun, A., Wurtz, E., & Muselli, M. (2015a). Assessment of different airflow modelling approaches on a naturally ventilated Mediterranean building. *Energy and Buildings*. <http://doi.org/10.1016/j.enbuild.2015.08.038>
- Faggianelli, G. A., Brun, A., Wurtz, E., Muselli, M., Corse, D., Spe, U. M. R. C., & Bourget, L. (2015b). GREY-BOX MODELLING FOR NATURALLY VENTILATED BUILDINGS. *Building Simulation Conference*, 720–727.
- Fiedler, a. M., & Müller, H.-J. (2011). Emissions of ammonia and methane from a livestock building natural cross ventilation. *Meteorologische Zeitschrift*, 20(1), 59–65. <http://doi.org/10.1127/0941-2948/2011/0490>
- Frausto, H. U., Pieters, J. G., & Deltour, J. M. (2003). Modelling Greenhouse Temperature by means of Auto Regressive Models. *Biosystems Engineering*, 84(2), 147–157. [http://doi.org/10.1016/S1537-5110\(02\)00239-8](http://doi.org/10.1016/S1537-5110(02)00239-8)
- Gao, Z., Mauder, M., Desjardins, R. L., Flesch, T. K., & van Haarlem, R. P. (2009). Assessment of the backward Lagrangian Stochastic dispersion technique for continuous measurements of CH₄ emissions. *Agricultural and Forest Meteorology*, 149(9), 1516–1523. <http://doi.org/10.1016/j.agrformet.2009.04.004>
- Gay, S. W., Ph, D., & Tech, V. (2004). Ammonia Emissions from Animal Housing Facilities.

- Hassouna, M., Robin, P., Charpiot, A., Edouard, N., & Méda, B. (2013). Infrared photoacoustic spectroscopy in animal houses: Effect of non-compensated interferences on ammonia, nitrous oxide and methane air concentrations. *Biosystems Engineering*, 114(3), 318–326. <http://doi.org/10.1016/j.biosystemseng.2012.12.011>
- Heiselberg, P. (2006). *Modelling of Natural and Hybrid Ventilation*, DCE Lecture Notes No. 004, Aalborg University - Department of Civil Engineering -Indoor Environmental Engineering, ISSN 1901-7286.
- Heiselberg, P., Li, Y., Andersen, a., Bjerre, M., & Chen, Z. (2004). Experimental and CFD evidence of multiple solutions in a naturally ventilated building. *Indoor Air*, 14(1), 43–54. <http://doi.org/10.1046/j.1600-0668.2003.00209.x>
- Hempel, S., Wiedemann, L., Ammon, C., Fiedler, M., Saha, C., Loebstin, C., ... Amon, T. (2015). Assessment of the through-flow patterns in naturally ventilated dairy barns – Three methods , one complex approach. *Conference Paper - Rural Urban Symbiosis*, (September), 8–11.
- Herrero, M., Gerber, P., Vellinga, T., Garnett, T., Leip, a., Opio, C., ... McAllister, T. a. (2011). Livestock and greenhouse gas emissions: The importance of getting the numbers right. *Animal Feed Science and Technology*, 166-167, 779–782. <http://doi.org/10.1016/j.anifeedsci.2011.04.083>
- Hoff, S. J. (2001). Assessing Air Infiltration Rates of Agricultural Use Ventilation Curtains.
- Hoff, S. J. (2004). Automated control logic for naturally ventilated agricultural structures. *Applied Engineering in Agriculture*, 20(1), 47–56.
- I. A. Nääs, D. J. Moura, R. A. Bucklin, F. B. F. (1988). An algorithm for determining opening effectiveness in natural ventilation by wind. *Transactions of the ASAE*, 41(3).
- Jacobson, L. D., Hetchler, B. P., Schmidt, D. R., Nicolai, R. E., Heber, A. J., Ni, J.-Q., ... Parker, D. B. (2008). Quality assured measurements of animal building emissions: odor concentrations. *Journal of the Air & Waste Management Association* (1995), 58(6), 806–11. Retrieved from <http://www.ncbi.nlm.nih.gov/pubmed/18581810>
- Joo, H. S., Ndegwa, P. M., Heber, A. J., Ni, J.-Q., Bogan, B. W., Ramirez-Dorransoro, J. C., & Cortus, E. L. (2013). Particulate matter dynamics in naturally ventilated freestall dairy barns. *Atmospheric Environment*, 69, 182–190. <http://doi.org/10.1016/j.atmosenv.2012.12.006>
- Joo, H. S., Ndegwa, P. M., Heber, A. J., Bogan, B. W., Ni, J.-Q., Cortus, E. L., & Ramirez-Dorransoro, J. C. (2014). A direct method of measuring gaseous emissions from naturally ventilated dairy barns. *Atmospheric Environment*, 86, 176–186. <http://doi.org/10.1016/j.atmosenv.2013.12.030>
- Joo, H. S., Ndegwa, P. M., Heber, a. J., Ni, J.-Q., Bogan, B. W., Ramirez-Dorransoro, J. C., & Cortus, E. (2015). Greenhouse gas emissions from naturally ventilated freestall dairy barns. *Atmospheric Environment*, 102, 384–392. <http://doi.org/10.1016/j.atmosenv.2014.11.067>
- Kalogirou, S., Eftekhari, M., & Marjanovic, L. (2003). Predicting the pressure coefficients in a naturally ventilated test room using artificial neural networks. *Building and Environment*, 38(3), 399–407. [http://doi.org/10.1016/S0360-1323\(02\)00032-X](http://doi.org/10.1016/S0360-1323(02)00032-X)
- Karava, P., Stathopoulos, T., & Athienitis, A. K. (2011). Airflow assessment in cross-ventilated buildings with operable façade elements. *Building and Environment*, 46(1), 266–279. <http://doi.org/10.1016/j.buildenv.2010.07.022>
- Kim, K. Y., Jong Ko, H., Tae Kim, H., Shin Kim, Y., Man Roh, Y., Min Lee, C., & Nyon Kim, C. (2008). Quantification of ammonia and hydrogen sulfide emitted from pig buildings in Korea. *Journal of Environmental Management*, 88(2), 195–202. <http://doi.org/10.1016/j.jenvman.2007.02.003>
- Kiwan, A., Berg, W., Brunsch, R., Özcan, S., Müller, H. J., Gläser, M., ... Berckmans, D. (2012). Tracer gas technique, air velocity measurement and natural ventilation method for estimating ventilation rates through naturally ventilated barns. *Agricultural Engineering International: CIGR Journal*, 14(4), 22–36.

- Kiwan, A., Berg, W., Fiedler, M., Ammon, C., Gläser, M., Müller, H.-J., & Brunsch, R. (2013). Air exchange rate measurements in naturally ventilated dairy buildings using the tracer gas decay method with ^{85}Kr , compared to CO_2 mass balance and discharge coefficient methods. *Biosystems Engineering*, 116(3), 286–296. <http://doi.org/10.1016/j.biosystemseng.2012.11.011>
- Laubach, J., & Kelliher, F. M. (2005). Methane emissions from dairy cows: Comparing open-path laser measurements to profile-based techniques. *Agricultural and Forest Meteorology*, 135(1-4), 340–345. <http://doi.org/10.1016/j.agrformet.2005.11.014>
- Li, Y., Delsante, A., & Symons, J. (2000). Prediction of natural ventilation in buildings with large openings. *Building and Environment*, 35(3), 191–206. [http://doi.org/10.1016/S0360-1323\(99\)00011-6](http://doi.org/10.1016/S0360-1323(99)00011-6)
- Lo, L. J., & Novoselac, A. (2012). Cross ventilation with small openings: Measurements in a multi-zone test building. *Building and Environment*, 57, 377–386. <http://doi.org/10.1016/j.buildenv.2012.06.009>
- López, A., Valera, D. L., & Molina-Aiz, F. (2011a). Sonic anemometry to measure natural ventilation in greenhouses. *Sensors (Basel, Switzerland)*, 11(10), 9820–38. <http://doi.org/10.3390/s111009820>
- López, D. L. Valera, F. D. Molina-Aiz, A. P. (2011b). Effects of surrounding buildings on air patterns and turbulence in two naturally ventilated mediterranean greenhouses using tri-sonic anemometry, 54(5), 1941–1950.
- Loyon, L., Burton, C. H., Misselbrook, T., Webb, J., Philippe, F. X., Aguilar, M., ... Sommer, S. G. (2015). Best available technology for European livestock farms: Availability, effectiveness and uptake. *Journal of Environmental Management*, 166, 1–11. <http://doi.org/10.1016/j.jenvman.2015.09.046>
- Lule, I., Eren Özcan, S., & Berckmans, D. (2014). Characterisation of ventilation rate in naturally-ventilated buildings using heat dissipation from a line source. *Biosystems Engineering*, 124, 53–62. <http://doi.org/10.1016/j.biosystemseng.2014.05.009>
- Maertens, W., Vangeyte, J., Baert, J., Jantuan, A., Mertens, K. C., De Campeneere, S., ... Van Nuffel, A. (2011). Development of a real time cow gait tracking and analysing tool to assess lameness using a pressure sensitive walkway: The GAITWISE system. *Biosystems Engineering*, 110(1), 29–39. <http://doi.org/10.1016/j.biosystemseng.2011.06.003>
- Mendes, L. B., Edouard, N., Ogink, N. W. M., van Dooren, H. J. C., Tinôco, I. D. F. F., & Mosquera, J. (2015a). Spatial variability of mixing ratios of ammonia and tracer gases in a naturally ventilated dairy cow barn. *Biosystems Engineering*, 129, 360–369. <http://doi.org/10.1016/j.biosystemseng.2014.11.011>
- Mendes, L., Ogink, N., Edouard, N., van Dooren, H., Tinôco, I., & Mosquera, J. (2015b). NDIR Gas Sensor for Spatial Monitoring of Carbon Dioxide Concentrations in Naturally Ventilated Livestock Buildings. *Sensors*, 15(5), 11239–11257. <http://doi.org/10.3390/s150511239>
- Mendes, L. B., Pieters, J. G., Snoek, D., Ogink, N. W. M., Brusselman, E., & Demeyer, P. (2016). Reduction of ammonia emissions from free stall dairy cattle barns via improved management- or design-based strategies: A modeling approach. *Journal of the Total Environment*, (October). <http://doi.org/10.1017/CBO9781107415324.004>
- Miller, D. J., Sun, K., Tao, L., Khan, M. a., & Zondlo, M. a. (2014). Open-path, quantum cascade-laser-based sensor for high-resolution atmospheric ammonia measurements. *Atmospheric Measurement Techniques*, 7(1), 81–93. <http://doi.org/10.5194/amt-7-81-2014>
- Molina-Aiz, F. D., Valera, D. L., Pena, a. a., Gil, J. a., & Lopez, A. (2009). A study of natural ventilation in an Almeria-type greenhouse with insect screens by means of tri-sonic anemometry. *Biosystems Engineering*, 104(2), 224–242. <http://doi.org/10.1016/j.biosystemseng.2009.06.013>
- Monteny, G. J., Schulte, D. D., Elzing, A., & Lamaker, E. J. J. (1998). A conceptual mechanistic model for the ammonia emissions from free stall cubicle dairy cow houses. *Trans. ASAE*, (41), 193–201. <http://doi.org/10.13031/2013.17151>

- Morsing, S., Ikeguchi, A., Bennetsen, J. C., Ravn, P., & Okushima, L. (2002). Wind induced isothermal airflow patterns in a scale model of a naturally ventilated swine barn with cathedral ceiling, 18(1), 97–101.
- Morsing, S., Strøm, J. S., Zhang, G., & Kai, P. (2008). Scale model experiments to determine the effects of internal airflow and floor design on gaseous emissions from animal houses. *Biosystems Engineering*, 99(1), 99–104. <http://doi.org/10.1016/j.biosystemseng.2007.09.028>
- Mosquera, J., Hofschreuder, P., Erisman, J. W., Mulder, E., Klooster, C. E. Van, & Ogink, N. (2002). Meetmethoden gasvormige emissies uit de veehouderij.
- Ngwabie, N. M., Jeppsson, K.-H., Nimmermark, S., Swensson, C., & Gustafsson, G. (2009). Multi-location measurements of greenhouse gases and emission rates of methane and ammonia from a naturally-ventilated barn for dairy cows. *Biosystems Engineering*, 103(1), 68–77. <http://doi.org/10.1016/j.biosystemseng.2009.02.004>
- Ngwabie, N. M., Vanderzaag, A., Jayasundara, S., & Wagner-Riddle, C. (2014). Measurements of emission factors from a naturally ventilated commercial barn for dairy cows in a cold climate. *Biosystems Engineering*, 127, 103–114. <http://doi.org/10.1016/j.biosystemseng.2014.08.016>
- Nielsen, P. V. (2015). Fifty Years of CFD for Room Air Distribution. *Building and Environment*, 91, 78–90. <http://doi.org/10.1016/j.buildenv.2015.02.035>
- Nikolopoulos, N., Nikolopoulos, A., Larsen, T. S., & Nikas, K.-S. P. (2012). Experimental and numerical investigation of the tracer gas methodology in the case of a naturally cross-ventilated building. *Building and Environment*, 56, 379–388. <http://doi.org/10.1016/j.buildenv.2012.04.006>
- Norton, T., Sun, D.-W., Grant, J., Fallon, R., & Dodd, V. (2007). Applications of computational fluid dynamics (CFD) in the modelling and design of ventilation systems in the agricultural industry: a review. *Bioresource Technology*, 98(12), 2386–414. <http://doi.org/10.1016/j.biortech.2006.11.025>
- Norton, T., Grant, J., Fallon, R., & Sun, D.-W. (2009). Assessing the ventilation effectiveness of naturally ventilated livestock buildings under wind dominated conditions using computational fluid dynamics. *Biosystems Engineering*, 103(1), 78–99. <http://doi.org/10.1016/j.biosystemseng.2009.02.007>
- Norton, T., Grant, J., Fallon, R., & Sun, D.-W. (2010). Assessing the ventilation performance of a naturally ventilated livestock building with different eave opening conditions. *Computers and Electronics in Agriculture*, 71(1), 7–21. <http://doi.org/10.1016/j.compag.2009.11.003>
- Ogink, N. W. M., Mosquera, J., Calvet, S., & Zhang, G. (2013a). Methods for measuring gas emissions from naturally ventilated livestock buildings: Developments over the last decade and perspectives for improvement. *Biosystems Engineering*, 116(3), 297–308. <http://doi.org/10.1016/j.biosystemseng.2012.10.005>
- Ogink, N. W. M., Mosquera, J., & Hol, J. M. G. (2013b). Protocol voor meting van ammoniakemissie uit huisvestingssystemen in de veehouderij 2013, (September), 31.
- Olden, J. D., & Jackson, D. A. (2002). Illuminating the “black box”: a randomization approach for understanding variable contributions in artificial neural networks, 154, 135–150.
- Özcan, S. E., Vranken, E., & Berckmans, D. (2009). Measuring ventilation rate through naturally ventilated air openings by introducing heat flux. *Building and Environment*, 44(1), 27–33. <http://doi.org/10.1016/j.buildenv.2008.01.011>
- Ozcan, S. (2011). Techniques to determine ventilation rate and airflow characteristics through naturally ventilated buildings, Doctoral dissertation, K. U. Leuven.
- P. Karava, Stathopoulos, T., & Athienitis, A. K. (2004). Wind Driven Flow through Openings – A Review of Discharge Coefficients. *International Journal of Ventilation*.
- Passe, U., & Battaglia, F. (2015). Designing spaces for natural ventilation: an architecture's guide.

- Phillips, V. R. ;, Lee, D. S. ;, Scholtens, R. ., A., G. J. ., & Sneath, R. W. (2001). A Review of Methods for measuring Emission Rates of Ammonia from Livestock Buildings and Slurry or Manure Stores, Part 2: monitoring Flux Rates, Concentrations and Airflow Rates. *Structures and Environment*, 78(1), 1–14. <http://doi.org/10.1006/jaer.2000.0618>
- Riffat, S. B. (1991). Algorithms for Airflows Through Large Internal and External Openings. *Applied Energy*, 40, 171–188.
- Rigakis, N., Katsoulas, N., Teitel, M., Bartzanas, T., & Kittas, C. (2015). A simple model for ventilation rate determination in screenhouses. *Energy and Buildings*, 87, 293–301. <http://doi.org/10.1016/j.enbuild.2014.11.057>
- Rong, L., Liu, D., Pedersen, E. F., & Zhang, G. (2015). The effect of wind speed and direction and surrounding maize on hybrid ventilation in a dairy cow building in Denmark. *Energy and Buildings*, 86, 25–34. <http://doi.org/10.1016/j.enbuild.2014.10.016>
- Rong, L., Bjerg, B., Bartzanas, T., & Zhang, G. (2016). Mechanisms of natural ventilation in livestock buildings: Perspectives on past achievements and future challenges. *Biosystems Engineering*, 151, 200–217. <http://doi.org/10.1016/j.biosystemseng.2016.09.004>
- Saha, C. K., Zhang, G., & Ni, J.-Q. (2010). Airflow and concentration characterisation and ammonia mass transfer modelling in wind tunnel studies. *Biosystems Engineering*, 107(4), 328–340. <http://doi.org/10.1016/j.biosystemseng.2010.09.007>
- Saha, C. K., Ammon, C., Berg, W., Loebstin, C., Fiedler, M., Brunsch, R., & von Bobrutzki, K. (2013). The effect of external wind speed and direction on sampling point concentrations, air change rate and emissions from a naturally ventilated dairy building. *Biosystems Engineering*, 114(3), 267–278. <http://doi.org/10.1016/j.biosystemseng.2012.12.002>
- Saha, C. K., Ammon, C., Berg, W., Fiedler, M., Loebstin, C., Sanftleben, P., ... Amon, T. (2014). Seasonal and diel variations of ammonia and methane emissions from a naturally ventilated dairy building and the associated factors influencing emissions. *The Science of the Total Environment*, 468-469, 53–62. <http://doi.org/10.1016/j.scitotenv.2013.08.015>
- Samer, M., Loebstin, C., Fiedler, M., Ammon, C., Berg, W., Sanftleben, P., & Brunsch, R. (2011 a). Heat balance and tracer gas technique for airflow rates measurement and gaseous emissions quantification in naturally ventilated livestock buildings. *Energy and Buildings*, 43(12), 3718–3728. <http://doi.org/10.1016/j.enbuild.2011.10.008>
- Samer, M., Müller, H.-J., Fiedler, M., Ammon, C., Gläser, M., Berg, W., ... Brunsch, R. (2011b). Developing the 85Kr tracer gas technique for air exchange rate measurements in naturally ventilated animal buildings. *Biosystems Engineering*, 109(4), 276–287. <http://doi.org/10.1016/j.biosystemseng.2011.04.008>
- Samer, M., Ammon, C., Loebstin, C., Fiedler, M., Berg, W., Sanftleben, P., & Brunsch, R. (2012). Moisture balance and tracer gas technique for ventilation rates measurement and greenhouse gases and ammonia emissions quantification in naturally ventilated buildings. *Building and Environment*, 50, 10–20. <http://doi.org/10.1016/j.buildenv.2011.10.008>
- Sandberg, M., & Blomqvist, C. (1985). A quantitative estimate of the accuracy of tracer gas methods for the determination of the ventilation flow rate in buildings. *Building and Environment*, 20(3), 139–150. [http://doi.org/10.1016/0360-1323\(85\)90009-5](http://doi.org/10.1016/0360-1323(85)90009-5)
- Seifert, J., Li, Y., Axley, J., & Rösler, M. (2006). Calculation of wind-driven cross ventilation in buildings with large openings. *Journal of Wind Engineering and Industrial Aerodynamics*, 94(12), 925–947. <http://doi.org/10.1016/j.jweia.2006.04.002>

- Shen, X., Zhang, G., & Bjerg, B. (2012a). Investigation of response surface methodology for modelling ventilation rate of a naturally ventilated building. *Building and Environment*, 54, 174–185. <http://doi.org/10.1016/j.buildenv.2012.02.009>
- Shen, X., Zong, C., & Zhang, G. (2012b). Optimization of sampling positions for measuring ventilation rates in naturally ventilated buildings using tracer gas. *Sensors (Basel, Switzerland)*, 12(9), 11966–88. <http://doi.org/10.3390/s120911966>
- Shen, X., Zhang, G., Wu, W., & Bjerg, B. (2013). Model-based control of natural ventilation in dairy buildings. *Computers and Electronics in Agriculture*, 94, 47–57. <http://doi.org/10.1016/j.compag.2013.02.007>
- Shen, X., Su, R., Ntinias, G. K., & Zhang, G. (2016). Influence of sidewall openings on air change rate and airflow conditions inside and outside low-rise naturally ventilated buildings. *Energy and Buildings*. <http://doi.org/10.1016/j.enbuild.2016.08.056>
- Sherman, M. h. (1989). Uncertainty in Air Flow Calculations Using Tracer Gas Measurements. *Building and Environment*, 24(4).
- Sherman, M. H. (1990). Tracer-Gas Techniques For Measuring Ventilation in a Single Zone. *Building and Environment*, 25(4), 365–374.
- Shilo, E., Teitel, M., Mahrer, Y., & Boulard, T. (2004). Air-flow patterns and heat fluxes in roof-ventilated multi-span greenhouse with insect-proof screens. *Agricultural and Forest Meteorology*, 122(1-2), 3–20. <http://doi.org/10.1016/j.agrformet.2003.09.007>
- Simon Haykin. (2005). *Neural networks: a comprehensive foundation*. The Knowledge Engineering Review. Pearson. <http://doi.org/10.1017/S0269888998214044>
- Snoek, D. J. W., Stigter, J. D., Ogink, N. W. M., & Groot Koerkamp, P. W. G. (2014). Sensitivity analysis of mechanistic models for estimating ammonia emission from dairy cow urine puddles. *Biosystems Engineering*, 121, 12–24. <http://doi.org/10.1016/j.biosystemseng.2014.02.003>
- Snoek, D. W. J. (2016). Refining a model-based assessment strategy to estimate the ammonia emission from floors in dairy cow houses. <http://doi.org/10.18174/387486>
- Society, C., June, C., & Science, G. (2010). *World Congress of the International Commission of Agricultural and Biosystems Engineering (CIGR)*, (1998), 1–8.
- Takai, H., & Banhazi, T. (2013a). Special issue on emissions from naturally ventilated livestock buildings. *Biosystems Engineering*, 116(3), 213. <http://doi.org/10.1016/j.biosystemseng.2013.08.006>
- Takai, H., Nimmermark, S., Banhazi, T., Norton, T., Jacobson, L. D., Calvet, S., ... Berckmans, D. (2013b). Airborne pollutant emissions from naturally ventilated buildings: Proposed research directions. *Biosystems Engineering*, 116(3), 214–220. <http://doi.org/10.1016/j.biosystemseng.2012.12.015>
- Teitel, M., Tanny, J., Ben-Yakir, D., & Barak, M. (2005). Airflow Patterns through Roof Openings of a Naturally Ventilated Greenhouse and their Effect on Insect Penetration. *Biosystems Engineering*, 92(3), 341–353. <http://doi.org/10.1016/j.biosystemseng.2005.07.013>
- Teitel, M. (2007). The effect of screened openings on greenhouse microclimate. *Agricultural and Forest Meteorology*, 143(3-4), 159–175. <http://doi.org/10.1016/j.agrformet.2007.01.005>
- Teitel, M., Liran, O., Tanny, J., & Barak, M. (2008a). Wind driven ventilation of a mono-span greenhouse with a rose crop and continuous screened side vents and its effect on flow patterns and microclimate. *Biosystems Engineering*, 101(1), 111–122. <http://doi.org/10.1016/j.biosystemseng.2008.05.012>
- Teitel, M., Ziskind, G., Liran, O., Dubovsky, V., & Letan, R. (2008b). Effect of wind direction on greenhouse ventilation rate, airflow patterns and temperature distributions. *Biosystems Engineering*, 101(3), 351–369. <http://doi.org/10.1016/j.biosystemseng.2008.09.004>

- Ulens, T., Daelman, M. R. J., Mosquera, J., Millet, S., van Loosdrecht, M. C. M., Volcke, E. I. P., ... Demeyer, P. (2015). Evaluation of sampling strategies for estimating ammonia emission factors for pig fattening facilities. *Biosystems Engineering*, 140, 79–90. <http://doi.org/10.1016/j.biosystemseng.2015.09.009>
- Van Buggenhout, S., Van Brecht, a., Eren Özcan, S., Vranken, E., Van Malcot, W., & Berckmans, D. (2009). Influence of sampling positions on accuracy of tracer gas measurements in ventilated spaces. *Biosystems Engineering*, 104(2), 216–223. <http://doi.org/10.1016/j.biosystemseng.2009.04.018>
- Van Hooff, T., & Blocken, B. (2010). On the effect of wind direction and urban surroundings on natural ventilation of a large semi-enclosed stadium. *Computers and Fluids*, 39(7), 1146–1155. <http://doi.org/10.1016/j.compfluid.2010.02.004>
- Van Overbeke, P., De Vogeleer, G., Pieters, J. G., & Demeyer, P. (2014a). Development of a reference method for airflow rate measurements through rectangular vents towards application in naturally ventilated animal houses: Part 2: Automated 3D approach. *Computers and Electronics in Agriculture*, 106, 20–30. <http://doi.org/10.1016/j.compag.2014.05.004>
- Van Overbeke, P., Pieters, J. G., De Vogeleer, G., & Demeyer, P. (2014b). Development of a reference method for airflow rate measurements through rectangular vents towards application in naturally ventilated animal houses: Part 1: Manual 2D approach. *Computers and Electronics in Agriculture*, 106, 31–41. <http://doi.org/10.1016/j.compag.2014.05.005>
- Van Overbeke, P. (2015a). Development of a reference method for ventilation rate measurements in a naturally ventilated test facility. PhD Thesis. Ghent University, Belgium.
- Van Overbeke, P., De Vogeleer, G., Brusselman, E., Pieters, J. G., & Demeyer, P. (2015b). Development of a reference method for airflow rate measurements through rectangular vents towards application in naturally ventilated animal houses: Part 3: Application in a test facility in the open. *Computers and Electronics in Agriculture*, 115, 97–107. <http://doi.org/10.1016/j.compag.2015.05.009>
- Van Overbeke, P., De Vogeleer, G., Mendes, L. B., Brusselman, E., Demeyer, P., & Pieters, J. G. (2016). Methodology for airflow rate measurements in a naturally ventilated mock-up animal building with side and ridge vents. *Building and Environment*, 105, 153–163. <http://doi.org/10.1016/j.buildenv.2016.05.036>
- VERA. (2011). Test Protocol for Livestock Housing and Managements Systems.
- Verlinde, W., Gabriels, D., & Christiaens, J. P. A. (1998). Ventilation coefficient for wind-induced natural ventilation in cattle buildings: a scale model study in a wind tunnel, 41(3), 783–788.
- Wang, H., & Chen, Q. (2012). A new empirical model for predicting single-sided, wind-driven natural ventilation in buildings. *Energy and Buildings*, 54, 386–394. <http://doi.org/10.1016/j.enbuild.2012.07.028>
- Wang, S., Boulard, T., & Haxaire, R. (1999a). Air speed pro® les in a naturally ventilated greenhouse with a tomato crop, 96.
- Wang, S., & Deltour, J. (1999b). Lee-side Ventilation-induced Air Movement in a Large-scale Multi-span Greenhouse, 103–110.
- Wang, X., Ndegwa, P. M., Joo, H., Neerackal, G. M., Stöckle, C. O., Liu, H., & Harrison, J. H. (2016). Indirect method versus direct method for measuring ventilation rates in naturally ventilated dairy houses. *Biosystems Engineering*, 144, 13–25. <http://doi.org/10.1016/j.biosystemseng.2016.01.010>
- Wu, W., Zhai, J., Zhang, G., & Nielsen, P. V. (2012a). Evaluation of methods for determining air exchange rate in a naturally ventilated dairy cattle building with large openings using computational fluid dynamics (CFD). *Atmospheric Environment*, 63, 179–188. <http://doi.org/10.1016/j.atmosenv.2012.09.042>
- Wu, W., Zhang, G., & Kai, P. (2012b). Ammonia and methane emissions from two naturally ventilated dairy cattle buildings and the influence of climatic factors on ammonia emissions. *Atmospheric Environment*, 61, 232–243. <http://doi.org/10.1016/j.atmosenv.2012.07.050>

- Yu, H., Hou, C.-H., & Liao, C.-M. (2002). Scale Model Analysis of Opening Effectiveness for Wind-induced Natural Ventilation Openings. *Biosystems Engineering*, 82(2), 199–207. <http://doi.org/10.1006/bioe.2002.0072>
- Zhai, Z. (John), Mankibi, M. El, & Zoubir, A. (2015). Review of Natural Ventilation Models. *Energy Procedia*, 78, 2700–2705. <http://doi.org/10.1016/j.egypro.2015.11.355>
- Zhang, G., Strøm, J. S., Li, B., Rom, H. B., Morsing, S., Dahl, P., & Wang, C. (2005). Emission of Ammonia and Other Contaminant Gases from Naturally Ventilated Dairy Cattle Buildings. *Biosystems Engineering*, 92(3), 355–364. <http://doi.org/10.1016/j.biosystemseng.2005.08.002>

Curriculum vitae

Personal particulars

Gerlinde Diana Jeroentsje De Vogeleer

Gent, 13 November 1985

gerlindedv@gmail.com

married to Hans Bossaer (on 9 June 2012)

Children:

Wolf Bossaer (15 March 2012)

Hazel Bossaer (3 October 2013)

Basic education

2003 – 2006 Mercator Polytechnic

Environmental Management

2006 – 2009 PIH - association UGent

Master in Industrial Sciences: Environmental Engineering

Student Council representative (2007-2009)

Environmental coordinator type A

Employment

August 2009 - December 2011

Linea Trovata Suntec nv: project engineer

- Feasibility studies heat pump projects (industrial, agricultural and domestic application)
- Engineering aquaculture: heating and cooling; design of hydraulic schemes, monitoring installation.
- Engineering domestic heatpump projects; technical support salesmen; design offers (design, material and installation of boreholes and central heating systems); applications environmental permits boreholes

August 2009 - July 2012

Linea Trovata Eco bvba: project engineer

- Feasibility studies of renewable energy sources; optimisation energy processes (*manure mining projects, (combustion) plant mushroom compost*)
- Support manure drying and air scrubber projects from offer to completion (design offers and hydraulic schemes, acquisition material, technical support, contact with clients)
- Monitoring relevant Flemish and European legislation
- Design support of manuals for air scrubbers and manure dryers

August 2012 - September 2012

VREG - Flemish Government: handling expertise files

- Checking applications for the combined heat and power (CHP) and green power certificate system to conformity of the Flemish legislation and VREG procedures

October 2012 – February 2017

Ghent University, Department of Biosystems Engineering

- Research in view of obtaining a PhD degree:
'Reduced measuring strategies to assess ventilation rates in naturally ventilated animal houses'

Supervisors: Prof. dr. ir. Jan G. Pieters, dr. ir. Peter Demeyer

From March 2017

FLEMISH RESEARCH INSTITUTE FOR AGRICULTURE, FISHERIES AND FOOD

- Energy coordinator

Publications

Papers in international journals with reading committee

De Vogeleer G., Van Overbeke P., Brusselman E., Mendes L.B., Pieters J.G., Demeyer (2016) P. Assessing airflow rates of a naturally ventilated test facility using a fast and simple algorithm supported by local air velocity measurements. *Building and Environment*. 10.1016/j.buildenv.2016.05.006.

Van Overbeke, P., Pieters, J. G., **De Vogeleer, G.**, & Demeyer, P. (2014). Development of a reference method for airflow rate measurements through rectangular vents towards application in naturally ventilated animal houses: Part 1: Manual 2D approach. *Computers and Electronics in Agriculture*, 10.1016/j.compag.2014.05.005

Van Overbeke, P., **De Vogeleer, G.**, Pieters, J. G., & Demeyer, P. (2014). Development of a reference method for airflow rate measurements through rectangular vents towards application in naturally ventilated animal houses: Part 2: Automated 3D approach. *Computers and Electronics in Agriculture*. 10.1016/j.compag.2014.05.004

Van Overbeke, P., **De Vogeleer, G.**, Brusselman, E., Pieters, J.G., Demeyer, P., (2015). Development of a reference method for airflow rate measurements through rectangular vents towards application in naturally ventilated animal houses: Part 3 : Application in a test facility in the open. *Computers and Electronics in Agriculture*. 10.1016/j.compag.2015.05.009

Van Overbeke, P., **De Vogeleer, G.**, Brusselman, E., Demeyer, P., Pieters, J.G., (2015). Development of a reference method for airflow rate measurements through rectangular vents towards application in naturally ventilated animal houses: Part 4: Cross and ridge ventilated test facility. *Buildings and Environment*. 10.1016/j.buildenv.2016.05.036

Oral presentations at conferences

De Vogeleer, G., Van Overbeke, P., Pieters, J. G., & Demeyer, P. (2014). Assessing natural ventilation rates using a combined measuring and modelling approach. In proceedings of International Conference of Agricultural Engineering - Engineering for Improving Resource Efficiency. The European Society of Agricultural Engineers (EurAgEng), Zurich, Switzerland

G. De Vogeleer, J. G. Pieters, P. Demeyer (2016). Hoe het precies meten van het ventilatiedebiet in een natuurlijk geventileerde veestal een link heeft naar de natuur. In proceedings of 'Startersdag' INBO – Instituut Voor Natuur- en Bosonderzoek, Brussel.

Van Overbeke, P., **De Vogeleer, G.**, Pieters, J., & Demeyer, P. (2014). Development of a Reference Test Facility for the Validation of Naturally Ventilated Airflow Rate Measurement Techniques. In proceedings of the 18th World Congress of CIGR - International Commission of Agricultural and Biosystems Engineering, Beijing, China. - Presented by Philippe Van Overbeke

Van Overbeke, P., Pieters, J., **De Vogeleer, G.**, & Demeyer, P. (2013). Development of a reference method for the measurement of the ventilation rate through rectangular ventilation openings using ultrasonic anemometers. In proceedings of the 11th Conference "Construction, Engineering and Environment in Livestock Farming, Vechta, Germany. - Presented by Philippe Van Overbeke

Mendes B. L., **De Vogeleer G.**, Van Overbeke P., Demeyer P., Pieters J.G. (2015). Effects of Standard k- ϵ and LES Turbulence Models on a Full Scale Numerical CFD Simulation for a Naturally Ventilated Pig Barn Prototype ASABE 2015, Annual International Meeting, At New Orleans, United States of America - Presented by Luciano B. Mendes

De Vogeleer G., Van Overbeke P., Pieters J.G. , Demeyer P. (2016) Assessing airflow rates in a naturally ventilated test facility using ridge vent velocity data. The European Society of Agricultural Engineers (EurAgEng), Aarhus, Denmark. - Presented by Peter Demeyer

Other conference contributions

De Vogeleer, G., Pieters, J., Van Overbeke, P., & Demeyer, P. (2013). Field test facility for the development of a reference method for ventilation rate and emission measurements in naturally ventilated pig houses. In proceedings of the 11th Conference "construction, engineering and environment in livestock farming", Vechta, Germany. Poster Presentation – Award for best poster

Van Overbeke, P., **De Vogeleer, G.**, Demeyer, P., & Pieters, J. (2013). Development of a real life measuring technique for the ventilation rate of naturally ventilated animal houses. In proceedings of 18th National Symposium on Applied Biological Sciences, Ghent, Belgium. Poster Presentation

MSc theses

De Vogeleer G. (2009). Technologieverkenning van industriële drogers en optimalisatie van een banddroger voor digestaat- en mestverwerking (in collaboration with Spiessens nv).

Promotor: Ing. Bruno Vanslambrouck

BSc thesis

Evens K., De Meyer L., **De Vogeleer G.** (2006). Blauwe Vlag-audits en afvalproblematiek in jachthavens", (in collaboration with BBL).

Promotors: Benjamin Clarysse, Annie Van Goethem, Quirin Vyvey